MEASURING AND SIMULATING THE ENVIRONMENTAL EFFECTS OF PURSUING HIGH MAIZE YIELDS IN GEORGIA

by

DIMITRIOS PAVLOU

(Under the Direction of George Vellidis)

ABSTRACT

A three-year study was conducted from 2016 to 2018 to assess the water quality effects of high fertilization rates on maize. The study was conducted in a 1.44 ha field located on the University of Georgia's (UGA) Tifton Campus, in the southeastern Coastal Plain of Georgia, USA. Two fertilizer treatments were applied based on the University of Georgia Extension Service (C_E) and the Georgia maize growers (C_G) recommendations for achieving high yields. Conventional tillage was used in 2016 while conservation tillage was used during the following two years. Throughout the course of the study, groundwater and surface runoff samples were collected. Implementation of conservation tillage in the second and third growing seasons resulted in reduced surface runoff and increased infiltration. Statistically higher NO_3-N concentrations in groundwater resulted from the C_G treatment and NO_3-N concentrations in groundwater increased over time. The data collected from the field study were used in to simulate the water flow and solute transport with the HYDRUS-1D model. Groundwater data from 2018 were used to calibrate the model while the data from 2016 and 2017 were used for evaluating the model. In general, the correspondence between simulated and observed data was good especially in 2016 and 2018. Additionally, after HYDRUS-1D was successfully calibrated

and evaluated, it was used in parallel with the DSSAT CERES Maize model to evaluate three maize irrigation scenarios. The scenarios were the University of Georgia Checkbook Method, a sensor-based method, and rainfed production. The simulation results indicated that the sensor-based scheduling method could achieve higher maize yields along with lower water and NO_3-N leaching.

INDEX WORDS: water quality, non-point source pollution, maize, simulation modelling, HYDRUS-1D, DSSAT CERES Maize

MEASURING AND SIMULATING THE ENVIRONMENTAL EFFECTS OF PURSUING HIGH MAIZE YIELDS IN GEORGIA

by

DIMITRIOS PAVLOU

Bachelor of Science, University of Thessaly, Greece, 2009

Master of Science, Aarhus University, Denmark, 2012

A Dissertation Submitted to the Graduate Faculty of The University of Georgia in Partial Fulfillment of the Requirements for the Degree

DOCTOR OF PHILOSOPHY

ATHENS, GEORGIA

2020

MEASURING AND SIMULATING THE ENVIRONMENTAL EFFECTS OF PURSUING HIGH MAIZE YIELDS IN GEORGIA

by

DIMITRIOS PAVLOU

Major Professor:	George Vellidis
Committee:	Miguel L. Cabrera
	Gerrit Hoogenboom
	Wesley M. Porter
	David E. Radcliffe

Electronic Version Approved:

Ron Walcott
Vice Provost for Graduate Education and Dean of the Graduate School
The University of Georgia
December 2020

ACKNOWLEDGEMENTS

I would like to acknowledge the Georgia Corn Commission for proving the funding for this project. I would like to express my deepest gratitude to my supervisor Dr. George Vellidis. His guidance and support throughout this project brought my work to a higher level and his insightful feedback made a better person and scientist. I am deeply indebted to the members of my committee Dr. Wesley Porter, Dr. Radcliffe, Dr. Miguel Cabrera and Dr Gerrit Hoogenboom for helping me to improve my research. Special thanks to my partner and colleague Anna Orfanou for her wise counseling and encouragement. I could not have completed this dissertation without her assistance.

TABLE OF CONTENTS

Page

LIST OF TABLES

Page

LIST OF FIGURES

Page

CHAPTER 1

INTRODUCTION AND LITERATURE REVIEW

Introduction

Rapid population growth which is expected to reach 10 billion by 2050 has brought the agricultural sector to the forefront of interest as the increased needs for food, feed and energy must be met. To achieve that, yields of several crops must be increased. To some extent, this is something that modern agriculture has already accomplished with the mechanization of many operations, the use of new hybrids and agrochemicals such as pesticides and fertilizers.

Increasing yields and environmental consequences

Maize is one of the world's most cultivated crops and the USA is the largest world's maize producer (USDA, 2018). Total production of maize in the USA for 2019/2020 was 345.89 million Mg with the USA the world's largest maize exporter (Shahbandeh, 2020). Approximately, 130K ha are used for maize production in Georgia with an average production of 10K kg ha^{-1} (Toffanin, 2019). Farmers, though, are always pursuing higher maize yields. One way they attempt to achieve this goal is to use higher fertilizer rates. Although this practice may lead to higher yields, it can also lead to unintentional environmental effects and more specifically to water quality problems resulting from nonpoint source (NPS) pollution such as eutrophication of surface waters and nitrate (NO_3-N) contamination of ground waters from leaching (Addiscott and Benjamin, 2006; Berg et al., 2017; Conley et al., 2009; Mehdi et al., 2015; Menció et al., 2016; Sogbedji et al., 2000). This is because maize, like most crops, does not used all of the fertilizer applied. For example, nitrogen use efficiency (NUE) in maize production is less than

50% on average (Raun and Johnson, 1999), meaning that about half the nitrogen (N) applied is not utilized by the plants but instead is lost to the environment.

Phosphorus (P) is also a concern in NPS pollution because it too can lead to eutrophication problems. Total P in soil that moves through surface runoff is mainly transported in particulate form bound to sediment particles, but it can also be lost as P in solution (Haygarth et al., 1999). Agricultural production is responsible for more than 70% of total P being lost into rivers (Yu et al., 2006). Conservation practices, such as reduced tillage methods and the utilization of cover crops can reduce while when conventional practices are used the leaching can reach up to 80 kg ha^{-1} (Gold et al., 1990a).

Simulation models

In general, the interactions between plants, water, soil, and management practices can influence each other. Additionally, the agricultural decisions a consultant or farmer makes are complex. For these reasons, the use of simulation models can be an important tool that can provide essential insights to farmers which can lead to their financial and environmental sustainability.

A large number of simulation models have been developed and are widely used around the world. HYDRUS-1D is a finite-element model for simulating the one-dimensional movement of water, heat, and multiple solutes in variably saturated media. The model numerically solves the Richards equation for saturated–unsaturated water flow and convection–dispersion type equations for heat and solute transport (Šimůnek et al., 2016; Simunek et al., 2008). It has been proven by other studies to successfully simulate the water movement along with NO_3-N solute transport. For instance, Wang et al. (2010) used HYDRUS-1D to simulate NO_3-N leaching under heavy rainfall and high intensity irrigation rates. Their results showed that rainy years can

produce higher NO_3-N leaching while it was recommended to increase the irrigation times by applying smaller water doses. Iqbal et al. (2020) simulated soil water dynamics in sweet corn production for two seasons under rainfed conditions. The results showed that HYDRUS-1D successfully simulated the water balance components of the study while the water leaching reached up 10.6% and 26.8% of total water input of the two seasons, respectively. HYDRUS-1D was applied to simulate water movement and solute transport in two experiments which involved irrigating maize with saline water by Ramos et al. (2011). The model performed satisfactorily, showing that can be used for analyzing solute concentrations.

Although water and solute transport models like HYDRUS-1D include crop growth functions, dedicated crop growth models are best used to simulate crop response to environmental conditions and the response of yield to irrigation and fertilization management practices. The Decision Support System for Agrotechnology Transfer (DSSAT) is a suite of crop models that is widely used around the globe (Hoogenboom et al., 2012; Hoogenboom et al., 2019; Jones et al., 2003). The DSSAT maize model known as CERES-Maize has been used since 1986 for conducting experiments in a simulation environment (Jones, 1986). Saseendran et al. (2008) calibrated and validated CERES-Maize for northeastern Colorado to assess irrigation methods and to optimize irrigation WUE. The study included rainfed production. Kisekka et al. (2016) used CERES-Maize model to simulate yield while evaluating management practices for improving the use of limited water for irrigating maize.

Goals and objectives

The overall goal of this project was to evaluate the environmental and yield effects of maize to high fertilization rates in the southeastern Coastal Plain of Georgia, USA. Specific objectives were to

- evaluate the water quality effects of fertilization rates used to achieve high yield goals;
- use the HYDRUS-1D transport model to simulate the system and estimate N leaching losses; and
- use the HYDRUS-1D and CERES-Maize models to evaluate maize irrigation scheduling management scenarios that would result in high yields while minimizing NO3-N leaching.

CHAPTER 2

THE IMPACT OF HIGH INPUT MAIZE PRODUCTION IN WATER QUALITY[1]

[1] Pavlou, D., A. Orfanou, M.L. Cabrera, G. Hoogenboom, W.M. Porter, D.E. Radcliffe, and G. Vellidis. To be submitted to *Journal of Environmental Quality*.

Abstract

A three-year study was conducted to evaluate the water quality effects of fertilization rates used to achieve high maize yields in the southeastern Coastal Plain of Georgia, USA and different management practices. The study included two fertilizer treatments, based on University of Georgia Extension (C_E) and Georgia maize grower (C_G) recommendations for achieving yields in excess of 22 Mg ha^{-1} (350 bu ac^{-1}). Fertilizer application rates varied slightly from year to year based on soil test results but averaged 348 kg N ha^{-1} and 514 kg N ha^{-1} for the C_E and C_G treatments, respectively. Groundwater and surface runoff samples were collected throughout the course of the project. Samples were analyzed for NO_3-N, NH_4-N, PO_4-P and Cl^-. Surface runoff was also analyzed for total N (TN), total P (TP), and suspended solids. Yield differences between the two treatments were not significantly different. During the first year of the study, conventional tillage in combination with high irrigation application rates resulted in runoff occurring with each irrigation event. In subsequent years, irrigation application rates were reduced and conservation tillage in combination with a winter cover crop was used. This resulted in significantly less runoff and lower concentrations of NO_3-N in runoff in Years 2 and 3. Concentrations and loads of nutrients in surface runoff were not statistically different between the two fertilization treatments. Significantly higher NO_3-N concentrations in groundwater resulted from the C_G treatment and NO_3-N concentrations in groundwater increased over time under both treatments. Under the physical and management conditions used in this study, higher fertilizer application rates did not result in increased maize yield but did result in increased nonpoint source pollution that was somewhat tempered by adopting cover crops, conservation tillage, and lower irrigation water application rates.

Introduction

Maize (*Zea mays*) is the world's most productive grain crop in terms of yield (Goldschein, 2011) and the most cultivated crop in the United States of America (USA) with about 33 million hectares harvested in 2018 (Capehart and Olson, 2020). Demand for maize has consistently increased due to its many uses including as livestock feed, processed foods, industrial products, and biofuel. Growers in the USA Growers across the world are constantly exploring management strategies that may lead to higher yields including use of irrigation, planting hybrids better suited to their growing conditions, and using higher rates of fertilizers. Intensification of inputs may lead to increased nonpoint source (NPS) pollution.

According to United States Environmental Protection Agency (EPA), NPS pollution occurs through surface runoff, precipitation, atmospheric deposition, drainage, seepage or hydrologic modification (EPA, 2017b). As runoff moves, it transports natural and anthropogenic pollutants and deposits them into lakes, rivers, and groundwater. Pollutants associated with crop production are typically fertilizers, pesticides, and sediments.

Nonpoint Source Pollution

The primary nutrients of concern in NPS pollution are nitrogen (N) and phosphorus (P). Both are essential for plant growth, but when transported to receiving waters, they may lead to eutrophication (Bricker et al., 1999). N exists in the environment in many forms. It changes forms as it moves through the N cycle, for instance gaseous nitrogen, ammonia nitrogen, nitrates, nitrites and organic nitrogen. Nitrate (NO_3^-) is often seen as a worldwide agricultural pollutant of groundwater (Addiscott and Benjamin, 2006; Bouchaou et al., 2008; Cruz-Fuentes et al., 2014; Karr et al., 2001; Mehdi et al., 2015; Menció et al., 2016; Tagma et al., 2009; Weyer et al., 2001). Depending on management practices, soils, and geology, NO_3^- can become a significant

contaminant of both shallow and deep groundwater systems. Ammonium (NH_4^+) is another form of N sometimes found in groundwater (Hussain et al., 2015). Like with NO_3^-, high concentrations of NH_4^+ in groundwater are typically associated with anthropogenic activities.

NO_3^- and NH_4^+ contribute to the eutrophication of aquatic ecosystems through surface runoff (Galloway et al., 2008; Nolan et al., 1997; Rabalais et al., 2002). Eutrophication induces overgrowth of phytoplankton, thus deteriorating water quality, depopulating aquatic species and accelerating water scarcity (Sellner et al., 2003). As a result, the global concern about nutrient overload into the environment has been increased and there are strict regulations for the protection of water resources.

Soil P is composed of organic and inorganic P. These two forms together make up the total soil phosphorus (TP). About 80% of TP is immobile and not available for uptake by the plants. Inorganic P in the soil is found in three pools – plant available P in the soil solution, sorbed P, and mineral P. Soil solution and P sorbed to sediments are the generally associated with NPS pollution. (Gardner, 1990; Lane et al., 2011; Stewart and Tiessen, 1987). P in the soil solution is in the form of HPO_4^{2-} and $H2PO_4^-$and are commonly referred to as orthophosphates (Haygarth et al., 1999). P-sorption occurs when the orthophosphate ions bind to soil particles. Because these ions bind readily to soils, they are not usually concerns for contaminating groundwater. PO_4^{3-} is the dissolved ionic form of P for which water samples are analyzed. P bound to sediment that moves with surface runoff is the primary vector by which P contaminates receiving waters.

Factors that influence the amount of P in surface runoff could are the local soils, geology, and topography, the duration and intensity of a rain or irrigation event, the temperature and in general the management practices that take place in each field (Yu et al., 2006; Zhang et al.,

2012). Over 70% of TP discharged into rivers originates from agricultural land (Yu et al., 2006) and contributes to accelerated eutrophication of natural waters (Sims et al., 1998; Toor et al., 2003).

Soil erosion by water is a major worldwide environmental problem. It results in the degradation of quality of landscapes, has negative effects on agricultural productivity, influences sustainable development and contributes to transferring sediment and contaminants into surface waters (Novara et al., 2011; Palacio et al., 2014). Because of the ecological damage that soil erosion can cause, it is crucial to find ways for minimizing it. Practices such as conservation tillage and proper management of residues can help with the reduction of sediment movement from agricultural fields, slow runoff and create small ponds where sediment can be deposited and runoff can infiltrate the soil (Alberts and Neibling, 1994; Steiner, 1994).

Regulatory controls for NPS

The European Union's (EU) Nitrate Directive 91/676/EEC was implemented to protect receiving waters from NO_3^- derived from agricultural sources (EU, 2019). EPA has established a drinking water standard of 10 mg L^{-1} NO_3-N (Oram, 2018a). NH_4^+ concentrations in receiving waters are generally not regulated because concentrations are typically below levels that pose health concerns (WHO, 1996). However, the EU has set a NH_4^+ threshold of 0.5 mg L^{-1} (EU, 1998) primarily to serve as an indicator of fecal contamination. According to Water Research Center the maximum level of phosphates to avoid accelerated eutrophication is 0.1 mg L^{-1}.

NPS pollution from maize production

Phillips et al. (1993) tested four different management approaches in 100 croplands in Illinois which included continuous maize and a rotation of maize with soybean under conventional and no-till systems. The results showed that no-till could reduce N and P losses in

eroded soils. However, the concentrations of NO_3-N in groundwater samples exceeded the threshold of 10 mg L^{-1}, something that indicates contamination. 10 to 30% lower soluble N losses in surface runoff, subsurface flow and percolation were achieved with rotating maize and soybean production compared to continuous maize under both tillage systems. The P losses of maize soybean rotation in surface runoff were greater under no-till compared to conational tillage probably because P fertilizer was not incorporated into the soil.

The management practices followed in a maize field can play an important role in NPS pollution issues. A study which conducted in Minnesota compared two tillage methods and showed that soluble nutrient losses through surface runoff and drainage can be greater in tillage systems that do not incorporate plant residues. Conversely, sediment and particulate P losses can be greater in tillage systems that thoroughly mix residues (Zhao et al., 2001). A study which took place in maize fields in two areas in Wisconsin showed that when the P inputs exceed the plant demand can increase the P concentrations and loads in runoff. Furthermore, by using sources with high organic matter the P loads in runoff can be increased (Bundy et al., 2001).

Goals and Objectives

In Georgia, a relatively small group of growers have been able to achieve maize yields approaching and sometimes exceeding 31,000 kg ha^{-1} (500 bu ac^{-1}) by using high fertilizers rates as well as intensive management practices (Miller, 2016). This has put pressure on other growers to adopt these practices. The overall goal of this study was to evaluate the yield and environmental response of maize production to high fertilization rates in the southeastern Coastal Plain of Georgia, USA. The specific objective of the work reported here was to evaluate the water quality effects of these production practices.

Materials and methods

Field description

The study was conducted in the 1.44 ha NESPAL field located on the University of Georgia's (UGA) Tifton campus (31° 28.736'N, 83° 31.916'W) which is located in the Tifton–Vidalia Upland portion of the Gulf-Atlantic Coastal Plain in the headwaters of the Suwannee River basin. The climate of the Tifton–Vidalia Upland is humid subtropical providing abundant rainfall and a long growing season. Average monthly temperatures range from 11^{o}C in January to 27^{o}C in July and August with a 47-yr mean annual temperature of 19.2^{0}C (Vellidis et al., 2003). The average frost-free season is 253 d. Precipitation follows a definite seasonal pattern with generally low rainfall from September through November and an increase in precipitation in December through early May. Rainfall typically decreases again in May and early June. Summer thunderstorms and tropical depressions cause July and August to be wetter months on average. The study was conducted for three years from 15 March 2016 – 15 March 2019. Average annual precipitation for the study period was 1236 mm.

The NESPAL field was divided into six blocks of cultivated land separated by grassed berms. The berms prevent overland water flow between blocks and capture surface runoff. The three western blocks were labeled W1, W2, and W3 and the three eastern blocks were labeled E1, E2, and E3 as shown in Figure 2.1. Block size ranged from 0.18 ha to 0.34 ha. The blocks were further divided into four or six plots depending on the size and shape of each block (Figure 2.2). This resulted in 32 plots ranging in size from 121 m^2 to 526 m^2. Crop rows ran from west to east. Each plot contained twelve 0.91-m wide (36 in) rows.

The soil series in blocks W1, W2, and W3 and the western half of blocks E1, E2, E3 is a Tifton loamy sand with 2 to 5 % slope. The soil series in the eastern half of blocks E1, E2, E3 is

an Alapaha loamy sand with 0 to 2% slope. There is a visible color difference between the two soil series that is visible in Figure 2.1. Tifton loamy sand is described by the NRCS Soil Survey as deep, well drained, and commonly found on ridgetops and hillsides. This soil is low in natural fertility and organic matter and very strongly acid. Alapaha loamy sand is described as deep, poorly drained nearly level soil found along the upper part of drainage ways. This soil is also low in natural fertility and organic matter and very strongly acid. The eastern edge of the field is bordered by a forested riparian area drained by a second order stream.

A tractor equipped with a Trimble RTK GPS was used to collect elevation data with better than 50-mm x, y, and z, accuracy. A digital elevation model (DEM) of the field's terrain was created using ArcGIS (ESRI. ArcGIS Desktop, Redlands, CA: Environmental Systems Research Institute). The field slopes from north to south but also to the southeast and to the southwest along its north-south axis (Figure 2.3a). There is maximum elevation change of 8 m in the field with the maximum elevation being approximately 103 m and the minimum 95 m ASL (above sea level). The highest elevation is found at the northwest corner and the lowest at the southeast corner. ArcGIS and the DEM were used to develop the hydrography of the field. The lines in Figure 2.3b indicate surface runoff flow paths. Darker lines indicate less concentrated flow while white lines indicate concentrated flow that occurs along the berms of the blocks. The DEM-derived flow paths coincide well with the physical flow paths shown in the aerial photograph underlying Figure 2.1.

Experimental design

Two maize fertilization treatments based on high maize yield goals were selected for the study. The first treatment was recommended by Georgia maize producers who have consistently achieved high yields. This treatment was designated as C_G and had a yield goal of 28 Mg ha^{-1}

(450 bu ac^{-1}). The second treatment's yield goal was based on recommendations from UGA Extension specialists on what might be an aspirational statewide yield goal and was set to 22 Mg ha^{-1} (350 bu ac^{-1}). It was designated as C_E. The fertilizer application rates associated with the two treatments are shown in Table 2.1.

Three blocks were randomly assigned to the C_G treatment (W1, E2, and W3) and the remaining three to the C_E treatment (E1, W2, and E3) as shown in Figure 2.2. All plots within each block were then assigned to the block's treatment. As a result, there were eight plots (replicates) of each treatment. Because of the project's three-year duration, an annual maize-soybean rotation was established among the plots of each block. Half of the plots in each block were planted with maize and the other half with soybeans. Each growing season, the maize and soybeans were rotated. Figure 2.2 shows the location of the maize (C_G and C_E) and soybean (S) plots during the three growing seasons. The soybean plots were not fertilized.

Table 2.1 presents the crop production management practices used during the project and Figure 2.4 presents a timeline of the project. Project years (Year 1, Year 2, Year 3) were defined as shown in Figure 2.4. During each project year, maize was planted in March and harvested in August. In 2016, because instrumentation was being installed in the field prior to the planting of the first maize crop, a cover crop was not planted. As a result, conventional tillage was used for the 2016 growing season. After the 2016, 2017, and 2018 growing seasons, a cover crop was planted. The field remained fallow with corn residue until October or November when a wheat or rye cover crop was planted. Rye was the preferred cover crop, but seed was not available during Year 1 and Year 3. The cover crop was planted with a seed drill into the maize residue and fertilized as shown in Table 2.1. The cover crop was terminated using herbicides in late February

in preparation for spring maize planting and strip tillage used to plant the corn in the cover crop residue.

Management practices were adjusted during the study to address observed problems. The field was irrigated by a center pivot irrigation system and runoff was observed consistently during irrigation in 2016. To correct this problem, the sprinkler package on the pivot was changed to reduce the intensity of water application (Table 2.1). Fertilizer side-dress applications were reduced in amount but increased in frequency during Years 2 and 3 to increase yields. Seeding rate was increased in the C_G treatment during Year 3 for the same reason. The factors driving these changes are discussed in detail below.

Irrigation scheduling

The UGA Smart Sensor Array (UGA SSA), wireless soil moisture sensing system was used to measure soil moisture continuously and schedule irrigation (Vellidis et al., 2013). A UGA SSA sensor node consisted of three Watermark® sensors incorporated into a probe. The sensors were located at depths of 0.2 m, 0.4 m and 0.6 m below the soil surface. A UGA SSA sensor node was installed in each of the 16 maize plots. The nodes were installed near the center of each plot within a row of maize. A field-average of soil water tension (SWT) at 07:00 each morning was used to make irrigation scheduling decisions. Irrigation was initiated when the field-average SWT was between 30-35 kPa (Orfanou et al., 2019).

Soil sampling

Intact 0.75 m soil cores were collected twice per year, in February before the maize was planted, and in September, after the maize was harvested. The cores were segmented into 0.15 m increments and were analyzed with Mehlich 1 by a commercial laboratory for analysis. The semi-annual analyses included organic matter, pH, Total N (TN), NH_4-N, NO_3-N, P, and

micronutrients. The initial analysis also included soil texture and cation exchange capacity (CEC). The soil test results were used for making agronomic decisions such as liming and adding phosphorus, potassium, and micronutrients. The results were also used to assess transport of nutrients through the soil profile.

Sampling surface runoff and groundwater

To assess the water quality effects of the fertilization treatments, shallow groundwater and surface runoff was sampled and analyzed for nutrients and suspended solids. In the landscape where the study was conducted, a plinthic soil horizon (irreversibly hardened mixture of iron sesquioxides and quartz) begins at a depth of 1 to 1.5 m. As a result, most of the excess precipitation in the Tifton–Vidalia Upland moves either laterally in shallow saturated and unsaturated flow or moves in surface runoff during storm events (Vellidis et al., 2003) and creates a dense dendritic network of first and second order streams. The general hydrology of the Tifton–Vidalia Upland is reflected at the NESPAL field.

Surface runoff was measured using 0.45-m H-flumes installed at the locations shown by the circled “R” in Figure 2.1. A Druck pressure transducer (Baker Hughes, Houston, Texas, USA) connected to a Campbell Scientific CR-10 data logger (CAMPBELL SCIENTIFIC, Logan, Utah, USA) was used to measure pressure head in the flume’s stilling well (Figure 2.5). Head data were converted to flow with a rating curve stored in the data logger’s memory. Hydrographs were created from the flow data and used to estimate volumes of surface runoff for individual precipitation or irrigation events.

Flow proportional water samples were collected with an ISCO 2910 compositing sampler contained in a metal instrument house on a raised metal stand adjacent to the flume (Figure 2.5). The data logger instructed the sampler to collect a sample when a predetermined volume of

runoff passed through the flume. The volume of runoff was a function of block surface area and differed for each sampler. Sample volume was set at 250 mL. Consequently, the ISCO sampler collected samples more frequently when flow was high and less frequently when flow was low. The individual samples were accumulated in a 10-L glass jar to create a single composite sample for each runoff event. When feasible, manual grab samples were collected from the flumes during runoff events as backups in case of instrument failure. The samples were analyzed for NO_3-N, NH_4-N, TN, PO_4-P, TP, and Cl^- by a commercial laboratory. Samples were analyzed for total suspended solids (TSS) by project team members.

Loads of TN, TP, and suspended solids were calculated for individual runoff events by multiplying estimated volume by concentrations of nutrients and TSS. Loads from individual events were aggregated by crop and annually.

Groundwater was captured by installing drain tile along the western, southern, and eastern boundaries of each block (Figure 2.1) prior to the 2016 growing season. Drain tile depth ranged from 1.1 m at the center of the field to 0.6 m along the edges of the field to accommodate the field's slope. The drain tile also isolated the blocks from any shallow groundwater moving laterally from higher positions of the landscape. Blocks W1 and E1 were located at the top of the slope and were unlikely to receive shallow groundwater flows from the north (top of the figure). The location of the drain tile is shown by the blue lines in Figure 2.1. Drain tile was also installed along the length and in the middle of blocks E1, E2, and E3, to replace existing drain tile that was cut during installation of the new tile. The circled "G" indicates where the drain tile was sampled to collect ground water samples from each block. Groundwater samples were collected manually twice per week in 1-L plastic bottles when there was flow. The first sample was collected after the first fertilizer application in 2016 and the last was collected on 15th of

March 2019. The samples were analyzed for NO_3-N, NH_4-N, PO_4-P and Cl^- by a commercial laboratory.

Statistical analysis

A statistical analysis was performed with JMP® Pro 14.1.0 (JMP®, Pro 14.1.0, SAS Institute Inc., Cary, NC, 1989-2019) to determine significant differences in the response variables between the fertilization treatments and management practices. The response variables were surface runoff volume and analytes in groundwater and surface runoff. The comparison of means was done using the Tukey-Kramer HSD test with $\alpha = 0.05$ and $\alpha = 0.1$. In the cases that the results of the statistical analysis were different between the α values, the connected letters report of $\alpha = 0.1$ are represented with bold letters in Appendices and tables. There were not many differences between the α values and for that reason the $\alpha = 0.05$ was used for describing the results of the study.

Results

Surface runoff

A total of 540 surface runoff samples was collected of which 293 were collected during the Year 1, 76 during Year 2, and 171 during Year 3 (Table 2.2). Figure 2.6 shows the relationship between precipitation, irrigation, and number of samples collected annually. The numbers within the bars of Figure 2.6 indicate the percentage of irrigation and precipitation events that resulted in runoff. More samples were collected during Year 1 because the combination of conventional tillage and the higher application rate of the pivot resulted in runoff from all irrigation events. Crusting of the soil surface was observed throughout the field and runoff began almost immediately after irrigation was initiated.

Figure 2.7 shows the volume of runoff per unit area (dark blue bars) and total of water received via irrigation or precipitation by block and cropping season. Also shown is the percent of water received lost to surface runoff. A larger percentage of water received was lost to runoff during the Year 1 maize cropping season than in the corresponding periods in Years 2 and 3 because of the issues described above. This trend continued during the fallow period (maize residue – no irrigation) and during the wheat cover crop period. Irrigation was applied only to promote germination of the cover crop during these two periods, so runoff was generated by precipitation. Table 2.3 presents the percentage of precipitation and irrigation lost to surface runoff by block during the maize cropping period for each of the project's three years. Blocks W3 and E3 which were located lower in the landscape lost a higher percentage of precipitation and irrigation to runoff. Across all blocks, more precipitation than irrigation was consistently lost to runoff.

Appendix A presents mean concentrations of TSS, NO_3-N, NH_4-N, TN, PO_4-P, and TP in runoff by treatment, block, year, and cropping period. Across the entire study period, mean concentrations between the C_G and C_E treatments were similar without significant differences. Mean TSS concentrations showed a sharp decrease from Year 1 to Year 2 but increased just as sharply during Year 3. This is likely due to the precipitation differences between years. There were significant differences in mean TSS concentrations between cropping periods within blocks and years. The nine highest mean cropping period concentrations ranged from 472 to 1325 mg L^{-1} and were measured during the wheat cover crop of Year 3 and the maize crop of Year 1. The Year 3 cover crop was planted in November 2018. Heavy rain after planting resulted in poor germination and a poor stand. Because of the poor stand, the field was eroded by runoff over the winter especially in the eastern blocks as shown in the aerial photo of the field from April 2019

(Figure 2.1). High mean cropping period concentrations were measured in the Year 1 maize crop because of the conventional tillage, soil crusting, and high intensity irrigation described earlier.

Mean NO_3-N concentrations in runoff were greater during the maize cropping period of Year 1 and Year 3 regardless of block and treatment, while there were cases that mean NO_3-N concentrations were greater during the residue and rye cropping periods of Year 2. The combination of high rates of N fertilizers applied during the maize cropping period, along with the large amount of water received via precipitation and irrigation explains the results of Years 1 and 3. Year 2 received the least precipitation and irrigation. In addition, the side-dress fertilizer was split into more applications in the C_G treatment (Table 2.1). This strategy may have reduced NO_3-N losses during the maize cropping period. There were significant differences in mean NO_3-N concentrations between years, with Year 1 having the highest concentrations, regardless of block and treatment.

Mean NH_4-N concentrations in runoff were statistically higher in Year 3, regardless of treatment or block perhaps because more precipitation events occurred more frequently after fertilizer applications. The four highest NH_4-N concentrations (1.5 – 1.7 mg L^{-1}) were observed during the fallow period and may have been the result of mineralization of maize residues.

Mean TN concentrations in runoff were consistently higher for the Year 1 maize cropping period. There was a decrease in concentrations of TN from Years 1 to 3, regardless of treatment. There were significant differences in concentrations of TN between years for all treatments. The five highest TN mean cropping period concentrations were from the Year 2 rye cover crop (7.4 – 17.8 mg L^{-1}). These concentrations were all from different blocks.

Mean PO_4-P and TP concentrations in runoff were significantly higher during Year 2 regardless of block and treatment. This was likely the result of the greatest amount of P_2O_5

fertilizer being applied during Year 2. The concentrations of PO_4-P were significantly greater during the residue periods in every year and block except for Year 3 in the W2 and E1 blocks. TP concentrations were significantly greater during the residue periods apart from Year 3 in W2 block. Larger PO_4-P and TP concentrations during residue periods is likely the result of decomposition and or transport of maize residue. The four highest PO_4-P (2.2 – 5 mg L^{-1}) concentrations and the seven highest TP concentrations (2.5 – 5.4 mg L^{-1}) were also observed during the residue periods.

Figure 2.8 shows cumulative runoff per unit area for the entire project period. The greatest cumulative runoff was observed in blocks W3 and E3. The greatest annual cumulative runoff was observed during Year 1 for all six blocks. Because of the changes in management practices described earlier, and because there was less precipitation, runoff decreased sharply in Year 2. More rain events resulted in increased runoff in Year 3 compared to Year 2 but in almost all cases, the amount was less than half that of Year 1. The same trend was observed in the annual cumulative loads of TSS, NO_3-N, NH_4-N, TN, PO_4-P and is an indicator of how management practices can reduce runoff-driven nonpoint source pollution.

Table 2.4 presents the loads of TSS, NO_3-N, NH_4-N, TN, PO_4-P, and TP in surface runoff by treatment, block, and year. Cumulative NO_3-N and NH_4-N runoff loads were higher in C_E than in C_G treatment by 0.2 kg ha^{-1} and 0.6 kg ha^{-1}, respectively. Conversely, cumulative TN was higher in C_G than C_E by 1 kg ha^{-1}. Cumulative PO_4-P loads were higher in C_G than C_E by 0.1 kg ha^{-1} and TP loads were greater in C_G than C_E by 0.9 kg ha^{-1}. However, these differences between treatments were not statistically significant.

Despite the much great fertilizer rates applied to the C_G treatment, only blocks W3 and E2 had consistently higher nutrient losses than the C_E treatment blocks. This is primarily because

the measured losses were affected by the response of individual blocks whose response was a function of topographical position and soil type. For example, block W1 which is located in the northwestern section of the field (Figures 2.1 and 2.2), had the least topographical relief (Figure 2.3). This resulted in block W1 producing the lowest volume of runoff and smallest loads of all the six blocks. W3 and E2, the other two blocks of the C_G treatment had more topographical relief (Figure 2.3) and had greater runoff volumes and larger loads. If the randomization of treatments assigned to blocks had resulted in block W1 being assigned to the C_E, it is quite likely that the C_G treatment would have resulted in consistently higher nutrient losses.

Table 2.5 presents the losses of runoff (%) in comparison to total water received via precipitation and irrigation and losses of TN (%) and TP (%) through surface runoff in comparison to total fertilizer applied. In all cases, block W1 had the lowest percentage of runoff and TN and TP losses. The highest percentage of runoff was observed in block W3 while the highest losses of TN and TP were in block W2. The percentage of runoff, TN and TP was higher in C_E than C_G treatment during Years 1 and 3.

Appendix B presents the volumes of runoff and loads per unit area of TSS, NO_3-N, NH_4-N, TN, PO_4-P, and TP in runoff by treatment, block, year, and cropping period. Across the entire study period, mean volumes and loads between the C_G and C_E treatments were similar without statistically significant differences.

In Years 1 and 3, mean runoff volume per unit area was highest during the wheat cropping period of Years 1 and 3, while during Year 2 it was highest during the maize period. In Year 2, rye was used as cover crop and it had a better stand and much more cover when compared to the two wheat crops. This was especially true in Year 3 when poor wheat germination resulted in a very poor stand and little cover in the field. The eight highest values of

runoff were between 39 and 64 m^3 ha^{-1} and occurred during wheat and residue periods in Year 1. By block, the highest mean surface runoff volume per unit area was observed in W3 (14.2 m^3 ha^{-1}) and E3 (13.1 m^3 ha^{-1}) both located lower in the landscape, while the lowest was at W1 block (6.9 m^3 ha^{-1}) in the northern part of the field and with the highest elevation and lowest topographical relief. Mean runoff volume per unit area was statistically higher in Year 1. A sharp decrease was noticed in Year 2 due to less rainfall and irrigation combined with the utilization of cover crop and conservation tillage. The increased rainfall and irrigation in Year 3 resulted in higher runoff losses but not significantly different than Year 2. This was occurred in all treatments and blocks.

Mean TSS loads matched the patterns of runoff volume. They were higher in Years 1 and 3 during the wheat period and during the maize period during Year 2. However, there were no significant differences between the cropping periods. Similarly, TSS loads matched runoff volume trends with the highest loads in Year 1 and the lowest in Year 2. However, there were no significant differences between years. In contrast, blocks did not follow the same trends as years and cropping periods. While blocks W3 and E3 had the highest mean runoff volume per unit area, blocks E2 (18.3 kg ha^{-1}) and E1 (12.6 kg ha^{-1}) had the highest mean TSS loads. Both blocks E1 and E2 had a sand soil texture at the top 15 cm while the soil texture of the other blocks was loamy sand to sandy loam although this does not explain the observations.

In Year 1, mean NO_3-N loads were higher during the residue period except for block W1, in which mean NO_3-N loads were greater during the wheat cropping period. In Years 2 and 3, mean NO_3-N loads were greater during the maize period. Significant differences were observed between cropping periods only in the C_E treatment. The mean NO_3-N loads were statistically

greater in Year 1 for both treatments, something that can be related to the greater runoff volumes per unit area in Year 1.

Mean NH_4-N loads were higher during maize cropping periods for all the years of the project likely because of the type of fertilizer applied but there were no significant differences. By year, the NH_4-N loads were significantly greater in Year 3. This is the same as for surface runoff concentrations and likely due to the reasons described earlier.

Similar to mean NO_3-N loads, mean TN loads were higher during the residue period in Year 1. In Years 2 and 3, the losses of TN through surface runoff were greater during the maize cropping periods. By year, mean TN loads were significantly greater in Year 1 for both treatments.

During Year 1, mean PO_4-P loads were significantly higher during the residue period. In Year 2, mean loads were higher during the maize period but differences between cropping periods were not statistically different. In Year 3, mean PO_4-P loads were higher during the maize period and there were statistical differences between some blocks. Although the values of PO_4-P loads were lower than 0.2 kg ha1, regardless of cropping period, the three highest cases ranged from 0.6 to 1.4 kg ha1 and were measured either during the maize residue period or the wheat cropping period. Comparing the results by year there were no significant differences except for block W1. A similar pattern to mean PO_4-P loads was observed in mean TP loads as well. They were higher during residue periods in Year 1 but in Years 2 and 3 they were higher during the maize cropping periods. The P2O5 fertilizers applied during Years 2 and 3 were higher in both treatments compared to Year 1. Comparing the results by year, there were no significant differences.

Groundwater

A total of 932 groundwater samples were collected of which 285 were collected during Year 1, 238 during Year 2, and 409 during Year 3 (Table 2.2). The number of samples reflected the precipitation received in each of the three years.

NO_3-N concentrations of all collected groundwater samples are shown in Figure 2.9. Concentrations ranged from a low of 0.01 mg L^{-1} (block E1) to a high of 33.21 mg L^{-1} (block W3). Concentrations most frequently exceed 10 mg L^{-1} in block E3 which contained the sandiest soils but also the shallowest water table due to its proximity to the riparian area on the east edge of the field and the farm pond south of the field (Figure 2.1). Mean concentrations of NO_3-N, NH_4-N, PO_4-P and Chloride (Cl) in groundwater are presented in Appendix C by treatment, block, year, and cropping period. By crop, mean NO_3-N concentration was higher either during the residue periods or wheat cropping periods in all blocks and years. In Year 1, the highest mean NO_3-N concentration was observed during the wheat cropping period however, there were no rainfall events during the residue period, which led to no groundwater sample collections (Figure 2.9). Rainfall began again at the end of November. In Year 2, the highest mean NO_3-N concentration was observed during the residue period while during Year 3, the highest mean NO_3-N concentrations were observed during the residue period and the wheat cropping period. A likely explanation for these observations is that unused fertilizer remaining from the maize fertilizer applications moved through the soil profile over time and began leaching. At the same time, N from the maize residue was likely mineralized and contributed to leaching.

The western blocks (W1, W2, and W3) generally had higher mean NO_3-N concentrations. By treatment, Year 3 had higher NO_3-N concentrations, but this was statistically different only in the C_G treatment. Overall, the C_G treatment had statistically higher mean NO_3-N

concentrations than the C_E treatment that indicates that continuous use of high N fertilizer applications contributed to higher NO_3-N concentration in groundwater over the long term.

Mean NH_4-N concentrations in groundwater were consistently highest after the maize cropping period. Specifically, in Year 1, the highest mean NH_4-N concentrations in groundwater were observed during the wheat cropping period, in Year 2 during the rye period, while in Year 3 during the residue period. The six highest mean NH_4-N concentrations ranged from 0.9 to 1.2 and were observed during the residue cropping period of Year 3. By year, mean NH_4-N concentrations were significantly higher in Year 3, regardless of block and treatment. This increase could be related to higher precipitation in Year 3 in combination with overall low soil CEC values. Table 2.6 shows that CEC was low in the entire soil profile (0.75 m), independent of the blocks, something that indicated low cation retention. The low CEC values in combination with the high precipitation in Year 3 could have resulted in the increased mean NH_4-N concentrations in groundwater. Comparing the two fertilization treatments, no significant differences were observed with a=0.05, while C_E is significantly higher than C_G with a=0.1.

Mean PO_4-P concentration was higher during cover crop periods (wheat and rye) in Year 1 and 2, while in Year 3 the concentrations were higher during the residue period. By year, mean PO_4-P concentration was significantly higher in Year 3 while the lowest average concentrations were observed in Year 1. Table 2.7 shows that available P in the soil was significantly higher in the first 30 cm and then there was a decrease. Adding more P fertilizer during the course of the study resulted in an increase of the amount of P. This, in combination with the increased precipitation in Year 3, may have led to increased leaching. Mean PO_4-P concentrations between the two treatments were not significantly different.

Cl^- concentrations were used primarily to ensure that observed differences in concentrations were not affected by dilution. Although overall mean concentrations in the C_G treatment were significantly higher than the C_E treatment (Appendix C), the numerical difference between the means was small (C_E = 35.0 mg L^{-1} and C_G = 38.6 mg L^{-1}). There were no consistent trends in the data between cropping periods, blocks, years, or treatments that would indicate dilution effects. Effects of fertilizers used were found in the Cl^- concentrations. For example, Year 2 concentrations were significantly higher, and this could be attributed to a combination of the use of MOP (Muriate of Potash), which contains 45% to 47% Cl^- and lower precipitation.

Discussion and conclusions

The goal of this study was to evaluate the water quality effects of the fertilization treatments used to achieve high maize yields in the southeastern Coastal Plains of Georgia, USA. Adaptive management was implemented throughout the project's duration to improve growing conditions based on field observations. Although the intention from the beginning was to use conservation tillage, installation of the drain tile prior to the initiation of the project required the use of conventional tillage during the first cropping season. As described in the results, the combination of conventional tillage and high application rates from the irrigation system caused surface runoff to occur with all of the irrigation events in addition to excessive runoff during precipitation events. Incorporating a cover crop with strip tillage the subsequent years reduced the number of surface runoff events by 74% and 42% during Years 2 and 3, respectively. Runoff volume per unit area was reduced by an average of 72% and 43%. The impact of cover crop and conservation tillage is especially shown during Year 3 when 49% more rainfall was received compared to Year 1 but 43% less surface runoff was measured.

Although many studies have documented reduced runoff and increased infiltration from the use of cover crops and reduced tillage practices (Kaspar et al., 2001; Raczkowski et al., 2009; Zhu et al., 1989), few studies have shown this for maize production in the southeastern Coastal Plain. Furthermore, few studies have documented runoff reductions of this magnitude in sandy soils. Zhu et al. (1989) found that cover crops and conservation tillage reduced runoff by 53% when compared to conventional tillage in a plot study conducted in Missouri on heavier soils. One of the problems encountered in this project by using conventional tillage during Year 1 was soil crusting. Cassel et al. (1995) found that tillage practices that leave crop residues on the soil surface (no tillage, in-row subsoiling and chisel plow) can reduce crusting, increase infiltration and reduce surface runoff.

Surface runoff results in soil and nutrient losses. The volume of surface runoff affects TSS concentrations but is not always a predictor of TSS concentrations. For instance, block W1 had the lowest mean TSS concentration and the least runoff among the blocks. However, blocks E2 and E1 blocks had the highest mean TSS concentrations but the volume of surface runoff was not as high as in other blocks. Consequently, higher runoff volume did not necessarily lead to higher TSS losses. This was also shown in the study by Mailapalli et al. (2013), where the highest amount of runoff did not contribute to the highest TSS losses. Other factors that affected the TSS losses were the topographical location of each block, soil texture in the top 15 cm, and slope. The east blocks and W3 had higher cumulative TSS losses compared to blocks W1 and W2 due to a steeper slope (Figure 2.3). The concentration of TSS in runoff samples was greater during the first year of the project. The total load of TSS (kg ha^{-1}) was 97% and 80% less during Years 2 and 3, respectively. The primary reason for this reduction was the use of cover crop and conservation tillage after the Year 1 residue period. A study by Singh et al. (2018) found that

TSS were reduced by 33% to 34% due to cover crops. This occurred because erosion was reduced due to the presence of cover crop which does not allow water droplets to impact the soil directly (Dillaha et al., 1988). Consequently, cover crops can reduce erosion and crusting and increase infiltration. A study by Baker and Laflen (1983) showed that erosion was reduced by half when the percentage of cover crop was increased by 9 to 16 %. Another possible reason for the reduction in runoff is the rotation between maize and soybean. This rotation has been shown to reduce TSS and TP concentration in Midwestern streams Mbonimpa et al. (2014).

Cover crops and conservation tillage improve water infiltration rates. Although these rates were not directly measured in this study, the increase can be determined indirectly from the number of groundwater samples collected. Even though Year 2 was considerably drier than Year 1, approximately the same number of groundwater samples were collected. Year 3 was the wettest and the amount of groundwater samples collected was 44% and 72% higher than Year 1 and Year 2, respectively.

Mean concentrations of TN in runoff were 4.00 mg L^{-1} and 4.53 mg L^{-1} during Years 1 and 2 of the project, respectively. Mean TN concentration was reduced to 1.74 mg L^{-1} in Year 3. Although Georgia does not have nutrient criteria for streams, the adjacent state of Florida does. The watershed in which the project was conducted as well as many of the watersheds in southwestern Georgia drain to north-central Florida. The surface water criterion for TN there is 1.87 mg L^{-1}, (FDS, 2016). Although surface runoff concentrations are greatly diluted in receiving waters, if many growers begin pursuing high maize yields by increasing fertilizer applications, surface water quality in receiving waters may be adversely affected. However, conservation practices like the ones used during Years 2 and 3 of the project may have long-term positive effects on water quality. The ability of conservation tillage to reduce TN losses have been

documented in other studies including (McDowell and McGregor, 1984) in northern Mississippi, USA.

Soil residual N -- primarily NH_4-N and NO_3-N can be lost through leaching, surface runoff, volatilization and N_2O emissions. Under the best of circumstances, crops use between 50% - 70% of applied N (Sainju et al., 2018), so applying fertilizer to crops in large doses increases the chances of losses to the environment and especially via leaching. The concentration of NO_3-N in groundwater samples was high during the three years of the project. There were samples throughout the three years with concentrations exceeding 10 mg L^{-1}, which is the U.S. EPA drinking water standard (Oram, 2018a). Although mean NO_3-N concentrations increased over time, the differences were not consistently statistically different. This is consistent with other studies that have linked increased infiltration to increases in NO_3-N leaching (Daryanto et al., 2017; St. Luce et al., 2011). In this study, there was a statistically significant difference between the two fertilization treatments indicating that a higher fertilization rate does increase the concentration of NO_3-N in groundwater.

Although the area in which the study was conducted is not a groundwater recharge zone, much of southwestern Georgia where maize is grown is a major recharge zone for the Floridan Aquifer that provides drinking water to major metropolitan areas as well as thousands of rural communities and individual homeowners. In the recharge area, NO_3-N leached from excessive fertilizer applications can further contaminate the regional aquifer. Crandall et al. (2013) found that NO_3-N concentrations in the upper Floridan Aquifer underlying the Dougherty Plain in southwestern Georgia, the Marianna Lowlands in the Florida panhandle, and the lower Apalachicola–Chattahoochee–Flint River Basin (ACFB) in southeastern Alabama from 1993 to 2007 showed an upward trend in most cases and ranged from 0.37 to 12.73 mg L^{-1}.

Groundwater is the drinking water source for 37% of the U.S. population. In Georgia 92% of rural drinking water sources come from groundwater (Hawkins and Thomas, 2014). Samples collected from rural drinking water wells in the Georgia-Florida coastal plain showed that 25% of them exceeded the 10 mg NO_3-N L^{-1} threshold (Berndt et al., 1998).

The published maximum acceptable concentration of PO_4-P in fresh surface water bodies to prevent eutrophication varies but 0.1 mg L^{-1} is frequently used (Oram, 2018b). In this project, the mean PO_4-P concentration levels were above this threshold during all three years of the project in surface runoff. This threshold was also exceeded in groundwater samples during Years 2 and 3. High concentrations in groundwater are relevant in the Tifton-Vidalia Upland because shallow groundwater recharges the ecoregion's many first and second order streams. In the Floridan Aquifer recharges zone, groundwater feeds springs that discharge directly to streams and rivers.

As P concentrations in topsoil are increased, its transport in surface runoff tends to increase as well (Czapar, 2008). Conservation tillage practices generally reduce the loss of particulate P in runoff but increases the concentration of dissolved P in runoff increases (Soileau et al., 1994). The lowest TP and PO_4-P concentrations were measured in surface runoff samples collected during Year 1 which was the year with the smallest amount of applied P fertilizer but also the year with the largest volume of runoff. Because of the large volume of runoff, Year 1 had by far the largest TP and PO_4-P loads. The most P fertilizer was applied in Year 2, which had the highest mean TP and PO_4-P concentrations in surface runoff samples. Year 2 also had the highest P concentrations in February soil samples up to 450 mm depth. According to Sharpley et al. (1994), the amount and timing of fertilizer application in combination with a rain event can lead to loss of soluble P through runoff. Another explanation for the increasing

concentration of TP and PO_4-P in runoff samples could be the release of P from maize and cover crop residues (McDowell and McGregor, 1984).

Maize yields were not significantly different between treatments for each of the three years of the study (Orfanou et al., 2020a). Although the NESPAL field is considered representative of agricultural areas in the Tifton-Vidalia Upland of the southeastern Coastal Plain, factors specific to this field that may have limited maize yield, simulation studies using crop models did not identify specific variables that may have limited the yield of the treatments (Orfanou et al., 2020b). The work described in this paper clearly shows that increased fertilizer application rates resulted in increased NPS pollution that was somewhat tempered by adopting cover crops, conservation tillage, and lower irrigation water application rates. Nevertheless, if growers in southern Georgia, southeastern Alabama, and northern Florida pursue higher maize yields through higher fertilizer applications, both surface and groundwater resources may see increased concentrations of nutrients.

Table 2.1 Management practices used during each of the project's three years.

Operation	Year					
	2016		2017		2018	
	C_E	C_G	C_E	C_G	C_E	C_G
Tillage	Conventional		Conservation		Conservation	
Soil core sampling	22 Feb		6 Feb		5 Feb	
Maize planting date	16 Mar		21 Mar		28 Mar	
Maize harvest dates	19 Aug		29 Aug		22 Aug	
Variety	P1794VYHR		P1794VYHR		P1794VYHR	
Plant density (plants ha^{-1})	79000	79000	79000	79000	79000	97850
Irrigation SWT threshold (kPa)	<35		<35		<35	
Irrigation application rate (mm h^{-1})	71		36		36	
Total irrigation applied (mm)	408		235		261	
Cover crop planting date	4 Nov, Wheat		27 Oct, Rye		28 Nov, Wheat	
Cover crop termination	14 Feb 2017		19 Feb 2018		22 Apr 2019	
Fertilizer Applications	Date and application rate in kg N ha^{-1}					
Pre-plant fertilizer (granular)	15 Mar, 110	15 Mar, 110	15 Mar, 90	15 Mar, 90	22 Mar, 30	22 Mar, 64
At planting fertilizer (liquid)	16 Mar, 47	16 Mar, 47	21 Mar, 48	21 Mar, 48	28 Mar, 48	28 Mar, 48
Side-dress fertilizer(liquid)	8 Apr, 100 25 Apr, 100	8 Apr, 110 25 Apr, 230	13 Apr, 123 21 Apr, 123	13 Apr, 123 21 Apr, 63 2 May, 63 12 May, 63 26 May, 63 2 Jun, 27	24 Mar, 112 8 May, 56 23 May, 56	24 Mar, 112 8 May, 56 23 May, 112 5 Jun, 112
Cover crop fertilizer application	4 Nov, 34		27 Oct, 34		28 Nov, 34	

Table 2.2 Total water received through rainfall and irrigation and number of samples collected.

Year	Tillage	Rainfall (mm)	Irrigation (mm)	Groundwater samples	Runoff samples
1	Conventional	1070	408	285	293
2	Conservation	1034	235	238	76
3	Conservation	1591	261	409	171

Table 2.3 Water lost through runoff due to rainfall or irrigation during maize cropping periods.

Trt	Block	Runoff (%)					
		2016		2017		2018	
		Rainfall	Irrigation	Rainfall	Irrigation	Rainfall	Irrigation
C_G	W1	6.86%	0.50%	5.12%	0.09%	7.75%	2.68%
	W3	29.02%	1.42%	8.23%	0.90%	10.94%	2.64%
	E2	21.37%	6.62%	1.42%	0.21%	6.66%	1.23%
C_E	W2	16.14%	0.92%	5.47%	0.16%	5.71%	0.78%
	E1	10.67%	3.30%	3.66%	0.00%	6.67%	1.89%
	E3	27.36%	10.46%	2.69%	0.59%	12.96%	4.65%

Table 2.4 Annual cumulative loads of TSS, TN, NO_3-N, NH_4-N, TP and PO_4-P in surface runoff. Volume and loads are reported in terms of unit area because the six blocks varied in size. Means followed by different letters between treatments and within the same treatments between years are significantly different ($p<0.05$) for $\alpha=0.05$ and **$\alpha=0.1$**.

Trt	Blocks	Year	Runoff (m^3 ha^{-1})	TSS (kg ha^{-1})	TN (kg ha^{-1})	NO_3-N (kg ha^{-1})	NH_4-N (kg ha^{-1})	TP (kg ha^{-1})	PO_4-P (kg ha^{-1})
By year									
C_E	W2	1	3600	625.6	6.6	3.1	0.4	3.8	1.5
		2	290	35.1	0.6	0.4	0.0	0.2	0.4
		3	1300	239.1	1.5	1.2	4.4	0.8	0.7
		Total	5190	899.8	8.7	4.7	4.8	4.8	2.6
	E1	1	3200	1156.4	8.4	3.0	0.5	5.5	2.4
		2	180	45.1	0.3	0.3	0.0	0.2	0.3
		3	880	114.3	1.1	1.2	4.0	0.5	0.8
		Total	4260	1315.8	9.8	4.5	4.5	6.2	3.5
	E3	1	4100	1235.6	10.3	2.4	0.5	6.7	1.0
		2	190	13.1	0.5	0.2	0.0	0.1	0.2
		3	1700	259.5	1.7	1.8	4.0	0.6	1.1
		Total	5990	1508.2	12.5	4.4	4.5	7.4	2.3
	Treatment	1	3633^a	1005.9^a	8.4^a	2.8^a	0.5^b	5.3^a	1.6^a
		2	220^b	31.1^b	0.5^b	0.3^c	0.0^c	0.2^b	0.3^b
		3	1293^c	204.3^b	1.4^b	1.4^b	4.1^a	0.6^b	0.9^{ab}
		Total	5146	1241.3	10.3	4.5	4.6	6.1	2.8

Trt	Blocks	Year	Runoff (m^3 ha^{-1})	TSS (kg ha^{-1})	TN (kg ha^{-1})	NO_3-N (kg ha^{-1})	NH_4-N (kg ha^{-1})	TP (kg ha^{-1})	PO_4-P (kg ha^{-1})
C_G	W1	1	1900	332.4	3.9	0.9	0.4	2.0	0.5
		2	280	29.3	0.6	0.5	0.0	0.4	0.4
		3	1000	87.6	1.4	0.8	1.3	0.7	0.6
		Total	3180	449.3	5.9	2.2	1.7	3.1	1.5
	W3	1	4100	1245.5	11.2	2.3	1.2	7.7	1.4
		2	470	43.1	1.4	0.8	0.0	0.8	0.7
		3	1900	351.5	2.8	2.0	3.9	1.2	1.1
		Total	6470	1640.1	15.4	5.1	5.1	9.7	3.2
	E2	1	3300	1898.5	11.7	4.3	0.5	8.0	3.2
		2	76	17.4	0.2	0.1	0.0	0.1	0.1
		3	910	259.7	0.8	1.0	4.8	0.3	0.6
		Total	4286	2175.6	12.7	5.4	5.3	8.4	3.9
	Treatment	1	3100^{a}	$1158.8^{a\ \mathbf{a}}$	8.9^{a}	2.5^{a}	$0.7^{ab\ \mathbf{b}}$	5.9^{a}	1.7^{a}
		2	275^{b}	$29.9^{a\ \mathbf{b}}$	0.7^{b}	0.5^{a}	$0.0^{b\ \mathbf{b}}$	0.4^{b}	0.4^{a}
		3	1270^{b}	$232.9^{a\ \mathbf{ab}}$	1.7^{b}	1.3^{a}	$3.3^{a\ \mathbf{a}}$	0.7^{b}	0.8^{a}
		Total	4645	1421.6	11.3	4.3	4	7	2.9
By treatment									
C_E			5146^{a}	1241.3^{a}	10.3^{a}	4.5^{a}	4.6^{a}	6.1^{a}	2.8^{a}
C_G			4645^{a}	1421.6^{a}	11.3^{a}	4.3^{a}	4^{a}	7^{a}	2.9^{a}

Table 2.5 Percentages of surface runoff compared to the total amount of water received and TN and TP lost through surface runoff compared to the amount of fertilizer received each year of the project. Means followed by different letters between treatments and within the same treatments between years are significantly different ($p<0.05$) for $\alpha=0.05$ and **$\alpha=0.1$**.

Trt	Plot	Year	Runoff (%)	TN (%)	TP (%)
By year					
C_E	W2	1	24.7	6.8	9.3
		2	2.3	0.4	0.7
		3	7.0	1.4	2.5
		Mean	11.33	2.87	4.17
	E1	1	22.3	6.1	7.0
		2	1.4	0.2	0.4
		3	4.9	1.0	2.2
		Mean	9.53	2.43	3.20
	E3	1	27.2	5.6	4.5
		2	1.4	0.4	0.4
		3	9.1	1.4	3.0
		Mean	12.57	2.47	2.63
	Mean	1	24.7^{a}	$6.2^{a\ \mathbf{a}}$	7^{a}
		2	1.7^{c}	$0.4^{b\ \mathbf{c}}$	0.5^{b}
		3	7^{b}	$1.3^{b\ \mathbf{b}}$	2.5^{b}

Trt	Plot	Year	Runoff (%)	TN (%)	TP (%)
C_G	W1	1	12.4	1.6	0.7
		2	2.2	0.3	0.5
		3	5.3	0.6	0.8
		Mean	6.63	0.83	0.67
	W3	1	27.7	5.0	2.3
		2	3.7	1.0	1.1
		3	9.9	1.7	2.4
		Mean	13.77	2.57	1.93
	E2	1	22.4	7.7	5.2
		2	0.6	0.1	0.1
		3	4.9	0.4	1.0
		Mean	9.30	2.73	2.10
	Mean	1	20.8^{a}	$4.8^{a\ \mathbf{a}}$	2.7^{a}
		2	2.2^{b}	$0.4^{a\ \mathbf{b}}$	0.6^{a}
		3	6.7^{b}	$0.9^{a\ \mathbf{b}}$	1.4^{a}
By treatment					
C_E			11.1^{a}	2.6^{a}	3.3^{a}
C_G			9.9^{a}	2^{a}	1.6^{a}

Table 2.6 CEC levels at various depths for each block and sampling events. Means followed by different letters between treatments and within the same treatments between years are significantly different ($p<0.05$) for $\alpha=0.05$ and **$\alpha=0.1$**.

Depth (mm)	Date	CEC (cmol(+) kg^{-1})					
		C_E			C_G		
		W2	E1	E3	W1	W3	E2
0-150	Feb 2016	$3.3^{d\ \mathbf{d}}$	3.7^{b}	4^{cd}	3.4^{b}	4.2^{b}	$3.8^{cd\ \mathbf{c}}$
	Sep 2016	$3.9^{cd\ \mathbf{cd}}$	4^{b}	4.1^{cd}	4.5^{b}	4.8^{b}	$4^{bc\ \mathbf{c}}$
	Feb 2017	$6^{ab\ \mathbf{b}}$	4.4^{b}	5.6^{b}	4.4^{b}	5.4^{b}	$5^{b\ \mathbf{b}}$
	Sep 2017	$5.9^{bc\ \mathbf{bc}}$	4.7^{b}	5.2^{bc}	4.8^{b}	5.7^{b}	$4.3^{bc\ \mathbf{bc}}$
	Feb 2018	$4^{cd\ \mathbf{cd}}$	3.6^{b}	3.4^{d}	4^{b}	5.1^{b}	$2.7^{d\ \mathbf{d}}$
	Sep 2018	$7.6^{a\ \mathbf{a}}$	8.4^{a}	7.5^{a}	7^{a}	8.1^{a}	$6.9^{a\ \mathbf{a}}$
150-300	Feb 2016	$3.5^{c\ \mathbf{c}}$	3.7^{b}	$4.5^{ab\ \mathbf{abc}}$	$3.9^{bc\ \mathbf{bc}}$	4.1^{b}	3.3^{c}
	Sep 2016	$4^{bc\ \mathbf{bc}}$	3.8^{b}	$4.1^{b\ \mathbf{bc}}$	$4.3^{bc\ \mathbf{b}}$	4.4^{b}	3.6^{c}
	Feb 2017	$4.9^{b\ \mathbf{b}}$	4.3^{b}	$5.6^{a\ \mathbf{a}}$	$4.2^{bc\ \mathbf{bc}}$	4.9^{b}	4.6^{b}
	Sep 2017	$4^{bc\ \mathbf{c}}$	4.2^{b}	$3.6^{b\ \mathbf{bc}}$	$4.3^{b\ \mathbf{b}}$	4.6^{b}	4.5^{c}
	Feb 2018	$3.7^{c\ \mathbf{c}}$	3.8^{b}	$3.4^{b\ \mathbf{c}}$	$3.1^{c\ \mathbf{c}}$	3.9^{b}	3.5^{c}
	Sep 2018	$6.4^{a\ \mathbf{a}}$	5.7^{a}	$4.7^{ab\ \mathbf{ab}}$	$6.3^{a\ \mathbf{a}}$	7.9^{a}	5.7^{a}
300-450	Feb 2016	$4.6^{abc\ \mathbf{bc}}$	$3.8^{a\ \mathbf{b}}$	$3.6^{ab\ \mathbf{bc}}$	4.8^{ab}	$4.7^{a\ \mathbf{ab}}$	3.9^{bc}
	Sep 2016	$4.3^{c\ \mathbf{c}}$	$4.7^{a\ \mathbf{ab}}$	$4.1^{ab\ \mathbf{abc}}$	5^{ab}	$4.6^{a\ \mathbf{ab}}$	4.6^{abc}
	Feb 2017	$5.6^{a\ \mathbf{ab}}$	$5.4^{a\ \mathbf{a}}$	$5.3^{a\ \mathbf{a}}$	5.2^{ab}	$5.1^{a\ \mathbf{ab}}$	5.2^{ab}
	Sep 2017	$5.4^{ab\ \mathbf{ab}}$	$4.7^{a\ \mathbf{ab}}$	$4.1^{ab\ \mathbf{abc}}$	4.5^{ab}	$4.8^{a\ \mathbf{ab}}$	4.2^{abc}
	Feb 2018	$4.4^{bc\ \mathbf{c}}$	$4.1^{a\ \mathbf{ab}}$	$3.3^{b\ \mathbf{c}}$	4^{b}	$3.9^{a\ \mathbf{b}}$	3.7^{c}

	Sep 2018	5.6$^{a\ a}$	4.8$^{a\ ab}$	5.2$^{a\ ab}$	5.6^{a}	5.5$^{a\ a}$	5.4^{a}
450-600	Feb 2016	5.3^{ab}	4.4$^{b\ b}$	5.1$^{ab\ abc}$	5.1^{bc}	5$^{b\ b}$	4.9^{b}
	Sep 2016	4.8^{b}	4.8$^{b\ b}$	4.2$^{b\ c}$	5.3^{abc}	5.7$^{ab\ ab}$	5.1^{b}
	Feb 2017	5.4^{ab}	5.1$^{ab\ ab}$	5.7$^{ab\ ab}$	5.8^{ab}	6.3$^{a\ a}$	5.6^{ab}
	Sep 2017	5.4^{ab}	4.8$^{ab\ b}$	4.5$^{b\ bc}$	5.4^{abc}	5.4$^{ab\ b}$	5.1^{b}
	Feb 2018	4.7^{b}	4.9$^{ab\ b}$	6.3$^{a\ a}$	4.7^{c}	5.1$^{b\ b}$	6.5^{a}
	Sep 2018	5.8^{a}	6$^{a\ a}$	4.1$^{b\ c}$	6.2^{a}	6.3$^{a\ a}$	4.8^{b}
600-750	Feb 2016	6.7^{a}	5.4^{a}	6.2^{a}	6.1$^{b\ b}$	6.7^{ab}	5.9^{a}
	Sep 2016	5^{b}	5^{a}	5.2^{b}	5.3$^{c\ c}$	5.3^{c}	4.8^{b}
	Feb 2017	5.5^{b}	5.4^{a}	5.5^{b}	5.8$^{bc\ bc}$	6.3^{b}	5.5^{ab}
	Sep 2017	5.2^{b}	4.9^{a}	5.2^{b}	5.2$^{c\ c}$	5.4^{c}	5.2^{ab}
	Feb 2018	6.4^{a}	5.4^{a}	5.4^{b}	6.9$^{a\ a}$	7.2^{a}	4.9^{b}
	Sep 2018	4.8^{b}	5.2^{a}	5.4^{b}	5.5$^{bc\ c}$	5.5^{c}	5^{b}

Table 2.7 Soil P levels at various depths for each block and sampling events. Means followed by different letters between treatments and within the same treatments between years are significantly different ($p<0.05$) for $\alpha=0.05$ and **$\alpha=0.1$**.

Depth (mm)	**Date**	**P (kg ha^{-1})**					
		C_E			**C_G**		
		W2	**E1**	**E3**	**W1**	**W3**	**E2**
0-150	Feb 2016	108.5^{c}	92.1$^{b\ c}$	68.2$^{bc\ c}$	82.7$^{b\ d}$	74.7$^{b\ b}$	111$^{cd\ cd}$
	Sep 2016	102.2^{c}	94.4$^{b\ c}$	57.3$^{c\ c}$	86.3$^{b\ cd}$	88.9$^{b\ b}$	94$^{cd\ d}$
	Feb 2017	226.23^{b}	161.1$^{b\ bc}$	165.9$^{a\ a}$	157.8$^{b\ bc}$	146.5$^{b\ b}$	210$^{ab\ ab}$
	Sep 2017	213.7^{b}	174.6$^{ab\ ab}$	114.9$^{b\ b}$	163.9$^{b\ b}$	173.7$^{ab\ b}$	176.7$^{bc\ bc}$
	Feb 2018	140.1^{c}	117.4$^{b\ bc}$	71.9$^{bc\ c}$	120.5$^{b\ bcd}$	140.1$^{b\ b}$	79.8$^{d\ d}$
	Sep 2018	324.3^{a}	252.8$^{a\ a}$	183.8$^{a\ a}$	267.6$^{a\ a}$	288.8$^{a\ a}$	279.8$^{a\ a}$
150-300	Feb 2016	138.1$^{bc\ b}$	75.1^{a}	59.6^{b}	91.5^{b}	65$^{ab\ ab}$	106.5$^{ab\ bc}$
	Sep 2016	108.7$^{c\ b}$	68.7^{a}	55.6^{b}	64.7^{b}	54.2$^{ab\ b}$	80$^{b\ c}$
	Feb 2017	220.6$^{ab\ a}$	119.9^{a}	150.6^{a}	113.8^{ab}	99$^{ab\ ab}$	174.5$^{a\ a}$
	Sep 2017	136.7$^{c\ b}$	78.5^{a}	58.9^{b}	102.6^{ab}	73$^{ab\ ab}$	107$^{ab\ bc}$
	Feb 2018	94.5$^{c\ b}$	62.8^{a}	54.4^{b}	67.3^{b}	49.5$^{b\ b}$	61.7$^{b\ c}$
	Sep 2018	241.9$^{a\ a}$	137.6^{a}	59.6^{b}	169.5^{a}	149.8$^{a\ a}$	163.8$^{a\ ab}$
300-450	Feb 2016	26.2^{a}	10.3^{a}	18.2$^{a\ ab}$	12.8^{a}	12.1^{a}	28$^{ab\ ab}$
	Sep 2016	28^{a}	12.1^{a}	32$^{a\ ab}$	12.6^{a}	11.8^{a}	17.8$^{ab\ b}$
	Feb 2017	62^{a}	25.2^{a}	53.8$^{a\ a}$	34.2^{a}	12.3^{a}	43$^{a\ a}$
	Sep 2017	12.1^{a}	7.9^{a}	15.9$^{a\ b}$	7.6^{a}	4.9^{a}	9.3$^{b\ b}$
	Feb 2018	17.8^{a}	12.3^{a}	33.4$^{a\ ab}$	10.1^{a}	5.2^{a}	13.3$^{b\ b}$
	Sep 2018	19.8^{a}	11.2^{a}	17.4$^{a\ b}$	28.3^{a}	15.3^{a}	16.1$^{ab\ b}$
450-600	Feb 2016	4^{a}	4^{a}	9$^{a\ b}$	3.4^{a}	3.6^{a}	5.4^{b}
	Sep 2016	11.2^{a}	4.2^{a}	10.6$^{a\ b}$	3.9^{a}	2.6^{a}	4.3^{b}
	Feb 2017	6.5^{a}	5.6^{a}	22.2$^{a\ ab}$	4.8^{a}	3.7^{a}	8.2^{b}
	Sep 2017	4.1^{a}	3.1^{a}	9.3$^{a\ b}$	3.6^{a}	3.2^{a}	3.7^{b}
	Feb 2018	19.6^{a}	4.5^{a}	33.3$^{a\ a}$	5.6^{a}	4.5^{a}	32.1^{a}

Depth (mm)	Date	P (kg ha^{-1})					
		C_E			C_G		
		W2	E1	E3	W1	W3	E2
	Sep 2018	6.9^{a}	3.9^{a}	9.5^{a} **b**	4.8^{a}	11^{a}	4.5^{b}
600-750	Feb 2016	14.1^{ab}	14.6^{a}	10.1^{ab} **ab**	16.8^{a} **b**	13.9^{ab}	15.2^{b} **b**
	Sep 2016	5.4^{b}	1.7^{b}	3.7^{b} **b**	2^{b} **c**	1.5^{b}	1.7^{d} **d**
	Feb 2017	5.2^{b}	5^{b}	14.2^{ab} **ab**	3.4^{b} **c**	4.5^{ab}	8^{c} **c**
	Sep 2017	3.9^{b}	2.8^{b}	5.8^{b} **b**	2.2^{b} **c**	3.6^{b}	2.4^{cd} **d**
	Feb 2018	39.6^{a}	18.8^{a}	20.2^{a} **a**	27.2^{a} **a**	18.3^{a}	21.3^{a} **a**
	Sep 2018	4.1^{b}	1.4^{b}	7.3^{ab} **a**	2^{b} **c**	11^{ab}	3^{cd} **cd**

Figure 2.1 C_E (light green) and C_G (dark green) fertilization treatments, location of the drain tiles outlets with blue lines. Sampling points for groundwater and runoff. Blocks of NESPAL field.

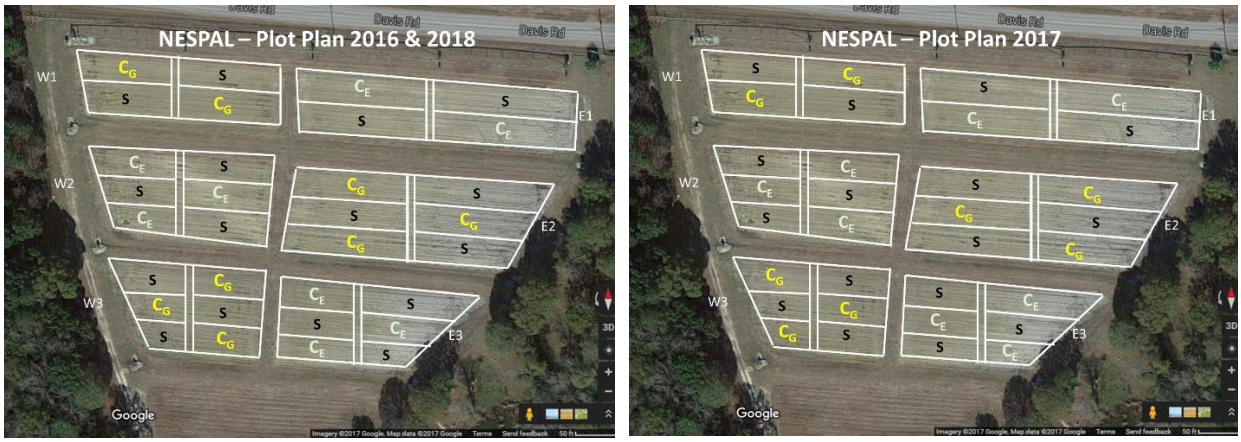

(a) (b)

Figure 2.2 Plot plans of NESPAL field during the (a) 2016 and 2018, and (b) 2017 maize growing seasons.

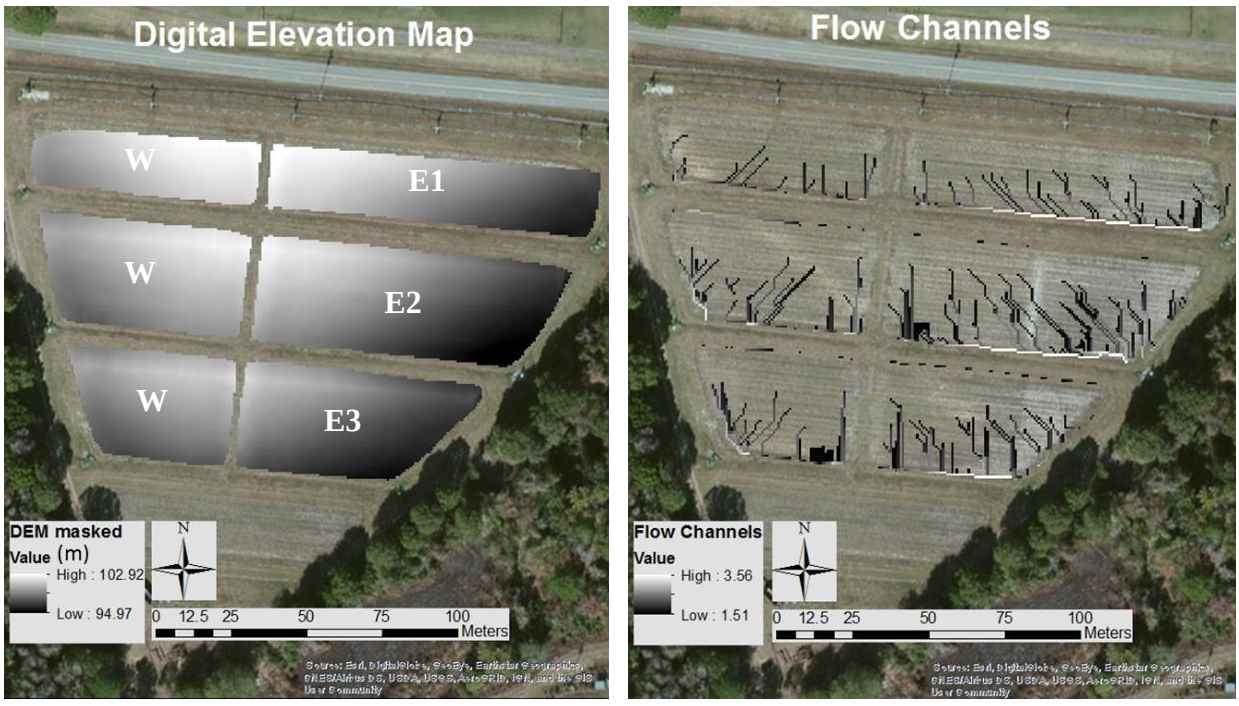

(a) (b)

Figure 2.3 (a) Digital Elevation Model and (b) flow channels of NESPAL field.

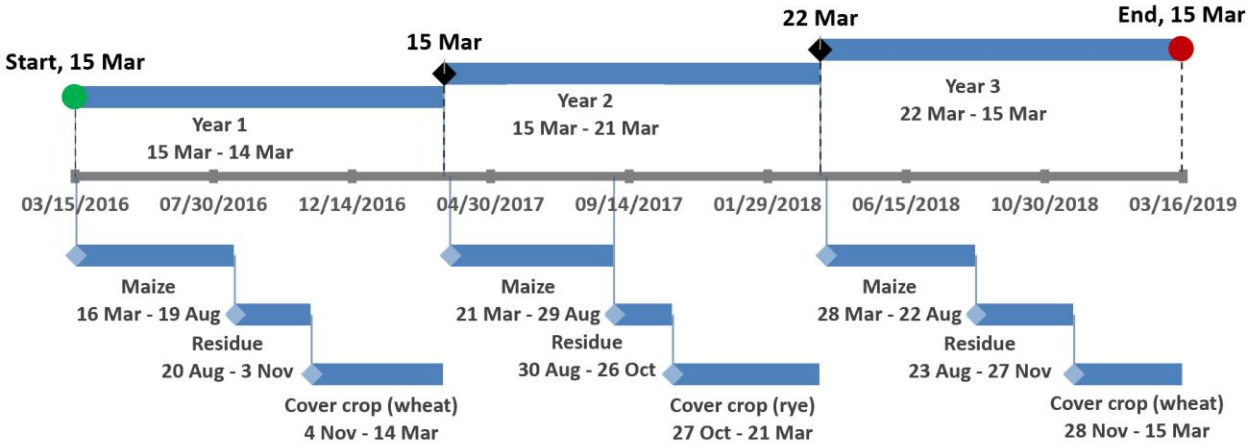

Figure 2.4 Project timeline, showing the beginning and end of the project, and the dates and duration of maize, fallow and cover crops.

(a) (b)

Figure 2.5 (a) Equipment used for flow proportional runoff sampling and (b) pressure transducer.

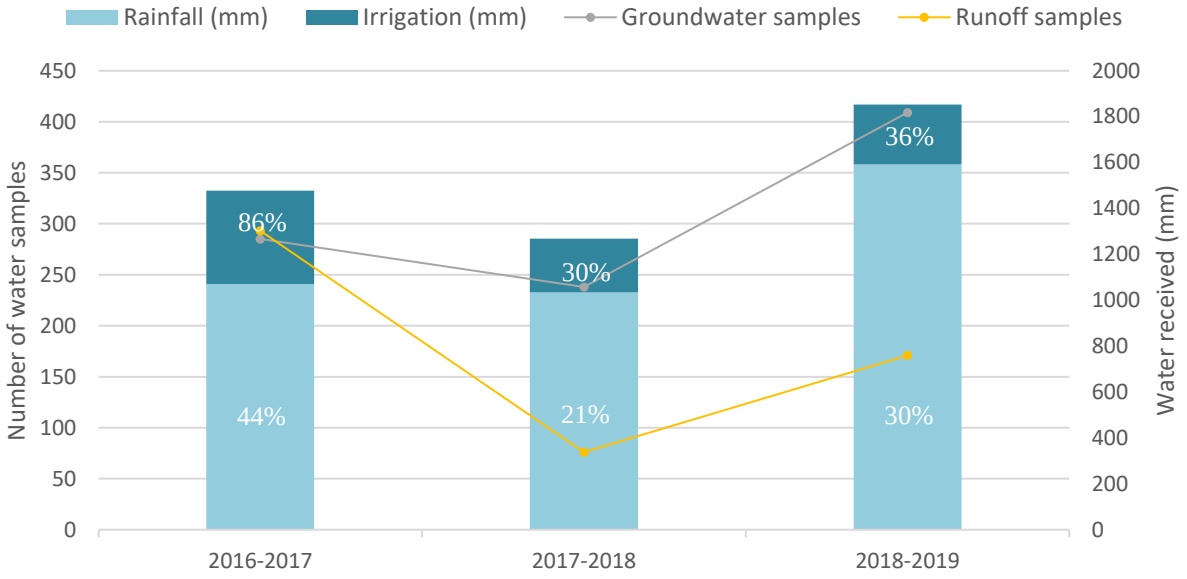

Figure 2.6 Total number of ground water and runoff samples collected in correlation to total water received either through rainfall or irrigation per year of the project.

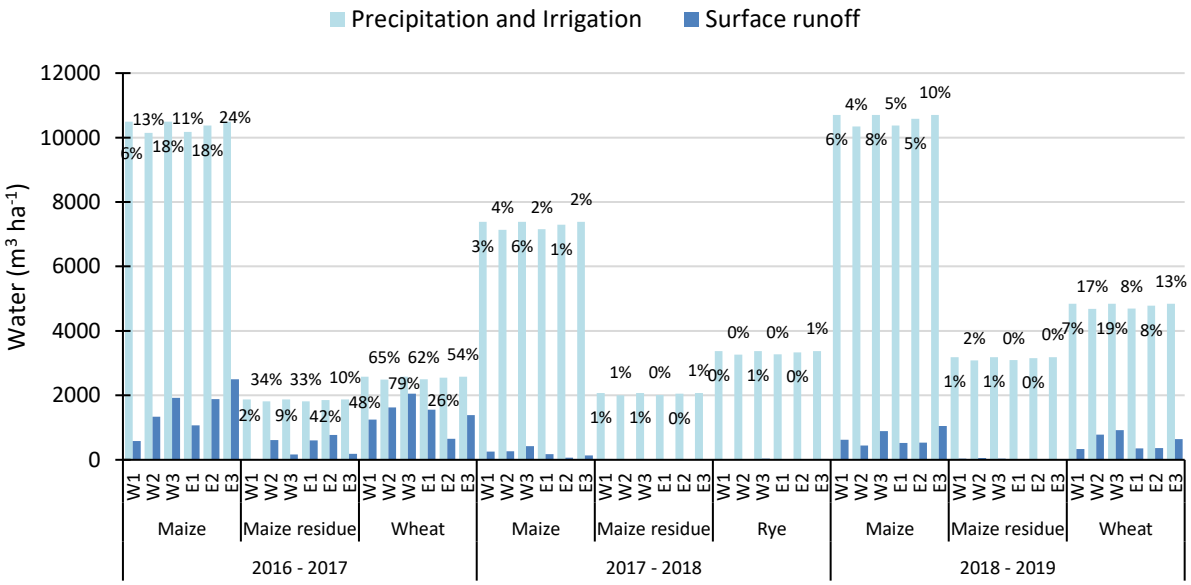

Figure 2.7 Volume and percent of precipitation and irrigation lost to surface runoff per block and cropping period.

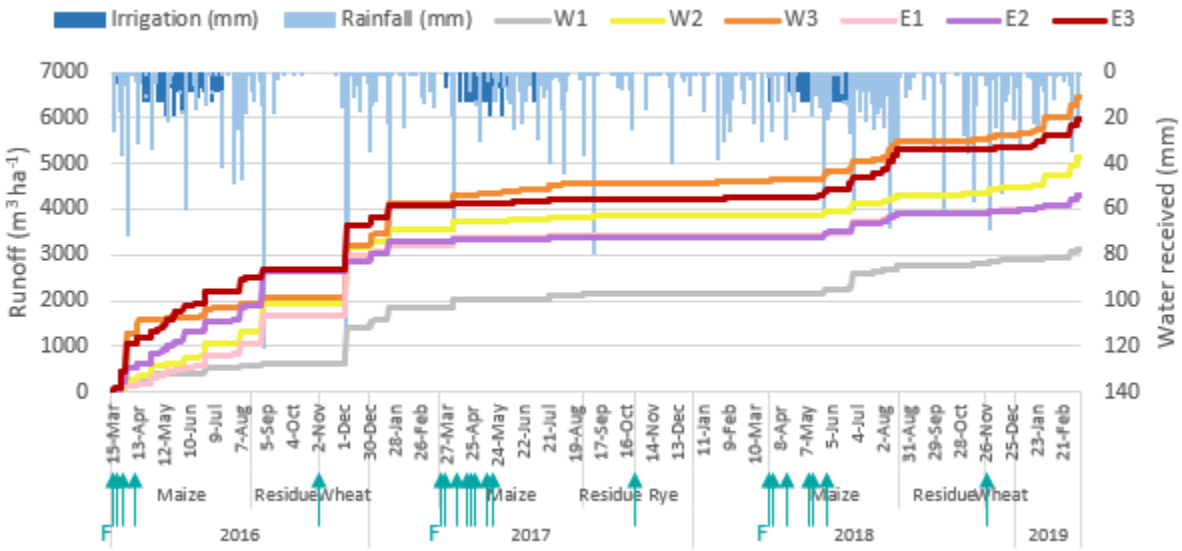

Figure 2.8 Cumulative surface runoff per block, total amount of irrigation and rainfall received.

Arrows indicate fertilization events.

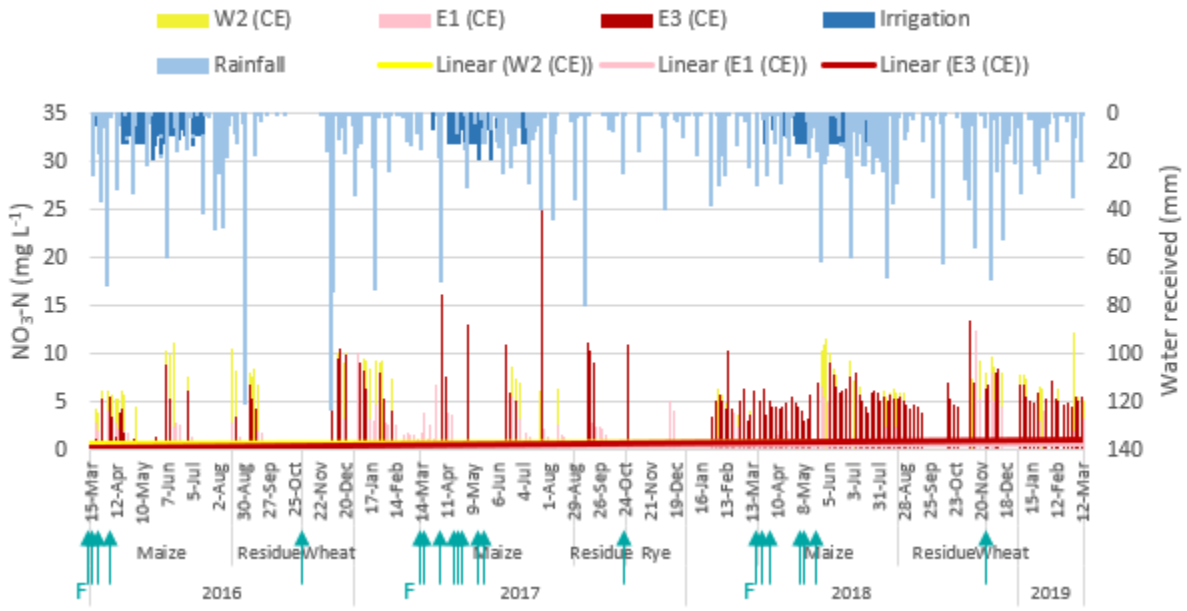

(a)

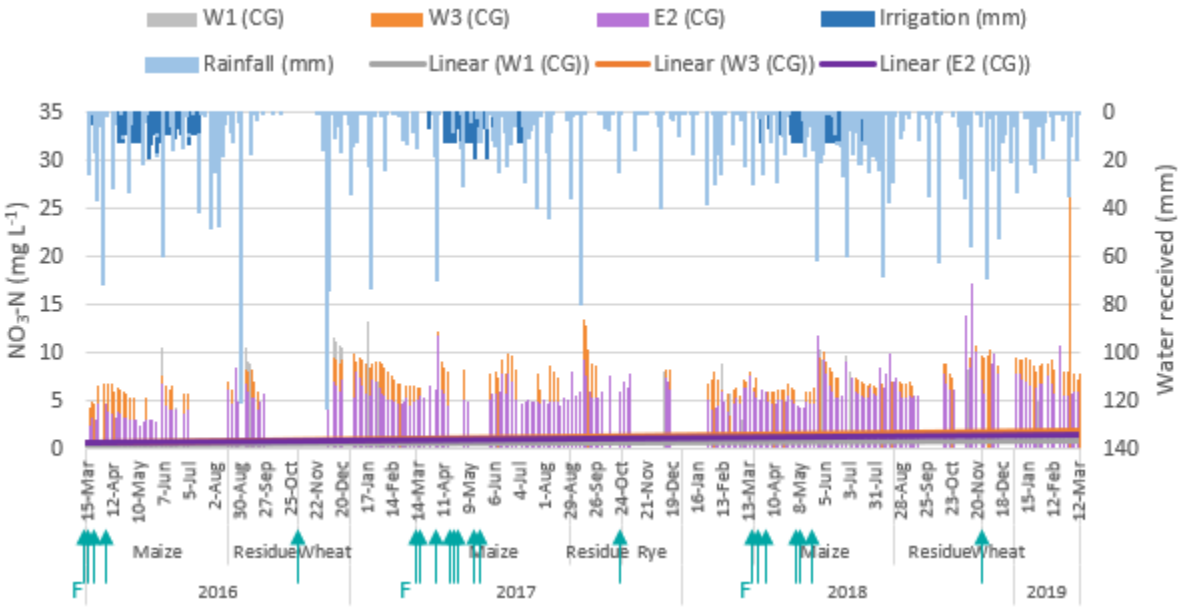

(b)

Figure 2.9 NO_3-N concentration in groundwater, total amount of irrigation and rainfall received for the (a) C_E treatment and the (b) C_G treatments. Arrows indicate fertilization events.

CHAPTER 3

APPLICATION OF HYDRUS-1D MODEL FOR SIMULATING WATER FLOW AND NO_3-N SOLUTE TRANSPORT IN MAIZE[2]

[2] Pavlou, D., A. Orfanou, M.L. Cabrera, G. Hoogenboom, W.M. Porter, D.E. Radcliffe, and G. Vellidis. To be submitted to *Agricultural Water Management*.

Abstract

Simulation models have become essential tools that provide insights on how an agricultural production system responds to management practices. The goal of this study was to use the HYDRUS-1D model to simulate water flow and N leaching losses measured in an experiment conducted in the 1.44 ha NESPAL field located on the University of Georgia's (UGA) Tifton campus. In the experiment, maize was planted in six blocks for three consecutive growing seasons (2016-2018). Two fertilization treatments based on the University of Georgia Extension Service (C_E) and Georgia grower (C_G) recommendations for achieving high yields were used. Experimental data collected from the NESPAL field during 2018 of the study were used to calibrate the HYDRUS-1D model and data from 2016 and 2017 were used to evaluate the model. Correspondence between simulated and observed data was better for the water flow models than the NO_3-N transport models. The simulation results generally fit the trends of the observed data well in in Years 1 and 3 but the model overpredicted the trends in observed data during Year 2. Because it received higher fertilizer rates, it was expected that the C_G treatment would result in greater N leaching than the C_E treatment, but the simulation results indicated no statistically significant differences between treatments. This was primarily because of high variability between blocks of the same treatment. HYDRUS-1D predicted NO_3-N leaching after large precipitation events indicating that irrigation was not a driver of leaching in this landscape. Overall, the HYDRUS-1D model was used successfully to simulate vertical water flow and NO_3-N transport and estimate NO_3-N leaching to groundwater.

Introduction

Fertilizers are applied to soils to provide nutrients that are essential for plant growth. One of the most important and challenging to manage plant nutrients is nitrogen (N). N fertilizers are typically applied as complex dry or liquid compounds. The United Nations Food and Agricultural Organization (FAO) estimates that N fertilizer use exceeded 100 million tons in 2018 – an increase of 25% over the past 10 years (FAO, 2015; Udvardi et al., 2015). Through biological and chemical processes in the soil, these compounds are eventually transformed to nitrate ($NO3^-$) – an ionic form of N that is biologically available to plants. For plants to absorb nitrate, it must be available in the soil solution – the water found in the pores or the soil matrix. Nitrogen use efficiency (NUE) is the fraction of applied N fertilizer that is absorbed and used by the plant. Under field conditions, NUE is at best around 50%. This means that up to 50% of the N applied to soil as fertilizer may be lost to the environment (Udvardi et al., 2015). Excess fertilizer not taken by the crop, can contaminate surface waters and lead to eutrophication (Mueller and Helsel, 1996). Likewise, excess N in the form of $NO3^-$ can leach to groundwater. This occurs because nitrate is highly soluble in water and easily transported below the crop root zone by rain or excess irrigation. Nitrate that leaches below the root zone is lost to the crop.

Maize fertilization

Proper fertilization is a crucial factor for achieving high maize yield and avoiding NPS pollution. Insufficient amounts of N could result in reductions of dry matter allocation and reproductive structures, which negatively influence maize yield (Below et al., 2000; Ding et al., 2005; Monneveux et al., 2005; O'Neill et al., 2004). A general recommendation for maize is to use 1.12 kg N ha^{-1} to 1.35 kg N ha^{-1} for 25.4 kg of expected yield goal (Hollis, 2013).

For many crops such as maize grown in the U.S., up to half of the N required by the crop is applied prior to planting. The remaining N is applied with one or more in-season (also referred to as side-dress) applications. Under these practices, more fertilizer than the crop needs is applied to ensure that nutrients are available throughout the growing season. Under good management, the amount of fertilizer applied is based on soil samples collected prior to planting and/or the farmer's yield goals (Kissel and Sonon, 2008). However, in areas with sandy soils, soil samples are not routinely tested for N because it is assumed that the soils retain little N because of leaching. As a result, the amount of N fertilizer applied is based only on the farmer's yield goal. In many regions of the country and the world, the amount of N applied before planting and during side-dress events is not directly related to the nutrients available to the crop in the soil solution.

NO_3^- leaching

Management practices, weather conditions, soil type etc. are important factors which affect the NO_3^- losses below root zone (Bouchaou et al., 2008; Cruz-Fuentes et al., 2014; Mehdi et al., 2015; Menció et al., 2016; Tagma et al., 2009). NO_3^- leaching is considered a worldwide threat (Addiscott and Benjamin, 2006; Karr et al., 2001; Weyer et al., 2001). Concentrations of $NO3^-$ in water are reported in terms of mg L^{-1} of NO3-N. A study that took place on 144 farms in Ontario, Canada, showed that at 23% of the sites, NO3-N concentrations exceeded the U.S. EPA drinking water standard of 10 mg L^{-1} (EPA, 2017a; Rudolph et al., 1998). Twenty-two percent of cultivated areas in Europe have groundwater NO3-N concentrations that exceed the drinking water standard. When maize is cultivated under conventional practices, NO_3-N leaching loads as

high as 100 kg ha^{-1} (Gold et al., 1990b) have been observed. Conservation management practices have the potential to minimizing NO_3^- leaching (Yadav, 1997).

Mathematical tools for simulating NO_3-N transport

HYDRUS-1D (Rassam et al., 2018; Simunek et al., 2008, 2016) is a widely-used water and solute transport simulation model. Li et al. (2014) used HYDRUS-1Dfor evaluating water flow and losses in a direct seeded rice field during two seasons where there were different amount of rainfall and irrigation management. In their study, the simulated pressure heads and vertical fluxes had a good match with observed data. HYDRUS-1D was also used by Tan et al. (2015) for simulating water movement, and N transport and transformations in experimental paddy fields under different irrigation management practices during 2007 and 2008. They concluded that HYDRUS-1D is an efficient tool for the simulation of water and N regime for improving water and N management for sustainable rice production. Saso et al. (2012) used HYDRUS-1D for simulating field measured chloride (Cl^-) leaching and near-surface soil water content in a Guelph loam and a Maryhill loam, planted with maize. The simulation accurately predicted Cl^- leaching and the timing of losses for both soil types. The model also predicted shallow soil water content well in the Maryhill loam during the early part of the growing season but it under-estimated shallow soil water content during the latter half of the growing season. The model overestimated soil water content in the Guelph loam. Tafteh and Sepaskhah (2012) used HYDRUS-1D for simulating water and NO_3^- leaching in rapeseed and maize fields. More specifically, in their experiment, different urea rates and variable and fixed alternate furrow irrigation and continuous furrow irrigation were applied. Their results indicated that HYDRUS-1D accurately simulated deep percolation and NO_3^- leaching for both rapeseed and maize.

However, the model did not predict crop N uptake well. This was explained as resulting from excluding root N uptake in the measured values and not including N mineralization, denitrification and microbial immobilization processes.

Goals and objectives

The goal of this study was to use the HYDRUS-1D model to evaluate the effect of high-yield maize management system practices on water flow and solute transport in the soil profile. Specific objectives were to simulate soil water flow through the soil profile, simulate NO3-N concentrations in leachate leaving the soil profile, and estimate N loads lost through leaching.

Materials and methods

Field experiment description

This work was based on a field experiment conducted at the 1.44 ha NESPAL field located on the University of Georgia's (UGA) Tifton campus (31° 28.736'N, 83° 31.916'W). The three-year experiment, beginning in 2016 and ending in 2018, was conducted to evaluate the effect of high fertilization rates on maize yield and water quality. Tifton is located in the southeastern coastal plain of the USA. The climate is subtropical providing abundant rainfall and a long growing season. Average annual precipitation for the study period was 1210 mm.

For the field experiment, the NESPAL field was divided into six blocks of cultivated land separated by grassed berms to prevent overland flow between blocks. The three western blocks were labeled W1, W2, and W3 and the three eastern blocks were labeled E1, E2, and E3 as shown in Figure 3.1. Block size ranged from 0.18 ha to 0.34 ha.

The soil type in blocks W1, W2, and W3 and the western half of blocks E1, E2, E3 is a Tifton loamy sand with 2 to 5 % slope. The soil type in the eastern half of blocks E1, E2, E3 is

an Alapaha loamy sand with 0 to 2% slope. There is a visible color difference between the two soil types that can be seen in Figure 3.1. Tifton loamy sand is described by the NRCS Soil Survey as deep, well drained, and commonly found on ridgetops and hillsides. This soil is low in natural fertility and organic matter and very strongly acid. Alapaha loamy sand is described as deep, poorly drained nearly level soil found along the upper part of drainage ways. This soil is low in natural fertility and organic matter and very strongly acid.

Two maize fertilization treatments based on high maize yield goals were used in the field experiment. The first was a treatment recommended by Georgia maize producers who have consistently achieved high yields. This treatment was designated as C_G and had a yield goal of 28 Mg ha^{-1} (450 bu ac^{-1}). The second treatment used the UGA Extension high yield goal of 22 Mg ha^{-1} (350 bu ac^{-1}) and was designated as C_E. There were three replicates of each treatment.

Table 3.1 presents the management practices used during each year of the project. These are pertinent to the modeling scenarios that are described below. Because instrumentation was being installed prior to the planting of the first maize crop which resulted in soil disturbance, conventional tillage was used for the 2016 growing season. A cover crop and strip tillage were used for the remaining two years of the study. Plant density was the same for the two first years of the project but increased to 97850 plants ha^{-1} for the C_G treatment in 2018. More fertilizer side-dress events were used in 2017 and 2018 than in 2016. Pavlou et al. (2020a) described the field experiment in detail.

Data collection

Soil data

Four to six 750 mm soil cores were collected before planting and after the maize was harvested from block depending on size. Each core was separated into five 150 mm segments (482 cm^3) for analysis that included bulk density, soil texture, and NH_4-N and NO_3-N concentrations. Samples were dried at a temperature of 100^oC and its mass was used to calculate bulk density (BD) in units of g cm^{-3} was estimated (Eq. 1). The samples were also analyzed for soil texture by following the Bouyoukos hydrometer method (Bouyoucos, 1962). NH_4-N and NO_3-N concentrations were measured using KCL-Cadmium reduction method by flow injection analysis. The soil texture and bulk density were used in the simulation models for estimating the soil hydraulic parameters with Rosetta Lite v.1.1 which is a neural network model for estimating soil hydraulic parameters with hierarchical pedotransfer functions that is incorporated into HYDRUS-1D. The NH_4-N and NO_3-N concentrations were used in the initial conditions of the soil profile.

$$\mathrm{BD} = \frac{\text{Dry soil weight}}{\text{Soil volume}} \qquad \text{Eq. 1}$$

At the beginning of each growing season, soil moisture sensor nodes were installed in each block during the growing season. Nodes contained Watermark® soil moisture sensors (Irrometer, Riverside, CA) at depths of 200 mm, 400 mm and 600 mm. Two nodes were installed in blocks W1 and E1 while three nodes were installed in blocks W2, W3, E2 and E3. Soil matric potential was measured hourly. The data were recorded in terms of soil water tension (SWT), the absolute value of matric potential. A daily average volumetric water content was estimated for each block and used in HYDRUS-1D as observed data. The observed data from the 2018

growing season were used for calibrating the soil hydraulic parameters while the data from 2016 and 2017 were used for evaluating model performance.

Irrigation and meteorological data

Irrigation scheduling was based on SWT data at 07:00 AM daily. A weighted average SWT was calculated by applying the SWT readings from the three sensor depths (200 mm, 400 mm and 600 mm) to equation (Eq. 2). The weighting factors β_1, β_2, β_3 varied by crop phenological stage and anticipated root depth at that stage as shown in Table 3.2. In general, as the root system lengthened, more weight was given to the deeper sensors (Orfanou et al., 2019). The weight was adjusted based on the growing degree days. The irrigation threshold was set at 30-35 kPa. This relatively low irrigation threshold was established because with sandy soils, SWT increases sharply after 35 kPa as plant available soil water is rapidly depleted. To avoid large SWT values and the associated crop water stress, the entire field was irrigated when the weighted SWT of at least one block was in the range of 30-35 kPa.

$$\text{SWT Weighted Average} = \beta_1 * \text{SWT}_{200\text{mm}} + \beta_2 * \text{SWT}_{400\text{mm}} + \beta_3 * \text{SWT}_{600\text{mm}} \quad \text{Eq. 2}$$

Where,

β_1, β_2 and β_3 are the weighting factors based on the phenological stage of the maize as reported in Table 3.2.

Daily meteorological data, i.e., minimum and maximum air temperature (^{o}C), solar radiation (MJ m^{-2}), relative humidity (%) and wind speed (m s^{-1}) were retrieved from the Tifton campus University of Georgia Weather Network (UGAWN) weather station which was

approximately 1.5 km from the field. Sunshine (hr) was retrieved from the Weather Atlas webpage. Precipitation was measured with an automated tipping bucket rain gage located approximately 100 m from the field. Irrigation data and meteorological and were used to define the boundary and meteorological conditions in the simulation models.

Maize growth data

Maize crop height and leaf area were measured during the V3, V4, V5, V6, V7, V8, V10, V12, V14, VT vegetative stages and the R1, R2, R3, R4, R5 and R6 reproductive stages during the 2018 growing season (Orfanou et al., 2020a). Leaf area was used to estimate the Leaf Area Index (LAI). Crop height and LAI were used in HYDRUS-1D to separate potential evapotranspiration (PET) into evaporation and transpiration.

Groundwater data

Groundwater was captured by installing drain tile along the western, southern, and eastern boundaries of each block (Figure 3.1) prior to the 2016 growing season. The drain tile also isolated the blocks from any shallow groundwater moving laterally from higher positions of the landscape. Blocks W1 and E1 were located at the top of the slope and are unlikely to receive shallow groundwater flows from the north (top of the figure). The circled "G" indicates where the drain tile was sampled to collect the ground water samples from each block. Groundwater samples were collected manually twice per week in 1 L plastic bottles when there was flow.

Groundwater samples were collected manually twice per week in 1 L plastic bottles when there was flow. The first sample was collected after the first fertilizer application in 2016 and the last was collected on final day of the project. The samples were analyzed for NO_3-N and NH_4-N

by a commercial laboratory. The NO_3-N and NH_4-N concentrations were used as observed data in the simulation models for calibrating the solute transport parameters.

Model description

HYDRUS-1D is a public domain windows-based modeling environment for analysis of water flow and solute transport in variably saturated porous media. This model was developed to simulate the vertical movement of soil water, solute and heat while it neglects the fluxes in the horizontal direction. HYDRUS-1D was chosen in this study to simulate water flow and solute transport since it has been used with success in other research studies (Li et al., 2014; Ramos et al., 2011). A graphical representation of the setup of the model is shown in Figure 3.2.

Soil water flow was simulated from the date that fertilizer was applied prior to planting maize until harvest during each growing season. Simulations were not conducted during the period between maize crops because soil moisture sensors were not installed during that time and data were not available for calibrating and evaluating the models during those periods. Solute transport was simulated from the day that the soil core samples were collected in February until harvest. Simulation of solute transport began earlier than because groundwater samples were collected throughout the project period. The start and end dates of the three simulation periods are shown in Table 3.3. Because of differences in soil texture, elevation, and yield, for modeling purposes, each block was treated as a different field. Consequently, models for soil water flow and solute transport were run individually for each block. This resulted in calibrating and validating six soil water flow and six solute transport models. To match the soil cores, the soil profile was set at 750 mm with five soil materials or layers each 150 mm in depth. The soil profile was separated into 101 nodes with 1 mm density at the top.

Soil water flow

The Richards equation (Eq. 3) governs variably saturated water flow in the unsaturated zone (Richards, 1931). The equation accounts for the effect of capillarity and gravity on water movement.

$$\frac{\partial \theta(h)}{\partial t} = \frac{\partial}{\partial z}\left[K(h) \cdot \left(\frac{\partial h}{\partial z} + 1\right)\right] - Q(h) \quad \text{Eq. 3}$$

Where,

θ is the volumetric soil water content ($cm^3\ cm^{-3}$),

h is the pressure head (cm),

t is the time (day)

z is the gravitational potential head (cm),

K is the hydraulic conductivity ($cm\ day^{-1}$), and

Q is the root water uptake ($cm\ day^{-1}$)

Initial conditions in the Richards equation were specified in terms of pressure head (Eq. 4).

$$h(z, t) = h_i(z, 0) \quad \text{Eq. 4}$$

Where,

h_i are the initial values for pressure head (cm)

Water flow parameters

The water retention curve was defined using the van Genuchten-Mualem model (van Genuchten, 1980) (Eq. 5) with a non-hysteretic approach.

$$\theta(h) = \begin{cases} \theta_r + \dfrac{\theta_s - \theta_r}{[1 + (-\alpha h)^n]^m} & h < 0 \\ \theta_s & h \geq 0 \end{cases} \quad \text{Eq. 5}$$

Where,

θ_s is the saturated water content (cm^3cm^{-3}),

θ_r is the residual water content (cm^3cm^{-3}),

α (cm^{-1}), m (dimensionless), and n (dimensionless) are empirical parameters and it is assumed that

$$m = 1 - \frac{1}{n} \quad \text{Eq. 6}$$

The unsaturated hydraulic conductivity function was described by the van Genuchten (1980) equation:

$$K(h) = K_s \left| \frac{\theta(h) - \theta_r}{\theta_s - \theta_r} \right|^{0.5} \left(1 - \left\{ 1 - \left| \frac{\theta(h) - \theta_r}{\theta_s - \theta_r} \right|^{1/m} \right\}^m \right) \quad \text{Eq. 7}$$

Where,

K_s is the saturated hydraulic conductivity (cm day^{-1}),

Rosetta Lite v.1.1 (Schaap et al., 2001) is a neural network model for estimating soil hydraulic parameters with hierarchical pedotransfer functions that is incorporated into HYDRUS-1D. It was used to estimate soil hydraulic properties (θ_s, θ_r, α, n and K_s) that were not measured experimentally. The first function, based on textural classes, contains a table for average hydraulic parameters for each textural class, while the other four are based on neural network analysis (Schaap et al., 1998) and use more input variables. In this project, the third function was used, which includes the percentage of sand, silt and clay along with the bulk density of the core samples that were collected. The texture and bulk density data of each soil layer and block are presented in Table 3.4. Table 3.5 presents the hydraulic properties estimated using Rosetta Lite.

Water flow boundary conditions

The upper water flow boundary conditions were set as an "atmospheric boundary with surface runoff". This condition is based on a system-dependent boundary since the potential fluid flux is controlled by external conditions, such as precipitation and evapotranspiration. When the precipitation rate exceeded the infiltration capacity of the soil, surface runoff was generated. This condition was implemented mathematically in HYDRUS-1D by using the Neuman et al. (1974) approach by satisfying two conditions (Eq. 8 and Eq. 9).

$$\left| K(h) \frac{\partial h}{\partial z} + 1 \right| \leq E \qquad \text{Eq. 8}$$

Where,

E is the maximum potential rate of infiltration or evapotranspiration (cm day^{-1})

$$h_A \leq h \leq h_S \quad \text{Eq. 9}$$

Where,

h_A is the minimum pressure head

h_S is the maximum pressure head

Instead of entering atmospheric fluxes into the model, i.e. PET, the PET was separated into evaporation and transpiration in the HYDRUS-1-D model by the input of crop height and LAI. The lower water flow boundary conditions were set as free drainage, which can occur in non-saturated conditions.

Solute transport

Solute transport and reaction parameters

The solute transport component of the HYDRUS-1D model was used to simulate N transport and transformation. Solute transport was estimated by the advection dispersion equation (ADE) (Eq. 10) which involves linear adsorption and chemical equilibrium.

$$\frac{\partial(\theta c + \rho_b K_d c)}{\partial t} = -\frac{\partial}{\partial t}\left(J_w c - \theta D_e \frac{\partial c}{\partial z}\right) - \theta \mu c - Sc \quad \text{Eq. 10}$$

Where,

c is the dissolved concentration of the solute (g cm^{-3})

K_d is the adsorption coefficient (cm^{-3} mg^{-1})

J_w is the flux of water from Darcy's law

D_e is the effective dispersion coefficient (cm^2 day^{-1})

z represents the vertical dimension (cm)

μ is the first-order rate constant for solute transformation processes (day^{-1})

S is any source or sink

Essentially the model simulated a simplified version of the N cycle that included nitrification of NH_4-N to NO_3-N resulting from the application of N fertilizer and the denitrification of NO_3-N to atmospheric N (N_2). Processes such as the mineralization of plant residues, nitrification from NO_2-N to NO_3-N and the volatilization of NH_4-N were not considered. Plant uptake of N was accounted for separately and is described further below. The first-order reaction rate for nitrification and denitrification processes are presented in Eq. 11 and Eq. 12 respectively.

$$\frac{\partial(\mathrm{NH_4 - N})}{\partial \mathrm{t}} = -\mathrm{k}(\mathrm{NH_4 - N}) \qquad \text{Eq. 11}$$

Where,

k is the nitrification coefficient (day^{-1})

$$\frac{\partial(\mathrm{NO_3 - N})}{\partial \mathrm{t}} = -\mathrm{k}(\mathrm{NH_4 - N}) - \mu(\mathrm{NO_3 - N}) \qquad \text{Eq. 12}$$

Where,

μ is the denitrification coefficient (day^{-1})

According to Bradshaw et al. (2013), the initial values of K_d were set at 10 cm^3 g^{-1} for NH_4-N and 0.78 cm^3 g^{-1} for NO_3-N. According to the literature, the initial values of k for all the

soil layers and blocks were set at 0.2 day^{-1} (Hanson et al., 2006). The initial μ values were also set at 0.2 day^{-1}. It was assumed that there was complete denitrification under saturated conditions. The longitudinal dispersivity, λ (cm), for field soils can range from 5-20 cm (Radcliffe and Simunek, 2018). In this study, $\lambda = 20\text{cm}$ gave the best fit.

The water content dependence of degradation coefficients is utilized in HYDRUS-1D by a modified function of Walker (1974) (Eq. 13).

Eq. 13

$$\psi(\theta) = \psi_r(\theta_{ref}) \min\left[1, \left(\frac{\theta}{\theta_{ref}}\right)^B\right]$$

Where,

ψ and ψ_r are the values of the reaction rate constant (day^{-1})

θ is the actual water content

ω_r is the reaction rate constant (day^{-1})

θ_{ref} is the reference water content

B is the solute dependent parameter

Solute transport boundary conditions

The upper solute transport boundary condition was set at concentration flux, while free drainage (zero concentration gradient) was used for the lower boundary conditions.

Root water uptake

The Feddes (1982) water uptake reduction model (Eq. 14) was used with threshold pressure heads selected for maize from a database (Wesseling, 1991). Eq. 14 shows the root

water uptake (Q) as a function of soil water pressure head (h) which is used with threshold pressure heads selected for maize.

$$Q(h) = \alpha(h)Q_p \qquad \text{Eq. 14}$$

Where,

Q_p is the potential water uptake rate, and

$\alpha(h)$ is a dimensionless stress response function of the pressure head ($0<=\alpha<=1$)

Table 3.6 presents the root water uptake parameters for maize (Wesseling, 1991), i.e. the parameters for the water stress response function (Feddes, 1982). Water uptake is assumed to be zero in two cases, close to saturation (h_0) and for pressure heads less than the wilting point (h_3). Water uptake is optimal between h_{Opt} and h_2. The pressure head h_2 can be adjusted based on the transpiration rate (r_2). Water uptake decreases (or increases) linearly with pressure heads when pressure heads are between h_2 and h_3.

Root uptake of solute N

Root nutrient uptake is a combination of passive and active nutrient uptake. In general, passive uptake depends on diffusion mechanisms, which allows ions dissolved in the soil solution to be taken up when the concentration inside the root cell is lower than the external concentration. Active nutrient uptake requires the root cells to spend energy by using the hydrolysis of ATP. The partitioning of passive and active nutrient uptake is controlled by the maximum allowed concentration of root nutrient uptake. When the soil solution concentration values are below the maximum allowed concentration, passive nutrient uptake is simulated by

multiplying the dissolved nutrient concentration with root water uptake. Plants typically take up N in the form of NH_4^+ or NO_3^-. The assimilation of NH_4^+ occurs near the roots and lower amounts of NH_4^+ are absorbed, compared to NO_3^-, for avoiding the toxic effect of high NH_4^+ (Bloom et al., 2012). For that reason, it was assumed that there was no passive root uptake of NH_4^+. Plants can store high NO_3^- concentrations without toxic effect (Bloom et al., 2012). Furthermore, in passive nutrient uptake, it is likely that roots take up all NO_3^- dissolved in water. In HYDRUS-1D, the active nutrient uptake is implemented only for one solute, in this case, NO_3^-. Active nutrient uptake is simulated by using Michaelis-Menten kinetics. Reduced potential solute uptake due to reduced water uptake was selected to provide a more realistic approach to the root nutrient uptake (Šimůnek and Hopmans, 2009).

Input data

Initial conditions

The initial conditions for pressure head in the models varied for each observation node, block and growing season based on the initial average daily readings of the soil moisture sensors. The soil moisture sensors were installed at depths of 200 mm, 400 mm and 600 mm. The value of the sensor located at 200 mm was assumed to be the same for the first 300 mm of the soil profile, the value of the sensor at 400 mm was the same from 300 mm to 500 mm depth. The initial conditions for pressure head from 500 mm to 750 mm depth were the value of the sensor placed at 600 mm.

The initial conditions of NH_4-N and NO_3-N concentrations in the soil profile were based on groundwater samples collected before the start of simulation in each growing season. Measured concentrations were reported in the model in units of g cm^{-3}.

Water and fertilizer

Figure 3.3 shows the SWT readings on the primary y-axis and the water received either through irrigation (light blue bar) or rainfall (dark blue bar) on the secondary y-axis. The red dashed line represents the irrigation threshold of 35 kPa. Figure 3.3(a) shows the data from blocks W1, W3 and E2, the three blocks fertilized with the C_G treatment. Figure 3.3(b) shows the data from W2, E1 and E3 blocks, the three blocks fertilized with the C_E treatment. The total amount of water applied through irrigation and precipitation, during the maize growing seasons, is shown in Table 3.7. The precipitation data are from the Tifton campus UGAWN weather station.

In all three years, fertilizer was applied prior to planting and at planting for both treatments. The number of in-season (side-dress) fertilizer applications varied from year to year and by treatment. In 2016, there were two side-dress applications for both treatments. In 2017, there were two side-dress applications for the C_E treatment and six for the C_G treatment. In 2018, there were three and four side-dress applications for the C_E and the C_G treatments, respectively. The amount of fertilizer applied (g cm^{-2}) was entered into the model in units of g cm^{-3} by dividing amount of fertilizer applied by amount of water flux.

Meteorological conditions

A summary of meteorological data for the project period from the Tifton campus UGAWN weather station are presented in Table 3.8. According to Weather Atlas, the daily period of sunshine (hr) in Georgia is 6.1 hr during February, 7.1 hr during March, 8.7 hr during April, 9.3 hr during May, 9.5 hr during June, 8.8 hr during July and 8.3 hr during August.

Potential evapotranspiration was calculated in HYDRUS-1D with the Penman-Montheith equation (Eq. 15) using parameters related to crop growth (crop height and root depth) and LAI. Crop height and LAI were collected from the field during the growing seasons.

$$ET_0 = \frac{0.408\Delta(R_n - G) + \gamma \frac{900}{T + 273} U_2(e_a - e_d)}{\Delta + \gamma(1 + 0.34U_2)} \quad \text{Eq. 15}$$

Where,

ET_0 is the reference crop evapotranspiration (mm day^{-1})

Δ is the slope of the vapor pressure curve (kPa ^{o}C^{-1})

R_n is net radiation at the crop surface (MJ m^{-2} day^{-1})

G is soil heat flux (MJ m^{-2} day^{-1})

γ is the psychometric constant (kPa ^{o}C^{-1})

T is the average air temperature (^{o}C)

U_2 is the wind speed at 2 m height (m s^{-1})

$(e_a - e_d)$ is the vapor pressure deficit (kPa)

e_a is the saturation vapor pressure at temperature T (kPa)

e_d is the vapor pressure at due point (kPa)

Root estimation

The planting depth was at 40 mm. The maize root depth increased linearly up to a maximum of 1530 mm in 86 days after planting (Mengel and Barber, 1974). This concept was implemented in the model for simulating root depth. The root distribution was simulated in a way that 70% of the roots were included in the top 200 mm of the soil profile while after that point there was a liner decrease for the remaining 30% (Mengel and Barber, 1974).

Inverse solution

Observed data from the 2018 growing season were used for calibrating the models, while observed data from 2016 and 2017 were used for model evaluation. Each block was calibrated and evaluated individually.

Inverse procedures were used for estimating the soil hydraulic and solute transport parameters from specified observed data weighting by standard deviation. Through inverse solution, HYDRUS-1D fits several analytical functions to soil water retention data by searching for new values that will minimize the least square errors of the objective function (Eq. 16) (Radcliffe and Simunek, 2018).

$$F(b) = \sum_{i=1}^{N} \{w_i[\theta_i - \widehat{\theta}_i(b)]\}^2 \qquad \text{Eq. 16}$$

Where,

b is the set of parameter estimates

θ_i observed water content

$\hat{\theta}_i$ is the fitted water content

N is the number of retention data points

w_i is the weighting coefficient

Observation nodes were set at 200 mm, 400 mm and 600 mm based on the depths that the soil moisture sensors were installed. The average daily observation data of the soil moisture sensors were used for performing the inverse solution. The parameters that were calibrated were α, n, and K_s.

Solute transport parameters were calibrated based on the observed data of NO_3-N concentrations measured from groundwater samples. An observation node was set at the bottom of the soil profile (750 mm). The parameters that were fitted were K_d, k and μ.

Statistical analysis

To assess the performance of the model, the experimental data were compared to the simulation results using three statistical indices: the coefficient of determination, mean absolute error (MAE, Eq. 17) and root mean square error (RMSE, Eq. 18).

$$\mathrm{MAE} = \frac{1}{N}\sum_{i=1}^{N}|O_i - P_i| \qquad \text{Eq. 17}$$

Where,

O_i is the observed value for the i measurement,

P_i is the predicted value for the i measurement,

N is the number of field observations

$$\mathrm{RMSE} = \sqrt{\frac{\sum_{i=1}^{N}(O_i - P_i)^2}{N - 1}} \qquad \text{Eq. 18}$$

Results

As described earlier, simulations of soil water flow and solute transport began in March and February, respectively, each year and ended in August. ET, amount of water received through irrigation and rainfall, and solar radiation were the same for all six blocks. Observed and simulated data of pressure head were compared at 200 mm, 400 mm and 600 mm. Observed and simulated data of NO_3-N concentrations were compared at 750 mm. Results are described in detail below.

Meteorological data

ET was estimated based on the Pennman-Monteith equation included in HYDRUS-1-D and is presented in Figure 3.4. HYDRUS-1D also estimates the amount of evaporation and transpiration separately by using measured plant physiological parameters such as height and LAI. Those results are also shown in Figure 3.4. When the plants were small, ET was dominated by evaporation from the soil. As the plants grew and leaf area increased, transpiration became the dominant component of ET. This was especially true after canopy closure. As the plants matured and began to dry down, transpiration was reduced, and evaporation again became the dominant component. ET was lower during the 2018 growing season with a peak rate of approximately 10 mm day^{-1}. In 2016 and 2017, the peak ET rate was approximately 12 mm day^{-1}, respectively. In general, the 2018 growing season was wetter (Table 3.7 and Figure 3.5) with lower total solar radiation (Table 3.8 and Figure 3.6).

Despite the sandy soil, crusting was observed throughout the field during the 2016 growing season because maize was planted using conventional tillage. The crusting resulted in reduced water infiltration and excessive runoff during irrigation and precipitation events. This also resulted in irrigation events not adequately wetting the soil profile as documented by the soil moisture sensor data. The dense cover crop in combination with strip tillage that was used during the 2017 and 2018 growing seasons resulted in irrigation decreasing by 42% in 2017 and 36% in 2018. Although 2018 was a wetter year with 61% more precipitation during the growing season than in 2017, 11% more irrigation water was applied. This may be the result of the higher plant density in the C_G treatment blocks which increased from 79000 to 97850 plants ha^{-1}."

Calibration and validation of water flow parameters

The observed SWT data from 2018 were converted to units of pressure head and used for calibrating the soil hydraulic parameters of each block individually. The initial values of the soil moisture sensors were used to initialize pressure head and therefore, initial values of pressure head differed between blocks and years. When comparisons between the experimental data and the simulation results were satisfactory, the calibrated soil hydraulic parameters were used to validate the models with data from the 2016 and 2017 growing seasons. Calibration and validation was an iterative process that was ended when the statistical indices were considered satisfactory for both calibration and validation runs of the models. The final values of the water flow parameters are shown in Table 3.9 while results of the statistical indices are presented in Table 3.10.

The comparison between simulated and observed data for pressure head is presented in Figure 3.7. The solid lines indicate simulation results at each depth (200, 400, 600 mm) while the

open circles indicate observations. The observations are the average of all pressure head data within a block at a given depth over a 24 hr period. In general, the simulated results matched the trends of the observations well although there were individual blocks and years where the fit between the two were either better or worse than the overall. The results show that even during the years in which cover crops and strip tillage were used; pressure head data indicate a drier profile than simulation results. These sensor data were perplexing even during the growing season when on occasion, soil moisture sensors at 400 and 600 mm did not respond to irrigation events while they responded to comparable precipitation events. This phenomenon has been observed by the authors in several other studies with maize. In this study, the soil moisture sensors were installed in the row and the irrigation sprinklers were on drops and well within the canopy once the corn exceeded 2 m in height. One possible explanation of the phenomenon is that during irrigation events, the corn canopy shed the irrigation water away from the row and towards the furrows between rows. Visual observations of irrigation events tended to support this hypothesis but it was not confirmed with destructive soil sampling. Validation results were better in 2016 than 2017 because there was better fit between simulated and measured pressure head data.

Validation results were better for blocks W2, E1 and E3, i.e. the blocks in which the C_E treatment was applied possibly because the plant density was the same for all three growing seasons. During the 2018 growing season which was used for calibration, the plant density of the C_G treatment was 97850 plants ha^{-1} compared to 79000 plants ha^{-1} in the C_E treatment. However, the difference in LAI_{max} between the two plant densities was less than 1 cm^2 cm^{-2} which did not result in differences in the ET results of the model. This was also observed by Ramos et al. (2011).

The consistent disagreement between experimental and simulated data at 200 mm likely occurred because the pressure head near the soil surface exhibits high inter daily variations because of differing evaporation, transpiration, root extraction rates, and redistribution of soil water during the night. Because the model operated on a daily time step, it used a constant flux for each simulated day.

The results of the indices used to evaluate the fit between the simulations and the experimental data are presented in Table 3.10. The numbers in the table combine the results for all three depths (observation nodes). The two indices used to evaluate the simulation results did not respond uniformly but MAE and RMSE results consistently showed a good fit. MAE and RMSE were used to determine when to terminate the iterative calibration process.

Calibration and validation of solute transport parameters

After the soil hydraulic parameters were calibrated and validated, the next step was the calibration and validation of the solute transport parameters, i.e. the adsorption coefficients K_d, the nitrification coefficients k, and the denitrification coefficients μ using the same iterative approach described earlier. Their final values are presented in Table 3.11.

Figure 3.8 shows the fit between observed concentrations in ground water samples and simulated concentrations at the bottom of the soil profile (750 mm) during each growing season. The open circles represent the concentrations of NO_3-N in groundwater samples (observed data), while the solid lines show the model predictions (simulated data). The number of groundwater observations differ between blocks and seasons because sampling was contingent on flow from the drain tile of each block. With the exception of block E3, fewer samples were collected from the blocks at higher elevations than the blocks at lower elevations. Because the drain tile outlet

of E3 emptied into the pond at the southeastern edge of the field, samples were not collected when the pond level was high to avoid contamination of the samples by surface water.

As described by Pavlou et al. (2020), the concentration of NO_3-N in groundwater samples ranged from 0 mg L^{-1} to approximately 33 mg L^{-1} during the project period. Mean concentrations ranged from 2.46 mg L^{-1} to 8.05 mg L^{-1} and 4.96 mg L^{-1} to 8.14 mg L^{-1} for all blocks of C_E and C_G treatment respectively during each year. This indicates that both fertilization treatments resulted in excessive leaching. The simulation results generally fit the trends of the observed data well in 2018 and 2016 but did not fit the trends in observed data from 2017. Possible explanations for this discrepancy could be the differences in management practices and weather conditions that might have affected model performance. In addition, the model does not simulate important biological processes such as the mineralization of crop residues and soil humus and the nitrification of NO_2-N to NO_3-N that are not simulated by the model.

The 2017 simulation results consistently over-predicted the observed NO_3-N concentrations. The poorest simulations were the models for blocks W2 and E2. A possible explanation for this discrepancy is that the highest amount of N fertilizer was applied during the 2017 growing season (11% and 7% more for C_G treatment, and 7% and 26% more for C_E treatment compared to 2016 and 2018, respectively) and this coincided with drier conditions than in 2016 and 2018. The water received through rainfall and irrigation during the 2017 growing season was 30% and 46% less than the 2016 and 2018 growing seasons, respectively. As a result, fewer ground water samples were collected during 2017 and there were longer periods without samples. The discrepancy between the model results and observations may have been caused by the overall drier conditions. The observed data are groundwater samples collected at the drain tile outlets while the simulated results are from the bottom of the soil profile. If the volume of

leachate leaving the bottom of the soil profile was small (see Figure 3.9 and discussion below), it may not have reached the drain tile or may not have traveled through the drain tile to sampling point.

Table 3.12 presents the results of the indices used to evaluate the fit between the simulations and the experimental data. The results reflect the differences described in Figure 3.8. MAE and RSME are about an order of magnitude larger than those for the soil water flow models but still good for 2016 and 2018.

Water and NO_3-N leaching

Figure 3.9 shows the water flux at the bottom of the simulated soil profile of each block for each year of the project. It is clear from the graphs that the amount of leachate draining below the bottom of the soil profile in 2017 is much less than in 2016 or 2018. Consequently, the discrepancy between the observed data and simulated data in Figure 3.8 can be explained.

The water fluxes are similar for the 2016 and 2018 growing seasons with the exception that in 2018 most leaching occurred late in the growing season while in 2016 it occurred early in the growing season. These patterns match the occurrence of large precipitation events in those years (Figure 3.3). Comparison of Figure 3.9 to Figure 3.3 also indicates that leaching events were driven primarily by precipitation events and not irrigation events. However, a difference that is observed is the period that bottom fluxes took place. In 2018 the main fluxes started after 150 days and finished close to the end of the simulations, while in 2016 the fluxes occurred after the first 50 days and finished at 100 days after the simulations. These peaks in the bottom fluxes, in both years, occurred due to heavy rainfall events that took place close to the day that the peaks

are observed. This means that the precipitation exceeded the water holding capacity of the soil. It is obvious that the bottom fluxes were more affected by rainfall than irrigation events.

Figure 3.10 shows the NO_3-N solute flux at the bottom of the simulated soil profile of each block for the three years of the project. Clearly, the NO_3-N solute flux is a function of the water flux. An interesting observation is that blocks with the same treatments had different solute fluxes indicating that the soil properties and soil moisture measurements directly affected leaching.

In most cases, 2017 had the least cumulative flux while 2016 and 2018 had similar results (Figure 3.11). The shape of the curves is affected by water and solute bottom fluxes and therefore there are periods when the cumulative solute fluxes are relatively stable and periods with steep increases indicating a leaching event. Every steep increase in the curves is the result of precipitation events.

During the 2016 growing season, conventional tillage resulted in much more runoff than in 2017 and 2018. As a result, it was expected that less N would be lost to leaching during 2017 and 2018 compared to in 2016. However, a large increase of solute flux was simulated on the 01 April 2016 (92^{nd} day) caused by a 72 mm precipitation event. This was the largest precipitation event of the entire project period and resulted in a large amount of leachate draining below the simulated soil profile. Furthermore, while the cumulative NO_3-N solute flux in 2018 was similar to that of 2016, in many cases, it was lower. A possible reason for this result is the higher number of fertilizer applications in smaller amounts during 2018.

Table 3.13 presents the simulated loss of N in kg ha^{-1} from leaching and the percent of N lost in leaching compared to total N applied. In general, there is a trend for higher leaching losses from the C_G treatment blocks, apart from W2 block, but there are no significant

differences between treatments. This may have been caused by high leaching loss from block W2 that belongs to the C_E treatment. There are no statistical differences between years.

Discussion and conclusions

The use of simulation models such as HYDRUS-1D is becoming a more common approach for understanding the soil, water, and nutrient interactions of a system because models are inexpensive, detailed, and methodical. Models can provide insights regarding the environmental impact of agricultural practices. Physics based models, meaning models that are based on numerical solutions of the Richards equation can be very beneficial in cases in which there are efforts to understand the movement of water, increase water use efficiency and minimize the risk of leaching. However, to address these issues, as accurately as possible, the models require large inputs of data and complex parameterization. Due to the variability that exists in fields, different weather conditions, soil hydraulic properties, etc., the calibration and evaluation processes are essential and necessary for accurately representing reality.

In this study, soil hydraulic parameters were estimated by using pedotransfer functions included in HYDRUS-1D by providing % of sand, silt and clay, and bulk density. Because these parameters were not measured experimentally, they could be a significant source of error in the simulation results as they are critical in estimating fluxes in the soil profile. Nevertheless, using pedotransfer functions is an accepted practice in simulation modeling. For instance, Espino et al. (1996) used the pedotransfer functions created by Vereecken et al. (1989) to define the soil hydraulic functions of $\theta(h)$ and $K(h)$. Their results showed that the model overpredicted the moisture content but predicted the pressure heads at shallow depths well. Another study conducted by Skaggs et al. (2004) used the pedotransfer functions of HYDRUS-2D in order to

obtain the values of the soil hydraulic parameters for simulating the water content distribution under drip irrigation technology, with good results. Ventrella et al. (2019) used HYDRUS-1D to simulate soil water fluxes in a drip irrigated watermelon cultivation and the values of θ_r and K_s were acquired by using pedotransfer functions. They stated that the values of θ_s, α and n can be obtained successfully with laboratory or field methods described in literature. In this study, the initial soil hydraulic parameters were estimated by applying the soil characteristics of sand (%), silt (%), clay (%) and bulk density, which were acquired from the soil core samples. There are studies which have shown that more input data can produce more accurate predictions (Schaap and Bouten, 1996; Schaap and Leij, 1998). However, the appropriateness of the parameters predicted through the Rosetta Lite v.1.1 depends on accuracy of the collected data.

During the calibration process of the soil hydraulic and solute transport parameters, it was assumed that by running the inverse optimization process with a limited number of parameters, and not all of them simultaneously, would be beneficial for minimizing parameters' variation and more accurate for calibrating the model. This idea is in agreement with the work of Hopmans et al. (2018). However, in a study by Sonnleitner et al. (2003), it was found that by using more variables in the objective function, meaning in the inverse solution, better predictions, regarding the water flow, were obtained. Hopmans et al. (2002) suggests that if various parameter sets produce similar model outcomes, the soil hydraulic parameters may be unidentifiable and the inverse optimization may be ill-posed. According to Konikow and Bredehoeft (1992) when a model can produce data in a subjectively acceptable level of agreement then it is successfully calibrated. In this study, the calibration of the soil hydraulic parameters was considered to be good since the simulated trends match the observed trends with MAE and RMSE values close to 0.00 in all cases. Furthermore, the calibration of the solute transport parameters was also

successful. MAE and RMSE values were less than 1 for the models in 2016 and 2018. In general, the correspondence between observed and simulated data was better for the water flow models than the NO_3-N transport models. This result is common in other studies as well (Moriasi et al., 2015; Tafteh and Sepaskhah, 2012).

The calibration process itself should not be considered adequate for showing if the model can predict a different set of experimental values. The validation process was necessary to confirm that the calibrated model can predict different datasets (Ji, 2017). According to Ji (2017), if the validation is not successful, the calibrated parameters should be changed to provide better results with the validation dataset. The new parameters should be tested again with the calibrated dataset. In this study, an iterative process was necessary to have acceptable validation results. Harrison (1990) and Mitchell (1997) showed that the statistical indices should not be used as deterministic but as descriptive tools. They showed that the regression of yield between simulated and experimental data could possibly lead to invalid conclusions. In these cases, graphs that compare trends between simulated and observed results can provide a better understanding of the calibration and validation success.

The models predicted NO_3-N leaching after large precipitation events indicating that irrigation was not a driver of leaching in this landscape. The total cumulative NO_3-N leaching that HYDRUS-1D predicted varied from 3.82 kg ha^{-1} to 49.96 kg ha^{-1} per year. Similar results were found by Tafteh and Sepaskhah (2012), that tested HYDRUS-1D to predict NO_3-N leaching during maize growing season under different fertilizer rates and irrigation conditions. At the beginning of the project, it was expected that the C_G treatment would result in higher N leaching than the C_E treatment. Although in general the simulation results indicate that this might be the case, the differences between treatments were not statistically significant due to the high

variability between blocks of the same treatment. It is also likely that differences were masked by the high N application rates used on both treatments even though the C_G rates were 30%, 34% and 50% higher than the C_E rates during 2016, 2017 and 2018 growing seasons, respectively. In a study by Donner and Kucharik (2003), NO_3-N leaching was increased by 53% when there was an increase by 30% of N fertilization.

The HYDRUS-1D model was used successfully in this study to carry out the vertical water flow and NO_3-N transport and estimate NO_3-N leaching to groundwater during 2016, 2017 and 2018 maize growing seasons in Tifton, GA. The models predicted that leaching occurred in large precipitations events, when precipitation exceeded the water holding capacity of the soil. However, it would be interesting to observe the NO_3-N leaching that the models would predict long term, i.e. after harvesting maize during fallow seasons and when cover crops were planted. For doing this, soil moisture sensors should be installed in the field to record soil water content and growth data of cover crops to be recorded.

Table 3.1 Management practices followed during 2016, 2017 and 2018.

Operation	**Year**					
	2016		**2017**		**2018**	
	C_E	**C_G**	**C_E**	**C_G**	**C_E**	**C_G**
Tillage	Conventional		Conservation		Conservation	
Soil core sampling	22 Feb		6 Feb		5 Feb	
Maize planting date	16 Mar		21 Mar		28 Mar	
Maize harvest dates	19 Aug		29 Aug		22 Aug	
Variety	P1794VYHR		P1794VYHR		P1794VYHR	
Plant density (plants ha^{-1})	79000	79000	79000	79000	79000	97850
Irrigation SWT threshold (kPa)	<35		<35		<35	
Irrigation application rate (mm h^{-1})	71		36		36	
Total irrigation applied (mm)	408		235		261	
Fertilizer Applications	Date and application rate in kg N ha^{-1}					
Pre-plant fertilizer (granular)	15 Mar, 110	15 Mar, 110	15 Mar, 90	15 Mar, 90	22 Mar, 30	22 Mar, 64
At planting fertilizer (liquid)	16 Mar, 47	16 Mar, 47	21 Mar, 48	21 Mar, 48	28 Mar, 48	28 Mar, 48
Side-dress fertilizer(liquid)	8 Apr, 100 25 Apr, 100	8 Apr, 110 25 Apr, 230	13 Apr, 123 21 Apr, 123	13 Apr, 123 21 Apr, 63 2 May, 63 12 May, 63 26 May, 63 2 Jun, 27	24 Mar, 112 8 May, 56 23 May, 56	24 Mar, 112 8 May, 56 23 May, 112 5 Jun, 112

Table 3.2 Weighted percentages of each sensor according to the GDDs.

GDDs (°C)	Stage	β_1 (200 mm)	β_2 (400 mm)	β_3 (600 mm)
0-354	VE-V4	0.80	0.20	0.00
355-724	V5-V8	0.60	0.30	0.10
725-878	V9-V11	0.50	0.30	0.20
879-1099	V12-VT	0.50	0.25	0.25
1100-end of irrigation	R1-black layer	0.40	0.30	0.30

Table 3.3 Simulation periods for the soil water flow and solute transport models.

Year	Simulation begun		Simulation terminated	
	Water flow	Solute transport	Water flow	Solute transport
2016	15 Mar	22 Feb	19 Aug	19 Aug
2017	15 Mar	6 Feb	29 Aug	29 Aug
2018	22 Mar	5 Feb	21 Aug	21 Aug

Table 3.4 Texture and bulk density data of each soil layer and block used in neural network prediction, Rosetta Lite v.1.1 (June 2003), for predicting the soil hydraulic properties.

Trt	Block	Soil layer (mm)	Texture	Sand (%)	Silt (%)	Clay (%)	Bulk Density (g cm^{-3})
C_E	W2	0 – 150	Loamy Fine Sand	82.0	8.3	9.7	1.1
		150 – 300	Loamy Fine Sand	85.5	9.7	4.8	1.4
		300 – 450	Sandy Loam	74.7	7.6	17.7	1.4
		450 – 600	Sandy clay loam	65.2	8.9	25.9	1.3
		600 – 750	Sandy clay loam	68.5	8.8	22.7	1.3
	E1	0 – 150	Fine Sand	87.7	8.5	3.9	1.1
		150 – 300	Loamy Fine Sand	84.9	10.2	4.9	1.4
		300 – 450	Sandy Loam	66.5	14.5	19.1	1.4
		450 – 600	Sandy clay loam	67.8	8.7	23.5	1.4
		600 – 750	Sandy clay loam	66.5	9.1	24.4	1.3
	E3	0 – 150	Loamy Fine Sand	85.5	7.7	6.8	1.1
		150 – 300	Fine Sand	90.1	7.2	2.7	1.4
		300 – 450	Sandy Loam	74.9	11.3	13.9	1.5
		450 – 600	Sandy Loam	73.20	7.40	19.40	1.4
		600 – 750	Sandy clay loam	71.80	6.47	21.73	1.4
C_G	W1	0 – 150	Sandy Loam	79.40	10.20	10.40	1.1
		150 – 300	Loamy Fine Sand	86.2	7.5	6.3	1.4
		300 – 450	Sandy clay loam	70.9	8.2	20.9	1.4
		450 – 600	Sandy clay loam	58.3	16.1	25.6	1.4
		600 – 750	Sandy clay loam	66.1	9.1	24.8	1.4
	W3	0 – 150	Sandy Loam	79.5	8.5	12.1	1.1
		150 – 300	Loamy Fine Sand	78.9	12.4	8.7	1.4

Trt	Block	Soil layer (mm)	Texture	Sand (%)	Silt (%)	Clay (%)	Bulk Density (g cm^{-3})
		300 – 450	Sandy Loam	70.7	9.8	19.5	1.3
		450 – 600	Sandy clay loam	60.1	10.3	29.5	1.3
		600 – 750	Sandy clay loam	61.7	7.9	30.4	1.3
	E2	0 – 150	Fine Sand	89.5	6.4	4.1	1.1
		150 – 300	Fine Sand	88.5	8.5	3.1	1.4
		300 – 450	Sandy Loam	71.1	11.6	17.3	1.4
		450 – 600	Sandy Loam	71.7	10.9	17.5	1.4
		600 – 750	Sandy clay loam	70.4	6.2	23.4	1.4

Table 3.5 Initial values of the water flow parameters predicted by Rosetta Lite v.1.1 (June 2003) of each block and soil layer.

Trt	Block	Soil layer (mm)	θ_r (cm^3cm^{-3})	θ_s (cm^3cm^{-3})	a (cm^{-1})	n	K_s (cm day^{-1})	I
C_E	W2	0 – 150	0.05	0.52	0.04	1.53	270.3	0.5
		150 – 300	0.05	0.41	0.04	2.11	247.6	0.5
		300 – 450	0.07	0.45	0.03	1.52	81.71	0.5
		450 – 600	0.08	0.46	0.02	1.40	55.38	0.5
		600 – 750	0.07	0.46	0.02	1.44	62.98	0.5
	E1	0 – 150	0.05	0.51	0.05	1.74	442.5	0.5
		150 – 300	0.05	0.42	0.04	2.02	252.8	0.5
		300 – 450	0.06	0.44	0.02	1.45	56.42	0.5
		450 – 600	0.07	0.45	0.02	1.43	53.72	0.5
		600 – 750	0.07	0.46	0.02	1.42	57.78	0.5
	E3	0 – 150	0.05	0.50	0.04	1.70	341.9	0.5
		150 – 300	0.05	0.40	0.04	2.66	453.4	0.5
		300 – 450	0.06	0.41	0.03	1.55	68.98	0.5
		450 – 600	0.07	0.44	0.03	1.49	66.46	0.5
		600 – 750	0.07	0.45	0.03	1.46	63.81	0.5
C_G	W1	0 – 150	0.05	0.51	0.04	1.50	237.6	0.5
		150 – 300	0.05	0.43	0.04	2.07	280.8	0.5
		300 – 450	0.07	0.44	0.03	1.46	55.30	0.5
		450 – 600	0.07	0.45	0.02	1.40	33.74	0.5
		600 – 750	0.07	0.44	0.02	1.41	44.84	0.5
	W3	0 – 150	0.06	0.52	0.04	1.50	222.4	0.5
		150 – 300	0.05	0.42	0.04	1.68	129.0	0.5
		300 – 450	0.07	0.45	0.03	1.47	68.66	0.5
		450 – 600	0.08	0.46	0.02	1.37	44.13	0.5
		600 – 750	0.08	0.48	0.02	1.37	53.72	0.5
	E2	0 – 150	0.05	0.52	0.05	1.81	476.9	0.5
		150 – 300	0.05	0.41	0.04	2.42	385.5	0.5
		300 – 450	0.06	0.44	0.03	1.49	69.76	0.5

Trt	Block	Soil layer (mm)	θ_r (cm^3cm^{-3})	θ_s (cm^3cm^{-3})	a (cm^{-1})	n	K_s ($cm\ day^{-1}$)	I
		450 – 600	0.06	0.44	0.03	1.49	72.90	0.5
		600 – 750	0.07	0.45	0.02	1.44	61.29	0.5

Table 3.6 Root water uptake parameters and the values selected based on the database for maize.

Parameters	Description	Values (mm)
h_0	Below this pressure head value roots start to extract water from the soil (mm).	-150
h_{Opt}	Below this pressure head value roots start to extract water at the maximum possible rate (mm).	-300
h_{2H}	Value of the limiting pressure head, below which roots cannot extract water at the maximum rate (assuming a potential transpiration rate of r_{2H}) (mm).	-3250
h_{2L}	Value of the limiting pressure head, below which roots cannot extract water at the maximum rate (assuming a potential transpiration rate of r_{2L}) (mm).	-6000
h_3	Bellow this pressure head value root water uptake stops (cm).	-80000
r_{2H}	Potential transpiration rate ($mm\ day^{-1}$)	5
r_{2L}	Potential transpiration rate ($mm\ day^{-1}$)	0.5

Table 3.7 Irrigation and precipitation received at the NESPAL field during the 2016, 2017 and 2018 growing seasons. Total indicates irrigation + precipitation.

Year	Rainfall (mm)	Irrigation (mm)	Total (mm)
2016	630	408	1038
2017	495	235	730
2018	797	261	1058

Table 3.8 Weather data during the maize growing seasons from 2016 to 2018 in Tifton, GA, where this study was conducted. The growing seasons were from middle of March to end of August.

Year	Min. temperature (°C)			Max. temperature (°C)			Avg relative humidity (%)	Avg wind speed ($m\ s^{-1}$)	Avg solar radiation ($MJ\ m^{-2}$)
	Min	Max	Avg	Min	Max	Avg			
2016	2.59	23.90	17.96	15.26	35.82	29.37	73.51	2.10	20.52
2017	3.91	24.71	18.70	16.32	35.36	29.95	75.55	2.09	19.54
2018	4.57	24.25	18.86	16.84	35.29	29.67	77.25	2.13	18.69

Table 3.19 Calibrated values of hydraulic parameters based on the van Genuchten equation for water retention used in the HYDRUS-1D model for each block of NESPAL field.

Trt	Block	Soil layer (mm)	θ_r ($cm^3\ cm^{-3}$)	θ_s ($cm^3\ cm^{-3}$)	α (cm^{-1})	n	K_s ($cm\ day^{-1}$)	I
C_E	W2	0 – 150	0.05	0.52	0.04	1.06	180.2	0.5
		150 – 300	0.05	0.41	0.02	2.11	176.3	0.5
		300 – 450	0.07	0.45	0.01	1.13	62.32	0.5
		450 – 600	0.08	0.46	0.05	1.26	51.35	0.5
		600 – 750	0.07	0.46	0.01	1.17	17.83	0.5
	E1	0 – 150	0.05	0.51	0.05	1.74	442.5	0.5
		150 – 300	0.05	0.42	0.05	2.02	174.3	0.5
		300 – 450	0.06	0.44	0.02	1.06	50.00	0.5
		450 – 600	0.07	0.45	0.01	1.10	45.37	0.5
		600 – 750	0.07	0.46	0.01	1.07	19.32	0.5
	E3	0 – 150	0.05	0.50	0.03	1.57	258.8	0.5
		150 – 300	0.05	0.40	0.15	1.23	897.9	0.5
		300 – 450	0.06	0.41	0.01	1.14	250.0	0.5
		450 – 600	0.07	0.44	0.07	1.10	149.6	0.5
		600 – 750	0.07	0.45	0.04	1.43	19.72	0.5
C_G	W1	0 – 150	0.05	0.51	0.04	1.14	150.0	0.5
		150 – 300	0.05	0.43	0.03	2.06	411.9	0.5
		300 – 450	0.07	0.44	0.01	1.09	26.79	0.5
		450 – 600	0.07	0.45	0.01	2.00	59.78	0.5
		600 – 750	0.07	0.44	0.01	1.08	10.00	0.5
	W3	0 – 150	0.06	0.52	0.05	1.26	210.4	0.5
		150 – 300	0.05	0.42	0.02	1.31	576.7	0.5
		300 – 450	0.07	0.45	0.01	1.13	168.5	0.5
		450 – 600	0.08	0.46	0.05	1.11	54.69	0.5
		600 – 750	0.08	0.48	0.01	1.11	10.00	0.5
	E2	0 – 150	0.05	0.52	0.04	1.63	350.0	0.5
		150 – 300	0.05	0.41	0.03	2.00	546.3	0.5
		300 – 450	0.06	0.44	0.01	1.09	250.0	0.5
		450 – 600	0.06	0.44	0.01	1.17	59.43	0.5
		600 – 750	0.07	0.45	0.08	1.19	10.23	0.5

Table 3.210 Statistical analysis between observed and simulated pressure head data for all the blocks of NESPAL field and maize growing seasons.

Treatment	Blocks	Year	MAE	RMSE
C_E	W2	2018	0.04	0.04
		2017	0.04	0.05
		2016	0.05	0.05
	E1	2018	0.04	0.05
		2017	0.05	0.06

		2016	0.03	0.04
	E3	2018	0.03	0.04
		2017	0.08	0.09
		2016	0.03	0.04
C_G	W1	2018	0.03	0.04
		2017	0.05	0.06
		2016	0.05	0.06
	W3	2018	0.03	0.04
		2017	0.07	0.09
		2016	0.03	0.04
	E2	2018	0.04	0.04
		2017	0.09	0.11
		2016	0.04	0.05
Perfect fit			0	0

*MAE: Mean weighted Absolute Error, RMSE: Root Mean Square Error

Table 3.311 Calibrated values of solute transport parameters after using the inverse solution in HYDRUS-1D model for each block of NESPAL field.

Trt	**Block**	**Soil layer (mm)**	**Adsorption coefficient K_d ($cm^3\ g^{-1}$)**		**Nitrification rate k (day^{-1})**	**Denitrification rate μ (day^{-1})**
			NH_4-N	**NO_3-N**		
C_E	W2	0 – 150	6.71	1.99	0.00	0.14
		150 – 300	14.28	0.17	0.00	0.72
		300 – 450	31.22	0.10	0.30	0.31
		450 – 600	5.18	1.58	0.05	0.10
		600 – 750	9.64	1.00	0.06	0.20
	E1	0 – 150	82.66	0.25	0.00	0.11
		150 – 300	7.78	0.01	0.25	1.00
		300 – 450	21.16	1.00	1.00	0.24
		450 – 600	26.27	2.00	0.23	0.08
		600 – 750	12.60	0.10	0.05	0.31
	E3	0 – 150	100	1.40	0.09	1.00
		150 – 300	1.03	1.86	0.21	0.89
		300 – 450	7.39	0.85	0.70	0.28
		450 – 600	2.58	1.97	0.10	0.06
		600 – 750	0.25	2.00	0.61	0.21
C_G	W1	0 – 150	99.17	1.32	0.00	0.08
		150 – 300	51.3	0.15	0.10	1.00
		300 – 450	58.69	0.25	0.32	0.02
		450 – 600	100	0.75	0.02	0.04
		600 – 750	100	0.33	0.08	0.43
	W3	0 – 150	49.35	0.23	0.00	0.20

Trt	Block	Soil layer (mm)	Adsorption coefficient K_d ($cm^3\ g^{-1}$)		Nitrification rate k (day^{-1})	Denitrification rate μ (day^{-1})
			NH_4-N	NO_3-N		
		150 – 300	51.68	0.61	0.71	0.20
		300 – 450	87.72	0.07	0.86	0.20
		450 – 600	46.88	0.78	0.27	0.20
		600 – 750	10.00	0.48	0.13	0.30
	E2	0 – 150	12.52	1.93	0.03	0.01
		150 – 300	0.15	1.08	0.20	0.90
		300 – 450	100	2.00	0.00	0.61
		450 – 600	16.03	2.00	0.24	0.03
		600 – 750	1.45	0.39	0.03	0.10

Table 3.12 Statistical analysis between observed and simulated NO_3-N concentrations data for all the blocks of NESPAL field and maize growing seasons.

Treatment	Blocks	Year	MAE	RMSE
C_E	W2	2018	0.09	0.13
		2017	3.31	3.78
		2016	0.15	0.18
	E1	2018	0.08	0.12
		2017	0.44	0.47
		2016	0.18	0.21
	E3	2018	0.10	0.14
		2017	0.38	0.45
		2016	0.33	0.39
C_G	W1	2018	0.21	0.24
		2017	0.89	1.04
		2016	0.24	0.37
	W3	2018	0.17	0.20
		2017	0.84	0.88
		2016	0.94	1.10
	E2	2018	0.07	0.11
		2017	2.98	3.27
		2016	0.28	0.35
Perfect fit			0	0

*MAE: Mean weighted Absolute Error, RMSE: Root Mean Square Error

Table 3.413 Simulated loss of N from leaching and percent of N lost in leaching as a function of N applied during 2016, 2017 and 2018 growing seasons. Means followed by different letters between the years are significantly different ($p<0.05$).

Treatment	Block	Year	Total NO_3-N (kg ha^{-1})	Lost (%)
By year				
C_E	W2	2016	27.68	7.75
		2017	49.96	13.01
		2018	27.99	9.27
	E1	2016	11.07	3.10
		2017	9.55	2.49
		2018	5.8	1.92
	E3	2016	13.89	3.89
		2017	7.27	1.89
		2018	13.67	4.53
	Mean	2016	17.55[a]	4.92
		2017	22.25[a]	5.79
		2018	15.82[a]	5.24
C_G	W1	2016	15.39	3.10
		2017	3.82	0.71
		2018	15.11	3.00
	W3	2016	27.62	5.56
		2017	10.51	1.95
		2018	18.6	3.69
	E2	2016	9.47	1.91
		2017	4.19	0.78
		2018	13.59	2.70
	Mean	2016	17.49[a]	3.52
		2017	6.17[a]	1.14
		2018	15.77[a]	3.13
By treatment				
C_E	Mean		18.54[a]	
C_G	Mean		13.14[a]	

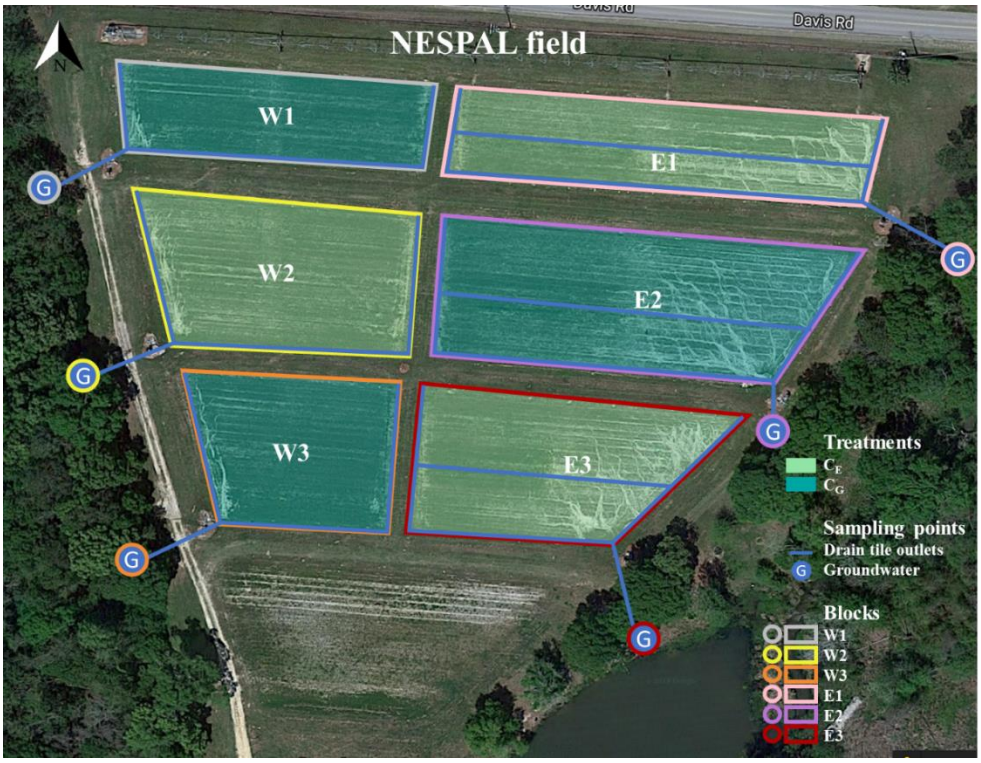

Figure 3.1 Map of the NESPAL field showing the six blocks, the two fertilization treatments (dark green for C_G and light green for C_E), the drain tile (blue lines) and the location of groundwater collection sites (G).

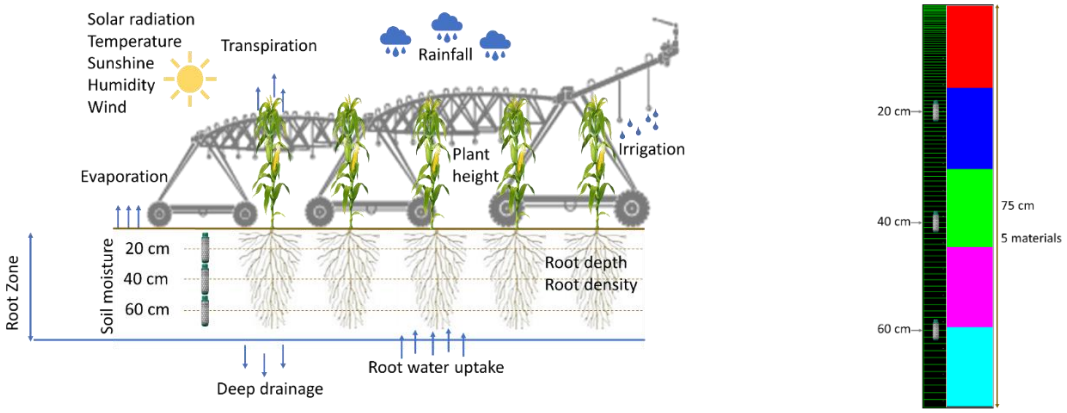

(a) (b)

Figure 3.2 (a) Representation of the model based on transient soil water flow processes and (b) graphical representation of the soil profile.

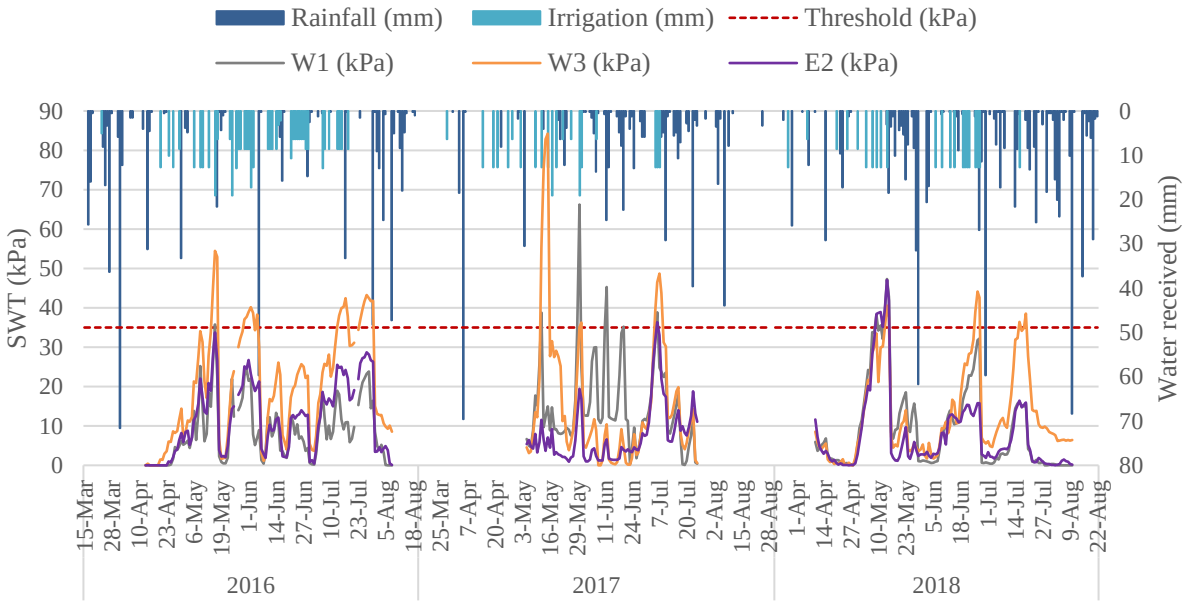

(a)

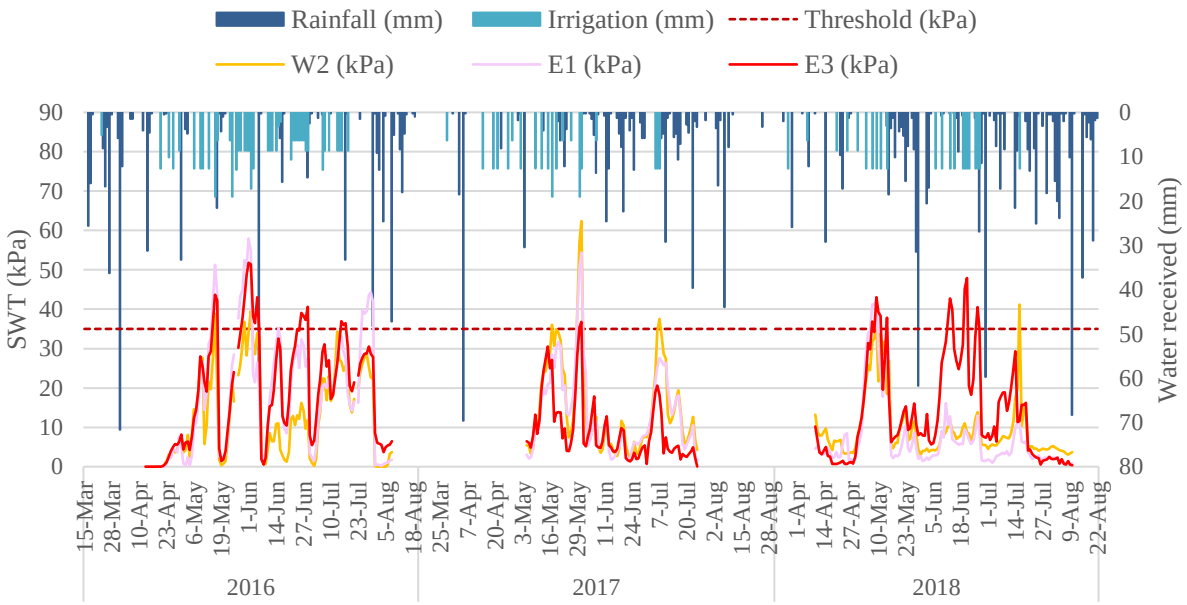

(b)

Figure 3.3 Daily SWT and amount of water received through applied irrigation or rainfall during the three growing seasons for (a) C_G and (b) C_E blocks.

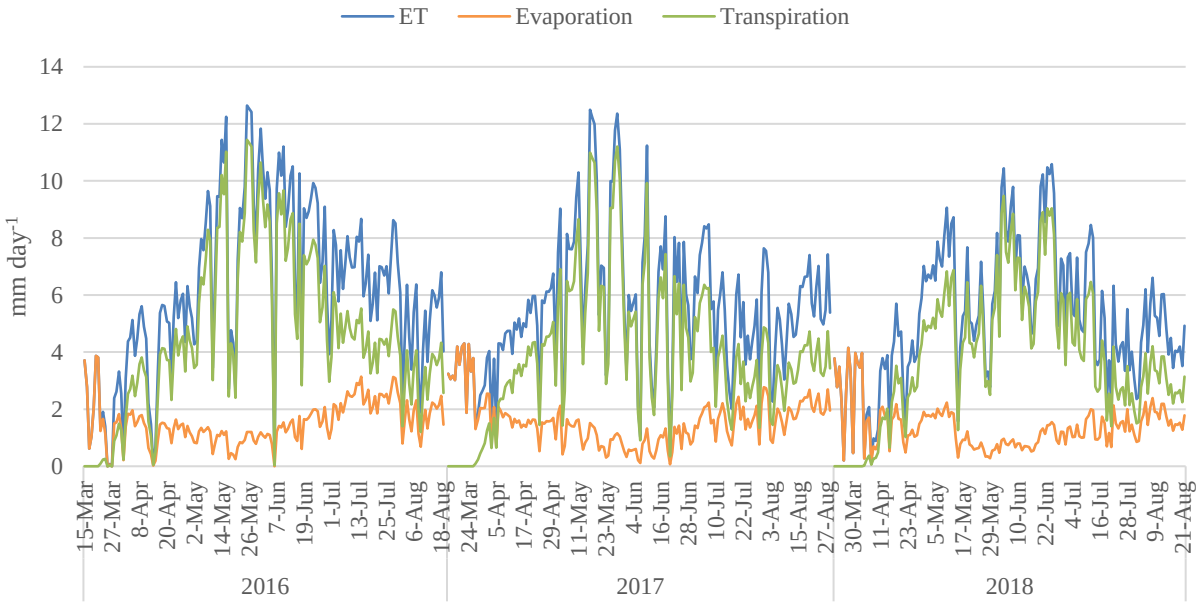

Figure 3.4 ET, evaporation, and transpiration estimated by HYDRUS-1D based on crop height and LAI data for 2016, 2017 and 2018.

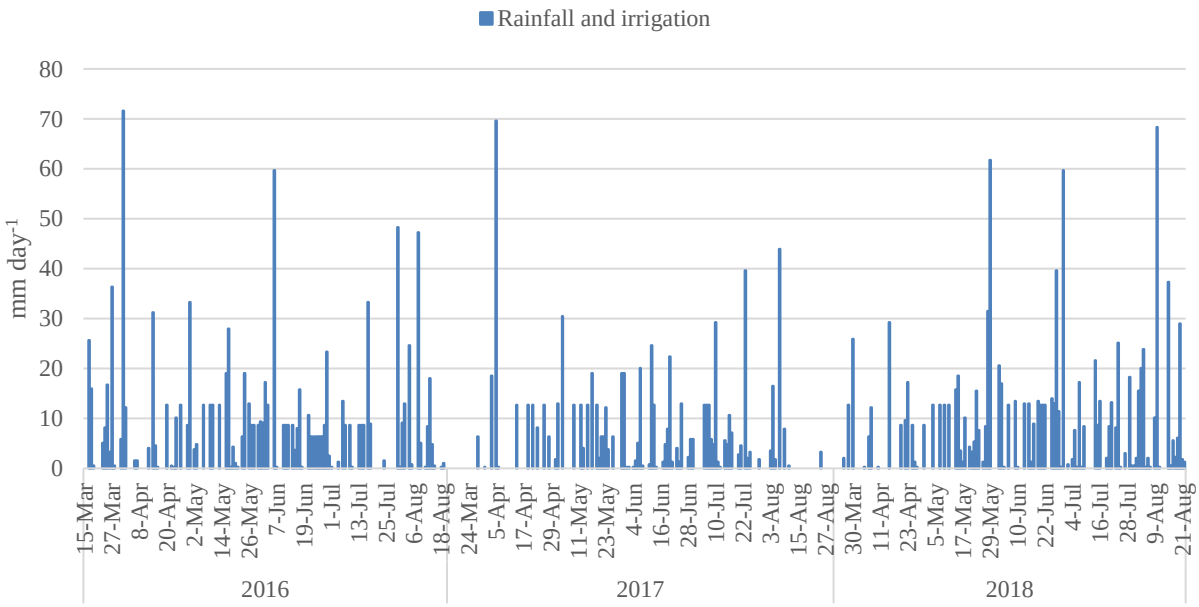

Figure 3.5 Daily total water received through rainfall and irrigation during 2016, 2017, and 2018 growing seasons.

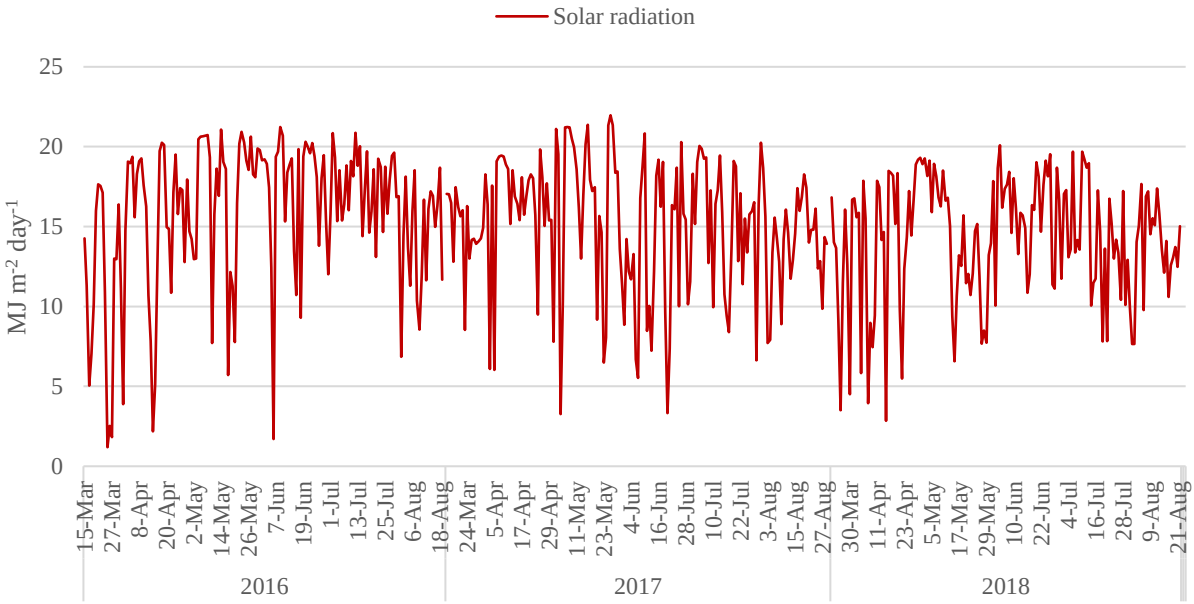

Figure 3.6 Daily short-wave radiation during 2016, 2017 and 2018 growing seasons.

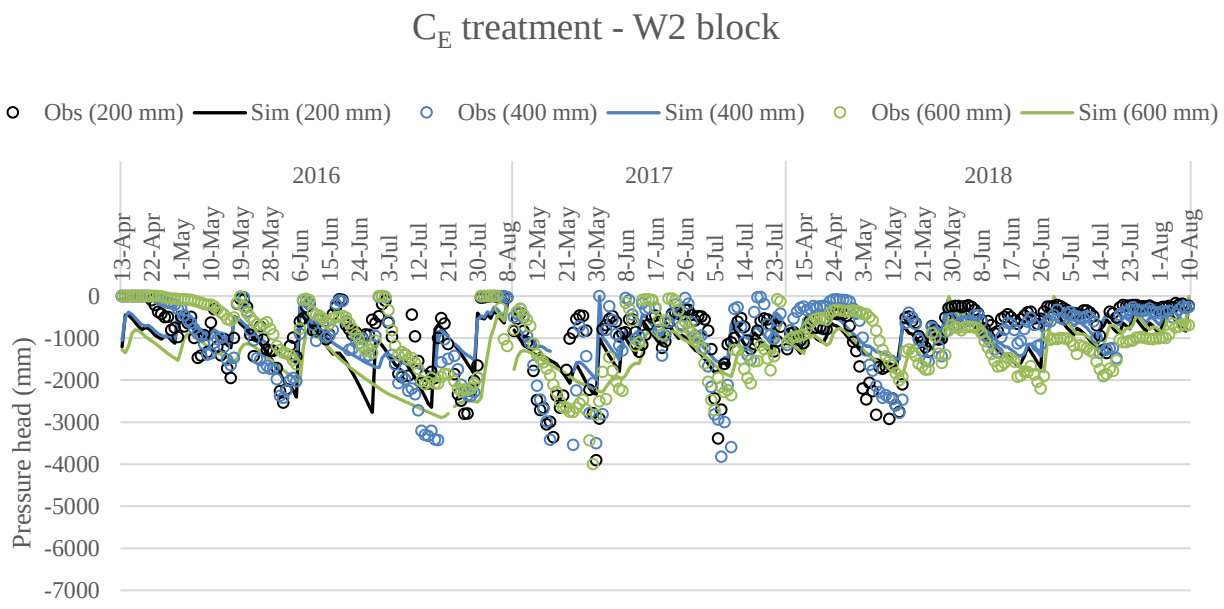
C_E treatment - W2 block
Obs (200 mm)
Sim (200 mm)
Obs (400 mm)
Sim (400 mm)
Obs (600 mm)
Sim (600 mm)
2016
2017
2018
13-Apr
22-Apr
1-May
10-May
19-May
28-May
6-Jun
15-Jun
24-Jun
3-Jul
12-Jul
21-Jul
30-Jul
8-Aug
12-May
21-May
30-May
8-Jun
17-Jun
26-Jun
5-Jul
14-Jul
23-Jul
15-Apr
24-Apr
3-May
12-May
21-May
30-May
8-Jun
17-Jun
26-Jun
5-Jul
14-Jul
23-Jul
1-Aug
10-Aug
0
-1000
-2000
-3000
-4000
-5000
-6000
-7000
Pressure head (mm)

(a)

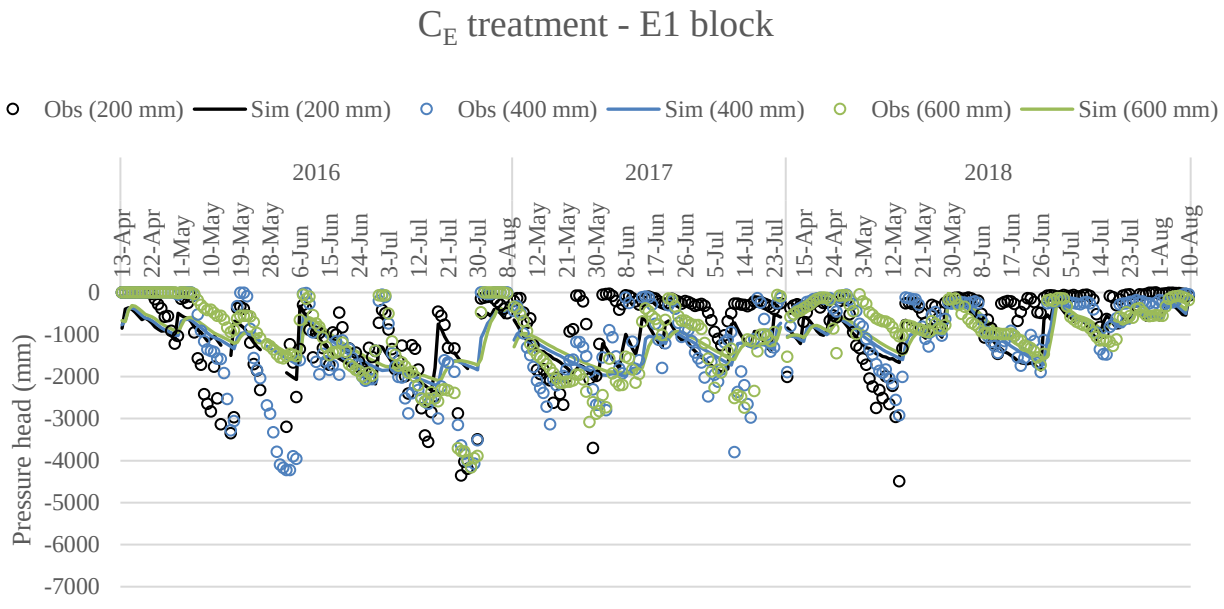
C_E treatment - E1 block
Obs (200 mm)
Sim (200 mm)
Obs (400 mm)
Sim (400 mm)
Obs (600 mm)
Sim (600 mm)
2016
2017
2018
13-Apr
22-Apr
1-May
10-May
19-May
28-May
6-Jun
15-Jun
24-Jun
3-Jul
12-Jul
21-Jul
30-Jul
8-Aug
12-May
21-May
30-May
8-Jun
17-Jun
26-Jun
5-Jul
14-Jul
23-Jul
15-Apr
24-Apr
3-May
12-May
21-May
30-May
8-Jun
17-Jun
26-Jun
5-Jul
14-Jul
23-Jul
1-Aug
10-Aug
0
-1000
-2000
-3000
-4000
-5000
-6000
-7000
Pressure head (mm)

(b)

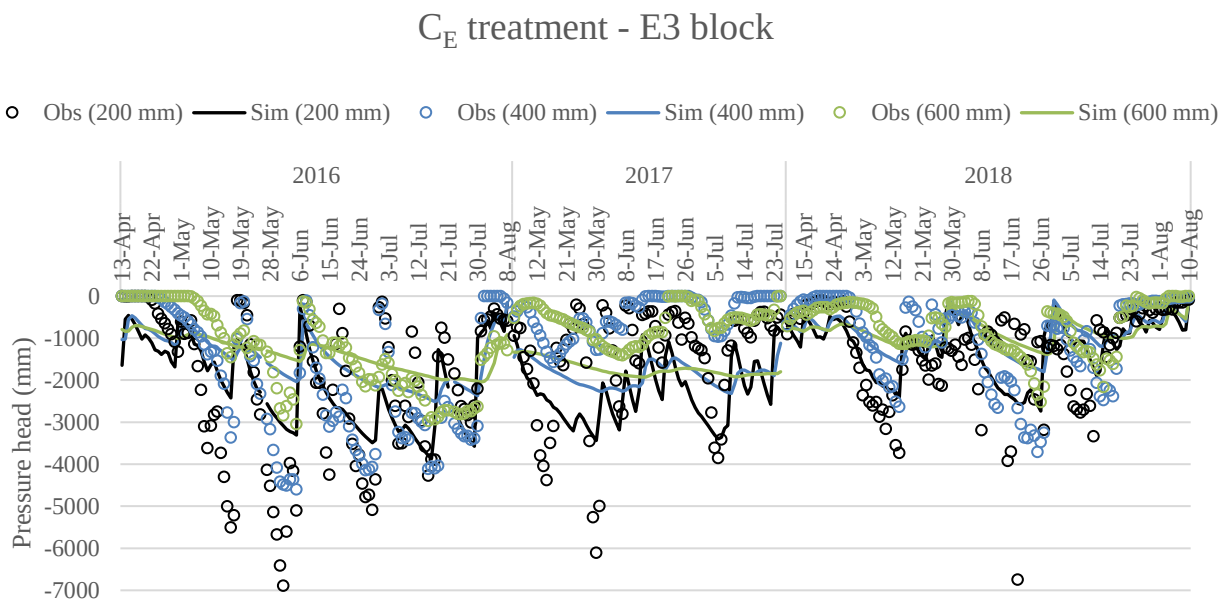
C_E treatment - E3 block
Obs (200 mm)
Sim (200 mm)
Obs (400 mm)
Sim (400 mm)
Obs (600 mm)
Sim (600 mm)
2016
2017
2018
13-Apr
22-Apr
1-May
10-May
19-May
28-May
6-Jun
15-Jun
24-Jun
3-Jul
12-Jul
21-Jul
30-Jul
8-Aug
12-May
21-May
30-May
8-Jun
17-Jun
26-Jun
5-Jul
14-Jul
23-Jul
15-Apr
24-Apr
3-May
12-May
21-May
30-May
8-Jun
17-Jun
26-Jun
5-Jul
14-Jul
23-Jul
1-Aug
10-Aug
0
-1000
-2000
-3000
-4000
-5000
-6000
-7000
Pressure head (mm)

(c)

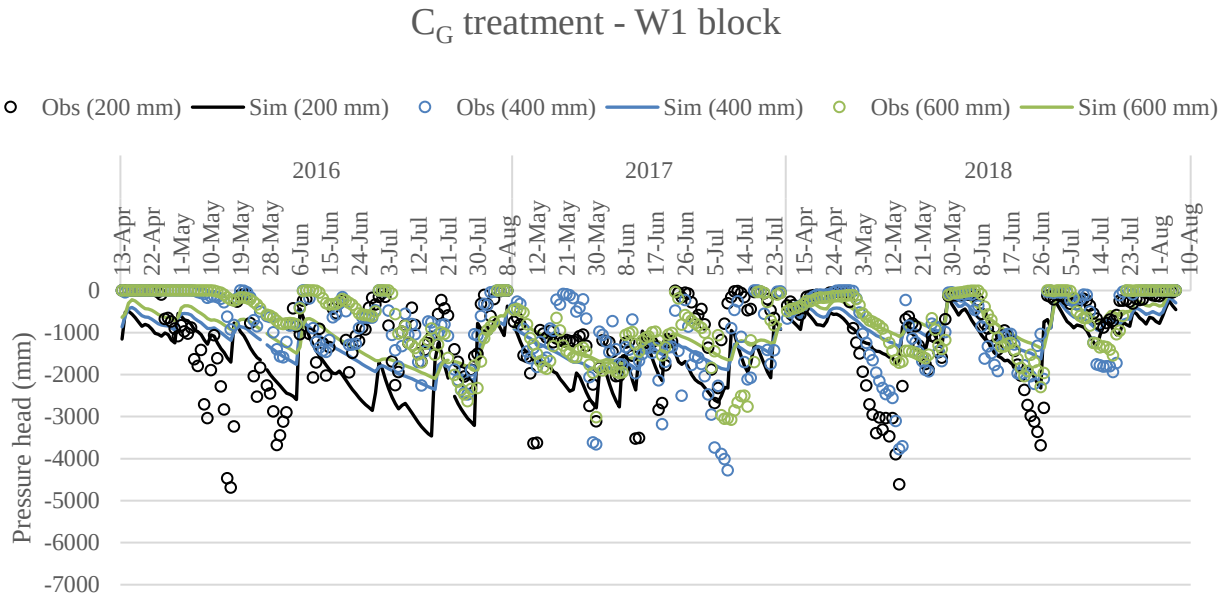
C_G treatment - W1 block
Obs (200 mm)
Sim (200 mm)
Obs (400 mm)
Sim (400 mm)
Obs (600 mm)
Sim (600 mm)
2016
2017
2018
13-Apr
22-Apr
1-May
10-May
19-May
28-May
6-Jun
15-Jun
24-Jun
3-Jul
12-Jul
21-Jul
30-Jul
8-Aug
12-May
21-May
30-May
8-Jun
17-Jun
26-Jun
5-Jul
14-Jul
23-Jul
15-Apr
24-Apr
3-May
12-May
21-May
30-May
8-Jun
17-Jun
26-Jun
5-Jul
14-Jul
23-Jul
1-Aug
10-Aug
0
-1000
-2000
-3000
-4000
-5000
-6000
-7000
Pressure head (mm)

(d)

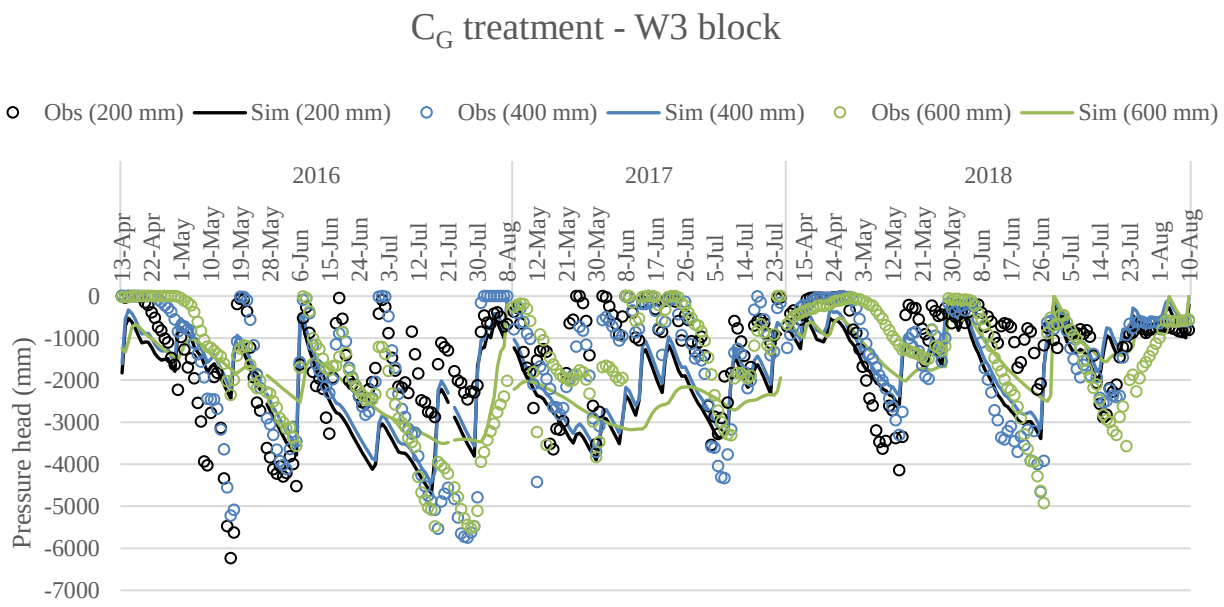

(e)

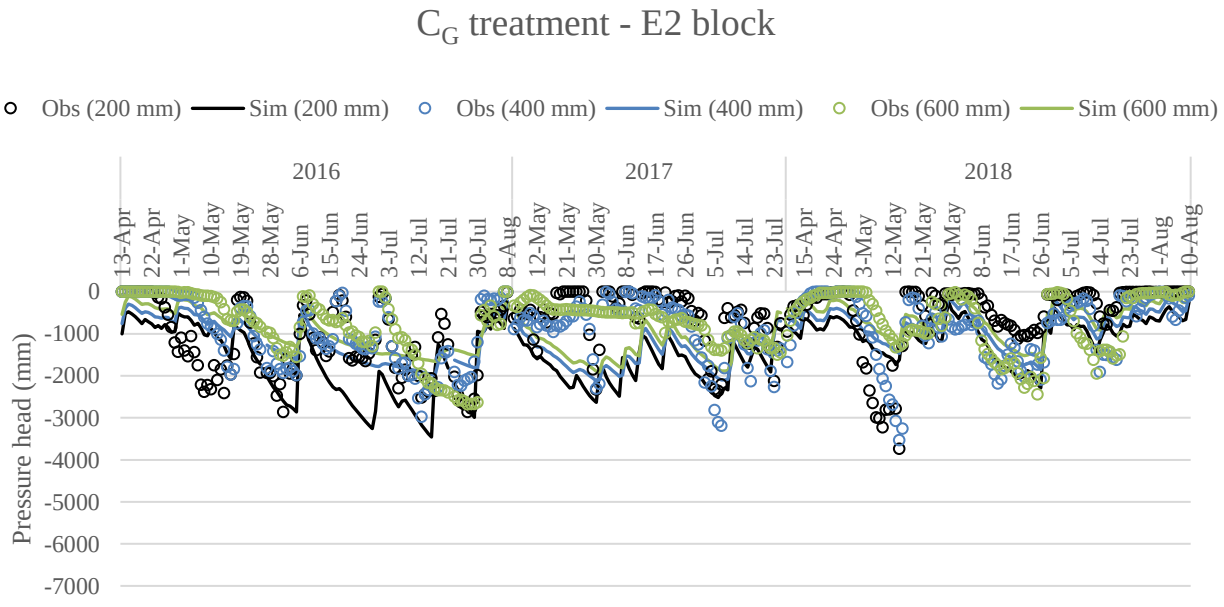

(f)

Figure 3.7 Fit between observed and simulated pressure heads during 2016, 2017 and 2018 growing seasons for C_E treatment (a) W2, (b) E1, (c) E3 and C_G treatment (d) W1, (e) W3, (f) E2.

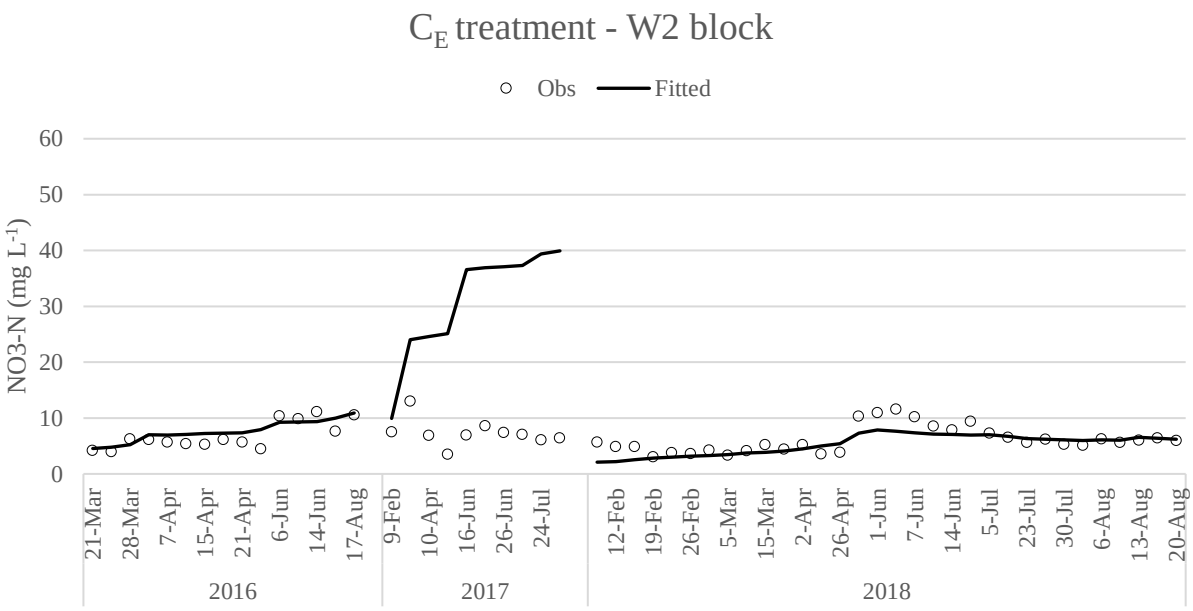
C_E treatment - W2 block
Obs
Fitted
NO3-N (mg L-1)
60
50
40
30
20
10
0
21-Mar
28-Mar
7-Apr
15-Apr
21-Apr
6-Jun
14-Jun
17-Aug
9-Feb
10-Apr
16-Jun
26-Jun
24-Jul
12-Feb
19-Feb
26-Feb
5-Mar
15-Mar
2-Apr
26-Apr
1-Jun
7-Jun
14-Jun
5-Jul
23-Jul
30-Jul
6-Aug
13-Aug
20-Aug
2016
2017
2018

(a)

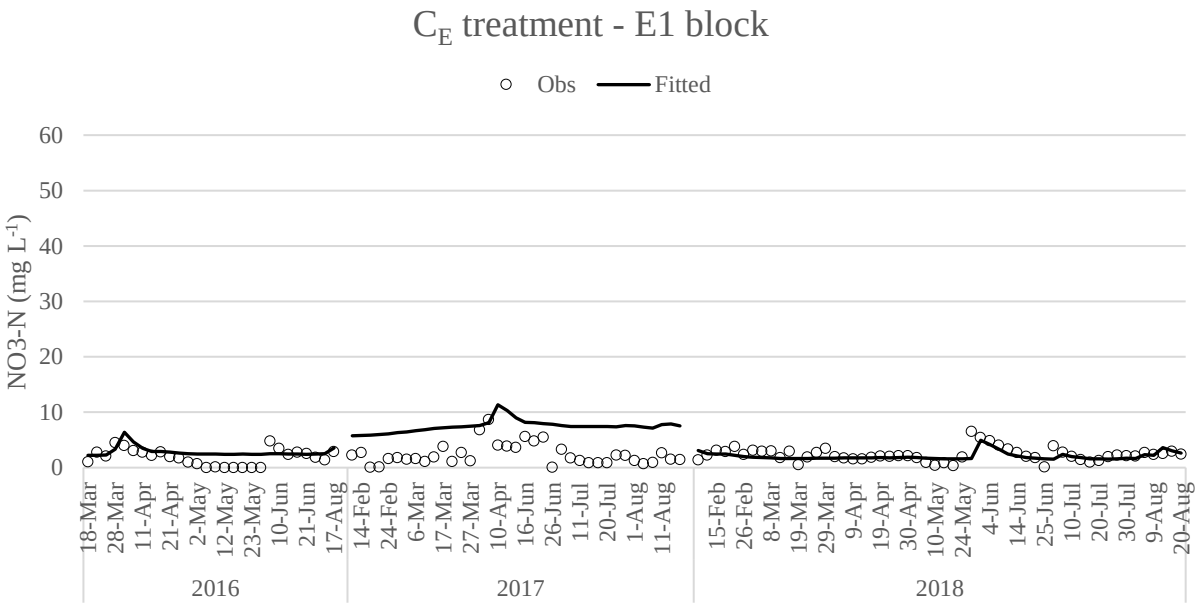
C_E treatment - E1 block
Obs
Fitted
NO3-N (mg L-1)
60
50
40
30
20
10
0
18-Mar
28-Mar
11-Apr
21-Apr
2-May
12-May
23-May
10-Jun
21-Jun
17-Aug
14-Feb
24-Feb
6-Mar
17-Mar
27-Mar
10-Apr
16-Jun
26-Jun
11-Jul
20-Jul
1-Aug
11-Aug
15-Feb
26-Feb
8-Mar
19-Mar
29-Mar
9-Apr
19-Apr
30-Apr
10-May
24-May
4-Jun
14-Jun
25-Jun
10-Jul
20-Jul
30-Jul
9-Aug
20-Aug
2016
2017
2018

(b)

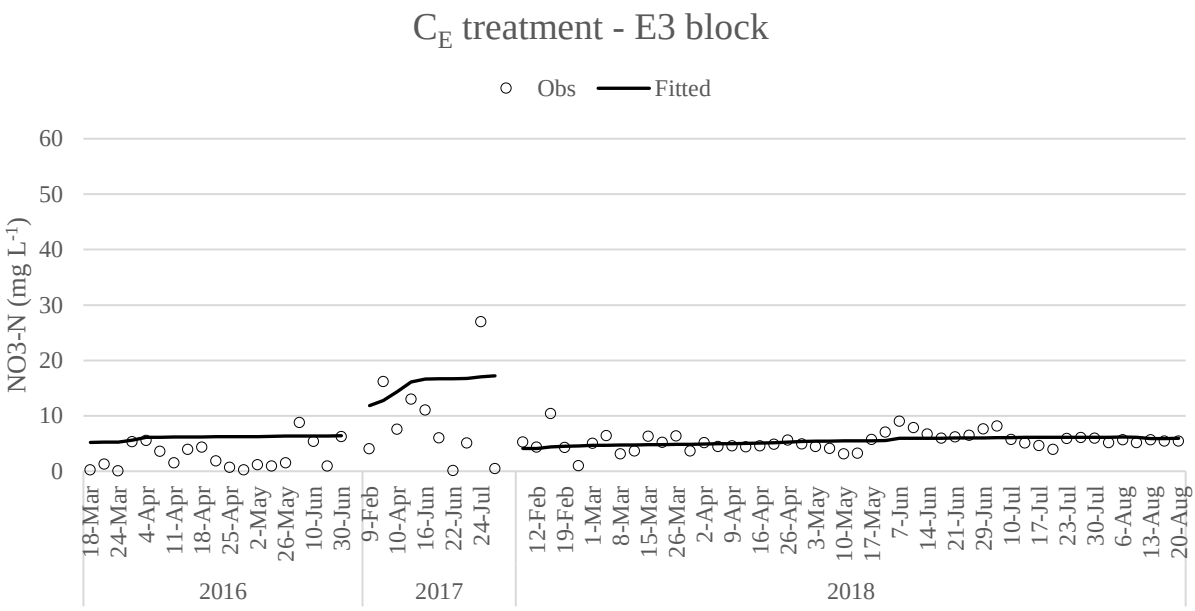
C_E treatment - E3 block
Obs
Fitted
NO3-N (mg L-1)
60
50
40
30
20
10
0
18-Mar
24-Mar
4-Apr
11-Apr
18-Apr
25-Apr
2-May
26-May
10-Jun
30-Jun
9-Feb
10-Apr
16-Jun
22-Jun
24-Jul
12-Feb
19-Feb
1-Mar
8-Mar
15-Mar
26-Mar
2-Apr
9-Apr
16-Apr
26-Apr
3-May
10-May
17-May
7-Jun
14-Jun
21-Jun
29-Jun
10-Jul
17-Jul
23-Jul
30-Jul
6-Aug
13-Aug
20-Aug
2016
2017
2018

(c)

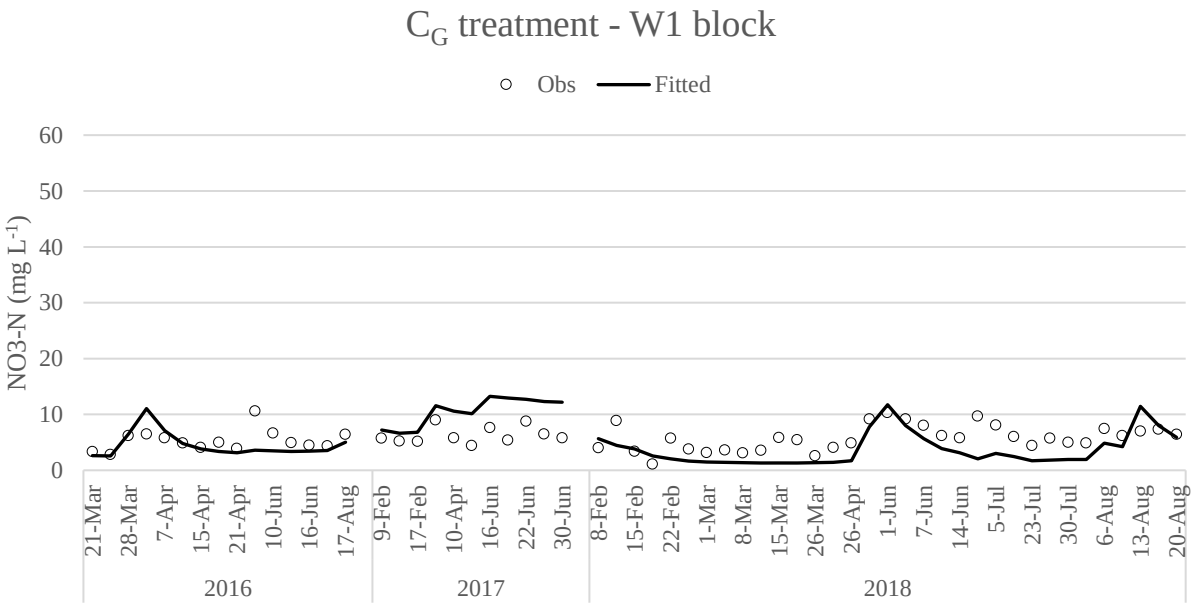
C_G treatment - W1 block
Obs
Fitted
NO3-N (mg L-1)
60
50
40
30
20
10
0
21-Mar
28-Mar
7-Apr
15-Apr
21-Apr
10-Jun
16-Jun
17-Aug
9-Feb
17-Feb
10-Apr
16-Jun
22-Jun
30-Jun
8-Feb
15-Feb
22-Feb
1-Mar
8-Mar
15-Mar
26-Mar
26-Apr
1-Jun
7-Jun
14-Jun
5-Jul
23-Jul
30-Jul
6-Aug
13-Aug
20-Aug
2016
2017
2018

(d)

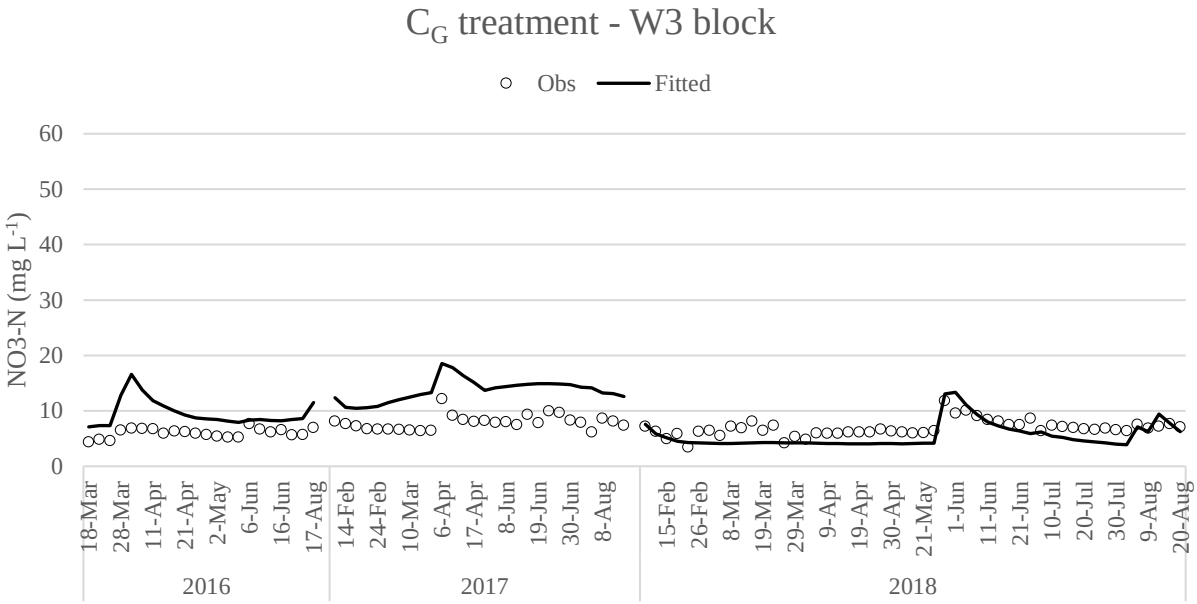

(e)

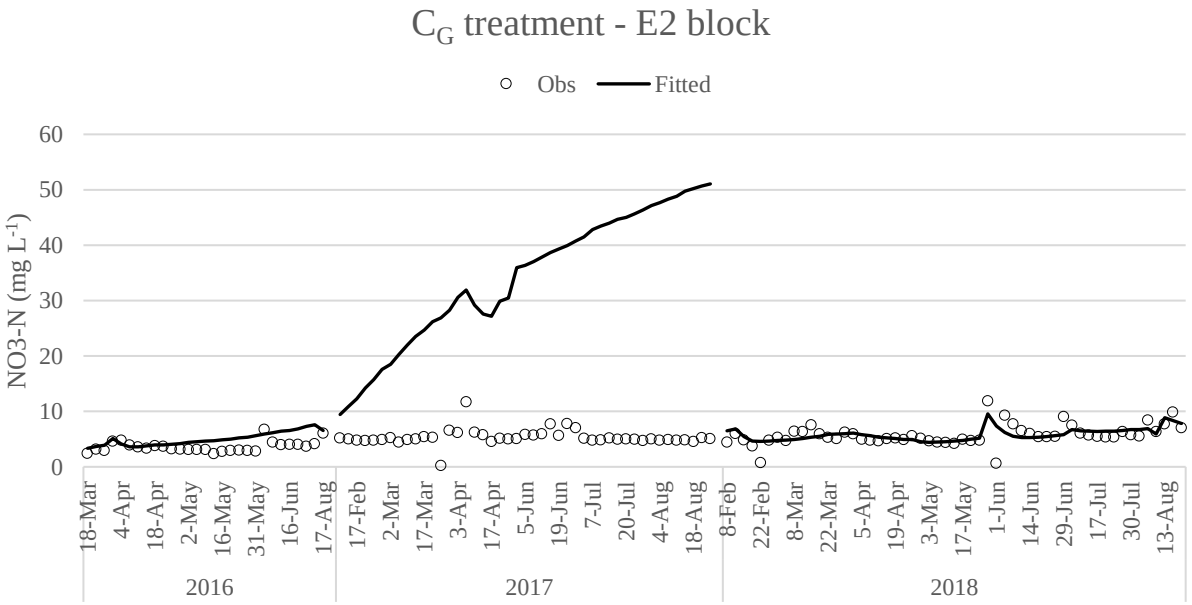

(f)

Figure 3.8 Fit between observed groundwater samples and simulated NO_3-N concentrations at 750 mm below the soil surface during 2016, 2017 and 2018 growing seasons for C_E treatment (a) W2, (b) E1, (c) E3 and C_G treatment (d) W1, (e) W3, (f) E2.

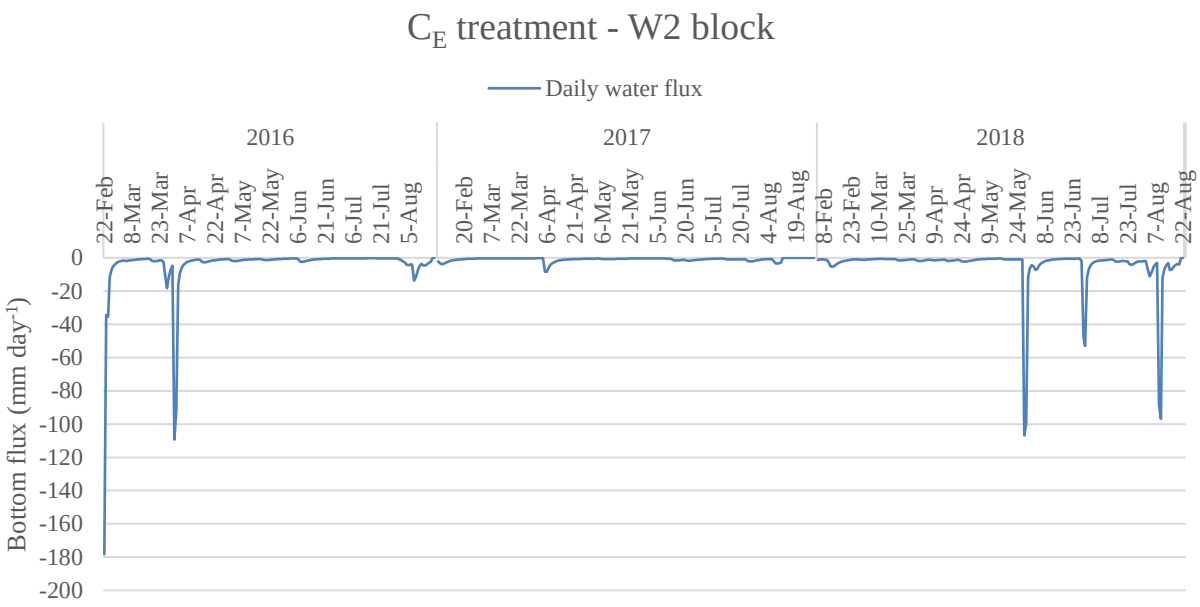
C_E treatment - W2 block
Daily water flux
2016
2017
2018
22-Feb
8-Mar
23-Mar
7-Apr
22-Apr
7-May
22-May
6-Jun
21-Jun
6-Jul
21-Jul
5-Aug
20-Feb
7-Mar
22-Mar
6-Apr
21-Apr
6-May
21-May
5-Jun
20-Jun
5-Jul
20-Jul
4-Aug
19-Aug
8-Feb
23-Feb
10-Mar
25-Mar
9-Apr
24-Apr
9-May
24-May
8-Jun
23-Jun
8-Jul
23-Jul
7-Aug
22-Aug
0
-20
-40
-60
-80
-100
-120
-140
-160
-180
-200
Bottom flux (mm day-1)

(a)

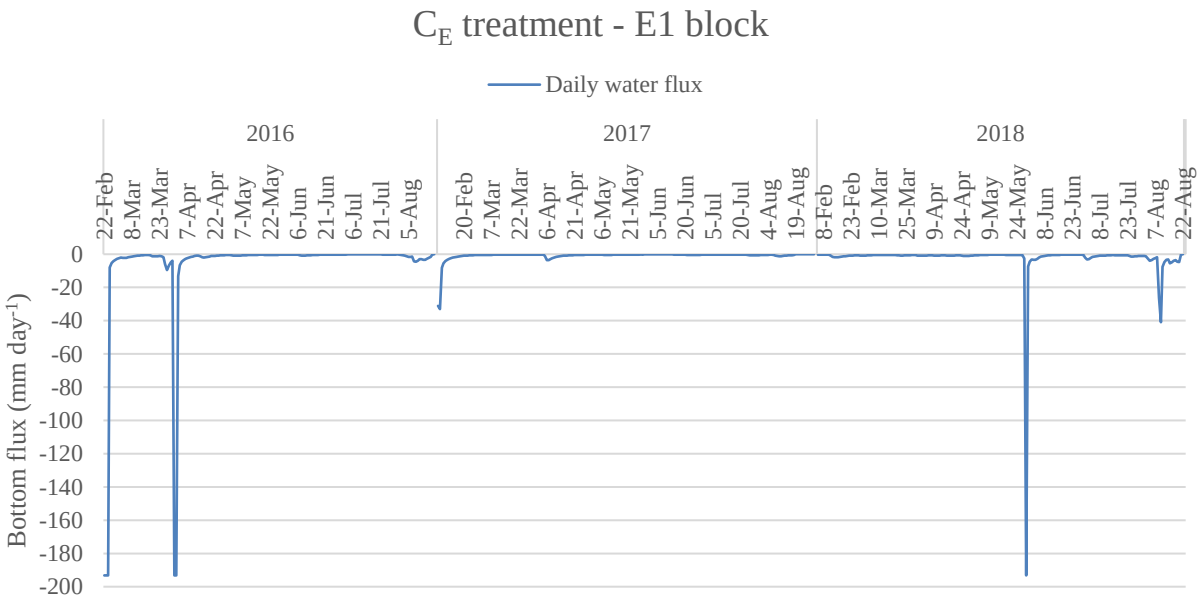
C_E treatment - E1 block
Daily water flux
2016
2017
2018
22-Feb
8-Mar
23-Mar
7-Apr
22-Apr
7-May
22-May
6-Jun
21-Jun
6-Jul
21-Jul
5-Aug
20-Feb
7-Mar
22-Mar
6-Apr
21-Apr
6-May
21-May
5-Jun
20-Jun
5-Jul
20-Jul
4-Aug
19-Aug
8-Feb
23-Feb
10-Mar
25-Mar
9-Apr
24-Apr
9-May
24-May
8-Jun
23-Jun
8-Jul
23-Jul
7-Aug
22-Aug
0
-20
-40
-60
-80
-100
-120
-140
-160
-180
-200
Bottom flux (mm day-1)

(b)

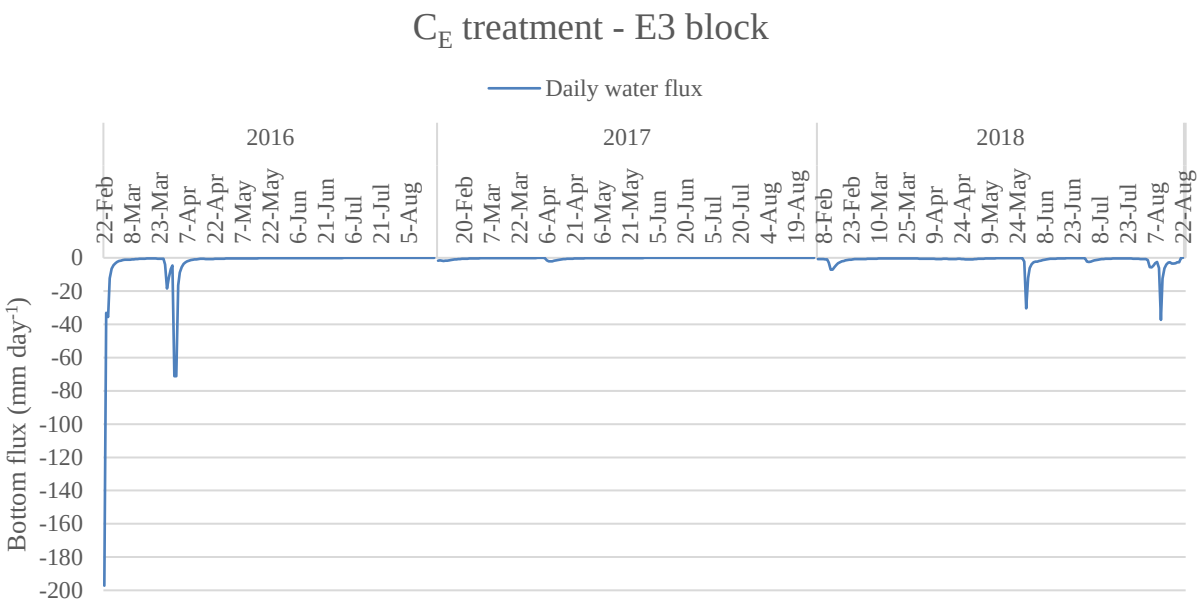
C_E treatment - E3 block
Daily water flux
2016
2017
2018
22-Feb
8-Mar
23-Mar
7-Apr
22-Apr
7-May
22-May
6-Jun
21-Jun
6-Jul
21-Jul
5-Aug
20-Feb
7-Mar
22-Mar
6-Apr
21-Apr
6-May
21-May
5-Jun
20-Jun
5-Jul
20-Jul
4-Aug
19-Aug
8-Feb
23-Feb
10-Mar
25-Mar
9-Apr
24-Apr
9-May
24-May
8-Jun
23-Jun
8-Jul
23-Jul
7-Aug
22-Aug
0
-20
-40
-60
-80
-100
-120
-140
-160
-180
-200
Bottom flux (mm day-1)

(c)

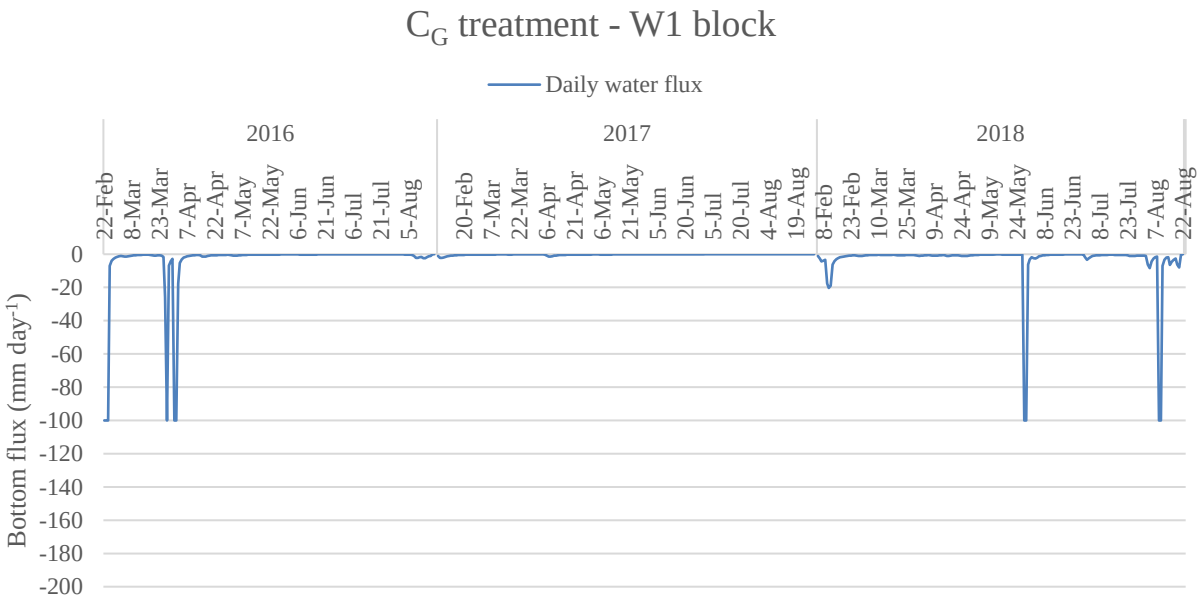
C_G treatment - W1 block
Daily water flux
2016
2017
2018
22-Feb
8-Mar
23-Mar
7-Apr
22-Apr
7-May
22-May
6-Jun
21-Jun
6-Jul
21-Jul
5-Aug
20-Feb
7-Mar
22-Mar
6-Apr
21-Apr
6-May
21-May
5-Jun
20-Jun
5-Jul
20-Jul
4-Aug
19-Aug
8-Feb
23-Feb
10-Mar
25-Mar
9-Apr
24-Apr
9-May
24-May
8-Jun
23-Jun
8-Jul
23-Jul
7-Aug
22-Aug
0
-20
-40
-60
-80
-100
-120
-140
-160
-180
-200
Bottom flux (mm day-1)

(d)

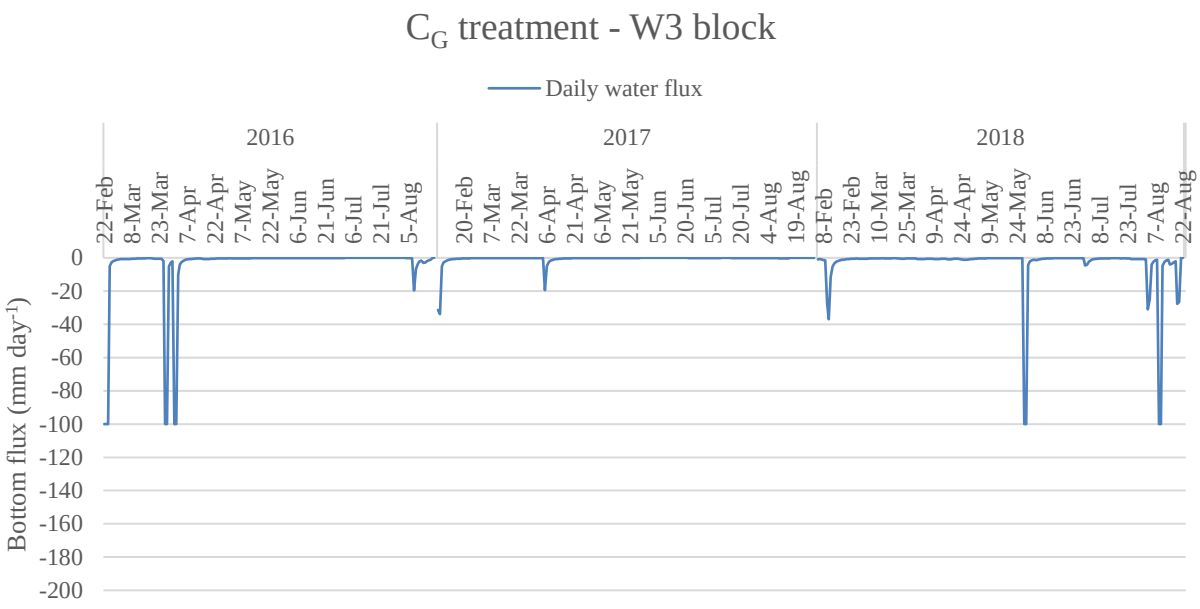

(e)

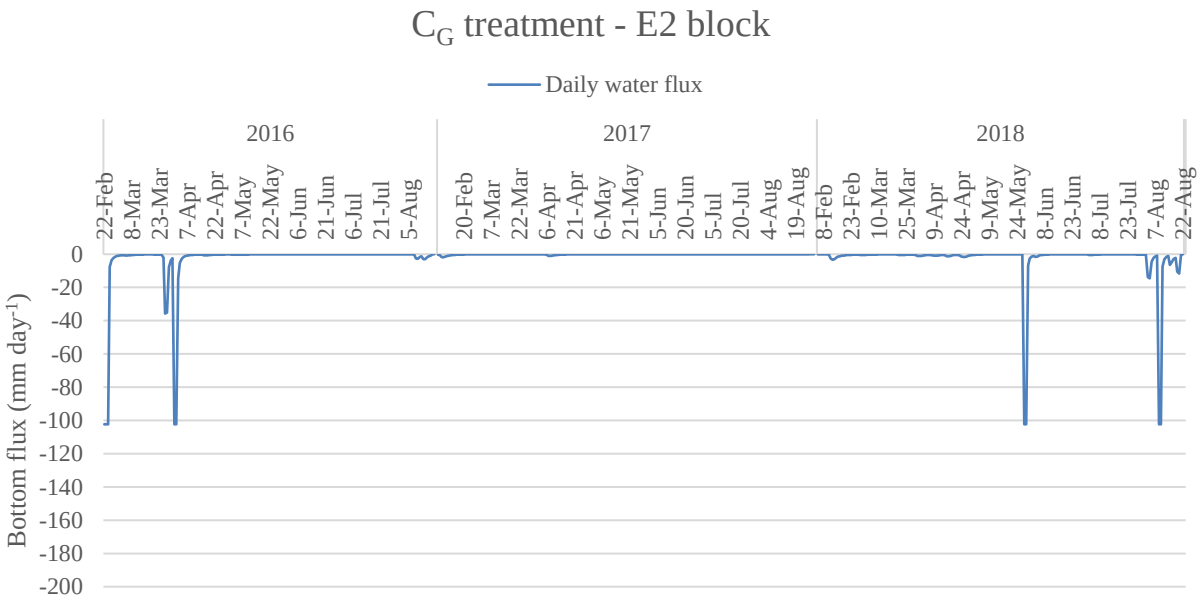

(f)

Figure 3.9 Daily simulated water fluxes from at 750 mm depth during 2016, 2017 and 2018 for C_E treatment (a) W2, (b) E1, (c) E3 and C_G treatment (d) W1, (e) W3, (f) E2.

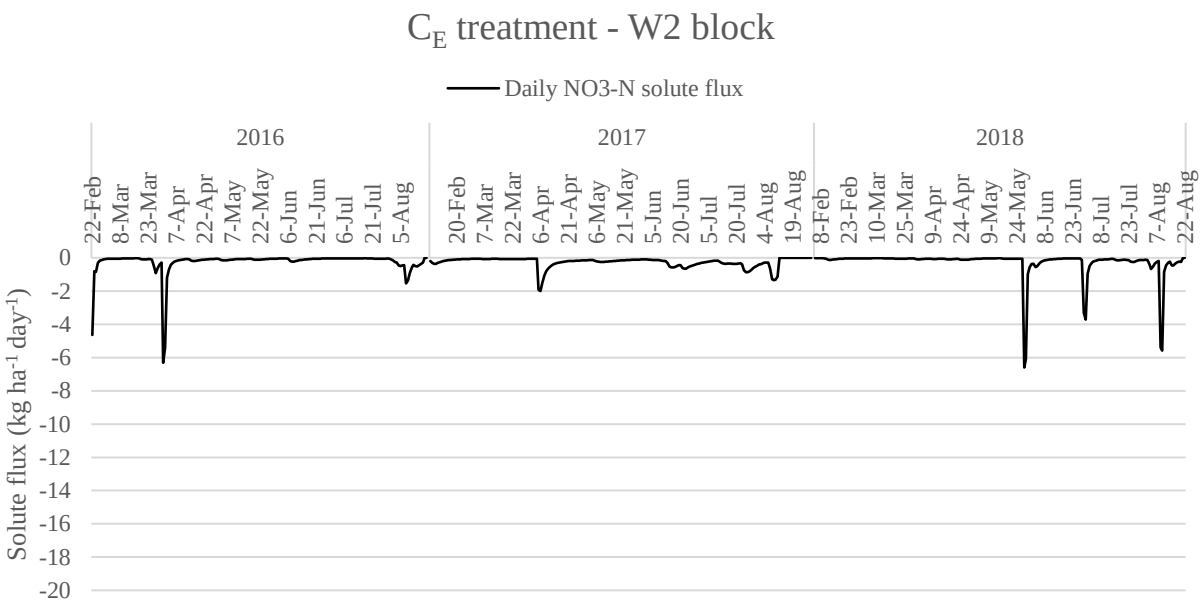
C_E treatment - W2 block
Daily NO3-N solute flux
2016
2017
2018
22-Feb
8-Mar
23-Mar
7-Apr
22-Apr
7-May
22-May
6-Jun
21-Jun
6-Jul
21-Jul
5-Aug
20-Feb
7-Mar
22-Mar
6-Apr
21-Apr
6-May
21-May
5-Jun
20-Jun
5-Jul
20-Jul
4-Aug
19-Aug
8-Feb
23-Feb
10-Mar
25-Mar
9-Apr
24-Apr
9-May
24-May
8-Jun
23-Jun
8-Jul
23-Jul
7-Aug
22-Aug
0
-2
-4
-6
-8
-10
-12
-14
-16
-18
-20
Solute flux (kg ha-1 day-1)

(a)

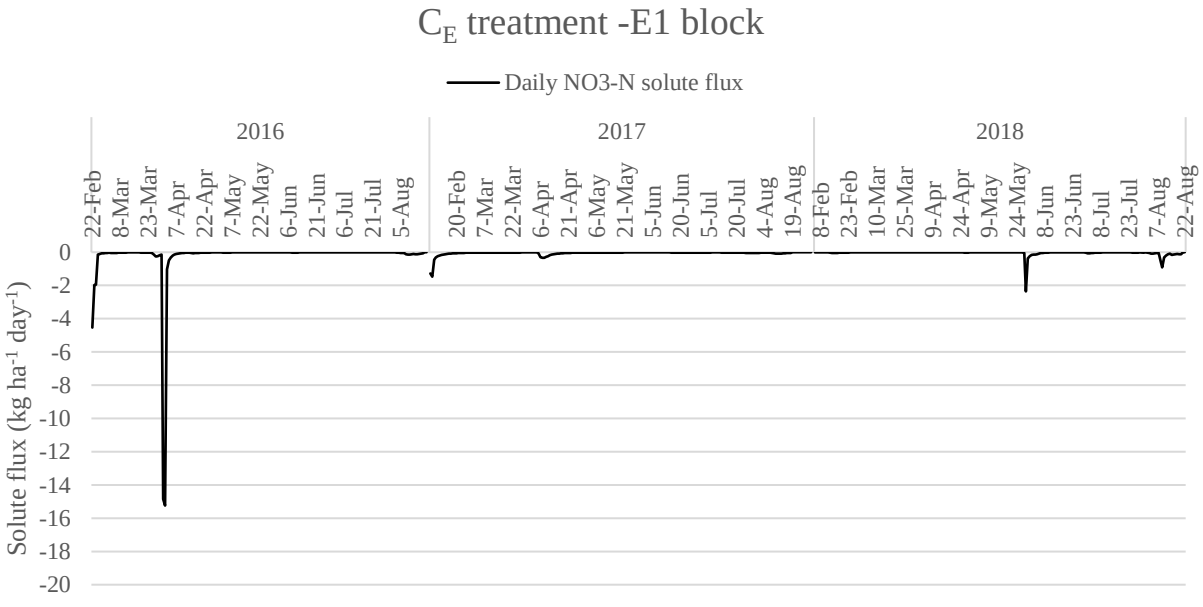
C_E treatment -E1 block
Daily NO3-N solute flux
2016
2017
2018
22-Feb
8-Mar
23-Mar
7-Apr
22-Apr
7-May
22-May
6-Jun
21-Jun
6-Jul
21-Jul
5-Aug
20-Feb
7-Mar
22-Mar
6-Apr
21-Apr
6-May
21-May
5-Jun
20-Jun
5-Jul
20-Jul
4-Aug
19-Aug
8-Feb
23-Feb
10-Mar
25-Mar
9-Apr
24-Apr
9-May
24-May
8-Jun
23-Jun
8-Jul
23-Jul
7-Aug
22-Aug
0
-2
-4
-6
-8
-10
-12
-14
-16
-18
-20
Solute flux (kg ha-1 day-1)

(b)

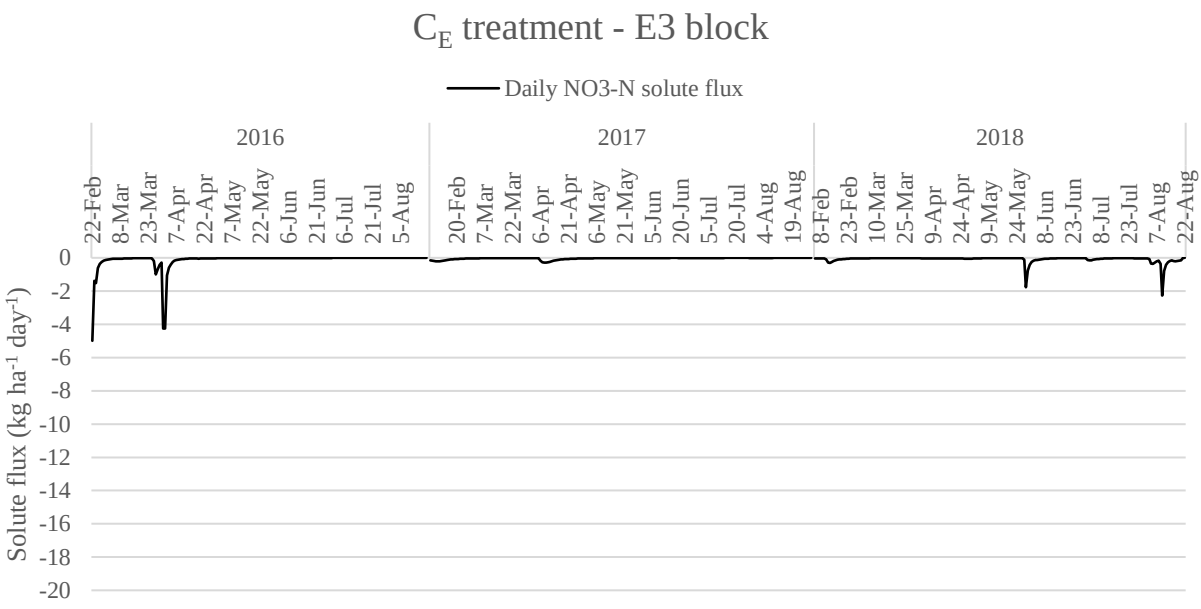
C_E treatment - E3 block
Daily NO3-N solute flux
2016
2017
2018
22-Feb
8-Mar
23-Mar
7-Apr
22-Apr
7-May
22-May
6-Jun
21-Jun
6-Jul
21-Jul
5-Aug
20-Feb
7-Mar
22-Mar
6-Apr
21-Apr
6-May
21-May
5-Jun
20-Jun
5-Jul
20-Jul
4-Aug
19-Aug
8-Feb
23-Feb
10-Mar
25-Mar
9-Apr
24-Apr
9-May
24-May
8-Jun
23-Jun
8-Jul
23-Jul
7-Aug
22-Aug
0
-2
-4
-6
-8
-10
-12
-14
-16
-18
-20
Solute flux (kg ha-1 day-1)

(c)

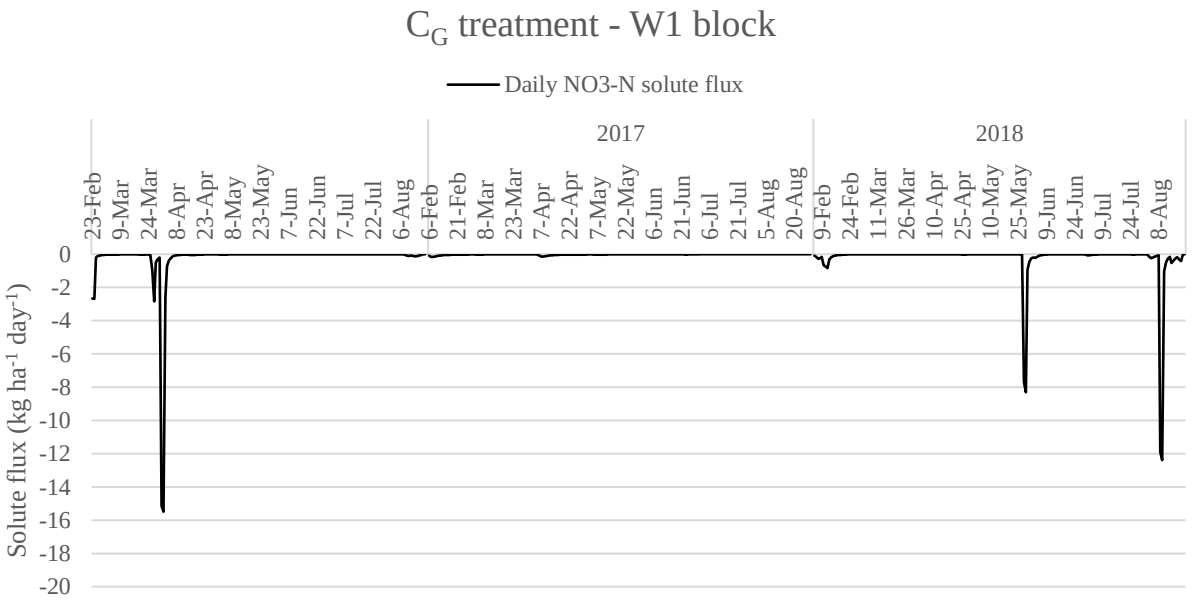
C_G treatment - W1 block
Daily NO3-N solute flux
2017
2018
23-Feb
9-Mar
24-Mar
8-Apr
23-Apr
8-May
23-May
7-Jun
22-Jun
7-Jul
22-Jul
6-Aug
6-Feb
21-Feb
8-Mar
23-Mar
7-Apr
22-Apr
7-May
22-May
6-Jun
21-Jun
6-Jul
21-Jul
5-Aug
20-Aug
9-Feb
24-Feb
11-Mar
26-Mar
10-Apr
25-Apr
10-May
25-May
9-Jun
24-Jun
9-Jul
24-Jul
8-Aug
0
-2
-4
-6
-8
-10
-12
-14
-16
-18
-20
Solute flux (kg ha-1 day-1)

(d)

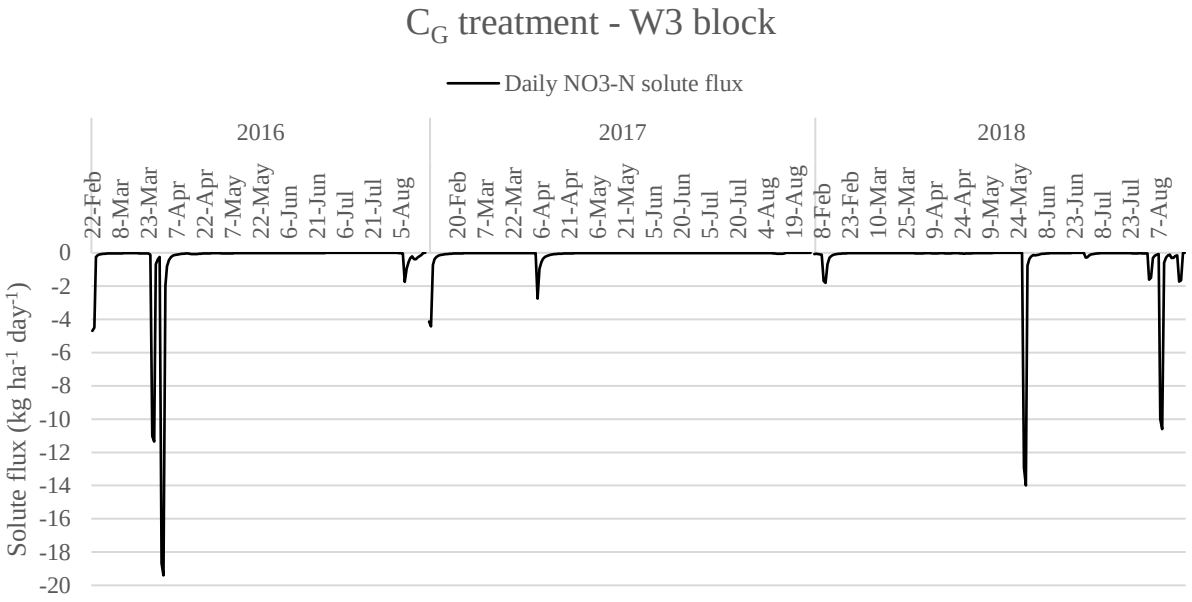

(e)

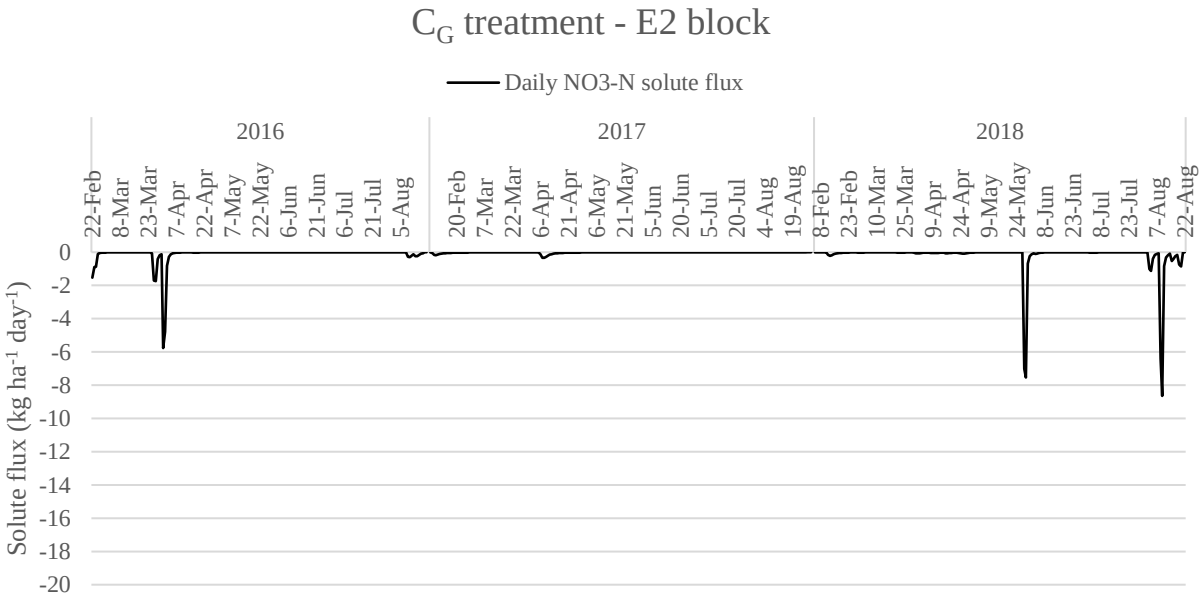

(f)

Figure 3.10 Daily NO_3-N solute fluxes at 750 mm depth during 2016, 2017 and 2018 for C_E treatment (a) W2, (b) E1, (c) E3 and C_G treatment (d) W1, (e) W3, (f) E2.

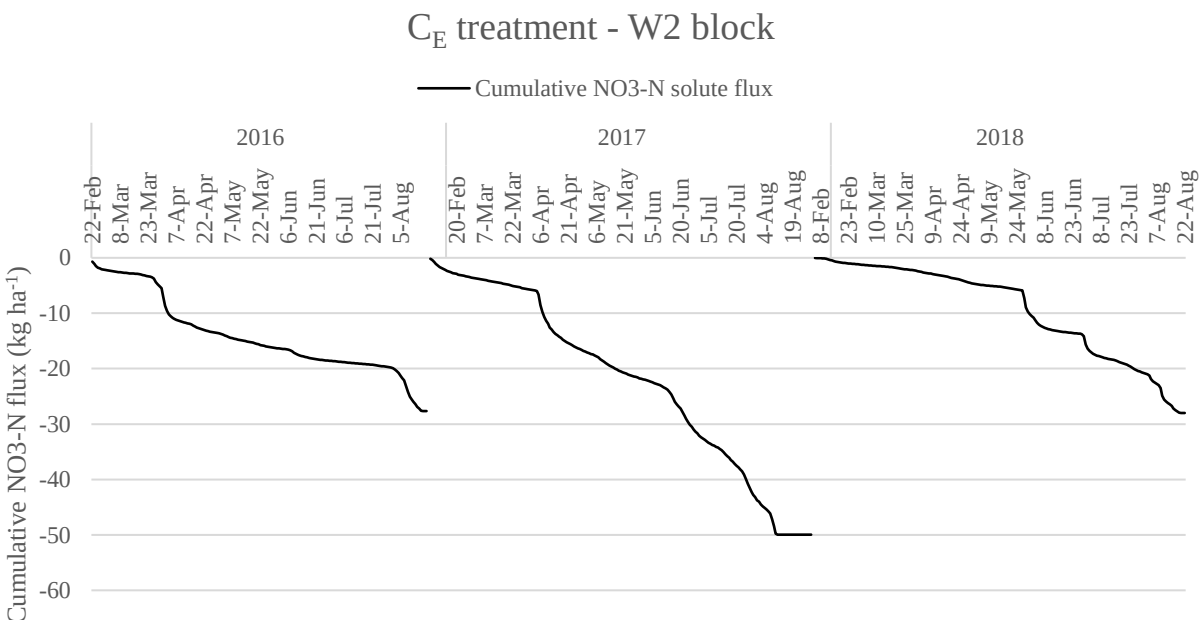
C_E treatment - W2 block
Cumulative NO3-N solute flux
2016
2017
2018
22-Feb
8-Mar
23-Mar
7-Apr
22-Apr
7-May
22-May
6-Jun
21-Jun
6-Jul
21-Jul
5-Aug
20-Feb
7-Mar
22-Mar
6-Apr
21-Apr
6-May
21-May
5-Jun
20-Jun
5-Jul
20-Jul
4-Aug
19-Aug
8-Feb
23-Feb
10-Mar
25-Mar
9-Apr
24-Apr
9-May
24-May
8-Jun
23-Jun
8-Jul
23-Jul
7-Aug
22-Aug
0
-10
-20
-30
-40
-50
-60
Cumulative NO3-N flux (kg ha-1)

(a)

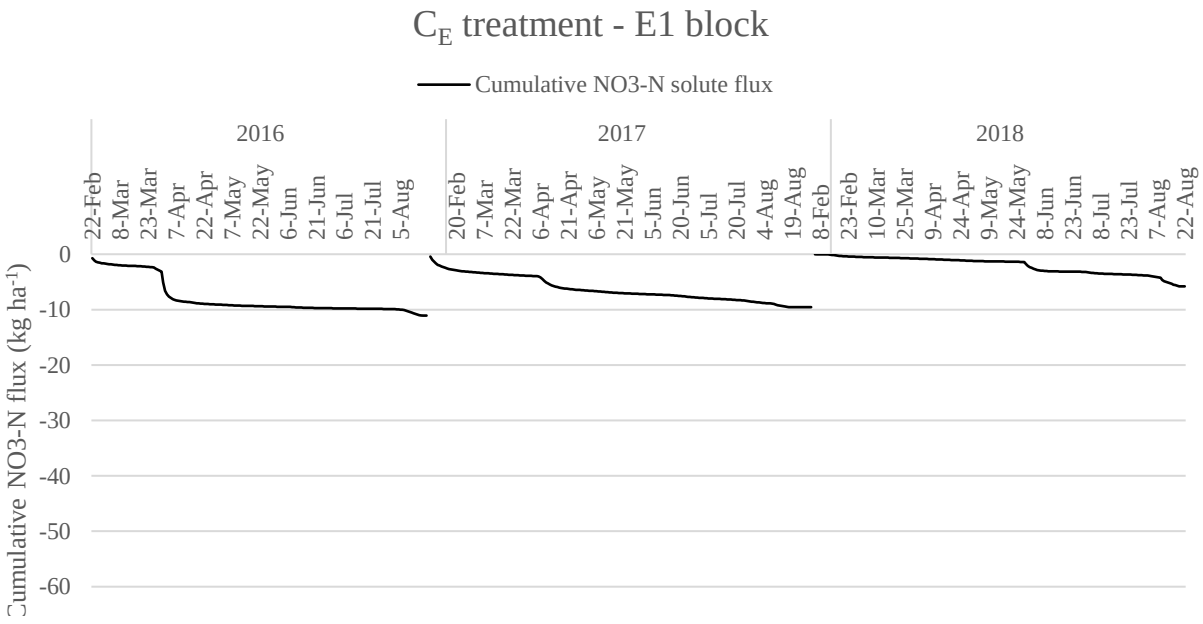
C_E treatment - E1 block
Cumulative NO3-N solute flux
2016
2017
2018
22-Feb
8-Mar
23-Mar
7-Apr
22-Apr
7-May
22-May
6-Jun
21-Jun
6-Jul
21-Jul
5-Aug
20-Feb
7-Mar
22-Mar
6-Apr
21-Apr
6-May
21-May
5-Jun
20-Jun
5-Jul
20-Jul
4-Aug
19-Aug
8-Feb
23-Feb
10-Mar
25-Mar
9-Apr
24-Apr
9-May
24-May
8-Jun
23-Jun
8-Jul
23-Jul
7-Aug
22-Aug
0
-10
-20
-30
-40
-50
-60
Cumulative NO3-N flux (kg ha-1)

(b)

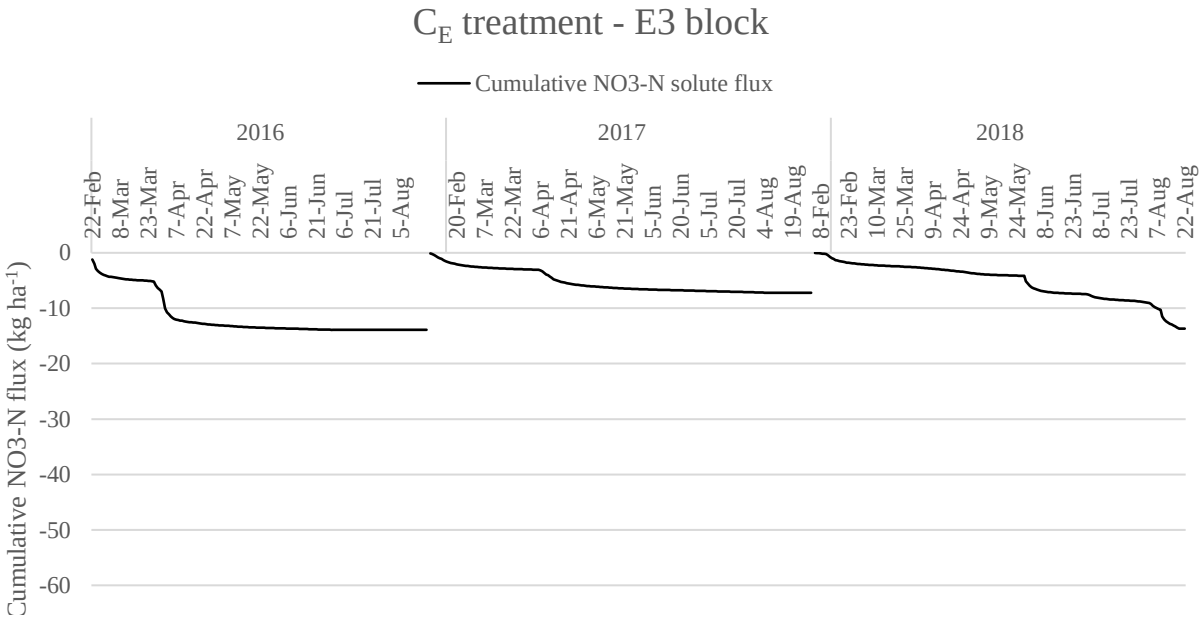
C_E treatment - E3 block
Cumulative NO3-N solute flux
2016
2017
2018
22-Feb
8-Mar
23-Mar
7-Apr
22-Apr
7-May
22-May
6-Jun
21-Jun
6-Jul
21-Jul
5-Aug
20-Feb
7-Mar
22-Mar
6-Apr
21-Apr
6-May
21-May
5-Jun
20-Jun
5-Jul
20-Jul
4-Aug
19-Aug
8-Feb
23-Feb
10-Mar
25-Mar
9-Apr
24-Apr
9-May
24-May
8-Jun
23-Jun
8-Jul
23-Jul
7-Aug
22-Aug
0
-10
-20
-30
-40
-50
-60
Cumulative NO3-N flux (kg ha-1)

(c)

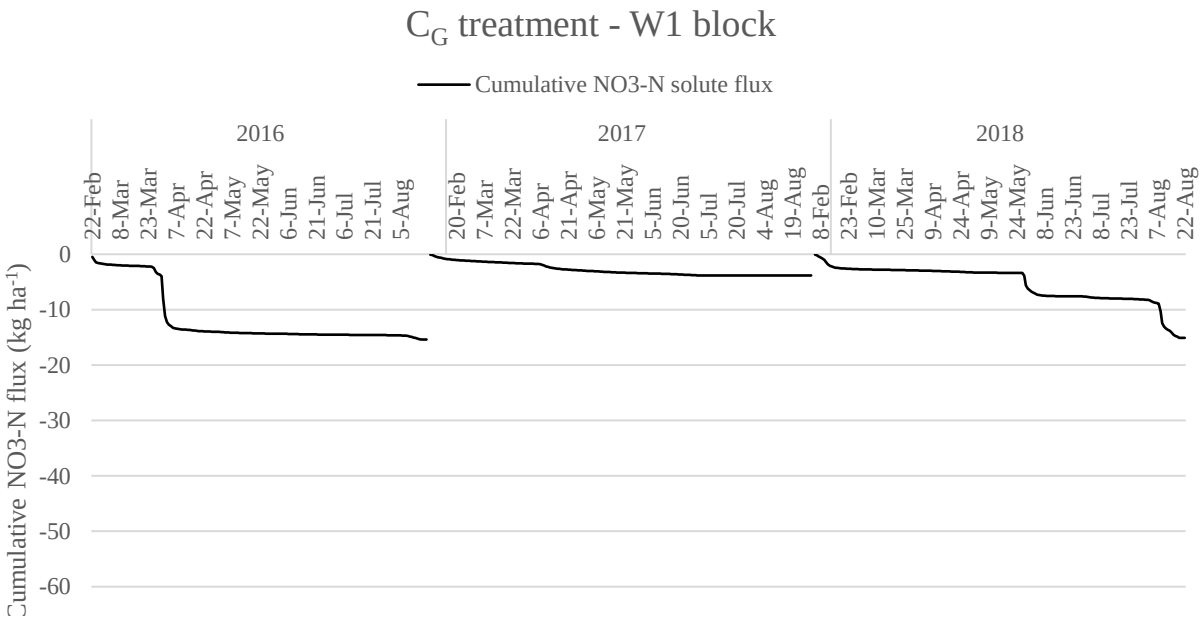
C_G treatment - W1 block
Cumulative NO3-N solute flux
2016
2017
2018
22-Feb
8-Mar
23-Mar
7-Apr
22-Apr
7-May
22-May
6-Jun
21-Jun
6-Jul
21-Jul
5-Aug
20-Feb
7-Mar
22-Mar
6-Apr
21-Apr
6-May
21-May
5-Jun
20-Jun
5-Jul
20-Jul
4-Aug
19-Aug
8-Feb
23-Feb
10-Mar
25-Mar
9-Apr
24-Apr
9-May
24-May
8-Jun
23-Jun
8-Jul
23-Jul
7-Aug
22-Aug
0
-10
-20
-30
-40
-50
-60
Cumulative NO3-N flux (kg ha-1)

(d)

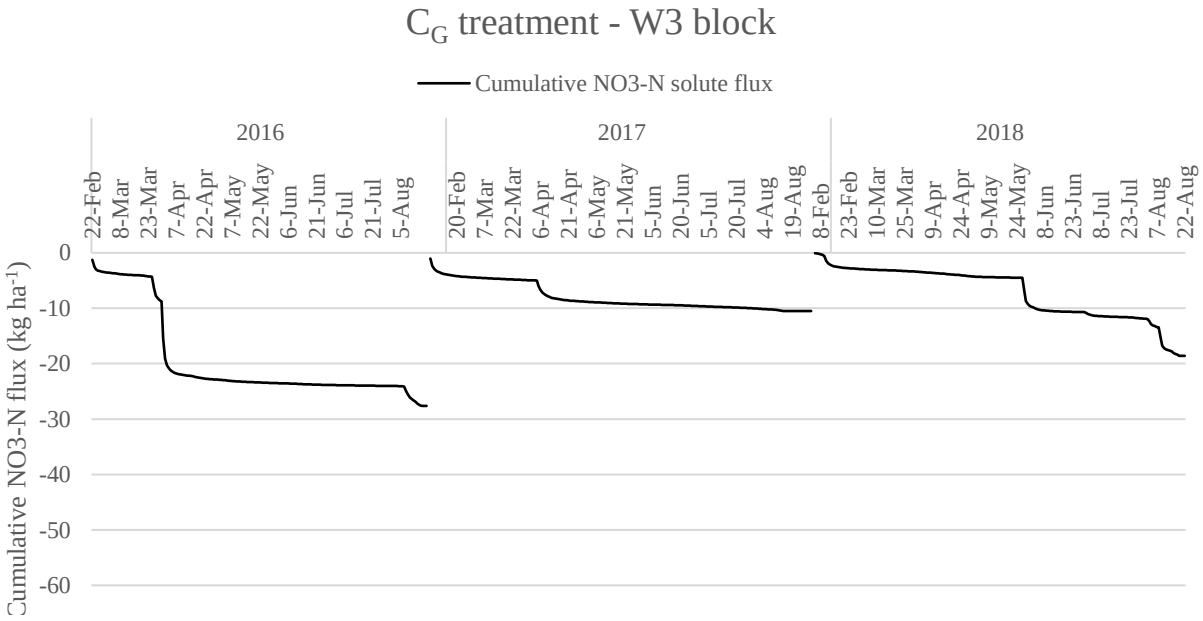

(e)

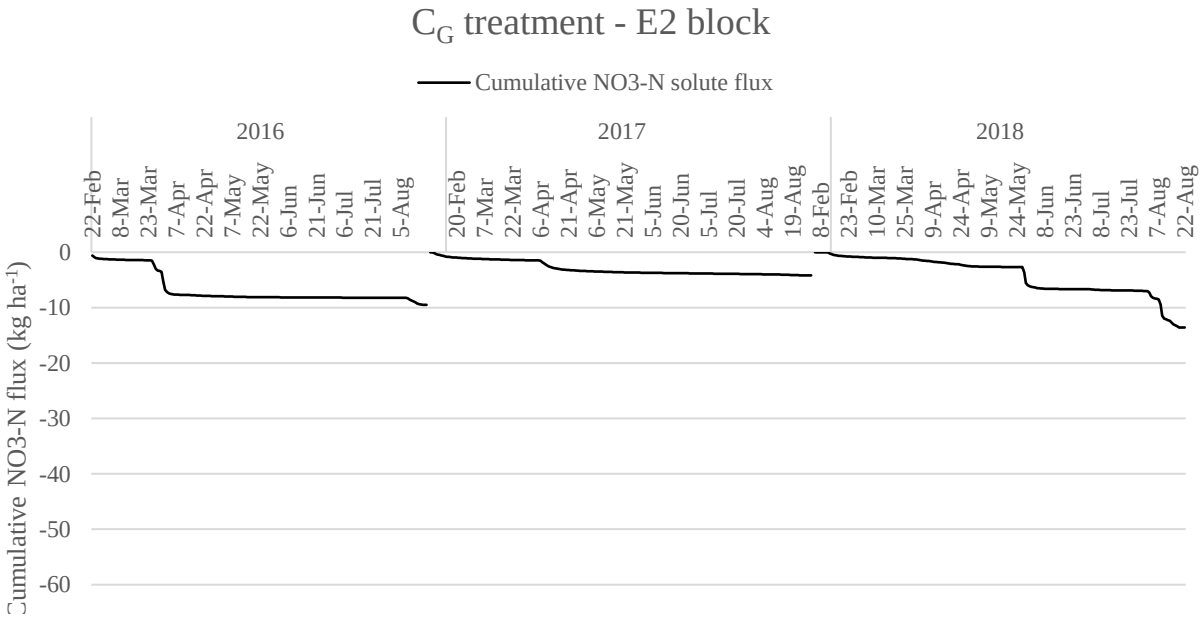

(f)

Figure 3.11 Cumulative NO_3-N solute fluxes at 750 mm depth during 2016, 2017 and 2018 for C_E treatment (a) W2, (b) E1, (c) E3 and C_G treatment (d) W1, (e) W3, (f) E2.

CHAPTER 4

SIMULATING THE EFFECT OF IRRIGATION SCHEDULING ON NITROGEN LEACHING AND MAIZE YIELD[3]

[3] Pavlou, D., A. Orfanou, M.L. Cabrera, G. Hoogenboom, W.M. Porter, D.E. Radcliffe, and G. Vellidis. To be submitted to *Agricultural Water Management*.

Abstract

In the southeastern U.S., irrigation is essential for crop production. However, used in excess, irrigation can lead to surface runoff and leaching. The goal of this study was to use HYDRUS-1D and DSSAT CERES Maize models to compare two maize irrigation scheduling management strategies to rainfed production and evaluate their effect on the amount of water used for irrigation, maize yield, and NO_3-N leaching. The irrigation scheduling management strategies were the University of Georgia Extension Checkbook method (hereafter referred to as the Checkbook method) and a sensor-based method that used a matric potential threshold of -35 kPa for triggering irrigation. The three strategies were evaluated under two high fertilization management scenarios used by growers pursuing high yields. The modeling study was based on an experiment conducted at the 1.44 ha NESPAL field located on the University of Georgia's (UGA) Tifton campus. The simulation results showed that the sensor-based method resulted in in the lower water use and less NO_3-N leaching as well as higher maize yields compared to the University of Georgia Extension Checkbook Method. The simulation results also showed that irrigation scheduling strategies influenced NO_3-N leaching more than fertilization treatments. The study indicates that irrigation scheduling methods that use real-time data to schedule irrigation, especially in sandy soils such as the ones used in this study, result in better overall management of resources.

Introduction

Farmers depend on irrigation and N fertilizers to increase yields (Erisman et al., 2008). Increasing use of irrigation water and fertilizers results in higher yields but may also result in unintended environmental problems. For example, Maize production in the USA uses an average

of 157 kg N ha^{-1} making it the largest consumer of N fertilizer in the country (USDA, 2013). The use of N fertilizer has resulted in significant maize yield increases but nitrogen use efficiency (NUE) is below 50% (Zhang et al., 2015) resulting in nonpoint source pollution and especially NO_3-N leaching below the root zone contaminating surface waters and groundwater (David et al., 2010). Similarly, water use has been increasing at more than twice the rate of population increase (UN, 2020). A major factor in this increase is water used for irrigation. Seventy percent of fresh water use worldwide is for agriculture (AQUASTAT, 2016). In the USA, 25% of the total irrigated acreage is used for maize production (USDA, 2019).

Irrigation scheduling methods

Data-driven irrigation scheduling methods have been shown to significantly improve irrigation water use efficiency (WUE) but also to result in higher profitability (Bhattarai et al., 2020; Vellidis et al., 2016a). The most commonly used methods by farmers in the USA are soil moisture sensors and evapotranspiration (ET) based water use models. Many farmers in Georgia (USA) utilize an ET-based method that uses historical average weekly ET rates to recommend weekly irrigation applications. This method is commonly referred to as the "checkbook" method and will be described in more detail later. Sensor-based scheduling is becoming more popular as wireless telemetry allows farmers to view data remotely on smartphone platforms. Orfanou et al. (2019) assessed these two methods by testing final maize yield under different plant densities and tillage systems in two locations in Georgia. The results of this study showed that less water was applied with the sensor-based method than with the checkbook method with similar yield results.

Increased NO_3^-N leaching is sometimes the unintended consequence of irrigation as excess irrigation water can push soluble nitrogen below the root zone (Gheysari et al., 2009; Spalding et al., 2001). Relatively few field studies have been conducted which quantify both the yield response of irrigation and the resulting environmental effects – especially in the southeastern coastal plain of the USA where soils are mostly sandy and require both high rates of fertilization and regular irrigation to produce high yields. This is primarily because of the expense and difficulty of conducting such multivariate studies.

Mathematical simulation models

Mathematical simulation models can be used to evaluate a wide variety of management scenarios provided the models are calibrated and validated appropriately. HYDRUS-1D (Rassam et al., 2018; Simunek et al., 2016) is a widely-used water and solute transport simulation model. It uses the Richards equation to simulate water flow and the Advection Dispersion Equation (ADE) to simulate solute transport. HYDRUS-1D has been used in different studies for irrigation management assessments. For instance, Tafteh and Sepaskhah (2012) used HYDRUS-1D for simulating water and NO_3^-N leaching by testing different irrigation methods and fertilization rates in rapeseed and maize production. In a cotton study, the AquaCrop model (Raes et al., 2009) was used in conjunction with HYDRUS-1D to develop the optimum and deficit irrigation schedule under shallow groundwater conditions (Akhtar et al., 2013). Zhang et al. (2020) applied HYDRUS-1D to simulate water movement and NO_3-N leaching in the unsaturated zone with success. A study by Shahrokhnia and Sepaskhah (2018) showed that the use of HYDRUS-1D can be beneficial for evaluating management practices such as irrigation, planting methods, and N fertilization rates regarding safflower.

Although water and solute transport models like HYDRUS-1D include crop growth functions, dedicated crop growth models are best used to simulate crop response to environmental conditions and the response of yield to irrigation and fertilization management practices. The Decision Support System for Agrotechnology Transfer (DSSAT) is a suite of crop models that is widely used around the globe (Hoogenboom et al., 2015; Hoogenboom et al., 2019; Jones et al., 2003). The DSSAT maize model known as CERES-Maize has been used since 1986 for conducting experiments in a simulation environment (Jones, 1986). Saseendran et al. (2008) calibrated and validated CERES-Maize for northeastern Colorado to assess irrigation methods and to optimize irrigation WUE. The study included rainfed production. Kisekka et al. (2016) used CERES-Maize model to simulate yield while evaluating management practices for improving the use of limited water for irrigating maize.

The goal of this study was to use the HYDRUS-1D and DSSAT-CERES Maize models to evaluate the environmental and yield effects of maize irrigation scheduling management strategies under two different fertilization regimes in the southeastern coastal plain of the USA.

Materials and Methods

Field experiment description

This work was based on a field experiment conducted at the 1.44 ha NESPAL field located on the University of Georgia's (UGA) Tifton campus (31° 28.736'N, 83° 31.916'W). The three-year experiment, beginning in 2016 and ending in 2018, was conducted to evaluate the effect of high fertilization rates on maize yield and water quality. Tifton is located in the southeastern coastal plain of the USA. The climate is subtropical providing abundant rainfall and a long growing season. Average annual precipitation for the study period was 1210 mm.

For the field experiment, the NESPAL field was divided into six blocks of cultivated land separated by grassed berms to prevent overland flow between blocks. The three western blocks were labeled W1, W2, and W3 and the three eastern blocks were labeled E1, E2, and E3 as shown in Figure 4.1. Block size ranged from 0.18 ha to 0.34 ha.

Two maize fertilization treatments based on high maize yield goals were used in the field experiment. The first was a treatment recommended by Georgia maize producers who have consistently achieved high yields. This treatment was designated as C_G and had a yield goal of 28 Mg ha^{-1} (450 bu ac^{-1}). The second treatment used the UGA Extension high yield goal of 22 Mg ha^{-1} (350 bu ac^{-1}) and was designated as C_E. There were three replicates of each treatment.

Table 4.1 presents the management practices used during each year of the project. These are pertinent to the modeling scenarios that are described below. Because instrumentation was being installed prior to the planting of the first maize crop which resulted in soil disturbance, conventional tillage was used for the 2016 growing season. A cover crop and strip tillage were used for the remaining two years of the study. Plant density was the same for the two first years of the project but increased to 97850 plants ha^{-1} for the C_G treatment in 2018. More fertilizer side-dress events were used in 2017 and 2018 than in 2016.

Field data collection

Four to six 750 mm soil cores were collected before planting and after the maize was harvested from block depending on size. Each core was separated into five 150 mm segments for analysis that included bulk density, soil texture, and NH_4-N and NO_3-N concentrations. Soil moisture data was collected hourly with a wireless soil moisture sensor network (Orfanou et al., 2020a).

Maize crop height and leaf area were measured during the V3, V4, V5, V6, V7, V8, V10, V12, V14, VT vegetative stages and the R1, R2, R3, R4, R5 and R6 reproductive stages during the 2018 growing season (Orfanou et al., 2020a). Leaf area was used to estimate the Leaf Area Index (LAI).

Daily meteorological data, i.e., minimum and maximum air temperature (^{o}C), solar radiation (MJ m^{-2}), relative humidity (%) and wind speed (m s^{-1}) were retrieved from the Tifton campus University of Georgia Weather Network (UGAWN) weather station which was approximately 1.5 km from the field. Sunshine (hr) was retrieved from the Weather Atlas webpage. Precipitation was measured with an automated tipping bucket rain gage located approximately 100 m from the field.

Groundwater was captured by installing drain tile along the western, southern, and eastern boundaries of each block (Figure 4.1) prior to the 2016 growing season. The drain tile also isolated the blocks from any shallow groundwater moving laterally from higher positions of the landscape. Blocks W1 and E1 were located at the top of the slope and are unlikely to receive shallow groundwater flows from the north (top of the figure). The circled "G" indicates where the drain tile was sampled to collect the ground water samples from each block. Groundwater samples were collected manually twice per week in 1 L plastic bottles when there was flow. (Pavlou et al., 2020a) described the field experiment in detail.

Simulation Scenarios

HYDRUS-1D and CERES-Maize were calibrated using the inputs, management practices, and field data from the 2018 growing season and evaluated using 2016 and 2017 growing seasons. Because of differences in soil texture, elevation, and yield, for modeling

purposes, each of the six blocks in the NESPAL field were simulated as individual field to increase model performance (Pavlou et al., 2020b). For the simulation scenarios described below, inputs and management practices were held constant except for the parameter being evaluated during the simulation.

HYDRUS-1D

HYDRUS-1D was used for simulating water flow, solute transport, and predicting water and NO_3-N bottom fluxes (leaching) during the maize growing seasons. As explained earlier, individual HYDRUS-1D models was used for each block. The management practices and field data described earlier were used to represent the natural system (Pavlou et al., 2020b). Soil water flow was simulated from the date that fertilizer was applied prior to planting maize until harvest during each growing season. Solute transport was simulated from the day that the soil core samples were collected prior to planting until harvest (Table 4.2). To match the soil cores, the models' soil profile was set to 750 mm with five soil materials or layers each 150 mm in depth. Water and solute fluxes exiting the profile at this depth were considered leachates.

The models of water flow and solute transport were calibrated by optimizing the soil hydraulic and solute transport parameters for each block individually. The soil hydraulic parameters consist of residual water content θ_r, water content at saturation θ_s, parameters α and n and soil hydraulic conductivity K_s. The solute transport parameters include adsorption coefficients for ammonium and nitrate K_d, nitrification rate k and denitrification rate μ. The soil hydraulic parameters were optimized for the water flow models by fitting the simulated to observed pressure heads. The observed data were obtained hourly by soil moisture sensors installed at 200, 400 and 600 mm. These data were averaged by day and block. When a good fit

was achieved, the optimized soil hydraulic parameters were used in the solute transport model. The solute transport parameters were optimized when there was good correspondence between simulated NO_3-N data in leachate at 750 mm depth and NO_3-N concentrations in groundwater samples. The optimized parameters are presented in Tables 4.3 and 4.4. More details about the setup, calibration and evaluation of model can be found in Pavlou et al. (2020b).

CERES-Maize

CERES-Maize was used by Orfanou et al. (2020b) to simulate growth, development of maize at the NESPAL field as a function of soil, plant, and atmosphere dynamics during the 2016, 2017 and 2018 growing seasons. Individual models was used for each block. The models were calibrated by adjusting the P1, P2, P5, G2, G3 and PHINT cultivar coefficients to achieve a good fit between simulated and observed data for leaf number, leaf weight, vegetative N concentration and final yield. The 2018 data were used for calibration while 2016 and 2017 data were used for model evaluation. Orfanou et al. (2020c) used models of the three years to evaluate different scenarios and identify the limiting factors for achieving high yields. This model, as calibrated by Orfanou et al. (2020b), was used in this study for predicting maize yields resulting from the different management scenarios evaluated for this study.

Management scenarios

The response of leaching to the two irrigation scheduling management strategies (Checkbook method and a sensor-based method) as well as rainfed production for the two fertilization treatments (C_G and C_E) was evaluated using the HYDRUS-1D model.

The Checkbook method is a calendar method for scheduling irrigation that provides the user with the amount of water needed by the crop for each week after planting. The weekly water

requirements were developed by using the FAO-56 crop coefficient (Kc) (Allen et al., 1998) values for maize and a 30-year weekly average of evapotranspiration (ET) from the southeastern coastal plain region of Georgia (Figure 4.2). ET data were retrieved from the historical record of the University of Georgia Weather Network (http://weather.uga.edu/). Maize weekly and daily water requirements for Georgia are published in the University of Georgia's annual Corn Production Guide (Lee, 2019). To apply this method, the user subtracts rain received from the weekly requirement and provides the rest through irrigation. Daily crop water use is determined by dividing the weekly crop water use by seven.

To minimize leaching, the amount of irrigation water applied during each irrigation event during the Checkbook method simulations was based on the soil's water holding capacity. The soil type at the NESPAL field is a Tifton loamy sand with a water holding capacity of 0.1 mm per mm of soil. The amount of water applied at each event was 50% of water holding capacity. During peak water use periods, multiple irrigation events were applied each week to achieve the amounts recommended by the Checkbook method.

The sensor-based scenario used a matric potential threshold to schedule irrigation. The University of Georgia Smart Sensor Array (UGA SSA) (Vellidis et al., 2008) was used to measure matric potential (soil water tension). The UGA SSA is a wireless soil moisture sensing system that collects soil water tension (SWT) data continuously using Watermark® (Irrometer, Riverside, California, USA) soil moisture sensors. UGA SSA nodes consist of a probe with three Watermark® sensors and an electronics package to process and transmit data. This was also the method used to schedule irrigation in the field during the field experiment. A probe consisting of three Watermark® sensors was installed in each of the 16 maize plots. The sensors were centered at depths of 200, 400 and 600 mm. Irrigation scheduling was based on SWT at 07:00 daily. A

weighted average SWT was calculated by applying the SWT readings from the three sensor depths (200, 400 and 600 mm) to equation (Eq. 19). The weighting factors α, β, and γ varied by crop phenological stage and anticipated root depth at that stage as shown in Table 4.5. In general, as the root system lengthened, more weight was given to the deeper sensors (Orfanou et al., 2019). An irrigation threshold of 35 kPa was established based on past research. Although this is a relatively low irrigation threshold, it was established because with sandy soils, SWT increases sharply after 35 kPa as plant available soil water is rapidly depleted. To avoid large SWT values and the associated crop water stress, the entire field was irrigated when the weighted SWT of at least one block was in the range of 30-35 kPa.

$$\text{SWT Weighted Average} = \alpha * \text{SWT}_{20\text{cm}} + \beta * \text{SWT}_{40\text{cm}} + \gamma * \text{SWT}_{60\text{cm}} \quad \text{Eq. 19}$$

Where,

α, β and γ are the weighting factors based on the phenological stage of the maize as reported in Table 4.5.

Figure 4.3Figure 4. shows the measured response of SWT in each of the field experiment's six blocks during the three maize growing seasons. The primary y-axis shows SWT while the secondary y-axis shows water received through irrigation (light blue bar) or rainfall (dark blue bar). The red dashed line represents the irrigation threshold of 35 kPa. For reasons described by Pavlou et al. (2020a), SWT exceeded the 35 kPa irrigation threshold on some occasions. Actual irrigation events were used in this modeling scenario.

The third management scenario was the rainfed method where no irrigation was applied and the only source of water was precipitation. Only 23% of Georgia's maize fields are rainfed with most of those located in northern Georgia. However, rainfed treatments are typically used as a benchmark when comparing the response of maize to irrigation scheduling methods.

The amount of water applied by irrigation and received via precipitation during the three growing seasons for each of the scenarios is shown in Table 4.6. The sensor-based irrigation scheduling scenario resulted in 65%, 48%, and 33% more water received (irrigation + precipitation) than the rainfed scenario for 2016, 2017, and 2018, respectively. The Checkbook scenario resulted in 78%, 114%, and 49% more water received than the rainfed scenario for 2016, 2017, and 2018, respectively. Figure 4.4 shows the temporal distribution of irrigation and precipitation events during the simulation periods.

Results

HYDRUS-1D water bottom fluxes

The cumulative water bottom fluxes (leachate from the bottom of the 750 mm soil profile) are summarized in Figure 4.5 and Table 4.7 in units of cm. Both show the response of an individual block to the three irrigation scheduling scenarios during the three maize growing seasons. As a reminder, blocks W1, W3, and E2 received the C_G treatment while blocks W2, E1, and E3 received the C_E treatment. Figure 4.5 shows the response over time while Table 4.7 shows the total amount of leachate. The leachate results correspond to the amount of water used by each scenario (Table 4.6) with the Checkbook method resulting in the largest losses of water from the soil profile followed by the sensor-based scenario and the rainfed scenario. A statistical analysis of the simulation results using JMP® Pro 14.1.0 showed that these differences were

statistically significant by comparing the combined results of the three years. Comparing the results within years, the mean total leachate from the Checkbook method was statistically higher than the other two methods in 2017 ($p_{rainfed\text{-}checkbook} = 0.0084$, $p_{sensor\text{-}checkbook} = 0.0118$) and only different from rainfed in 2018 ($p_{rainfed\text{-}checkbook} = 0.0112$) . There were no statistical differences in 2016 ($p > 0.05$). Across all three years, the Checkbook method had statistically significantly more leachate than the other two scenarios.

In addition, the blocks with the C_E treatment had consistently larger losses than the blocks with the C_G treatment, something that can be explained by higher biomass in the C_G blocks (Orfanou et al., 2020a). However, no statistical differences were observed between the two treatments at the $a = 0.05$ level (Table 4.7).

Figure 4.5 represents the effect of irrigation and precipitation events on the movement of water through the soil profile. For example, at the end of the March 2016 growing season, two rainfall events totaling 107 mm occurred. The plants were still at the early vegetative stages, there was no cover crop and the field had been prepared using conventional tillage. As a result, a water flux of approximately 100 mm, an amount similar to the combined precipitation events was lost from the soil profile in all six blocks. After that event, the water flux was near zero for five of the six blocks until June which coincided with a period of less frequent precipitation events. Bottom fluxes began to occur again in June and the fluxes of the different irrigation scheduling strategies begin to diverge.

Overall, trends of bottom flux between blocks were similar but there were differences in the magnitude of the bottom flux. Especially surprising were the simulation results for block W2 (Figure 4.5d) where the bottom flux was two to three times larger than that of other blocks depending on the scheduling scenario that was compared. The HYDRUS-1D model calibration

and evaluation results were the poorest for this block for two of the three years of the simulation (Pavlou et al., 2020b) and it is likely that simulation results for this block are less accurate than for the other five blocks. Nevertheless, the differences observed between blocks reaffirms the observations made in other studies that spatial variability of soils and topography significantly affect irrigation scheduling (Liakos et al., 2018; Vellidis et al., 2016c).

It is also clear from the simulations that the Checkbook method results in more leachate than sensor-based irrigation scheduling management strategies. This is because the Checkbook method does not respond to current environmental conditions. It recommends the same amount of irrigation for a cool and cloudy week as for a hot and sunny week. If the Checkbook method is strictly applied as was done in the simulations and is done during field experiments (Vellidis et al., 2016b), it frequently results in excessive irrigation. However, growers using this method may adapt their irrigation events to match environmental conditions and thus reduce the overall amount of irrigation water applied. The differences between the Checkbook method and the other two scenarios are more apparent in 2017 and 2018 than 2016. This is likely the result of differences in tillage. As described earlier, conventional tillage was used in 2016 while strip tillage with heavy cover crop residue was used in 2017 and 2018. This resulted in more infiltration and less runoff in 2017 and 2018. Since more irrigation events were needed in the Checkbook method simulations, more of that irrigation water was lost to runoff and less infiltrated in 2016 which indirectly resulted in less leachate.

HYDRUS-1D NO_3-N bottom fluxes

The cumulative NO_3-N bottom fluxes (NO_3-N leached from the bottom of the 750 mm soil profile) are summarized in Figure 4.6 and Table 4.8 in units of kg ha^{-1}. The flux can also be

considered the load of N lost to leaching per unit area. The trends are similar to those for the water bottom fluxes which is expected as NO_3-N is dissolved in soil water and moves below the root zone with soil water. The largest NO_3-N bottom fluxes were associated with the Checkbook method irrigation scheduling scenario followed by the sensor-based irrigation scheduling scenario. The smallest NO_3-N bottom fluxes were associated with the rainfed scenario. A statistical analysis of the simulation results shows that these differences were statistically significant at the $a = 0.05$ level by comparing the combined results of the three years. When comparing the results by year, the Checkbook method was statistically different from the other two methods in 2018, while there were no statistically significant differences in 2016 and 2017.

If the W2 block is excluded from the treatment averages in Table 4.8 for the reasons described earlier, the C_G treatment resulted in higher cumulative NO_3-N bottom fluxes than the C_E treatment in 2016 and 2018. This was expected as more fertilizer was applied to the C_G treatment and the total fertilizer was split to almost the same number of applications for both treatments. In contrast, during 2017, six side-dress applications were used for the C_G treatment and only two for the C_E treatment. Six applications with a higher total amount of N resulted in the less leaching than two more concentrated applications with a lower total amount of N. Specifically, in 2017, 40% more N fertilizer was applied to the C_G treatment in six side-dress applications which resulted in 7%, 26%, and 29% less NO_3-N leaching than the C_E treatment's Checkbook method, sensor-based, and rainfed scenarios, respectively. The same trend was observed when comparing 2016 to 2018. In 2016, two side-dress applications were used for both treatments while in 2018, four side-dress applications were used for C_G and three for C_E. More leaching was simulated for 2016 than 2018 with similar precipitation patterns. These results emphasize the importance of splitting side-dress N into more applications and are consistent with

findings from both experimental and modeling studies (S. Kanwar et al., 1988; Thomas et al., 1990). The C_G treatment had consistently smaller losses than C_E, and a probable explanation is the higher biomass as mentioned earlier, but the differences between the C_E treatment and the C_G treatment were not statistically significant (Table 4.8).

Table 4.9 presents N leached as a percentage of N applied for each of the simulated scenarios. Overall, the percentage of N leached by the Checkbook method was consistently higher than the percentage leached by the other two scenarios. The percentage of N leached when the Checkbook method was applied was statistically higher than the other two scenarios for the C_G treatment during 2017 ($p < 0.0001$) and 2018 ($p_{rainfed\text{-}checkbook} < 0.0001$ and $p_{sensor\text{-}checkbook} = 0.0002$) growing seasons. This indicates that excess irrigation results in higher N leaching. Similarly, the percentage of N leached by the C_E treatment was consistently higher than the percentage leached by the C_G treatment across all irrigation scenarios but no significant differences were observed.

Overall, the simulation results indicated irrigation strategies had a higher influence on NO_3-N leaching than fertilization treatments. This conclusion is supported by comparing the average differences in simulated NO_3-N leaching between irrigation scheduling methods to differences between fertilization treatments in Table 4.9. In general, the average differences between irrigation scheduling strategies is larger than the difference between fertilization treatments.

CSM-CERES-Maize yield

CSM-CERES-Maize was used to simulate the yield response of the irrigation management scenarios (Figure 4.7). Figure 4.7a presents the simulated yields for the C_G

fertilization treatment and Figure 4.7b presents the simulated yields for the C_E fertilization treatment. Regardless of the fertilization treatment or the year, the sensor-based method produced the highest simulated yields. This is likely because sensor-based irrigation events coincided best with drying soil conditions in the model. As expected, the lowest yields resulted from the rainfed scenario. In 2016, the rainfed yield results were quite low because the temporal distribution of rainfall resulted in water stress at the beginning and during the grain filling period.

However, both fertilization treatments show a steady increase in rainfed yields that are not directly related to total precipitation received during the growing season which was 630 mm in 2016, 500 mm in 2017, and 800 mm in 2018 (Table 4.6). One possible explanation is the timing of the precipitation events – there were more precipitation events during the reproductive stage (May-July) in 2017 and 2018 than in 2016. Rainfed yields similar to the simulated rainfed results were measured by the University of Georgia State Wide Variety Trial program in Tifton. For example, the average rainfed yield across many maize varieties was 12.8 Mg ha^{-1} for 2017 and 11.8 Mg ha^{-1} for 2018 (Mailhot et al., 2017; Mailhot et al., 2018). Another possible explanation is that the cover crop and strip tillage used during the 2017 and 2018 growing seasons allowed for more infiltration and therefore more plant available soil water during the growing season. This explanation is supported by the HYDRUS-1D water bottom fluxes that were generally higher for the rainfed scenario in 2016 than 2017 and 2018 (Figure 4.5). It is also supported by surface runoff data collected during the field experiment that showed much higher runoff in 2016 than 2017 and 2018 (Pavlou et al., 2020a).

Simulated maize yields were consistently lower for the Checkbook Method scenarios than the sensor-based scenarios. This may be caused by overly high soil moisture conditions and by leaching of nutrients below the root zone (Tables 4.8 and 4.9, Figure 4.6). Overall, the best

simulated yields were for the sensor-based scenario of the C_G treatment in 2016. It is likely that these higher yields were driven by 10% higher solar radiation during the 2016 growing season.

Discussion and conclusions

The traditional process of decision making for a farmer can be described as a set of eight functions; values and goals, problem detection, problem definition, observation, analysis, development of intention, implementation, and responsibility bearing (Ohlmer et al., 1998). Most farmers depend on their intuition, experience, and available data for making decisions and taking action. However, the complexity of decisions due to the increasing scale of farming operations, field variability, weather conditions, crop varieties, markets, and government policies can make the decision process very difficult because of the permutation of options. Simulation models such as the ones applied in this study can be used as decision support systems (DSS) to assist farmers in making data-driven decisions. For example, the models used in this study clearly indicate that sensor-based irrigation scheduling results in less NO_3-N leaching as well as higher yields when compared to the more traditional ET calendar-based irrigation scheduling methods like the Checkbook method. Irrigation scheduling studies in Georgia (Orfanou et al., 2019) and Alabama (Filho, 2016) have shown that calendar scheduling methods produce similar yields to sensor-based scheduling methods but consume much more irrigation water.

There are few published field studies documenting leaching from maize associated with different irrigation scheduling methods in the southeastern United States which makes modeling results even more valuable. Another important finding of this study is that multiple side-dress applications resulted in lower leaching rates and this should increase nitrogen use efficiency. He

et al. (2012) also showed the environmental advantages of multiple fertilizer applications by using CSM-CERES Maize.

The relative response of modeling scenarios from this study can assist farmers in making decisions on whether or not to invest in soil moisture sensors as they can compare water use, fertilizer needs, and yields of different management strategies. The modeling results can also provide state and federal agencies with information that they can use to make decisions about best management practices that should be incentivized to increase adoption.

In analyzing 50-year trends in N use, Lassaletta et al. (2014) found that increasing N application rates leads to a disproportionately low increase of yields with disproportionately high environmental risks. In agreement with Lassaletta et al. (2014), the CSM-CERES Maize simulation results from this study indicate that there was little yield benefit from the significantly higher N rates used for the C_G treatment compared to lower N rates used for the C_E treatment. With the exception of block W2, the HYDRUS-1D results indicated that the C_G treatment resulted in higher NO_3-N leaching rates than the C_E treatment.

The results of this study showed that the total amount of water applied along with the frequency and timing of irrigation can be crucial factors affecting water use efficiency, nutrient losses, and eventually the final yield. The use of calendar irrigation scheduling methods tends to over-apply water to ensure that irrigation is not a limiting yield factor, which in turn may lead to unwanted leaching. A study that took place in South Florida showed that by using data-driven irrigation scheduling tools, it is possible to maintain nutrients in the soil, improve crop performance and reduce water and nutrient losses in sandy soils (Ayankojo et al., 2019). This means that irrigation scheduling methods that use real-time data should be a top priority for

farmers, especially in sandy soils, such as the ones in this study, in which the chances of water and nutrient losses are increased.

Table 4.1 Management practices followed during 2016, 2017 and 2018.

Operation	**Year**					
	2016		**2017**		**2018**	
	C_E	**C_G**	**C_E**	**C_G**	**C_E**	**C_G**
Tillage	Conventional		Conservation		Conservation	
Soil core sampling	22 Feb		6 Feb		5 Feb	
Maize planting date	16 Mar		21 Mar		28 Mar	
Maize harvest dates	19 Aug		29 Aug		22 Aug	
Variety	P1794VYHR		P1794VYHR		P1794VYHR	
Plant density (plants ha^{-1})	79000	79000	79000	79000	79000	97850
Irrigation SWT threshold (kPa)	<35		<35		<35	
Irrigation application rate (mm h^{-1})	71		36		36	
Total irrigation applied (mm)	408		235		261	
Fertilizer Applications	Date and application rate in kg N ha^{-1}					
Pre-plant fertilizer (granular)	15 Mar, 110	15 Mar, 110	15 Mar, 90	15 Mar, 90	22 Mar, 30	22 Mar, 64
At planting fertilizer (liquid)	16 Mar, 47	16 Mar, 47	21 Mar, 48	21 Mar, 48	28 Mar, 48	28 Mar, 48
Side-dress fertilizer(liquid)	8 Apr, 100 25 Apr, 100	8 Apr, 110 25 Apr, 230	13 Apr, 123 21 Apr, 123	13 Apr, 123 21 Apr, 63 2 May, 63 12 May, 63 26 May, 63 2 Jun, 27	24 Mar, 112 8 May, 56 23 May, 56	24 Mar, 112 8 May, 56 23 May, 112 5 Jun, 112

Table 4.2 Simulation period for the soil water flow and solute transport models.

Year	Simulation begun		Simulation terminated	
	Water flow	Solute transport	Water flow	Solute transport
2016	15 Mar	22 Feb	19 Aug	19 Aug
2017	15 Mar	6 Feb	29 Aug	29 Aug
2018	22 Mar	5 Feb	21 Aug	21 Aug

Table 4.3 Calibrated values of hydraulic parameters based on the van Genuchten equation for water retention used in the HYDRUS-1D model for each block of NESPAL field.

Trt	Block	Soil layer (mm)	θ_r ($cm^3\ cm^{-3}$)	θ_s ($cm^3\ cm^{-3}$)	α (cm^{-1})	n	K_s ($cm\ day^{-1}$)	I
C_E	W2	0 – 150	0.05	0.52	0.04	1.06	180.2	0.5
		150 – 300	0.05	0.41	0.02	2.11	176.3	0.5
		300 – 450	0.07	0.45	0.01	1.13	62.32	0.5
		450 – 600	0.08	0.46	0.05	1.26	51.35	0.5
		600 - 750	0.07	0.46	0.01	1.17	17.83	0.5
	E1	0 – 150	0.05	0.51	0.05	1.74	442.5	0.5
		150 – 300	0.05	0.42	0.05	2.02	174.3	0.5
		300 – 450	0.06	0.44	0.02	1.06	50.00	0.5
		450 – 600	0.07	0.45	0.01	1.10	45.37	0.5
		600 - 750	0.07	0.46	0.01	1.07	19.32	0.5
	E3	0 – 150	0.05	0.50	0.03	1.57	258.8	0.5
		150 – 300	0.05	0.40	0.15	1.23	897.9	0.5
		300 – 450	0.06	0.41	0.01	1.14	250.0	0.5
		450 – 600	0.07	0.44	0.07	1.10	149.6	0.5
		600 - 750	0.07	0.45	0.04	1.43	19.72	0.5
C_G	W1	0 – 150	0.05	0.51	0.04	1.14	150.0	0.5
		150 – 300	0.05	0.43	0.03	2.06	411.9	0.5
		300 – 450	0.07	0.44	0.01	1.09	26.79	0.5
		450 – 600	0.07	0.45	0.01	2.00	59.78	0.5
		600 - 750	0.07	0.44	0.01	1.08	10.00	0.5
	W3	0 – 150	0.06	0.52	0.05	1.26	210.4	0.5
		150 – 300	0.05	0.42	0.02	1.31	576.7	0.5
		300 – 450	0.07	0.45	0.01	1.13	168.5	0.5
		450 – 600	0.08	0.46	0.05	1.11	54.69	0.5
		600 - 750	0.08	0.48	0.01	1.11	10.00	0.5
	E2	0 – 150	0.05	0.52	0.04	1.63	350.0	0.5
		150 – 300	0.05	0.41	0.03	2.00	546.3	0.5
		300 – 450	0.06	0.44	0.01	1.09	250.0	0.5
		450 – 600	0.06	0.44	0.01	1.17	59.43	0.5
		600 - 750	0.07	0.45	0.08	1.19	10.23	0.5

Table 4.4 Calibrated values of solute transport parameters after using the inverse solution in HYDRUS-1D model for each block of NESPAL field.

Trt	Block	Soil layer (mm)	Adsorption coefficient K_d ($cm^3\ g^{-1}$)		Nitrification rate k (day^{-1})	Denitrification rate μ (day^{-1})
			NH_4-N	NO_3-N		
C_E	W2	0 – 150	6.71	1.99	0.00	0.14
		150 – 300	14.28	0.17	0.00	0.72
		300 – 450	31.22	0.10	0.30	0.31
		450 – 600	5.18	1.58	0.05	0.10
		600 - 750	9.64	1.00	0.06	0.20
	E1	0 – 150	82.66	0.25	0.00	0.11
		150 – 300	7.78	0.01	0.25	1.00
		300 – 450	21.16	1.00	1.00	0.24
		450 – 600	26.27	2.00	0.23	0.08
		600 - 750	12.60	0.10	0.05	0.31
	E3	0 – 150	100	1.40	0.09	1.00
		150 – 300	1.03	1.86	0.21	0.89
		300 – 450	7.39	0.85	0.70	0.28
		450 – 600	2.58	1.97	0.10	0.06
		600 - 750	0.25	2.00	0.61	0.21
C_G	W1	0 – 150	99.17	1.32	0.00	0.08
		150 – 300	51.3	0.15	0.10	1.00
		300 – 450	58.69	0.25	0.32	0.02
		450 – 600	100	0.75	0.02	0.04
		600 - 750	100	0.33	0.08	0.43
	W3	0 – 150	49.35	0.23	0.00	0.20
		150 – 300	51.68	0.61	0.71	0.20
		300 – 450	87.72	0.07	0.86	0.20
		450 – 600	46.88	0.78	0.27	0.20
		600 - 750	10.00	0.48	0.13	0.30
	E2	0 – 150	12.52	1.93	0.03	0.01
		150 – 300	0.15	1.08	0.20	0.90
		300 – 450	100	2.00	0.00	0.61
		450 – 600	16.03	2.00	0.24	0.03
		600 - 750	1.45	0.39	0.03	0.10

Table 4.5 Weighted percentages of each sensor according to the GDDs.

GDDs (ºC)	Stage	α (200 mm)	β (400 mm)	γ (600 mm)
0-354	VE-V4	0.80	0.20	0.00
355-724	V5-V8	0.60	0.30	0.10
725-878	V9-V11	0.50	0.30	0.20

879-1099	V12-VT	0.50	0.25	0.25
1100-end of irrigation	R1-black layer	0.40	0.30	0.30

Table 4.6 Water received by using the UGA checkbook, sensor-based and rainfed method. Total indicates irrigation + precipitation.

Year	Checkbook method		Sensor-based		Rainfed	
	Irrigation (mm)	Total (mm)	Irrigation (mm)	Total (mm)	Irrigation (mm)	Total (mm)
2016	492	1122	408	1038	0	630
2017	564	1059	235	730	0	495
2018	392	1189	261	1058	0	797

Table 4.7 Simulated cumulative water bottom fluxes based on the three irrigation scenarios for each block and growing season. Means followed by different letters within the same year are significantly different ($p < 0.05$).

Year	Trt	Block	Cumulative water bottom fluxes (mm)		
			Checkbook method	Sensor-based	Rainfed
By irrigation scenario					
2016	C_G	W1	-304	-247	-229
		W3	-311	-254	-237
		E2	-264	-252	-238
		Mean	-293^{b}	-251^{a}	-235^{a}
	C_E	W2	-682	-411	-374
		E1	-357	-319	-302
		E3	-266	-264	-254
		Mean	-435^{a}	-331^{a}	-310^{a}
	Mean		-364^{a}	-291^{a}	-272^{a}
2017	C_G	W1	-136	-41	-37
		W3	-252	-72	-65
		E2	-175	-20	-18
		Mean	-188^{b}	-44^{a}	-40^{a}
	C_E	W2	-568	-177	-143
		E1	-293	-134	-125
		E3	-226	-53	-49
		Mean	-362^{a}	-121^{a}	-106^{a}
	Mean		-275^{a}	-83^{b}	-73^{b}
2018	C_G	W1	-419	-265	-200
		W3	-399	-251	-194
		E2	-306	-175	-111
		Mean	-375^{b}	-230^{a}	-168^{a}

Year	Trt	Block	Cumulative water bottom fluxes (mm)		
			Checkbook method	Sensor-based	Rainfed
	C_E	W2	-699	-460	-383
		E1	-359	-220	-177
		E3	-370	-241	-182
		Mean	-476[a]	-307[a]	-247[a]
	Mean		-425[a]	-269[ab]	-208[b]
Mean			-355[a]	-214[b]	-184[b]
By fertilization treatment					
2016	C_G		-293[a]	-251[a]	-235[a]
	C_E		-435[a]	-331[a]	-310[a]
2017	C_G		-188[a]	-44[a]	-40[a]
	C_E		-362[a]	-121[a]	-106[a]
2018	C_G		-374[a]	-230[a]	-168[a]
	C_E		-476[a]	-307[a]	-247[a]

Table 4.8 Cumulative NO_3-N bottom fluxes based on the three irrigation scenarios for each block and growing season. Means followed by different letters within the same year are significantly different ($p < 0.05$).

Year	Trt	Block	Cumulative NO_3-N bottom fluxes (kg ha^{-1})		
			Checkbook method	Sensor-based	Rainfed
By irrigation method					
2016	C_G	W1	-18.10	-15.39	-14.44
		W3	-32.22	-27.62	-25.78
		E2	-10.56	-9.47	-8.79
		Mean	-20.29[a]	-17.50[a]	-16.34[a]
	C_E	W2	-52.37	-27.68	-25.01
		E1	-11.74	-11.07	-10.43
		E3	-14.05	-13.89	-13.27
		Mean	-26.05[a]	-17.55[a]	-16.24[a]
	Mean		-23.17[a]	-17.52[a]	-16.29[a]
2017	C_G	W1	-33.89	-3.816	-3.41
		W3	-39.21	-10.51	-9.56
		E2	-38.78	-4.19	-3.58
		Mean	-37.29[a]	-6.17[b]	-5.52[b]
	C_E	W2	-162.08	-49.96	-39.02
		E1	-30.00	-9.55	-8.89
		E3	-50.51	-7.23	-6.66
		Mean	-80.86[a]	-22.25[a]	-18.19[a]
	Mean		-59.08[a]	-14.21[a]	-11.85[a]
2018	C_G	W1	-35.82	-15.11	-10.60

Year	Trt	Block	Cumulative NO_3-N bottom fluxes (kg ha^{-1})		
			Checkbook method	Sensor-based	Rainfed
		W3	-34.65	-18.60	-15.69
		E2	-36.17	-13.59	-9.01
		Mean	-35.55[a]	-15.77[b]	-11.77[b]
	C_E	W2	-43.71	-27.99	-23.57
		E1	-13.57	-5.80	-4.60
		E3	-22.80	-13.67	-9.98
		Mean	-26.69[a]	-15.82[a]	-12.71[a]
	Mean		-31.12[a]	-15.79[b]	-12.24[b]
Mean			-37.79[a]	-15.84[b]	-13.46[b]
By fertilization treatment					
2016	C_G		-20.29[a]	-17.50[a]	-16.34[a]
	C_E		-26.05[a]	-17.55[a]	-16.24[a]
2017	C_G		-37.29[a]	-6.17[a]	-5.52[a]
	C_E		-80.86[a]	-22.25[a]	-18.19[a]
2018	C_G		-35.55[a]	-15.77[a]	-11.77[a]
	C_E		-26.69[a]	-15.82[a]	-12.71[a]

Table 4.9 N leached (%) by each irrigation method of the N applied in 2016, 2017 and 2018 growing seasons.

Year	Trt	Block	N leached as percentage of N applied (%)		
			Checkbook method	Sensor-based	Rainfed
2016	C_G	W1	3.64	3.10	2.91
		W3	6.48	5.56	5.19
		E2	2.12	1.91	1.77
		Mean	4.08[a]	3.52[a]	3.29[a]
	C_E	W2	14.67	7.75	7.01
		E1	3.29	3.10	2.92
		E3	3.94	3.89	3.72
		Mean	7.30[a]	4.92[a]	4.55[a]
2017	C_G	W1	6.28	0.71	0.63
		W3	7.26	1.95	1.77
		E2	7.18	0.78	0.66
		Mean	6.91[a]	1.14[b]	1.02[b]
	C_E	W2	42.21	13.01	10.16
		E1	7.81	2.49	2.32
		E3	13.15	1.88	1.73
		Mean	21.06[a]	5.79[a]	4.74[a]
2018	C_G	W1	7.11	3.00	2.10
		W3	6.88	3.69	3.11

Year	Trt	Block	N leached as percentage of N applied (%)		
			Checkbook method	Sensor-based	Rainfed
		E2	7.18	2.70	1.79
		Mean	7.05[a]	3.13[b]	2.34[b]
	C_E	W2	14.47	9.27	7.80
		E1	4.49	1.92	1.52
		E3	7.55	4.53	3.30
		Mean	8.84[a]	5.24[a]	4.21[a]

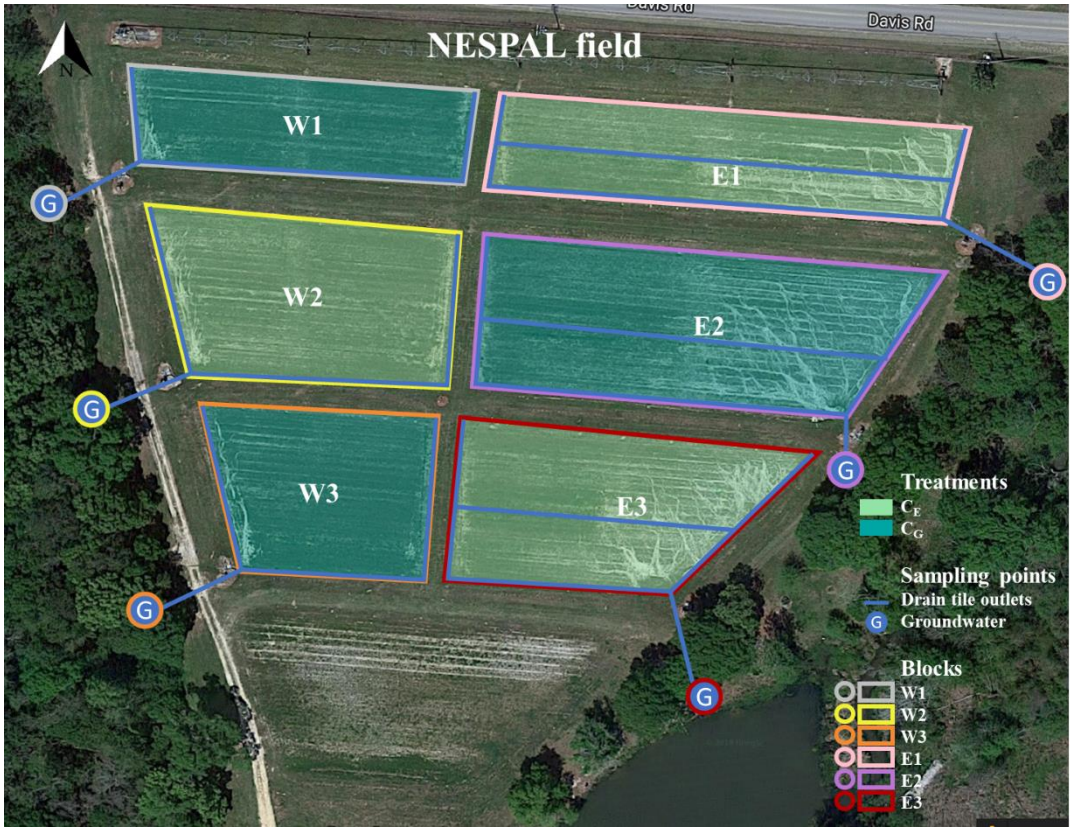

Figure 4.1 Map of NESPAL field showing the six blocks, the two fertilization treatments (dark green for C_G and light green for C_E), the drain tile (blue lines) and the location of groundwater collection sites (G).

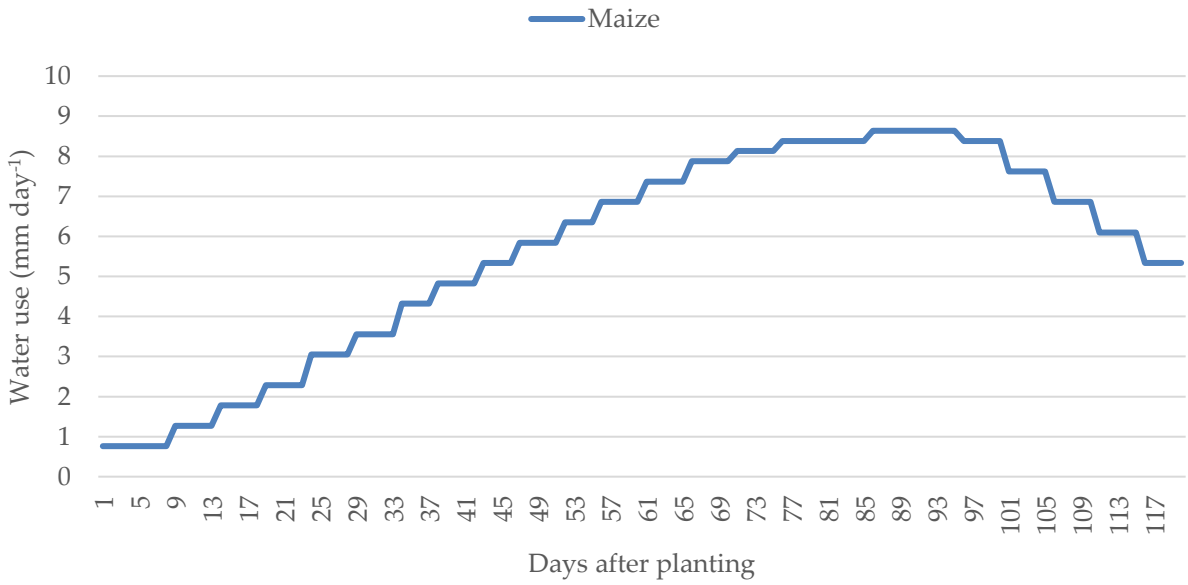

Figure 4.2 Maize weekly water use (mm day^{-1}) in Georgia according to UGA Extension Checkbook method (Lee, 2019).

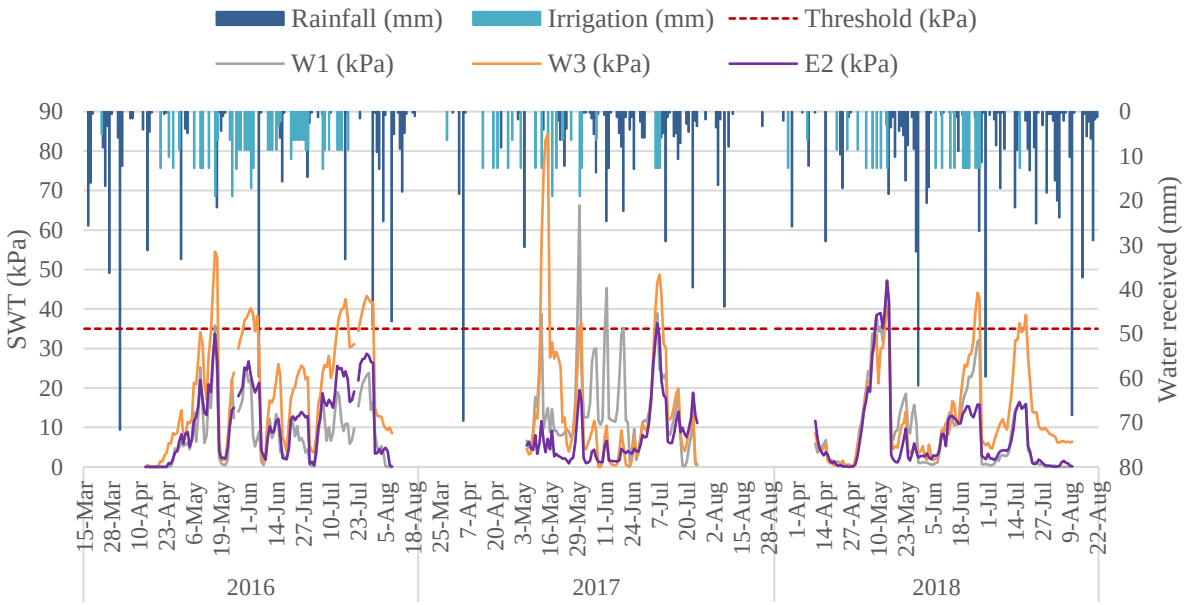

(a)

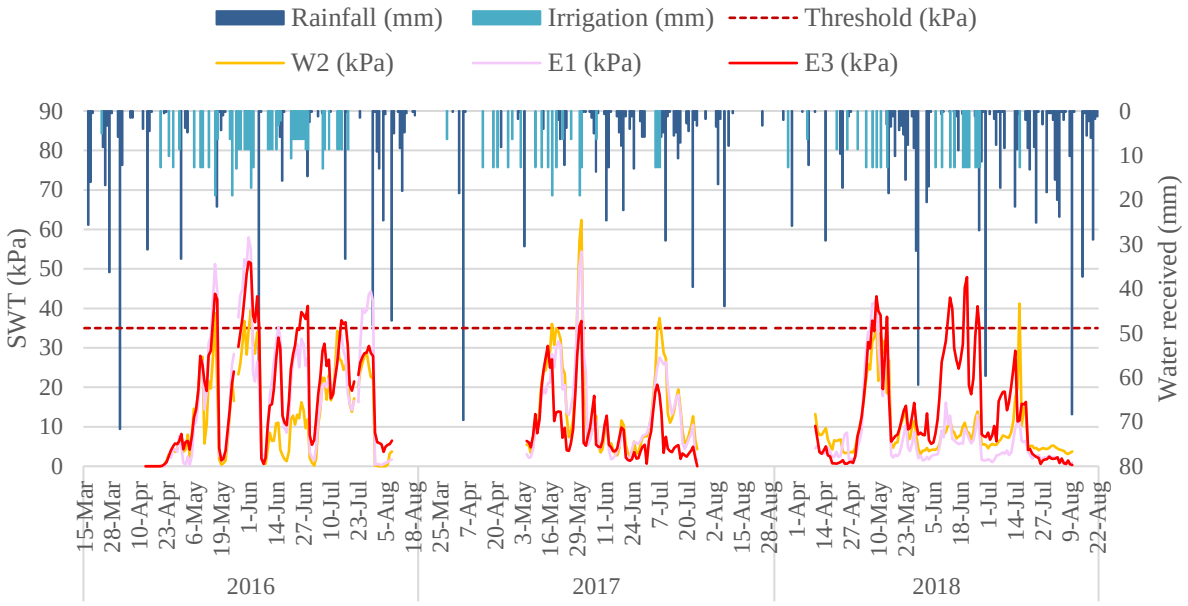

(b)

Figure 4.3 Daily SWT and amount of water received through applied irrigation or rainfall during the three growing seasons for (a) C_G and (b) C_E blocks.

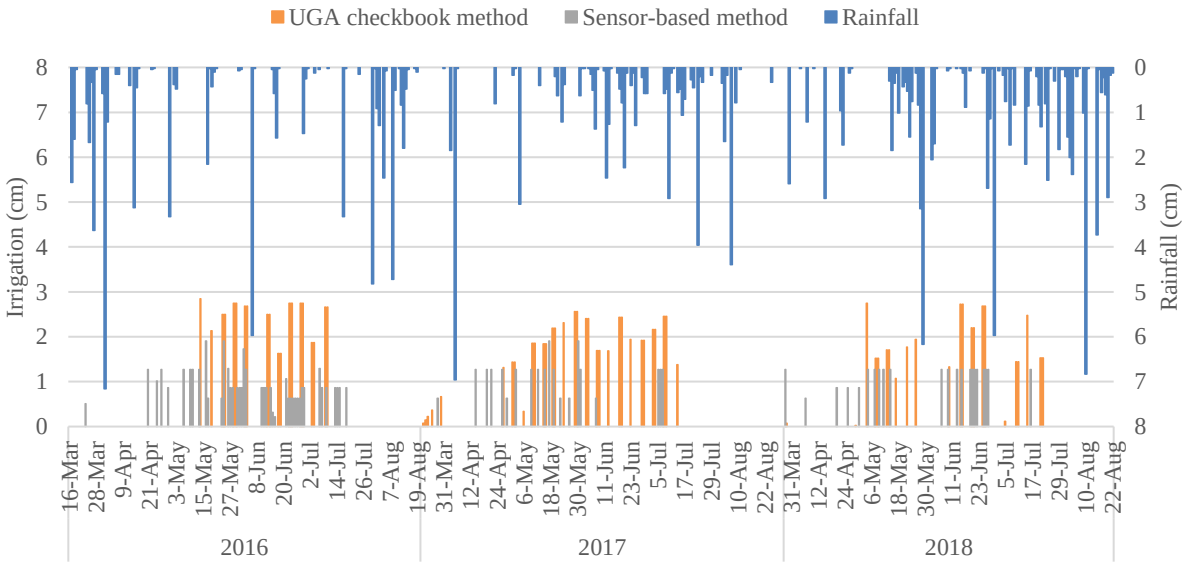

Figure 4.4 Daily amount and frequency of irrigation based on UGA checkbook and sensor-based method.

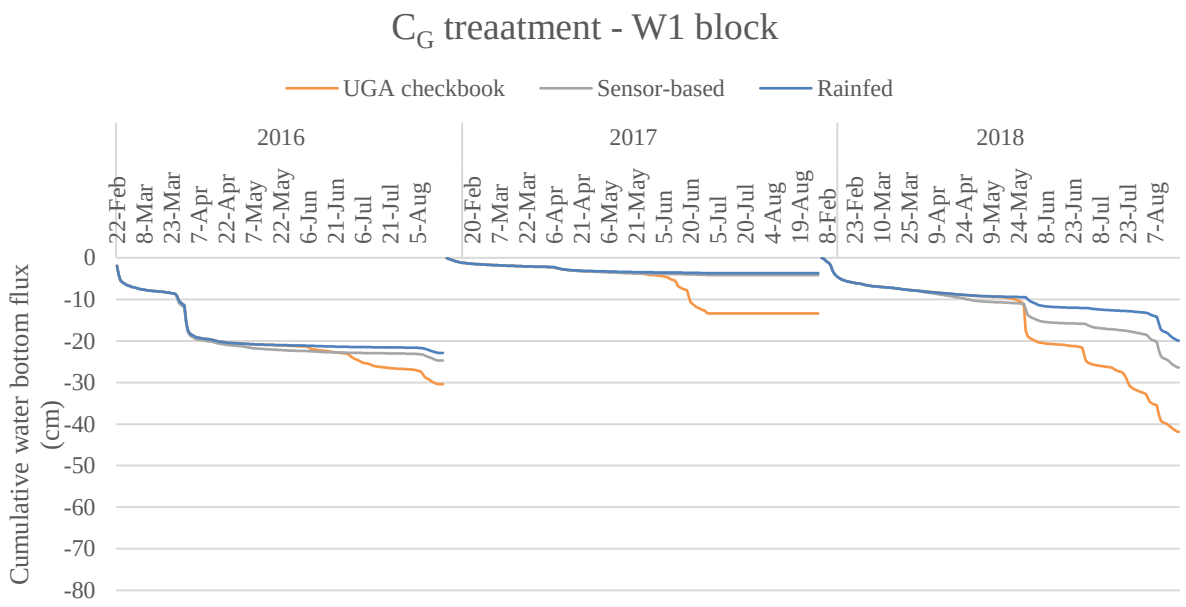
C_G treaatment - W1 block
UGA checkbook
Sensor-based
Rainfed
2016
2017
2018
22-Feb
8-Mar
23-Mar
7-Apr
22-Apr
7-May
22-May
6-Jun
21-Jun
6-Jul
21-Jul
5-Aug
20-Feb
7-Mar
22-Mar
6-Apr
21-Apr
6-May
21-May
5-Jun
20-Jun
5-Jul
20-Jul
4-Aug
19-Aug
8-Feb
23-Feb
10-Mar
25-Mar
9-Apr
24-Apr
9-May
24-May
8-Jun
23-Jun
8-Jul
23-Jul
7-Aug
0
-10
-20
-30
-40
-50
-60
-70
-80
Cumulative water bottom flux (cm)

(a)

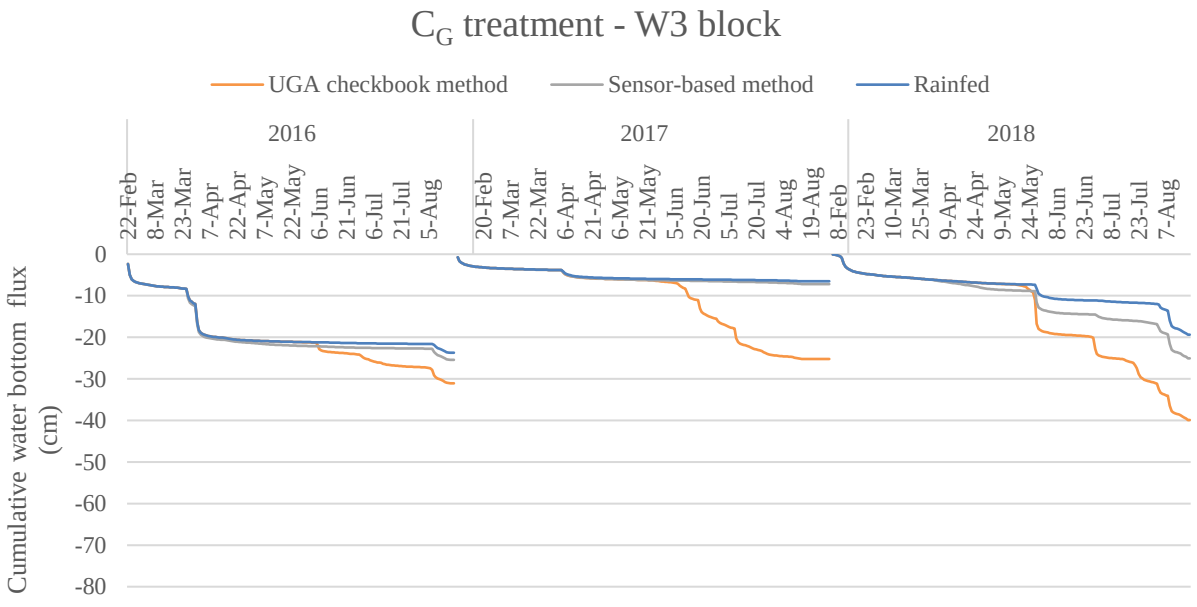
C_G treatment - W3 block
UGA checkbook method
Sensor-based method
Rainfed
2016
2017
2018
22-Feb
8-Mar
23-Mar
7-Apr
22-Apr
7-May
22-May
6-Jun
21-Jun
6-Jul
21-Jul
5-Aug
20-Feb
7-Mar
22-Mar
6-Apr
21-Apr
6-May
21-May
5-Jun
20-Jun
5-Jul
20-Jul
4-Aug
19-Aug
8-Feb
23-Feb
10-Mar
25-Mar
9-Apr
24-Apr
9-May
24-May
8-Jun
23-Jun
8-Jul
23-Jul
7-Aug
0
-10
-20
-30
-40
-50
-60
-70
-80
Cumulative water bottom flux (cm)

(b)

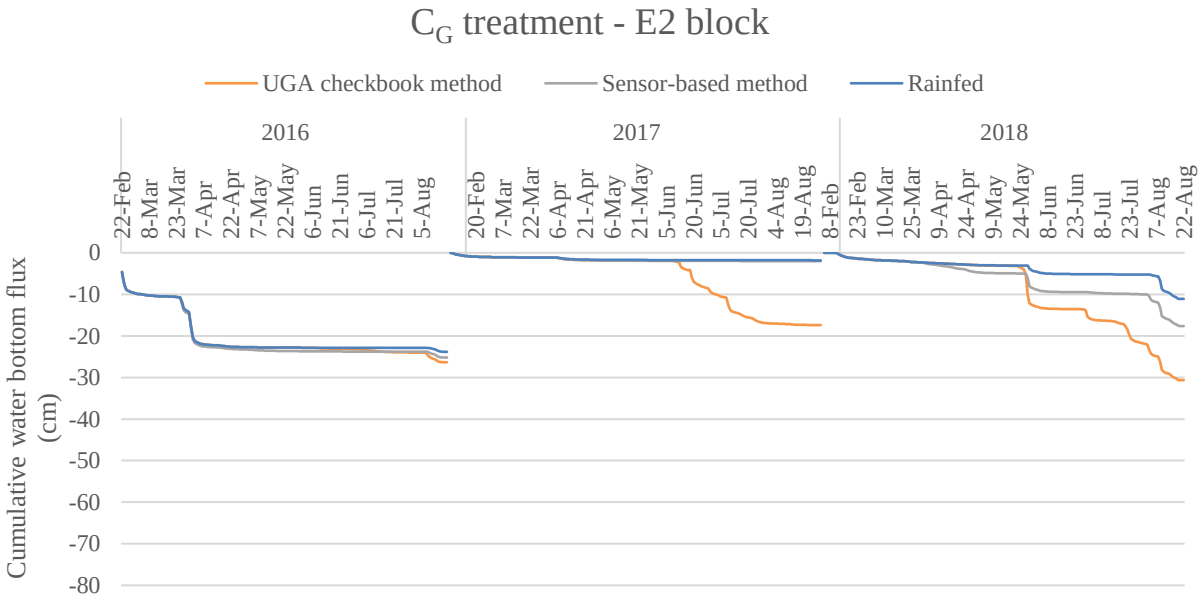
C_G treatment - E2 block
UGA checkbook method
Sensor-based method
Rainfed
2016
2017
2018
22-Feb
8-Mar
23-Mar
7-Apr
22-Apr
7-May
22-May
6-Jun
21-Jun
6-Jul
21-Jul
5-Aug
20-Feb
7-Mar
22-Mar
6-Apr
21-Apr
6-May
21-May
5-Jun
20-Jun
5-Jul
20-Jul
4-Aug
19-Aug
8-Feb
23-Feb
10-Mar
25-Mar
9-Apr
24-Apr
9-May
24-May
8-Jun
23-Jun
8-Jul
23-Jul
7-Aug
22-Aug
Cumulative water bottom flux (cm)
0
-10
-20
-30
-40
-50
-60
-70
-80

(c)

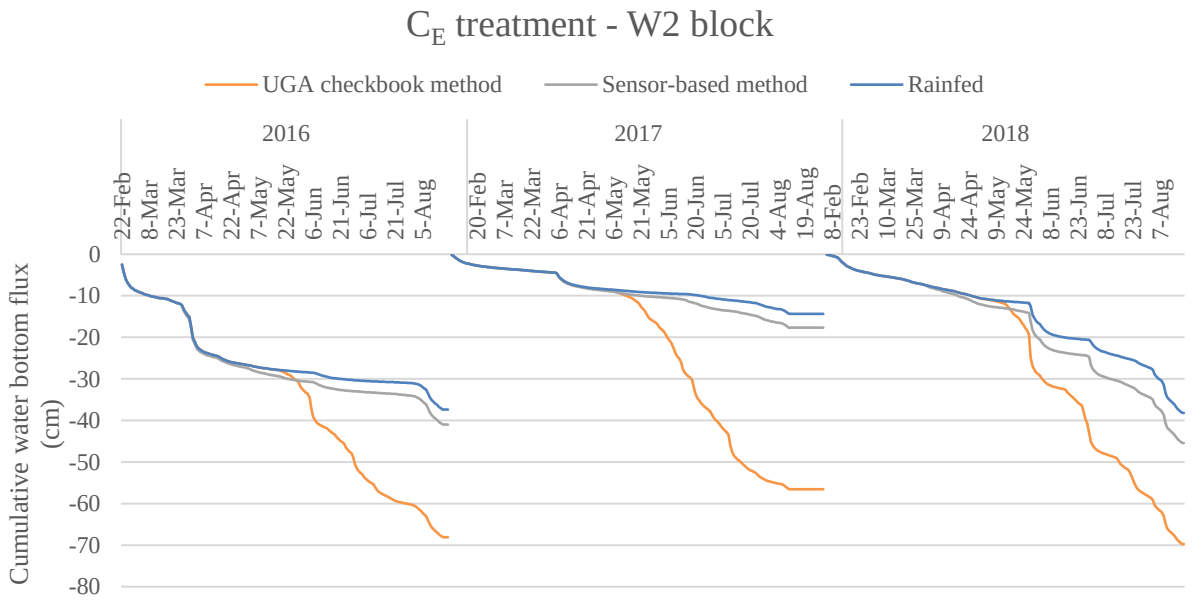
C_E treatment - W2 block
UGA checkbook method
Sensor-based method
Rainfed
2016
2017
2018
22-Feb
8-Mar
23-Mar
7-Apr
22-Apr
7-May
22-May
6-Jun
21-Jun
6-Jul
21-Jul
5-Aug
20-Feb
7-Mar
22-Mar
6-Apr
21-Apr
6-May
21-May
5-Jun
20-Jun
5-Jul
20-Jul
4-Aug
19-Aug
8-Feb
23-Feb
10-Mar
25-Mar
9-Apr
24-Apr
9-May
24-May
8-Jun
23-Jun
8-Jul
23-Jul
7-Aug
Cumulative water bottom flux (cm)
0
-10
-20
-30
-40
-50
-60
-70
-80

(d)

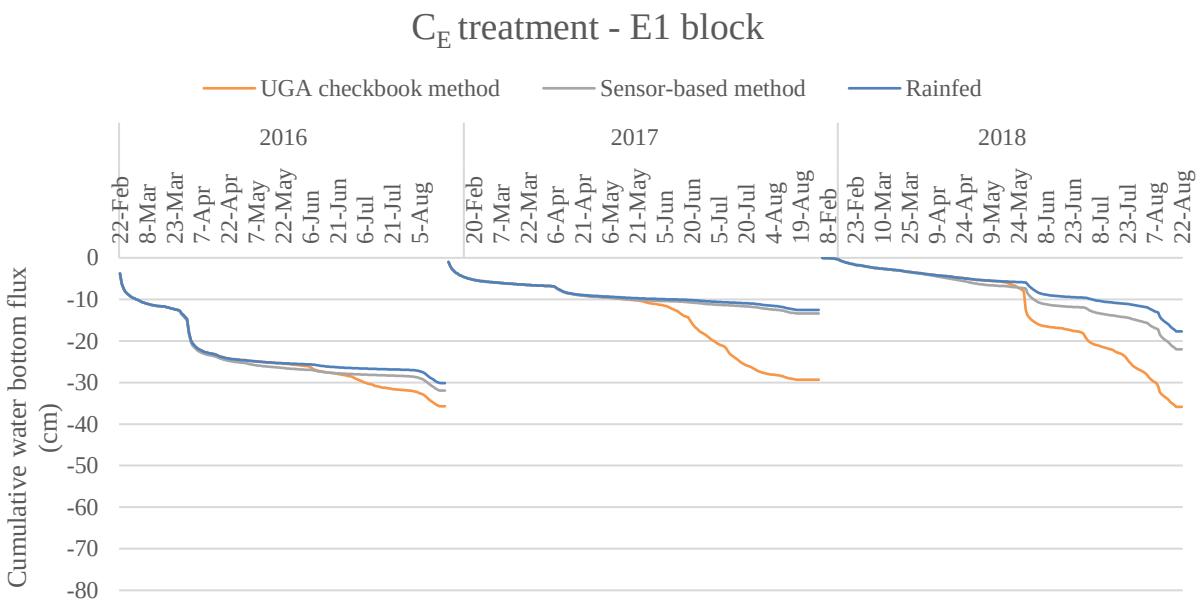

(e)

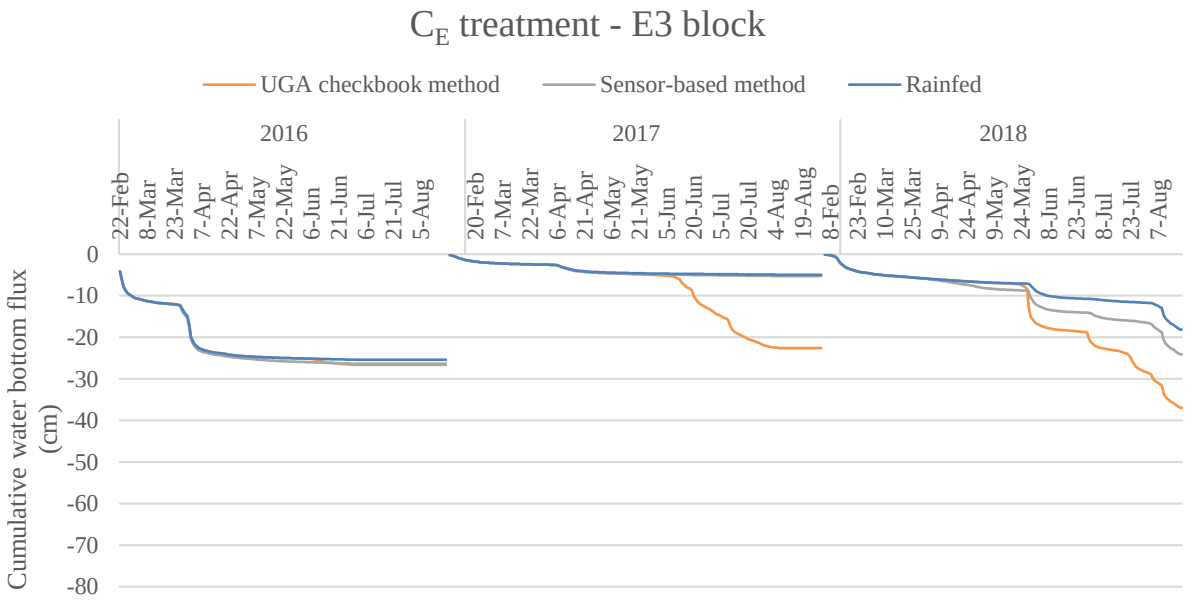

(f)

Figure 4.5 Cumulative water bottom flux comparisons between the different irrigation methods (UGA checkbook, sensor-based and rainfed) for the C_G treatment (a) W1, (b) W3, (c) E2 and C_E treatments (d) W2, (e) E1and (f) E3.

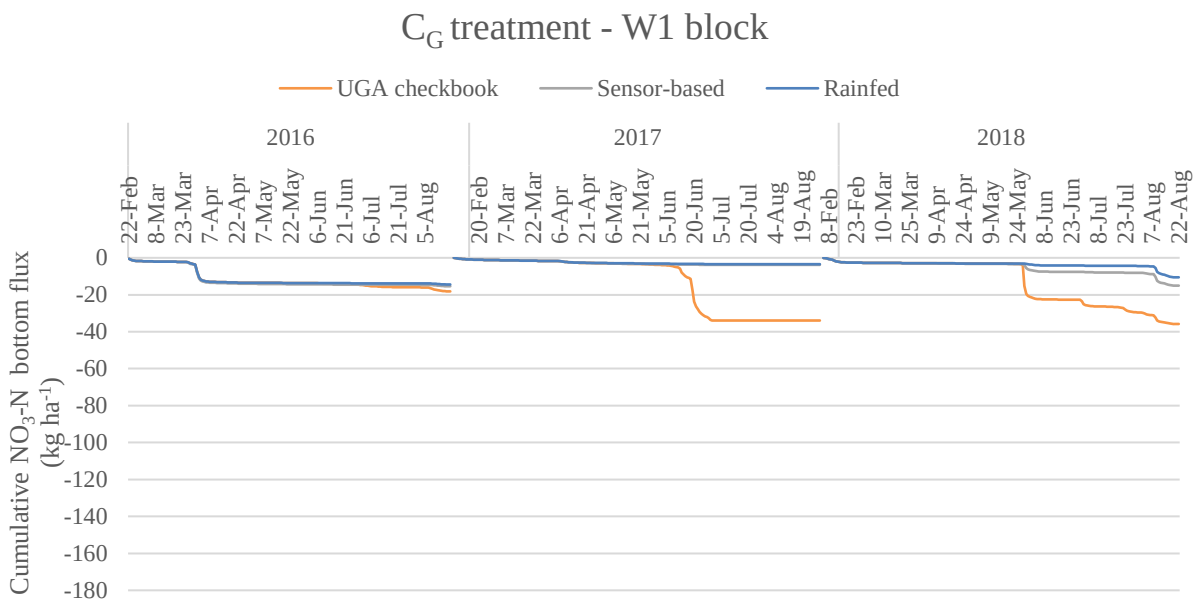
C_G treatment - W1 block
UGA checkbook
Sensor-based
Rainfed
2016
2017
2018
22-Feb
8-Mar
23-Mar
7-Apr
22-Apr
7-May
22-May
6-Jun
21-Jun
6-Jul
21-Jul
5-Aug
20-Feb
7-Mar
22-Mar
6-Apr
21-Apr
6-May
21-May
5-Jun
20-Jun
5-Jul
20-Jul
4-Aug
19-Aug
8-Feb
23-Feb
10-Mar
25-Mar
9-Apr
24-Apr
9-May
24-May
8-Jun
23-Jun
8-Jul
23-Jul
7-Aug
22-Aug
0
-20
-40
-60
-80
-100
-120
-140
-160
-180
Cumulative NO_3-N bottom flux (kg ha^{-1})

(a)

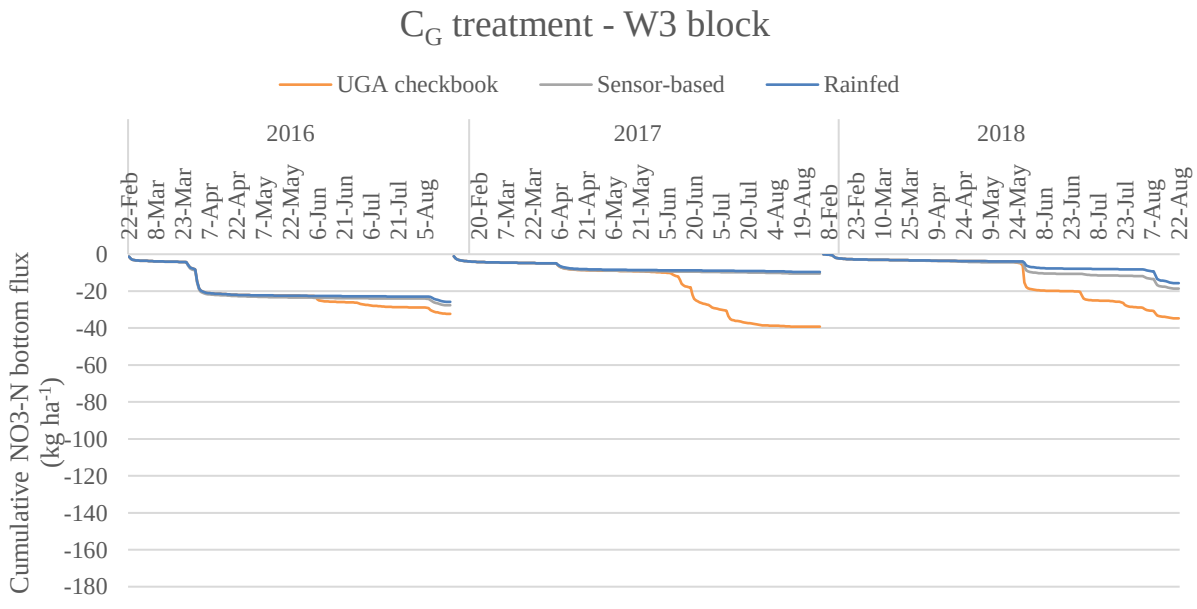
C_G treatment - W3 block
UGA checkbook
Sensor-based
Rainfed
2016
2017
2018
22-Feb
8-Mar
23-Mar
7-Apr
22-Apr
7-May
22-May
6-Jun
21-Jun
6-Jul
21-Jul
5-Aug
20-Feb
7-Mar
22-Mar
6-Apr
21-Apr
6-May
21-May
5-Jun
20-Jun
5-Jul
20-Jul
4-Aug
19-Aug
8-Feb
23-Feb
10-Mar
25-Mar
9-Apr
24-Apr
9-May
24-May
8-Jun
23-Jun
8-Jul
23-Jul
7-Aug
22-Aug
0
-20
-40
-60
-80
-100
-120
-140
-160
-180
Cumulative NO3-N bottom flux (kg ha^{-1})

(b)

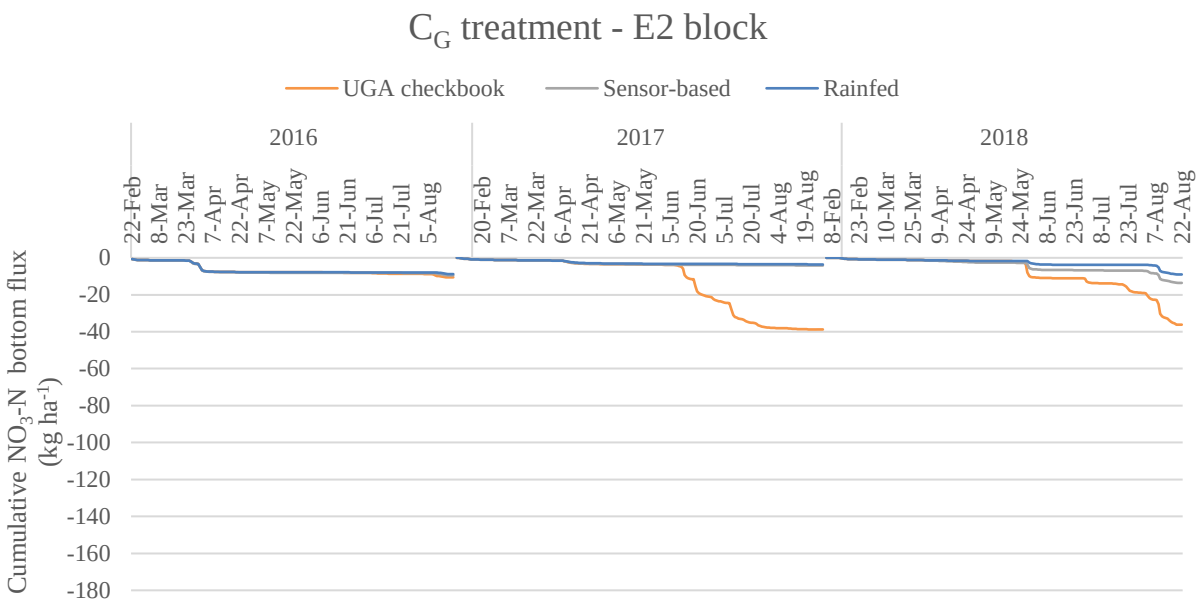
C_G treatment - E2 block
UGA checkbook
Sensor-based
Rainfed
2016
2017
2018
22-Feb
8-Mar
23-Mar
7-Apr
22-Apr
7-May
22-May
6-Jun
21-Jun
6-Jul
21-Jul
5-Aug
20-Feb
7-Mar
22-Mar
6-Apr
21-Apr
6-May
21-May
5-Jun
20-Jun
5-Jul
20-Jul
4-Aug
19-Aug
8-Feb
23-Feb
10-Mar
25-Mar
9-Apr
24-Apr
9-May
24-May
8-Jun
23-Jun
8-Jul
23-Jul
7-Aug
22-Aug
0
-20
-40
-60
-80
-100
-120
-140
-160
-180
Cumulative NO_3-N bottom flux (kg ha^{-1})

(c)

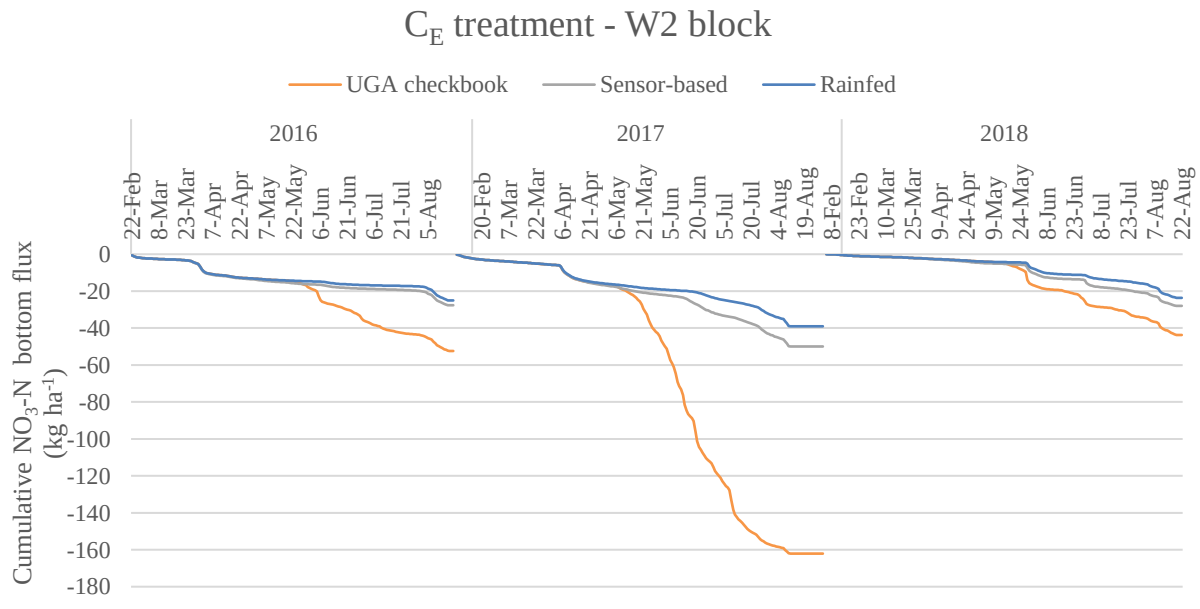
C_E treatment - W2 block
UGA checkbook
Sensor-based
Rainfed
2016
2017
2018
22-Feb
8-Mar
23-Mar
7-Apr
22-Apr
7-May
22-May
6-Jun
21-Jun
6-Jul
21-Jul
5-Aug
20-Feb
7-Mar
22-Mar
6-Apr
21-Apr
6-May
21-May
5-Jun
20-Jun
5-Jul
20-Jul
4-Aug
19-Aug
8-Feb
23-Feb
10-Mar
25-Mar
9-Apr
24-Apr
9-May
24-May
8-Jun
23-Jun
8-Jul
23-Jul
7-Aug
22-Aug
0
-20
-40
-60
-80
-100
-120
-140
-160
-180
Cumulative NO_3-N bottom flux (kg ha^{-1})

(d)

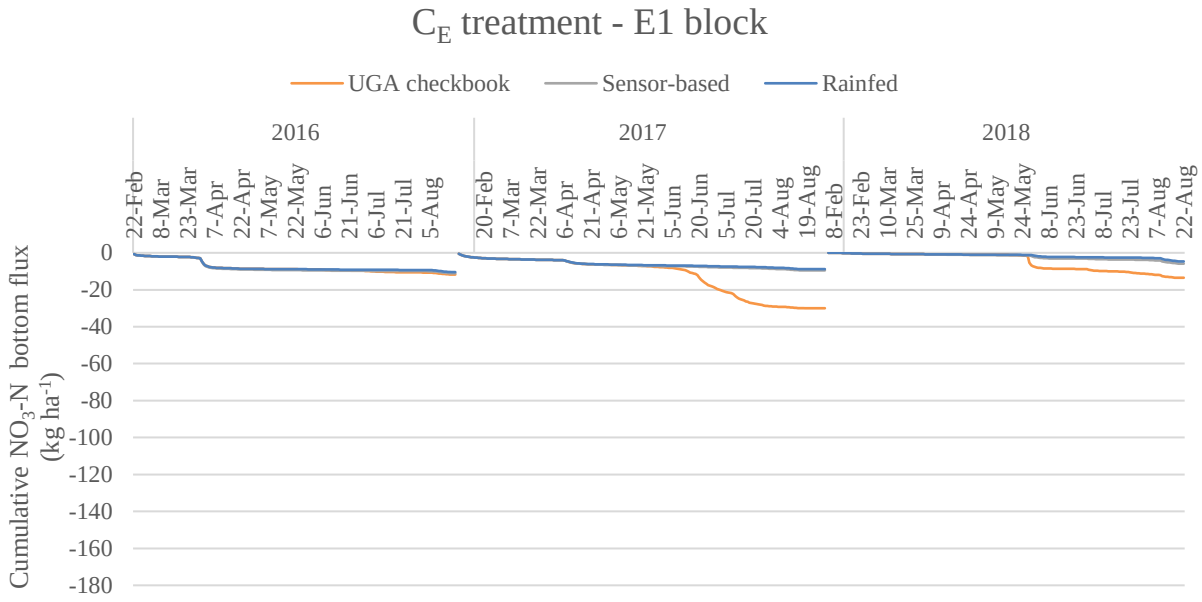

(e)

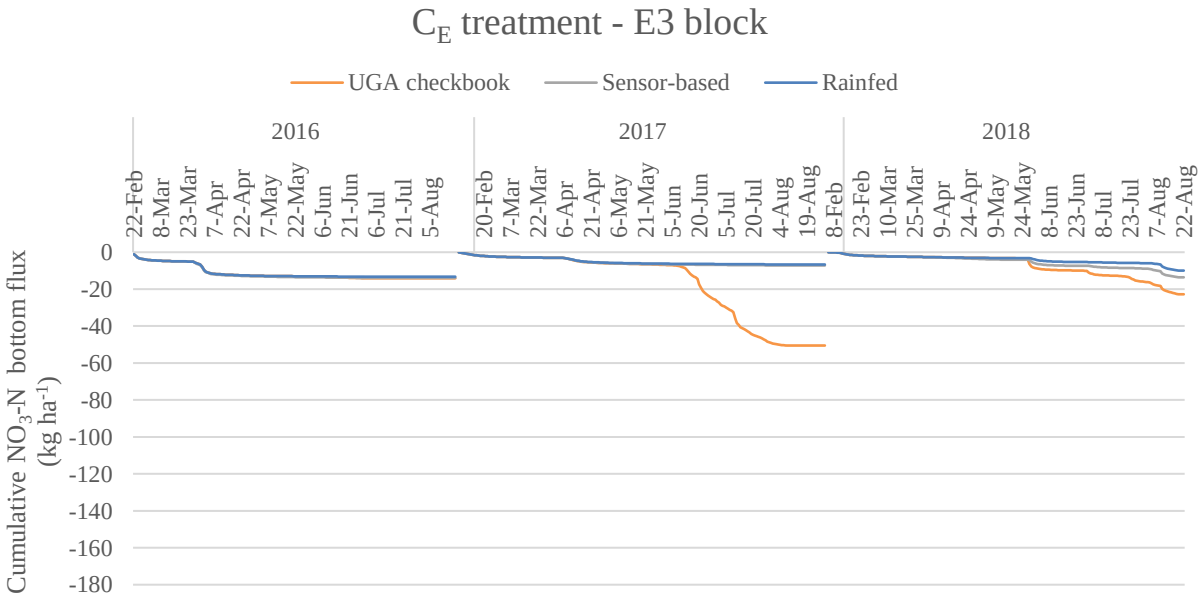

(f)

Figure 4.6 Cumulative NO_3-N bottom flux comparisons between the different irrigation methods (UGA checkbook, sensor-based method, rainfed) for the C_G treatment (a) W1, (b) W3, (c) E2 and C_E treatments (d) W2, (e) E1and (f) E3.

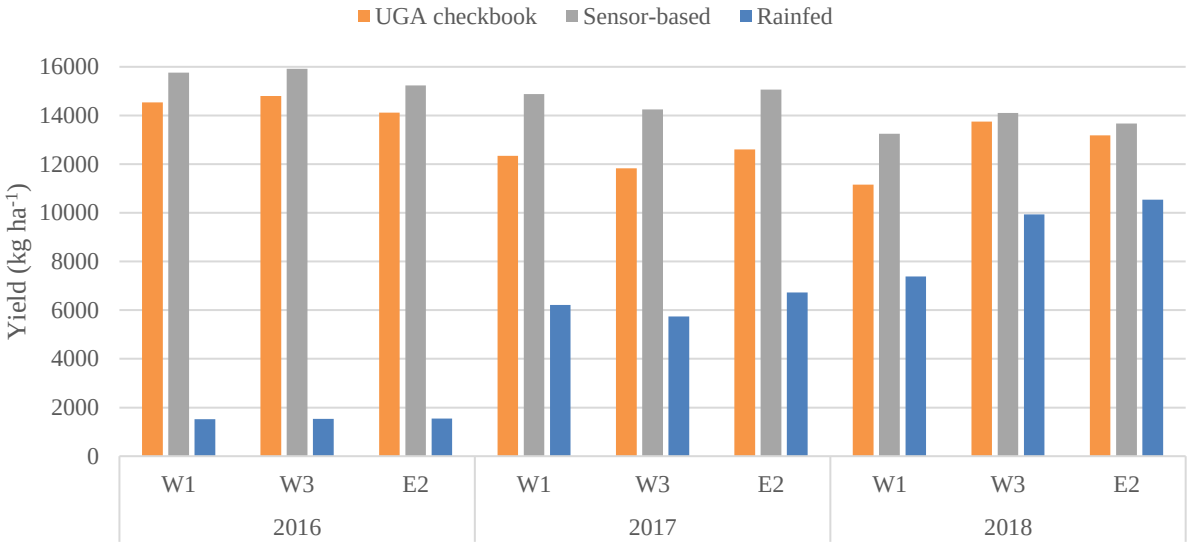

(a)

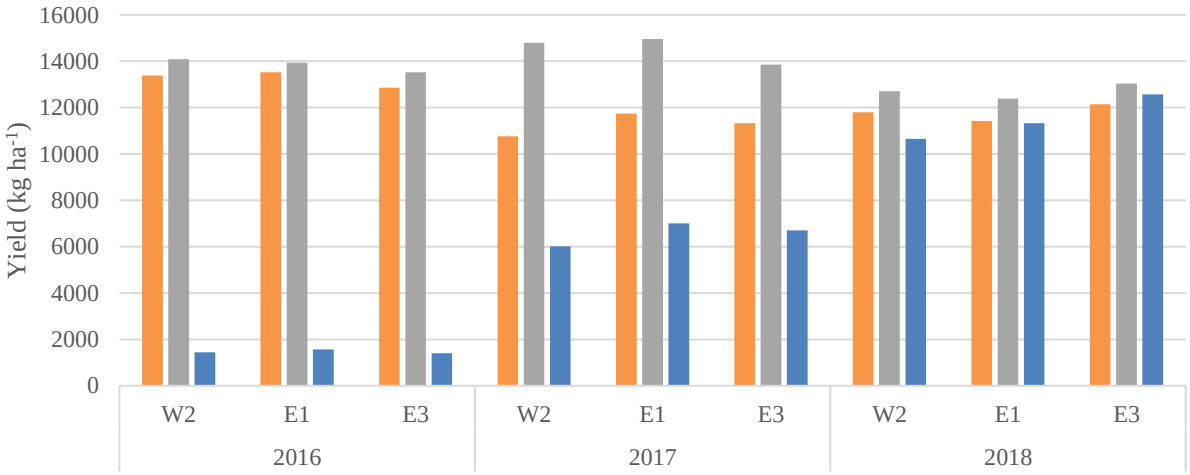

(b)

Figure 4.7 Maize yield results obtained from DSSAT-CERES Maize for (a) C_G and (b) C_E treatments after simulating UGA checkbook, sensor based and rainfed methods of irrigation.

CHAPTER 5

CONCLUSIONS

Maize yields were not significantly different between treatments for each of the three years of the study (Orfanou et al., 2020a). Although the NESPAL field is considered representative of agricultural areas in the Tifton-Vidalia Upland of the southeastern Coastal Plain, factors specific to this field that may have limited maize yield, simulation studies using crop models did not identify specific variables that may have limited the yield of the treatments (Orfanou et al., 2020b). The work described in this study and specifically in Chapter 2 clearly shows that increased fertilizer application rates resulted in increased NPS pollution that was somewhat tempered by adopting cover crops, conservation tillage, and lower irrigation water application rates. Nevertheless, if growers in southern Georgia, southeastern Alabama, and northern Florida pursue higher maize yields through higher fertilizer applications, both surface and groundwater resources may see increased concentrations of nutrients.

The HYDRUS-1D model was used successfully to simulate water flow in the soil profile and NO_3-N transport and estimate NO_3-N leaching to groundwater during the 2016, 2017 and 2018 maize growing seasons in Tifton, GA (Chapter 3). The models predicted that leaching occurred in large precipitations events, when precipitation exceeded the water holding capacity of the soil. However, it would be interesting to observe the NO_3-N leaching that the models would predict long term, i.e. after harvesting maize during fallow seasons and when cover crops were planted. For doing this, soil moisture sensors should be installed in the field to record soil water content and growth data of cover crops to be recorded. Additionally, it was shown that the

total amount of water applied along with the frequency and timing of irrigation can be crucial factors affecting water use efficiency, nutrient losses, and eventually the final yield (Chapter 4). The use of calendar irrigation scheduling methods tends to over-apply water to ensure that irrigation is not a limiting yield factor, which in turn may lead to unwanted leaching. This means that irrigation scheduling methods that use real-time data should be a top priority for farmers, especially in sandy soils, such as the ones in this study, in which the chances of water and nutrient losses are increased.

REFERENCES

Addiscott, T. M., and Benjamin, N. (2006). Nitrate and human health. *Soil Use and Management* **20**, 98-104.

Akhtar, F., Tischbein, B., and Awan, U. K. (2013). Optimizing Deficit Irrigation Scheduling Under Shallow Groundwater Conditions in Lower Reaches of Amu Darya River Basin. *Water Resources Management* **27**, 3165-3178.

Alberts, E. E., and Neibling, W. H. (1994). Influence of crop residues on water erosion. *Managing agricultural residues* **13**, 19-44.

Allen, R., Pereira, L., Raes, D., and Smith, M. (1998). FAO Irrigation and drainage paper No. 56. *Rome: Food and Agriculture Organization of the United Nations* **56**, 26-40.

AQUASTAT (2016). Annual freshwater withdrawals, agriculture (% of total freshwater withdrawal). Vol. 2016, https://data.worldbank.org/indicator/er.h2o.fwag.zs.

Atlas, W. (2019). Monthly weather forecast and climate Atlanta, GA Vol. 2019.

Ayankojo, I. T., Morgan, K. T., and Mahmoud, K. (2019). Evaluation of Soil Water and Nitrogen Distribution by Site-Specific Irrigation Scheduling Method in Tomato Crop Grown on Sandy Soil. *Soil Science Society of America Journal* **83**, 761-771.

Baker, J., and Laflen, J. (1983). Water quality consequences of conservation tillage: New technology is needed to improve the water quality advantages of conservation tillage. *Journal of Soil and Water Conservation* **38**, 186-193.

Below, F., Cazetta, J., and Seebauer, J. (2000). Carbon/nitrogen interactions during ear and kernel development of maize. *Physiology and modeling kernel set in maize*, 15-24.

Berg, M., Meehan, M., and Scherer, T. (2017). "Environmental Implications of Excess Fertilizer and Manure on Water Quality," NDSU.

Berndt, M. P., Hatzell, H. H., Crandall, C. A., Turtora, M., Pittman, J. R., and Oaksford, E. T. (1998). "Water Quality in the Georgia-Florida Coastal Plain ", USGS.

Bhattarai, A., Liu, Y., Liakos, V., and Vellidis, G. (2020). "Economic Analysis of Modern Irrigation Scheduling Strategies on Cotton Production Under Different Tillage Systems in South Georgia."

Bloom, A., Randall, L., Taylor, A., and Silk, W. (2012). Deposition of ammonium and nitrate in the roots of maize seedlings supplied with different nitrogen salts. *Journal of experimental botany* **63**, 1997-2006.

Bouchaou, L., Michelot, J. L., Vengosh, A., Hsissou, Y., Mohamed, Q., Gaye, C. B., Bullen, T. D., and Zuppi, G. M. (2008). Application of multiple isotopic and geochemical tracers for investigation of recharge, salinization, and residence time of water in the Souss-Massa aquifer, southwest of Morocco. *Journal of Hydrology* **352**, 267-287.

Bouyoucos, G. J. (1962). Hydrometer Method Improved for Making Particle Size Analyses of Soils1. *Agronomy Journal* **54**, 464-465.

Bradshaw, J. K., Radcliffe, D. E., Šimůnek, J., Wunsch, A., and McCray, J. E. (2013). Nitrogen Fate and Transport in a Conventional Onsite Wastewater Treatment System Installed in a Clay Soil: A Nitrogen Chain Model. *Vadose Zone Journal* **12**.

Bricker, S. B., Clement, C. G., Pirhalla, D. E., Orlando, S. P., and Farrow, D. R. G. (1999). "National Estuarine Eutrophication Assessment: Effects of Nutrient Enrichment in the Nation's Estuaries." NOAA National Ocean Service Special Projects Office and the National Centers for Coastal Ocean Science. .

Bundy, L. G., Andraski, T. W., and Powell, J. M. (2001). Management Practice Effects on Phosphorus Losses in Runoff in Corn Production Systems. *Journal of Environmental Quality* **30**, 1822-1828.

Capehart, T., and Olson, D. W. (2020). Feedgrains Sector at a Glance. USDA, https://www.ers.usda.gov/topics/crops/corn-and-other-feedgrains/feedgrains-sector-at-a-glance/.

Cassel, D. K., Raczkowski, C. W., and Denton, H. P. (1995). Tillage Effects on Corn Production and Soil Physical Conditions. *Soil Science Society of America Journal* **59**, 1436-1443.

Conley, D. J., Paerl, H. W., Howarth, R. W., Boesch, D. F., Seitzinger, S. P., Havens, K. E., Lancelot, C., and Likens, G. E. (2009). Controlling eutrophication: nitrogen and phosphorus. *Science* **323**, 1014-1015.

Crandall, C. A., Katz, B. G., and Berndt, M. P. (2013). "Estimating nitrate concentrations in groundwater at selected wells and springs in the surficial aquifer system and Upper Floridan aquifer, Dougherty Plain and Marianna Lowlands, Georgia, Florida, and Alabama, 2002-50," Rep. No. 2013-5150, Reston, VA.

Cruz-Fuentes, T., Cabrera Mdel, C., Heredia, J., and Custodio, E. (2014). Groundwater salinity and hydrochemical processes in the volcano-sedimentary aquifer of La Aldea, Gran Canaria, Canary Islands, Spain. *Sci Total Environ* **484**, 154-66.

Czapar, G. F. (2008). 9. Effects of Erosion Control Practices on Nutrient Loss.

Daryanto, S., Wang, L., and Jacinthe, P.-A. (2017). Impacts of no-tillage management on nitrate loss from corn, soybean and wheat cultivation: A meta-analysis. *Scientific Reports* **7**.

David, M. B., Drinkwater, L. E., and McIsaac, G. F. (2010). Sources of nitrate yields in the Mississippi River Basin. *Journal of Environmental Quality* **39**, 1657-1667.

Dillaha, T. A., Mostaghimi, S., and Heatwole, C. D. (1988). Tillage Effects on Nutrient Loadings of Waterways *Special Bulletin, Mississippi State, Mississippi Agricultural. Forestry Experiment Station 881, 83–85.*

Ding, L., Wang, K., Jiang, G., Biswas, D., Xu, H., Li, L., and Li, Y. (2005). Effects of nitrogen deficiency on photosynthetic traits of maize hybrids released in different years. *Annals of botany* **96**, 925-930.

Donner, S. D., and Kucharik, C. J. (2003). Evaluating the impacts of land management and climate variability on crop production and nitrate export across the Upper Mississippi Basin. *Global Biogeochemical Cycles* **17**.

EPA (2017a). National Primary Drinking Water Regulations.

EPA (2017b). Nonpoint Source: Agriculture. Vol. 2017, https://www.epa.gov/nps/nonpoint-source-agriculture.

Erisman, J. W., Sutton, M. A., Galloway, J., Klimont, Z., and Winiwarter, W. (2008). How a century of ammonia synthesis changed the world. *Nature Geoscience* **1**, 636-639.

Espino, A., Mallants, D., Vanclooster, M., and Feyen, J. (1996). Cautionary notes on the use of pedotransfer functions for estimating soil hydraulic properties. *Agricultural Water Management* **29**, 235-253.

EU (1998). "Council Directive 98/83/EC of 3 November 1998 on the quality of water intended for human consumption," https://eur-lex.europa.eu/legal-content/EN/TXT/?uri=CELEX:01998L0083-20151027.

EU (2019). The Nitrates Directive. https://ec.europa.eu/environment/water/water-nitrates/index_en.html.

FAO (2015). Fertilizer Use to Surpass 200 Million Tonnes in 2018. Food and Agricultural Organization of the United Nations, http://www.fao.org/news/story/en/item/277488/icode/.

FDS (2016). Surface Water uality Standards (D. o. E. Protection, ed.). Florida Department of State, https://www.flrules.org/gateway/ruleNo.asp?id=62-302.530.

Feddes, R. A. (1982). "Simulation of field water use and crop yield," Pudoc.

Filho, J. D. C. L. (2016). Irrigation Scheduling on Corn to Increase Profitability and Environmental Stewardship in Alabama. *In* "ASA Southern Regional Branch", San Antonio.

GAEMN (2019). Georgia Automated Environmental Monitoring Network.

Galloway, J. N., Townsend, A. R., Erisman, J. W., Bekunda, M., Cai, Z., Freney, J. R., Martinelli, L. A., Seitzinger, S. P., and Sutton, M. A. (2008). Transformation of the nitrogen cycle: recent trends, questions, and potential solutions. *Science* **320**, 889-892.

Gardner, L. R. (1990). The role of rock weathering in the phosphorus budget of terrestrial watersheds. *Biogeochemistry* **11**, 97-110.

Gheysari, M., Mirlatifi, S. M., Homaee, M., Asadi, M. E., and Hoogenboom, G. (2009). Nitrate leaching in a silage maize field under different irrigation and nitrogen fertilizer rates. *Agricultural Water Management* **96**, 946-954.

Gold, A., DeRagon, W., Sullivan, W., and Lemunyon, J. (1990a). Nitrate-Nitrogen Losses to Groundwater from Rural and Suburban Land Uses. *Journal of Soil and Water Conservation* **45**.

Gold, A. J., DeRagon, W. R., Sullivan, W. M., and Lemunyon, J. L. (1990b). Nitrate-nitrogen losses to groundwater from rural and suburban land uses. *Journal of soil and water conservation* **45**, 305-310.

Goldschein, E. (2011). The 10 Most Important Crops In The World. Vol. 2018, Business Insider.

Hanson, B. R., Šimůnek, J., and Hopmans, J. W. (2006). Evaluation of urea–ammonium–nitrate fertigation with drip irrigation using numerical modeling. *Agricultural water management* **86**, 102-113.

Harrison, S. R. (1990). Regression of a model on real-system output: an invalid test of model validity. *Agricultural systems* **34**, 183-190.

Hawkins, G. L., and Thomas, D. (2014). Protecting Georgia's Surface Water Resources. https://extension.uga.edu/publications/detail.html?number=B1217&title=Protecting%20Georgia%27s%20Surface%20Water%20Resources.

Haygarth, P., Heathwaite, A., Jarvis, S., and Harrod, T. (1999). Hydrological factors for phosphorus transfer from agricultural soils. *In* "Advances in agronomy", Vol. 69, pp. 153-178. Elsevier.

He, J., Dukes, M. D., Hochmuth, G. J., Jones, J. W., and Graham, W. D. (2012). Identifying irrigation and nitrogen best management practices for sweet corn production on sandy soils using CERES-Maize model. *Agricultural Water Management* **109**, 61-70.

Hollis, P. (2013). Fertilizer recommendations proving valid even with increasing corn yields. Farm Progress.

Hoogenboom, G., Jones, J., Wilkens, P., Porter, C., Boote, K., Hunt, L., Singh, U., Lizaso, J., White, J., and Uryasev, O. (2012). Decision support system for agrotechnology transfer (DSSAT) Version 4.5 [CD-ROM].

Hoogenboom, G., Jones, J. W., Wilkens, P. W., Porter, C. H., Boote, K. J., Hunt, L. A., Singh, U., Lizaso, J. I., White, J. W., Uryasev, O., Ogoshi, R., Koo, J., Shelia, V., and Tsuji, G. Y. (2015). Decision support system for agrotechnology transfer (DSSAT) Version 4.6 (www.DSSAT.net). DSSAT foundation, Prosser, Washington.

Hoogenboom, G., Porter, C. H., Boote, K. J., Shelia, V., Wilkens, P. W., Singh, U., White, J. W., Asseng, S., Lizaso, J. I., Moreno, P., Pavan, W., Ogoshi, R., Hunt, L., Tsuji, G. Y., and Jones, J. W. (2019). "The DSSAT crop modeling ecosystem," Burleigh Dodds Science Publishing, Cambridge, United Kingdom

Hopmans, J., Šimůnek, J., Romano, N., and Durner, W. (2002). "Inverse methods. In: Dane JH, Topp GC, editors. Methods of soil analysis. Part 4. Physical methods."

Hopmans, J. W., Šimůnek, J., Romano, N., and Durner, W. (2018). 3.6.2. Inverse Methods. *In* "Methods of Soil Analysis", pp. 963-1008.

Hussain, A., Kumar, P., and Mehrotra, I. (2015). NITROGEN AND PHOSPHORUS REQUIREMENT IN ANAEROBIC PROCESS: A REVIEW. *Environmental Engineering & Management Journal (EEMJ)* **14**.

Iqbal, M., Rowshon, M., Man, C., and Wayayok, A. (2020). HYDRUS-1D Simulation of Soil Water Dynamics for Sweet Corn under Tropical Rainfed Condition. *Applied Sciences* **10**, 1219.

Ji, Z.-G. (2017). "Hydrodynamics and Water Quality: Modeling Rivers, Lakes, and Estuaries," Second edition/Ed.

Jones, C. A. (1986). "CERES-Maize; a simulation model of maize growth and development."

Jones, J. W., Hoogenboom, G., Porter, C. H., Boote, K. J., Batchelor, W. D., Hunt, L., Wilkens, P. W., Singh, U., Gijsman, A. J., and Ritchie, J. T. (2003). The DSSAT cropping system model. *European journal of agronomy* **18**, 235-265.

Karr, J. D., Showers, W. J., Gilliam, J. W., and Andres, A. S. (2001). Tracing nitrate transport and environmental impact from intensive swine farming using delta nitrogen-15. *Journal of Environmental Quality* **30**, 1163-1175.

Kaspar, T., Radke, J., and Laflen, J. (2001). Small grain cover crops and wheel traffic effects on infiltration, runoff, and erosion. *Journal of Soil and Water Conservation* **56**, 160-164.

Kisekka, I., Aguilar, J., Rogers, D., Holman, J., O'Brien, D. M., and Klocke, N. (2016). Assessing Deficit Irrigation Strategies for Corn Using Simulation. *Transactions of the ASABE* **59**, 303-317.

Kissel, D. E., and Sonon, L. S. (2008). Soil test handbook for Georgia.

Konikow, L. F., and Bredehoeft, J. D. (1992). Ground-water models cannot be validated. *Advances in Water Resources* **15**, 75-83.

Lane, P. N., Noske, P. J., and Sheridan, G. J. (2011). Phosphorus enrichment from point to catchment scale following fire in eucalypt forests. *Catena* **87**, 157-162.

Lassaletta, L., Billen, G., Grizzetti, B., Anglade, J., and Garnier, J. (2014). 50 year trends in nitrogen use efficiency of world cropping systems: the relationship between yield and nitrogen input to cropland. *Environmental Research Letters* **9**, 105011.

Lee, D. (2019). "A guide to corn production in Georgia." University of Georgia College of Agricultural & Environmental Sciences, Cooperative Extension Crop and Soil Sciences.

Li, Y., Šimůnek, J., Jing, L., Zhang, Z., and Ni, L. (2014). Evaluation of water movement and water losses in a direct-seeded-rice field experiment using Hydrus-1D. *Agricultural water management* **142**, 38-46.

Liakos, V., Vellidis, G., Lacerda, L., Tucker, M., Porter, W. M., and Cox, C. (2018). Management Zone Delineation for Irrigation Based on Sentinel-2 Satellite Images and Field Properties *In* "14th International Conference on Precision Agriculture ", Montreal, Quebec, Canada

Mailapalli, D. R., Burger, M., Horwath, W. R., and Wallender, W. W. (2013). Crop Residue Biomass Effects on Agricultural Runoff. *Applied and Environmental Soil Science* **2013**, 805206.

Mailhot, D. J., Dunn, D., Jordan, H. J., and J., L. D. (2017). "2017 Corn Performance Tests." The Georgia Agricultural Expirement Stations. Department of Crop and Soil Sciences. College of Agricutural and Envirometal Services. University of Georgia Griffin Campus

Mailhot, D. J., Dunn, D., Jordan, H. J., and LaDon Day, J. (2018). "Georgia 2018 Corn Performance Tests," The Georgia Agricultural Experiment Stations. Department of Crop and Soil Sciences. College of Agricultural and Environmental Sciences. University of Georgia Griffin campus.

Mbonimpa, E. G., Yuan, Y., Nash, M. S., and Mehaffey, M. H. (2014). Sediment and total phosphorous contributors in Rock River watershed. *Journal of Environmental Management* **133**, 214-221.

McDowell, L. L., and McGregor, K. C. (1984). Plant nutrient losses in runoff from conservation tillage corn. *Soil and Tillage Research* **4**, 79-91.

Mehdi, B., Ludwig, R., and Lehner, B. (2015). Evaluating the impacts of climate change and crop land use change on streamflow, nitrates and phosphorus: A modeling study in Bavaria. *Journal of Hydrology: Regional Studies* **4**.

Menció, A., Mas-Pla, J., Otero, N., Regàs, O., Boy-Roura, M., Caminal, R., Bach, J., Domenech, C., Zamorano, M., Brusi, D., and Folch, A. (2016). Nitrate pollution of groundwater; all right…, but nothing else? *The Science of the total environment* **539**, 241-251.

Mengel, D., and Barber, S. (1974). Development and Distribution of the Corn Root System Under Field Conditions 1. *Agronomy Journal* **66**, 341-344.

Miller, D. (2016). Georgia's Dowdy Does It Again – Tops 500 Bushels In U.S. Corn Yield Contest – DTN. Vol. 2017, https://agfax.com/2016/12/20/georgia-farmer-at-top-of-500-bushel-national-corn-yield-contest-dtn/.

Mitchell, P. (1997). Misuse of regression for empirical validation of models. *Agricultural Systems* **54**, 313-326.

Monneveux, P., Zaidi, P., and Sanchez, C. (2005). Population density and low nitrogen affects yield-associated traits in tropical maize. *Crop Science* **45**, 535-545.

Moriasi, D. N., Gitau, M. W., Pai, N., and Daggupati, P. (2015). Hydrologic and Water Quality Models: Performance Measures and Evaluation Criteria. *Transactions of the ASABE* **2015 v.58 no.6**, pp. 1763-1785.

Mueller, D. K., and Helsel, D. R. (1996). Nutrients in the Nation's Waters--Too Much of a Good Thing?

Neuman, S. P., R. A. Feddes, a., and Bresler., E. (1974). Finite element simulation of flow in saturated - unsaturated soils considering water uptake by plants. Third Annual Report, Project No. A10-SWC-77, Hydraulic Engineering Lab., Technion, Haifa, Israel.

Nolan, B. T., Ruddy, B. C., Hitt, K. J., and Helsel, D. R. (1997). Risk of Nitrate in groundwaters of the United States a national perspective. *Environmental science & technology* **31**, 2229-2236.

Novara, A., Gristina, L., Saladino, S., Santoro, A., and Cerdà, A. (2011). Soil erosion assessment on tillage and alternative soil managements in a Sicilian vineyard. *Soil and Tillage Research* **117**, 140-147.

O'Neill, P. M., Shanahan, J. F., Schepers, J. S., and Caldwell, B. (2004). Agronomic responses of corn hybrids from different eras to deficit and adequate levels of water and nitrogen. *Agronomy journal* **96**, 1660-1667.

Ohlmer, B., Olson, K., and Brehmer, B. (1998). Understanding farmers' decision making processes and improving managerial assistance. *Agricultural Economics* **18**, 273-290.

Oram, B. (2018a). Nitrates and Nitrites in Drinking Water Groundwater and Surface Waters. Vol. 2018, https://water-research.net/index.php/nitrate.

Oram, B. (2018b). Phosphates in the Environment. Vol. 2019, https://www.water-research.net/index.php/phosphates.

Orfanou, A., Pavlou, D., Boote, K. J., Bryant, C. J., Cabrera, M., Vellidis, G., and Porter, W. M. (2020a). Effects of management practices in high input maize production, University of Georgia.

Orfanou, A., Pavlou, D., Boote, K. J., Bryant, C. J., Cabrera, M., Vellidis, G., and Porter, W. M. (2020b). Application of DSSAT CERES Maize for simulating high input maize production, University of Georgia.

Orfanou, A., Pavlou, D., Boote, K. J., Bryant, C. J., Cabrera, M., Vellidis, G., and Porter, W. M. (2020c). Simulation of management scenarios for identifying the limitng factors in maize production., University of Georgia.

Orfanou, A., Pavlou, D., and Porter, W. M. (2019). Maize Yield and Irrigation Applied in Conservation and Conventional Tillage at Various Plant Densities. *Water* **11**, 1726.

Palacio, R. G., Bisigato, A. J., and Bouza, P. J. (2014). Soil erosion in three grazed plant communities in northeastern Patagonia. *Land Degradation & Development* **25**, 594-603.

Pavlou, D., Orfanou, A., Cabrera, M., Hoogenboom, G., Radcliffe, D. E., Porter, W. M., and Vellidis, G. (2020b). Application of HYDRUS-1D for simulating water flow and NO_3-N solute transport in maize, University of Georgia.

Pavlou, D., Orfanou, A., Miguel, C., Hoogenboom, G., Porter, W. M., Radcliffe, D. E., and Vellidis, G. (2020a). Water qaulity effects of high input maize production, University of Georgia.

Pavlou, D., Orfanou, A., Porter, W. M., and Vellidis, G. (2020).

Phillips, D. L., Hardin, P. D., Benson, V. W., and Baglio, J. V. (1993). Nonpoint source pollution impacts of alternative agricultural management practices in Illinois: A simulation study. *Journal of Soil and Water Conservation* **48**, 449-457.

Rabalais, N. N., Turner, R. E., and Wiseman Jr, W. J. (2002). Gulf of Mexico hypoxia, aka "The dead zone". *Annual Review of ecology and Systematics* **33**, 235-263.

Raczkowski, C., Reyes, M., Reddy, G., Busscher, W. J., and Bauer, P. J. (2009). Comparison of conventional and no-tillage corn and soybean production on runoff and erosion in the southeastern US Piedmont. *Journal of Soil and Water Conservation* **64**.

Radcliffe, D. E., and Simunek, J. (2018). "Soil physics with HYDRUS: Modeling and applications," CRC press.

Raes, D., Steduto, P., Hsiao, T. C., and Fereres, E. (2009). AquaCrop—the FAO crop model to simulate yield response to water: II. Main algorithms and software description. *Agronomy Journal* **101**, 438-447.

Ramos, T. B., Šimůnek, J., Gonçalves, M. C., Martins, J. C., Prazeres, A., Castanheira, N. L., and Pereira, L. S. (2011). Field evaluation of a multicomponent solute transport model in soils irrigated with saline waters. *Journal of Hydrology* **407**, 129-144.

Rassam, D., Simunek, J. J., Mallants, D., and Van Genuchten, M. (2018). "The HYDRUS-1D Software Package for Simulating the Movement of Water, Heat, and Multiple Solutes in Variably Saturated Media: Tutorial."

Raun, W. R., and Johnson, G. V. (1999). Improving Nitrogen Use Efficiency for Cereal Production. *Agronomy Journal* **91**, 357-363.

Richards, L. A. (1931). CAPILLARY CONDUCTION OF LIQUIDS THROUGH POROUS MEDIUMS. *Physics* **1**, 318-333.

Rudolph, D., Barry, D., and Goss, M. (1998). Contamination in Ontario farmstead domestic wells and its association with agriculture:: 2. Results from multilevel monitoring well installations. *Journal of contaminant Hydrology* **32**, 295-311.

S. Kanwar, R., L. Baker, J., and G. Baker, D. (1988). Tillage and Split N-Fertilization Effects on Subsurface Drainage Water Quality and Crop Yields. *Transactions of the ASAE* **31**, 453-0461.

Sainju, U., Singh, H., Singh, B., Whitehead, W., Chiluwal, A., and Paudel, R. (2018). Cover Crop and Nitrogen Fertilization Influence Soil Carbon and Nitrogen Under Bioenergy Sweet Sorghum. *Agronomy Journal* **110**.

Saseendran, S. A., Ahuja, L. R., Nielsen, D. C., Trout, T. J., and Ma, L. (2008). Use of crop simulation models to evaluate limited irrigation management options for corn in a semiarid environment. *Water Resources Research* **44**.

Saso, J., Parkin, G., Drury, C., Lauzon, J., and Reynolds, W. (2012). Chloride leaching in two Ontario soils: Measurement and prediction using HYDRUS-1D. *Canadian Journal of Soil Science* **92**, 285-296.

Schaap, M., Leij, F., and Van Genuchten, M. (2001). ROSETTA: A computer program for estimating soil hydraulic parameters with hierarchical pedotransfer functions. *Journal of Hydrology* **251**, 163-176.

Schaap, M. G., and Bouten, W. (1996). Modeling water retention curves of sandy soils using neural networks. *Water Resources Research* **32**, 3033-3040.

Schaap, M. G., and Leij, F. J. (1998). Using neural networks to predict soil water retention and soil hydraulic conductivity. *Soil and Tillage Research* **47**, 37-42.

Schaap, M. G., Leij, F. J., and van Genuchten, M. T. (1998). Neural Network Analysis for Hierarchical Prediction of Soil Hydraulic Properties. *Soil Science Society of America Journal* **62**, 847-855.

Sellner, K. G., Doucette, G. J., and Kirkpatrick, G. J. (2003). Harmful algal blooms: causes, impacts and detection. *Journal of Industrial Microbiology and Biotechnology* **30**, 383-406.

Shahbandeh, M. (2020). Corn production worldwide 2019/2020, by country. https://www.statista.com/statistics/254292/global-corn-production-by-country/.

Shahrokhnia, M. H., and Sepaskhah, A. R. (2018). Water and nitrate dynamics in safflower field lysimeters under different irrigation strategies, planting methods, and nitrogen fertilization and application of HYDRUS-1D model. *Environmental Science and Pollution Research* **25**, 8563-8580.

Sharpley, A. N., Chapra, S., Wedepohl, R., Sims, J., Daniel, T. C., and Reddy, K. (1994). Managing agricultural phosphorus for protection of surface waters: Issues and options. *Journal of environmental quality* **23**, 437-451.

Sims, J. T., Simard, R. R., and Joern, B. C. (1998). Phosphorus loss in agricultural drainage: Historical perspective and current research. *Journal of environmental quality* **27**, 277-293.

Šimůnek, J., and Hopmans, J. W. (2009). Modeling compensated root water and nutrient uptake. *Ecological modelling* **220**, 505-521.

Šimůnek, J., van Genuchten, M. T., and Šejna, M. (2016). Recent Developments and Applications of the HYDRUS Computer Software Packages. *Vadose Zone Journal* **15**, vzj2016.04.0033.

Simunek, J. J., Van Genuchten, M., and Šejna, M. (2008). Development and applications of the HYDRUS and STANMOD software packages and related codes. *Vadose Zone Journal* **7**, 587-600.

Simunek, J. J., Van Genuchten, M., and Šejna, M. (2016). Recent Developments and Applications of the HYDRUS Computer Software Packages. *Vadose Zone Journal* **6**.

Singh, G., Schoonover, J., and Williard, K. (2018). Cover Crops for Managing Stream Water Quantity and Improving Stream Water Quality of Non-Tile Drained Paired Watersheds. *Water* **10**.

Skaggs, T., Trout, T., Nek, J., and Shouse, P. (2004). Comparison of HYDRUS-2D Simulations of Drip Irrigation with Experimental Observations. *Journal of Irrigation and Drainage Engineering-asce - J IRRIG DRAIN ENG-ASCE* **130**.

Sogbedji, J. M., van Es, H. M., Yang, C. L., Geohring, L. D., and Magdoff, F. R. (2000). Nitrate Leaching and Nitrogen Budget as Affected by Maize Nitrogen Rate and Soil Type. *Journal of Environmental Quality* **29**, 1813-1820.

Soileau, J. M., Touchton, J. T., Hajek, B. F., and Yoo, K. H. (1994). Sediment, nitrogen, and phosphorus runoff with conventional-and conservation-tillage cotton in a small watershed. *Journal of Soil and Water Conservation* **49**, 82-89.

Sonnleitner, M. A., Abbaspour, K. C., and Schulin, R. (2003). Hydraulic and transport properties of the plant–soil system estimated by inverse modelling. *European Journal of Soil Science* **54**, 127-138.

Spalding, R. F., Watts, D. G., Schepers, J. S., Burbach, M. E., Exner, M. E., Poreda, R. J., and Martin, G. E. (2001). Controlling Nitrate Leaching in Irrigated Agriculture. *Journal of Environmental Quality* **30**, 1184-1194.

St. Luce, M., Whalen, J. K., Ziadi, N., and Zebarth, B. J. (2011). Chapter two - Nitrogen Dynamics and Indices to Predict Soil Nitrogen Supply in Humid Temperate Soils. *In* "Advances in Agronomy" (D. L. Sparks, ed.), Vol. 112, pp. 55-102. Academic Press.

Steiner, J. L. (1994). Crop residue effects on water conservation. *Managing agricultural residues* **76**.

Stewart, J., and Tiessen, H. (1987). Dynamics of soil organic phosphorus. *Biogeochemistry* **4**, 41-60.

Tafteh, A., and Sepaskhah, A. R. (2012). Application of HYDRUS-1D model for simulating water and nitrate leaching from continuous and alternate furrow irrigated rapeseed and maize fields. *Agricultural Water Management* **113**, 19-29.

Tagma, T., Hsissou, Y., Bouchaou, L., Bouragba, L., and Boutaleb, S. (2009). Groundwater nitrate pollution in Souss-Massa basin. *African Journal of Environmental Science and Technology* **3**, 301-309.

Tan, X., Shao, D., Gu, W., and Liu, H. (2015). Field analysis of water and nitrogen fate in lowland paddy fields under different water managements using HYDRUS-1D. *Agricultural Water Management* **150**, 67-80.

Thomas, D. L., Smith, M. C., Leonard, R. A., and daSilva, F. J. K. (1990). Simulated effects of rapeseed production alternatives on pollution potential in the Georgia Coastal Plain. *Journal of Soil and Water Conservation* **45**, 148-154.

Toffanin, A. (2019). Scheduling Nitrogen Applications in Maize with a Simulation Model, University of Georgia.

Toor, G. S., Condron, L. M., Di, H. J., Cameron, K. C., and Cade-Menun, B. J. (2003). Characterization of organic phosphorus in leachate from a grassland soil. *Soil Biology and Biochemistry* **35**, 1317-1323.

Udvardi, M., Brodie, E. L., Riley, W., Kaeppler, S., and Lynch, J. (2015). Impacts of Agricultural Nitrogen on the Environment and Strategies to Reduce these Impacts. *Procedia Environmental Sciences* **29**, 303.

UN (2020). Water Scarcity. Vol. 2020, https://www.unwater.org/water-facts/scarcity/.

USDA (2018). World Agricultural Supply and Demand Estimates. USDA, Economics, Statistics and Market Information System. WASDE-575 March 8, 2018. .

USDA (2019). Irrigation & Water Use. Vol. 2019, https://www.ers.usda.gov/topics/farm-practices-management/irrigation-water-use/.

USDA, U. (2013). Fertilizer use and price. *US Department of Agriculture, Economic Research Service.*

van Genuchten, M. (1980). A Closed-form Equation for Predicting the Hydraulic Conductivity of Unsaturated Soils1. *Soil Science Society of America Journal* **44**.

Vellidis, G., Liakos, V., Andreis, J. H., Perry, C. D., Porter, W. M., Barnes, E. M., Morgan, K. T., Fraisse, C., and Migliaccio, K. W. (2016a). Development and assessment of a smartphone application for irrigation scheduling in cotton. *Computers and Electronics in Agriculture* **127**, 249-259.

Vellidis, G., Liakos, V., Debastiani Andreis, J., Perry, C. D., Porter, W. M., Barnes, E. M., Morgan, K., Fraisse, C., and Migliaccio, K. (2016b). Development and assessment of a smartphone application for irrigation scheduling in cotton. *Computers and Electronics in Agriculture* **127**, 249-259.

Vellidis, G., Liakos, V., Porter, W. M., Tucker, M., and Liang, X. (2016c). A Dynamic Variable Rate Irrigation Control System. *In* "13th International Conference on Precsion Agriculture ", St. Louis, Missouri, USA.

Vellidis, G., Lowrance, R., Gay, P., and Hubbard, R. (2003). Nutrient Transport in a Restored Riparian Wetland. *Journal of environmental quality* **32**, 711-26.

Vellidis, G., Tucker, M., Perry, C., Kvien, C., and Bednarz, C. (2008). A real-time wireless smart sensor array for scheduling irrigation. *Computers and Electronics in Agriculture* **61**, 44-50.

Vellidis, G., Tucker, M., Perry, C., Reckford, D., Butts, C., Henry, H., Liakos, V., Hill, R. W., and W., E. (2013). "A soil moisture sensor-based variable rate irrigation scheduling system," Precision agriculture '13. Wageningen Academic Publishers, Wageningen.

Ventrella, D., Castellini, M., Di Prima, S., Garofalo, P., and Lassabatere, L. (2019). Assessment of the Physically-Based Hydrus-1D Model for Simulating the Water Fluxes of a Mediterranean Cropping System. *Water* **11**, 1657.

Vereecken, H., Maes, J., Feyen, J., and Darius, P. (1989). Estimating the soil moisture retention characteristic from texture, bulk density, and carbon content. *Soil science* **148**, 389-403.

Walker, A. (1974). A simulation model for prediction of herbicide persistence. *J. Environ. Quality, 3(4), 396-401*.

Wang, H., Ju, X., Wei, Y., Li, B., Zhao, L., and Hu, K. (2010). Simulation of bromide and nitrate leaching under heavy rainfall and high-intensity irrigation rates in North China Plain. *Agricultural Water Management* **97**, 1646-1654.

Wesseling, J. (1991). Meerjarige simulaties van grondwateronttrekking voor verschillende bodemprofielen, grondwatertrappen en gewassen met het model SWATRE. *SC-DLO report* **152**, 40.

Weyer, P. J., Cerhan, J. R., Kross, B. C., Hallberg, G. R., Kantamneni, J., Breuer, G., Jones, M. P., Zheng, W., and Lynch, C. F. (2001). Municipal drinking water nitrate level and cancer risk in older women: the Iowa Women's Health Study. *Epidemiology* **12**, 327-338.

WHO (1996). "Guidelines for Drinking-Water Quality, 2nd edition." World Health Organization, https://www.who.int/water_sanitation_health/publications/gdwq2v1/en/index1.html.

Yadav, S. N. (1997). Formulation and estimation of nitrate-nitrogen leaching from corn cultivation. *Journal of Environmental Quality* **26**, 808-814.

Yu, S., He, Z., Stoffella, P., Calvert, D., Yang, X., Banks, D., and Baligar, V. (2006). Surface runoff phosphorus (P) loss in relation to phosphatase activity and soil P fractions in Florida sandy soils under citrus production. *Soil Biology and Biochemistry* **38**, 619-628.

Zhang, A., Chen, Z., Zhang, G., Chen, L., and Wu, Z. (2012). Soil phosphorus composition determined by 31P NMR spectroscopy and relative phosphatase activities influenced by land use. *European journal of soil biology* **52**, 73-77.

Zhang, H., Yang, R., Guo, S., and Li, Q. (2020). Modeling fertilization impacts on nitrate leaching and groundwater contamination with HYDRUS-1D and MT3DMS. *Paddy and Water Environment* **18**, 481-498.

Zhang, X., Davidson, E. A., Mauzerall, D. L., Searchinger, T. D., Dumas, P., and Shen, Y. (2015). Managing nitrogen for sustainable development. *Nature* **528**, 51-59.

Zhao, S. L., Gupta, S. C., Huggins, D. R., and Moncrief, J. F. (2001). Tillage and Nutrient Source Effects on Surface and Subsurface Water Quality at Corn Planting. *Journal of Environmental Quality* **30**, 998-1008.

Zhu, J., Gantzer, C., Anderson, S., Alberts, E., and Beuselinck, P. (1989). Runoff, soil, and dissolved nutrient losses from no-till soybean with winter cover crops. *Soil Science Society of America Journal* **53**, 1210-1214.

APPENDIX A

Connecting letters report showing the differences of concentrations in surface runoff between the crops, the three years of the project and the fertilization treatments. Means followed by different letters within the same year, block and treatment are significantly different ($p < 0.05$). Bold letters indicate statistics run with $a = 0.1$.

Trt	Block	Year	Crop	TSS (mg L^{-1})	NO_3-N (mg L^{-1})	NH_4-N (mg L^{-1})	TN (mg L^{-1})	PO_4-P (mg L^{-1})	TP (mg L^{-1})
By cropping period									
C_E	W2	1	Maize	494.8^{a}	2.72^{a} **a**	0.5^{a}	4.49^{a}	0.31^{b}	0.48^{b}
			Residue	7.2^{a}	1.16^{a} **ab**	0^{a}	2.15^{ab}	1.16^{a}	2.89^{a}
			Wheat	81^{a}	0.48^{a} **b**	0.01^{a}	0.83^{b}	0.28^{b}	0.42^{b}
			Mean	194.3	1.45	0.17	2.49	0.58	1.26
		2	Maize	43.1^{a}	0.75^{a}	0.16^{a}	2.45^{a}	1.74^{a} **b**	1.93^{a} **b**
			Residue	9.7^{a}	0.63^{a}	0.17^{a}	2.94^{a}	4.97^{a} **a**	5.43^{a} **a**
			Rye	40^{a}	0.13^{a}	0.02^{a}	2.17^{a}	1.06^{a} **ab**	1.48^{a} **ab**
			Mean	30.9	0.5	0.12	2.52	2.59	2.95
		3	Maize	37.5^{b}	1.23^{a}	1.48^{a}	3.16^{a} **a**	1.65^{a}	2.01^{a}
			Residue	259^{ab}	0.22^{b}	1.67^{a}	1.16^{ab} **b**	0.73^{b}	0.76^{b}
			Wheat	511.8^{a}	0.27^{b}	0.72^{b}	0.63^{b} **b**	0.25^{b}	0.64^{b}
			Mean	269.4	0.57	1.29	1.65	0.88	1.14
	E1	1	Maize	941.5^{a}	4.2^{a}	0.61^{a}	6^{a}	0.54^{b}	0.68^{b}
			Residue	22.4^{ab}	2.23^{ab}	0^{a}	2.99^{ab}	2.23^{a}	1.95^{a}
			Wheat	86.7^{b}	0.61^{b}	0.02^{a}	1.17^{b}	0.5^{b}	0.73^{ab}
			Mean	350.2	2.35	0.21	3.39	1.09	1.12
		2	Maize	127.2^{a}	0.91^{c}	0.24^{a}	2.23^{b} **c**	1.97^{a}	2.15^{a}
			Residue	66.6^{a}	1.33^{b}	0.37^{a}	3.44^{b} **b**	4.01^{a}	4.14^{a}
			Rye	26.2^{a}	3.2^{a}	0.11^{a}	16.93^{a} **a**	1.21^{a}	1.58^{a}
			Mean	73.3	1.81	0.24	7.53	2.40	2.62
		3	Maize	170.5^{a}	1.22^{a} **a**	1.42^{a}	2.42^{a}	1.35^{a}	1.65^{a}
			Residue	271.4^{a}	0.34^{a} **ab**	1.52^{a}	1.19^{ab}	1.05^{a}	2.11^{a}
			Wheat	828.0^{a}	0.31^{a} **b**	0.62^{b}	0.48^{b}	0.26^{b}	0.75^{b}
			Mean	423.3	0.62	1.19	1.36	0.89	1.50
	E3	1	Maize	395.2^{a}	2.47^{a}	0.12^{a}	3.85^{a}	0.31^{a}	0.5^{b}
			Residue	14.6^{a}	1.06^{ab}	0^{a}	1.81^{a}	1.06^{a}	1.8^{a}
			Wheat	73.4^{a}	0.57^{b}	0^{a}	1.15^{a}	0.48^{a}	0.75^{b}
			Mean	161.1	1.37	0.04	2.27	0.62	1.02
		2	Maize	32.6^{a}	0.41^{b}	0.07^{a}	2.07^{b}	1.16^{a}	1.39^{a}
			Residue	13.5^{a}	0.21^{ab}	0.09^{a}	1.83^{ab}	1.39^{a}	1.52^{a}
			Rye	16.9^{a}	1.51^{a}	0.07^{a}	8.39^{a}	1.04^{a}	1.23^{a}

Trt	Block	Year	Crop	TSS (mg L^{-1})	NO_3-N (mg L^{-1})	NH_4-N (mg L^{-1})	TN (mg L^{-1})	PO_4-P (mg L^{-1})	TP (mg L^{-1})
			Mean	21.0	0.71	0.08	4.1	1.2	1.38
		3	Maize	38.4^{b}	0.65^{a}	1.12^{a}	2.54^{a}	1.17^{a}	1.52^{b}
			Residue	55.1^{ab}	0.15^{ab}	1.45^{a}	1.22^{ab}	1.56^{a}	2.56^{a}
			Wheat	1229.5^{a}	0.28^{b}	0.61^{a}	0.42^{b}	0.28^{b}	0.72^{c}
			Mean	441	0.36	1.06	1.39	1	1.6
C_G	W1	1	Maize	243.2^{a}	1.89^{a}	0.45^{a}	4.23^{a}	0.3^{b}	0.46^{b}
			Residue	5.2^{a}	1.2^{a}	0^{a}	2.05^{ab}	1.2^{a}	1.66^{a}
			Wheat	83.7^{a}	0.81^{a}	0^{a}	1.47^{b}	0.34^{b}	0.41^{b}
			Mean	110.7	1.30	0.15	2.58	0.61	0.84
		2	Maize	48.3^{a}	2.03^{a}	0.02^{b}	2.94^{b}	1.52^{a}	1.65^{a}
			Residue	30.9^{a}	0.85^{a}	0.03^{b}	3.88^{b}	4.61^{a}	4.82^{a}
			Rye	196.2^{a}	2.05^{a}	0.3^{a}	17.84^{a}	0.67^{a}	0.4^{a}
			Mean	91.8	1.64	0.12	8.22	2.27	2.29
		3	Maize	102.7^{a}	1.04^{a}	1.38^{a}	2.62^{a}	0.97^{a}	1.22^{a}
			Residue	109.9^{a}	0.41^{ab}	1.49^{a}	1.42^{ab}	1.05^{a}	1.53^{a}
			Wheat	127.3^{a}	0.29^{b}	0.7^{b}	0.32^{b}	0.23^{b}	0.69^{a}
			Mean	113.3	0.58	1.19	1.45	0.75	1.15
	W3	1	Maize	471.5^{a}	3.43^{a}	0.44^{a}	4.52^{a}	0.27^{a}	0.45$^{a\ b}$
			Residue	9^{ab}	1.2^{a}	0^{a}	2.57^{ab}	1.2^{a}	1.63$^{a\ ab}$
			Wheat	89.2^{b}	1.22^{a}	0^{a}	1.77^{b}	0.6^{a}	0.93$^{a\ a}$
			Mean	189.9	1.95	0.15	2.95	0.69	1.00
		2	Maize	85.2^{a}	2.57^{a}	0.04^{a}	4.33^{a}	1.48^{a}	1.86$^{a\ a}$
			Residue	17.3^{a}	0.57^{a}	0.03^{a}	2.95^{a}	1.54^{a}	1.92$^{a\ ab}$
			Rye	24.1^{a}	1.46^{a}	0.07^{a}	7.43^{a}	0.95^{a}	1.23$^{a\ b}$
			Mean	42.2	1.53	0.05	4.90	1.32	1.67
		3	Maize	53.1^{b}	2.27^{a}	1.23^{a}	4.16^{a}	1.10^{a}	1.56^{a}
			Residue	214.5^{ab}	0.34^{ab}	1.46^{a}	2.07^{ab}	1.17^{a}	1.98^{a}
			Wheat	730.3^{a}	0.21^{b}	0.61^{a}	0.51^{b}	0.24^{b}	0.67^{b}
			Mean	332.6	0.94	1.1	2.25	0.84	1.40
	E2	1	Maize	850.5^{a}	3.55^{a}	0.48^{a}	4.75^{a}	0.62$^{a\ ab}$	0.75^{b}
			Residue	14.1^{ab}	1.64^{ab}	0^{a}	2.74^{ab}	1.64$^{a\ a}$	2.5^{a}
			Wheat	106.3^{b}	0.53^{b}	0.01^{a}	0.96^{b}	0.39$^{a\ b}$	0.58^{b}
			Mean	323.6	1.91	0.16	2.82	0.88	1.28
		2	Maize	127.8^{a}	0.85^{a}	0.14^{a}	2.24^{b}	1.52$^{a\ a}$	1.71^{a}
			Residue	27.8^{a}	1.12^{a}	0.08^{a}	2.59^{ab}	1.57$^{a\ a}$	1.74^{a}
			Rye	21.5^{a}	0.75^{a}	0.28^{a}	8.14^{a}	1.04$^{a\ b}$	1.24^{b}
			Mean	59.0	0.91	0.17	4.32	1.38	1.56
		3	Maize	31.1^{b}	0.46^{a}	1.43^{a}	1.60^{a}	1.21^{a}	1.57^{b}
			Residue	455.6^{ab}	0.1^{b}	1.53^{ab}	1.07^{ab}	1.59^{a}	2.77^{a}
			Wheat	1324.8^{a}	0.23^{b}	0.73^{b}	0.62^{b}	0.21^{b}	0.75^{c}
			Mean	603.8	0.26	1.23	1.1	1	1.7

Trt	Block	Year	Crop	TSS (mg L^{-1})	NO_3-N (mg L^{-1})	NH_4-N (mg L^{-1})	TN (mg L^{-1})	PO_4-P (mg L^{-1})	TP (mg L^{-1})
By year									
C_E	W2	1		406.5^{a}	2.27^{a}	0.39^{b}	3.75^{a}	0.33^{c}	0.53^{c}
		2		32.8^{a}	0.65^{b}	0.15^{b}	2.57^{ab}	2.64^{a}	2.94^{a}
		3		265.9^{a}	0.69^{b}	1.19^{a}	1.82^{b}	0.94^{b}	1.26^{b}
		Mean		235.1	1.20	0.58	2.71	1.30	1.58
	E1	1		791.3^{a} **a**	3.60^{a}	0.5^{a} **b**	5.19^{a}	0.56^{b}	0.71^{c}
		2		88.8^{a} **b**	1.5^{ab}	0.25^{a} **ab**	5.53^{a}	2.43^{a}	2.63^{a}
		3		491.3^{a} **ab**	0.69^{b}	1.06^{a} **a**	1.36^{b}	0.8^{b}	1.29^{b}
		Mean		457.3	1.93	0.60	4.03	1.26	1.54
	E3	1		330.9^{a}	2.11^{a}	0.1^{b}	3.33^{ab} **a**	0.35^{b}	0.56^{b}
		2		25.5^{a}	0.76^{b}	0.07^{b}	4.16^{a} **a**	1.14^{a}	1.35^{a}
		3		445^{a}	0.47^{b}	0.98^{a}	1.67^{b} **b**	0.91^{a}	1.35^{a}
		Mean		267.1	1.11	0.38	3.05	0.8	1.09
	Treatment	1		518.4^{a}	2.69^{a}	0.32^{b}	4.12^{a}	0.42^{c}	0.61^{c}
		2		41.9^{b}	0.9^{b}	0.13^{b}	4.11^{a}	1.77^{a}	2^{a}
		3		402.9^{a}	0.6^{b}	1.07^{a}	1.64^{b}	0.89^{b}	1.31^{b}
C_G	W1	1		199.9^{a}	1.61^{a}	0.33^{b}	3.52^{a}	0.33^{b} **c**	0.47^{c}
		2		62.4^{a}	1.74^{a}	0.06^{b}	5.04^{a}	2.19^{a} **a**	2.29^{a}
		3		114.2^{a}	0.63^{b}	1.11^{a}	1.46^{b}	0.67^{b} **b**	1.04^{b}
		Mean		125.5	1.33	0.50	3.34	1.06	1.27
	W3	1		386.6^{a}	2.95^{a}	0.34^{b}	3.93^{ab}	0.35^{c}	0.56^{b}
		2		63.5^{b}	2.11^{ab}	0.05^{b}	5.06^{a}	1.34^{a}	1.69^{a}
		3		315.3^{ab}	1.3^{b}	1.03^{a}	2.62^{b}	0.80^{b}	1.28^{a}
		Mean		255.1	2.12	0.47	3.87	0.83	1.18
	E2	1		705.5^{a}	3.01^{a}	0.39^{b}	4.08^{a}	0.61^{b}	0.78^{b}
		2		65.3^{b}	0.86^{b}	0.18^{b}	4.67^{a}	1.34^{a}	1.53^{a}
		3		617.3^{ab}	0.33^{b}	1.15^{a}	1.13^{b}	0.83^{b}	1.36^{a}
		Mean		462.7	1.40	0.57	3.29	0.93	1.22
	Treatment	1		460.2^{a}	2.63^{a} **a**	0.36^{b}	3.88^{a}	0.45^{c}	0.62^{c}
		2		63.9^{b}	1.67^{ab} **b**	0.1^{b}	4.94^{a}	1.48^{a}	1.74^{a}
		3		351.8^{a}	0.81^{b} **b**	1.09^{a}	1.83^{b}	0.77^{b}	1.24^{b}
By fertilization treatment									
C_E					1.72^{a}	0.56^{a}	3.24^{a}	0.77^{a}	1.04^{a}
C_G					1.87^{a}	0.57^{a}	3.34^{a}	0.7^{a}	0.99^{a}

APPENDIX B

Connecting letters report showing the differences of loads of surface runoff and TSS, TN, NO_3-N, NH_4-N, TP, PO_4-P in surface runoff between the crops, the years of the project and the fertilization treatments. Means followed by different letters within the same year, block and treatment are significantly different ($p < 0.05$). Bold letters indicate statistics run with $a = 0.1$.

Trt	Block	Year	Crop	Runoff (m^3 ha^{-1})	TSS (kg ha^{-1})	NO_3-N (kg ha^{-1})	NH_4-N (kg ha^{-1})	TN (kg ha^{-1})	PO_4-P (kg ha^{-1})	TP (kg ha^{-1})
By cropping period										
C_E	W2	1	Maize	14.03^{a}	11.37^{a}	0.07^{b}	0.01^{a}	0.12^{b}	0.01^{b}	0.02^{b}
			Residue	40.52^{a}	4.37^{a}	0.71^{a}	0^{a}	1.3^{a}	0.71^{a}	1.76^{a}
			Wheat	50.87^{a}	29.34^{a}	0.11^{b}	0^{a}	0.16^{b}	0.04^{b}	0.08^{b}
			Mean	35.14	15.03	0.3	0	0.53	0.25	0.62
		2	Maize	3.53^{a}	5.81^{a}	0.04^{a}	0^{a}	0.08^{a}	0.05^{a}	0.06^{a}
			Residue	0.95^{a}	0.05^{a}	0.01^{a}	0^{a}	0.02^{a}	0.02^{a}	0.02^{a}
			Rye	0.03^{a}	0.05^{a}	0^{a}	0^{a}	0^{a}	0^{a}	0^{a}
			Mean	1.50	1.97	0.02	0	0.03	0.02	0.03
		3	Maize	4.89$^{a\ \mathbf{b}}$	1.12^{a}	0.03^{a}	0.05^{a}	0.07^{a}	0.03^{a}	0.04^{a}
			Residue	1.42$^{a\ \mathbf{b}}$	2.87^{a}	0^{a}	0.02^{a}	0.01^{a}	0.01^{a}	0.01^{a}
			Wheat	16.21$^{a\ \mathbf{a}}$	13.79^{a}	0.02^{a}	0.02^{a}	0.02^{a}	0.01^{a}	0.04^{a}
			Mean	7.51	5.93	0.02	0.03	0.03	0.02	0.03
	E1	1	Maize	11.28^{a}	16.29^{a}	0.06^{b}	0.01^{a}	0.09^{b}	0.01^{b}	0.02^{c}
			Residue	40.28^{a}	13.55^{a}	1.35^{a}	0^{a}	1.81^{a}	1.35^{a}	1.18^{a}
			Wheat	48.59^{a}	29.59^{a}	0.1^{b}	0^{a}	0.17^{b}	0.04^{b}	0.11^{b}
			Mean	33.38	19.81	0.5	0	0.69	0.47	0.44
		2	Maize	2.37^{a}	9.01^{a}	0.03^{a}	0^{a}	0.06^{a}	0.05^{a}	0.06^{a}
			Residue	0.05^{a}	0.02^{a}	0^{a}	0^{a}	0^{a}	0^{a}	0^{a}
			Rye	0.02^{a}	0.01^{a}	0^{a}	0^{a}	0.01^{a}	0^{a}	0^{a}

Trt	Block	Year	Crop	Runoff (m^3 ha^{-1})	TSS (kg ha^{-1})	NO_3-N (kg ha^{-1})	NH_4-N (kg ha^{-1})	TN (kg ha^{-1})	PO_4-P (kg ha^{-1})	TP (kg ha^{-1})
			Mean	0.81	3.01	0.01	0.00	0.02	0.02	0.02
		3	Maize	5.74^{a}	1.70^{a}	0.02^{a}	0.07^{a}	0.08^{a}	0.05^{a}	0.07^{a}
			Residue	0.01^{a}	0.02^{a}	0^{a}	0^{a}	0^{ab}	0^{ab}	0^{a}
			Wheat	7.47^{a}	6.14^{a}	0.01^{a}	0.01^{a}	0.01^{b}	0^{b}	0.02^{a}
			Mean	4.41	2.62	0.01	0.03	0.03	0.02	0.03
	E3	1	Maize	26.27^{a}	18.66^{a}	0.11^{a}	0.01^{a}	0.17^{a}	0.01^{b}	0.03^{b}
			Residue	12.30^{a}	2.67^{a}	0.2^{a}	0^{a}	0.33^{a}	0.2^{a}	0.33^{a}
			Wheat	43.32^{a}	20.31^{a}	0.05^{a}	0^{a}	0.1^{a}	0.02^{b}	0.05^{b}
			Mean	27.30	13.88	0.12	0	0.2	0.08	0.14
		2	Maize	1.83^{a}	0.96^{a}	0.01^{a}	0^{a}	0.02^{a}	0.01^{a}	0.01^{a}
			Residue	0.95^{a}	0.14^{a}	0^{a}	0^{a}	0.02^{a}	0.01^{a}	0.01^{a}
			Rye	0.69^{a}	0.05^{a}	0^{a}	0^{a}	0.02^{a}	0^{a}	0.01^{a}
			Mean	1.16	0.38	0	0	0.02	0.01	0.01
		3	Maize	11.55^{a}	1.84^{b}	0.01^{a}	0.06^{a} **a**	0.06^{a} **a**	0.04^{a}	0.04^{a}
			Residue	0.34^{a}	0.15^{ab}	0^{a}	0^{a} **ab**	0^{a} **ab**	0^{ab}	0.01^{a}
			Wheat	13.48^{a}	12.19^{a}	0.01^{a}	0.01^{a} **b**	0.01^{a} **b**	0.01^{b}	0.03^{a}
			Mean	8.46	4.73	0.01	0.02	0.02	0.02	0.03
C_G	W1	1	Maize	6.12^{b}	4.83^{a}	0.04^{a}	0.01^{a}	0.08^{a}	0.01^{a}	0.01^{a}
			Residue	1.95^{ab}	0.15^{a}	0.04^{a}	0^{a}	0.06^{a}	0.04^{a}	0.05^{a}
			Wheat	38.87^{a}	15.28^{a}	0.06^{a}	0^{a}	0.11^{a}	0.02^{a}	0.04^{a}
			Mean	15.65	6.75	0.05	0	0.08	0.02	0.03
		2	Maize	3.42^{a}	5.57^{a}	0.07^{a}	0^{a}	0.1^{a}	0.08^{a}	0.09^{a}
			Residue	1.17^{a}	0.56^{a}	0.02^{a}	0^{a}	0.04^{a}	0.03^{a}	0.03^{a}
			Rye	0.04^{a}	0.29^{a}	0^{a}	0^{a}	0.03^{a}	0^{a}	0^{a}
			Mean	1.54	2.14	0.03	0	0.06	0.04	0.04
		3	Maize	6.88^{a}	3.17^{a}	0.04^{a}	0.08^{a}	0.09^{a} **a**	0.03^{a}	0.04^{a}
			Residue	0.95^{a}	0.75^{a}	0^{a}	0.01^{a}	0.01^{a} **ab**	0.01^{ab}	0.01^{a}
			Wheat	7.04^{a}	2.82^{a}	0.01^{a}	0.01^{a}	0.01^{a} **b**	0^{b}	0.02^{a}
			Mean	4.96	2.25	0.02	0.03	0.04	0.01	0.02

Trt	Block	Year	Crop	Runoff (m^3 ha^{-1})	TSS (kg ha^{-1})	NO_3-N (kg ha^{-1})	NH_4-N (kg ha^{-1})	TN (kg ha^{-1})	PO_4-P (kg ha^{-1})	TP (kg ha^{-1})
	W3	1	Maize	20.22^{a}	17.84^{a}	0.13^{a}	0.02^{a}	0.17^{a}	0.02^{b}	0.03$^{a\ b}$
			Residue	11.03^{a}	1.49^{a}	0.20^{a}	0^{a}	0.43^{a}	0.2^{a}	0.27$^{a\ a}$
			Wheat	64^{a}	27.09^{a}	0.08^{a}	0^{a}	0.16^{a}	0.02^{b}	0.06$^{a\ ab}$
			Mean	31.75	15.47	0.14	0.01	0.25	0.08	0.12
		2	Maize	5.65^{a}	2.49^{a}	0.04^{a}	0^{a}	0.07^{a}	0.03^{a}	0.04^{a}
			Residue	0.64^{a}	0.11^{a}	0^{a}	0^{a}	0.02^{a}	0.01^{a}	0.01^{a}
			Rye	0.77^{a}	0.07^{a}	0^{a}	0^{a}	0.02^{a}	0.01^{a}	0.01^{a}
			Mean	2.35	0.89	0.01	0	0.04	0.02	0.02
		3	Maize	9.75$^{a\ ab}$	1.84$^{a\ b}$	0.04^{a}	0.06^{a}	0.1^{a}	0.03^{a}	0.05^{a}
			Residue	1.06$^{b\ b}$	1.15$^{a\ ab}$	0^{a}	0.01^{a}	0.02^{a}	0.01^{a}	0.02^{a}
			Wheat	19.20$^{a\ a}$	17.63$^{a\ a}$	0.01^{a}	0.01^{a}	0.02^{a}	0.01^{a}	0.04^{a}
			Mean	10.01	6.87	0.02	0.03	0.05	0.02	0.04
	E2	1	Maize	19.82^{a}	32.93^{a}	0.12$^{a\ b}$	0.01^{a}	0.17^{b}	0.03^{b}	0.04^{b}
			Residue	51.29^{a}	5.41^{a}	0.63$^{a\ a}$	0^{a}	1.05^{a}	0.63^{a}	0.96^{a}
			Wheat	20.33^{a}	6.95^{a}	0.03$^{a\ b}$	0^{a}	0.05^{b}	0.02^{b}	0.03^{b}
			Mean	30.48	15.10	0.26	0	0.42	0.23	0.34
		2	Maize	0.94^{a}	2.88^{a}	0.01^{a}	0^{a}	0.02^{a}	0.02^{a}	0.02^{a}
			Residue	0.11^{a}	0.01^{a}	0^{a}	0^{a}	0^{a}	0^{a}	0^{a}
			Rye	0.09^{a}	0.01^{a}	0^{a}	0^{a}	0.01^{a}	0^{a}	0^{a}
			Mean	0.38	0.97	0.00	0.00	0.01	0.01	0.01
		3	Maize	5.83^{a}	0.85$^{a\ b}$	0.01^{a}	0.05^{a}	0.03^{a}	0.03^{a}	0.04^{a}
			Residue	0.39^{a}	2.26$^{a\ ab}$	0^{a}	0.01^{a}	0^{a}	0.01^{ab}	0.01^{a}
			Wheat	7.65^{a}	15.74$^{a\ a}$	0.01^{a}	0.01^{a}	0.01^{a}	0.00^{b}	0.02^{a}
			Mean	4.62	6.28	0.01	0.02	0.01	0.01	0.02
By year										
C_E	W2	1		25.13^{a}	14.55^{a}	0.09^{a}	0.01^{b}	0.15$^{a\ a}$	0.04^{a}	0.07^{a}
		2		2.1^{b}	3.51^{a}	0.02^{ab}	0^{ab}	0.06$^{a\ ab}$	0.04^{a}	0.04^{a}
		3		7.25^{b}	6.64^{a}	0.02^{b}	0.03^{a}	0.04$^{a\ b}$	0.02^{a}	0.03^{a}
		Mean		11.49	8.23	0.04	0.01	0.08	0.03	0.05

Trt	Block	Year	Crop	Runoff (m^3 ha^{-1})	TSS (kg ha^{-1})	NO_3-N (kg ha^{-1})	NH_4-N (kg ha^{-1})	TN (kg ha^{-1})	PO_4-P (kg ha^{-1})	TP (kg ha^{-1})
	E1	1		22.75^{a}	18.36^{a}	0.09^{a}	0.01$^{a\ b}$	0.13^{a}	0.04^{a}	0.05^{a}
		2		1.32^{b}	4.51^{a}	0.02^{a}	0$^{a\ ab}$	0.01^{a}	0.03^{a}	0.03^{a}
		3		5.01^{b}	3.57^{a}	0.01^{a}	0.03$^{a\ a}$	0.04^{a}	0.02^{a}	0.04^{a}
		Mean		9.69	8.81	0.04	0.01	0.06	0.03	0.04
	E3	1		28.64^{a}	18.72^{a}	0.10$^{a\ a}$	0.01^{b}	0.16$^{a\ a}$	0.02^{a}	0.04^{a}
		2		1.35^{b}	0.57^{a}	0.01$^{a\ ab}$	0.00^{b}	0.02$^{a\ b}$	0.01^{a}	0.01^{a}
		3		9.72^{b}	5.19^{a}	0.01$^{a\ b}$	0.04^{a}	0.03$^{a\ b}$	0.02^{a}	0.04^{a}
		Mean		13.24	8.16	0.04	0.02	0.07	0.02	0.03
	Treatment	1		25.51^{a}	17.54^{a}	0.09^{a}	0.01^{b}	0.15^{a}	0.03^{a}	0.05^{a}
		2		1.6^{b}	2.17^{b}	0.01^{b}	0^{b}	0.03^{b}	0.02^{a}	0.02^{a}
		3		7.32^{b}	5.19^{b}	0.02^{b}	0.03^{a}	0.04^{b}	0.02^{a}	0.04^{a}
C_G	W1	1		13.06$^{a\ a}$	7.23^{a}	0.04^{a}	0.01$^{a\ b}$	0.08^{a}	0.01^{b}	0.02^{a}
		2		2.07$^{a\ b}$	3.66^{a}	0.05^{a}	0$^{a\ ab}$	0.08^{a}	0.05^{a}	0.06^{a}
		3		5.68$^{a\ ab}$	2.65^{a}	0.02^{a}	0.04$^{a\ a}$	0.04^{a}	0.02^{b}	0.03^{a}
		Mean		6.94	4.51	0.04	0.02	0.07	0.03	0.04
	W3	1		29.12$^{a\ a}$	19.46^{a}	0.12^{a}	0.02^{a}	0.18^{a}	0.02^{a}	0.04^{a}
		2		3.44$^{b\ b}$	1.67^{a}	0.03^{a}	0^{a}	0.06^{a}	0.03^{a}	0.03^{a}
		3		10.50$^{ab\ b}$	7.48^{a}	0.03^{a}	0.04^{a}	0.06^{a}	0.02^{a}	0.04^{a}
		Mean		14.35	9.54	0.06	0.02	0.1	0.02	0.04
	E2	1		23.26^{a}	27.92^{a}	0.12^{a}	0.01^{b}	0.17$^{a\ a}$	0.05^{a}	0.06^{a}
		2		0.56^{b}	1.16^{a}	0.01^{a}	0^{b}	0.01$^{a\ ab}$	0.01^{a}	0.01^{a}
		3		5.19^{b}	7.21^{a}	0.01^{a}	0.03^{a}	0.02$^{a\ b}$	0.02^{a}	0.03^{a}
		Mean		9.67	12.10	0.05	0.01	0.07	0.03	0.03
	Treatment	1		21.81^{a}	19.53^{a}	0.10^{a}	0.01^{b}	0.15^{a}	0.03^{a}	0.04^{a}
		2		2.02^{b}	1.83^{a}	0.03^{ab}	0^{b}	0.05^{ab}	0.03^{a}	0.03^{a}
		3		7.12^{b}	6.02^{a}	0.02^{b}	0.04^{a}	0.04^{b}	0.02^{a}	0.03^{a}
By fertilization treatment										
C_E						0.06^{a}	0.02^{a}	0.09^{a}	0.03^{a}	0.04^{a}
C_G						0.06^{a}	0.02^{a}	0.1^{a}	0.03^{a}	0.04^{a}

APPENDIX C

Connecting letters report showing the difference of concentrations (mg L^{-1}) in groundwater between the crops, the years of the project and the fertilization treatments. Means followed by different letters within the same year, block and treatment are significantly different ($p < 0.05$). Bold letters indicate statistics run with $a = 0.1$.

Trt	Block	Year	Crop	NO_3-N (mg L^{-1})	NH_4-N (mg L^{-1})	PO_4-P (mg L^{-1})	Cl (mg L^{-1})
By cropping period							
C_E	W2	1	Maize	6.83^{b}	0.06^{b}	0.02^{a} **b**	23.84^{b} **c**
			Residue	7.82^{ab}	0.18^{ab}	0.03^{a} **ab**	38.74^{a} **b**
			Wheat	9.44^{a}	0.27^{a}	0.05^{a} **a**	46.66^{a} **a**
			Mean	8.03	0.17	0.03	36.41
		2	Maize	7.31^{a}	0.35^{a}	0.1^{b}	38.02^{b}
			Residue	8.67^{a}	0.01^{a}	0.08^{b}	56.44^{a}
			Rye	4.45^{b}	0.46^{a}	0.17^{a}	50.36^{a}
			Mean	6.81	0.27	0.12	48.27
		3	Maize	6.90^{a}	0.69^{a}	0.07^{b}	39.41^{a}
			Residue	8.01^{a}	0.87^{a}	0.28^{a}	38.43^{a}
			Wheat	7.47^{a}	0.62^{a}	0.21^{a}	26.60^{b}
			Mean	7.46	0.73	0.19	34.81
	E1	1	Maize	1.89^{b}	0.2^{a}	0.01^{b}	15.83^{b} **b**
			Residue	2.08^{ab}	0.26^{a}	0.03^{ab}	24.34^{ab} **a**
			Wheat	3.18^{a}	0.17^{a}	0.06^{a}	28.05^{a} **a**
			Mean	2.38	0.21	0.03	22.74
		2	Maize	2.73^{a}	0.04^{b}	0.09^{a} **b**	25.59^{b}
			Residue	2.09^{a}	0.06^{b}	0.12^{a} **ab**	39.45^{a}
			Rye	2.66^{a}	0.41^{a}	0.13^{a} **a**	37^{a}
			Mean	2.49	0.17	0.11	34.01
		3	Maize	2.29^{b}	0.51^{b}	0.09^{c}	31.5^{a}
			Residue	3.62^{a}	1.16^{a}	0.28^{a}	29.33^{a}
			Wheat	3.77^{a}	0.5^{b}	0.17^{b}	19.25^{b}
			Mean	3.23	0.72	0.18	26.69
	E3	1	Maize	2.79^{b}	0.25^{a}	0.01^{b}	29.7^{b}
			Residue	4.98^{ab}	0.22^{a}	0.02^{ab}	44.19^{ab}
			Wheat	7.91^{a}	0.24^{a}	0.07^{a}	48.62^{a}
			Mean	5.23	0.24	0.03	40.84
		2	Maize	9.57^{a}	0.07^{b}	0.10^{a}	47.74^{a} **b**
			Residue	10.13^{a}	0.02^{b}	0.07^{a}	53.76^{a} **ab**
			Rye	5.33^{a}	0.37^{a}	0.13^{a}	62.45^{a} **a**

Trt	Block	Year	Crop	NO_3-N (mg L^{-1})	NH_4-N (mg L^{-1})	PO_4-P (mg L^{-1})	Cl (mg L^{-1})
			Mean	8.34	0.15	0.1	54.65
		3	Maize	5.47^{a}	0.43^{b}	0.1^{b}	47.84^{a}
			Residue	5.96^{a}	0.99^{a}	0.25^{a}	49.08^{a}
			Wheat	5.62^{a}	0.47^{b}	0.14^{b}	37.95^{b}
			Mean	5.68	0.63	0.16	44.96
C_G	W1	1	Maize	5.34^{b} **b**	0.09^{b}	0.01^{b}	22.71^{b}
			Residue	8.37^{ab} **a**	0.18^{ab}	0.02^{ab}	33.51^{ab}
			Wheat	8.49^{a} **a**	0.24^{a}	0.05^{a}	39.85^{a}
			Mean	7.40	0.17	0.03	32.02
		2	Maize	6.67^{a}	0.05^{b}	0.13^{a}	37.82^{a} **b**
			Residue	7.89^{a}	0.04^{b}	0.08^{a}	59.23^{a} **a**
			Rye	4.43^{b}	0.39^{a}	0.14^{a}	41.86^{a} **ab**
			Mean	6.33	0.16	0.12	46.3
		3	Maize	6.55^{ab} **a**	0.59^{a}	0.11^{b}	38.86^{a}
			Residue	7.63^{a} **a**	1^{a}	0.27^{a}	38.9^{a}
			Wheat	4.83^{b} **b**	0.56^{a}	0.19^{ab}	21.44^{b}
			Mean	6.34	0.72	0.19	33.07
	W3	1	Maize	5.99^{b} **c**	0.05^{b} **b**	0.01^{b}	30.41^{c}
			Residue	7.18^{b} **b**	0.2^{ab} **a**	0.04^{ab}	38.01^{b}
			Wheat	8.48^{a} **a**	0.19^{a} **a**	0.08^{a}	48.48^{a}
			Mean	7.22	0.15	0.04	38.97
		2	Maize	8.38^{b}	0.03^{b}	0.11^{a}	46.2^{b}
			Residue	10.8^{a}	0.02^{b}	0.11^{a}	47.7^{ab}
			Rye	6.71^{c}	0.38^{a}	0.13^{a}	51.83^{a}
			Mean	8.63	0.14	0.12	48.58
		3	Maize	7.02^{b}	0.43^{b}	0.08^{b}	49.15^{a}
			Residue	8.38^{ab}	1.16^{a}	0.28^{a}	50^{a}
			Wheat	9.82^{a}	0.5^{b}	0.21^{a}	36.96^{b}
			Mean	8.41	0.7	0.19	45.37
	E2	1	Maize	3.67^{b}	0.08^{b} **b**	0.01^{b}	20.16^{c}
			Residue	5.63^{a}	0.22^{a} **a**	0.04^{ab}	28.06^{b}
			Wheat	6.13^{a}	0.17^{ab} **a**	0.06^{a}	36.15^{a}
			Mean	5.14	0.16	0.04	28.12
		2	Maize	5.49^{a}	0.02^{b}	0.09^{b}	35.3^{b}
			Residue	6.47^{a}	0.11^{b}	0.1^{ab}	38.75^{b}
			Rye	5.53^{a}	0.28^{a}	0.13^{a}	48.39^{a}
			Mean	5.83	0.14	0.11	40.81
		3	Maize	5.94^{b}	0.36^{b}	0.08^{b} **c**	42.16^{a}
			Residue	7.62^{a}	1.18^{a}	0.28^{a} **a**	41.12^{a}
			Wheat	6.74^{ab}	0.49^{b}	0.15^{b} **b**	31.3^{b}
			Mean	6.77	0.68	0.17	38.19

Trt	Block	Year	Crop	NO_3-N (mg L^{-1})	NH_4-N (mg L^{-1})	PO_4-P (mg L^{-1})	Cl (mg L^{-1})
By year							
C_E	W2	1		$8.05^{a\ \mathbf{a}}$	$0.16^{b\ \mathbf{b}}$	0.04^{b}	35.43^{b}
		2		$6.01^{b\ \mathbf{b}}$	$0.37^{ab\ \mathbf{b}}$	0.13^{a}	45.87^{a}
		3		$7.27^{ab\ \mathbf{a}}$	$0.69^{a\ \mathbf{a}}$	0.15^{a}	34.87^{b}
		Mean		7.11	0.41	0.11	38.72
	E1	1		2.46^{a}	0.2^{b}	0.04^{c}	22.05^{c}
		2		2.59^{a}	0.17^{b}	0.11^{b}	31.84^{a}
		3		2.98^{a}	0.63^{a}	0.15^{a}	27.47^{b}
		Mean		2.68	0.33	0.1	27.12
	E3	1		$4.5^{a\ \mathbf{b}}$	0.24^{b}	0.03^{b}	36.83^{c}
		2		$7.35^{a\ \mathbf{a}}$	0.23^{b}	0.11^{a}	56.35^{a}
		3		$5.6^{a\ \mathbf{b}}$	0.55^{a}	0.14^{a}	45.18^{b}
		Mean		5.82	0.34	0.09	46.12
	Treatment	1		4.45^{a}	0.2^{b}	0.03^{c}	29.3^{c}
		2		4.52^{a}	0.22^{b}	0.11^{b}	41.03^{a}
		3		4.90^{a}	0.61^{a}	0.15^{a}	35.6^{b}
C_G	W1	1		7.23^{a}	0.17^{b}	0.03^{b}	32.41^{b}
		2		5.56^{b}	0.24^{b}	0.13^{a}	42.65^{a}
		3		6.15^{ab}	0.66^{a}	0.17^{a}	32.60^{b}
		Mean		6.31	0.36	0.11	35.89
	W3	1		7.3^{a}	0.14^{b}	0.05^{b}	39.76^{b}
		2		7.95^{a}	0.18^{b}	0.12^{a}	48.79^{a}
		3		8.14^{a}	0.59^{a}	0.16^{a}	45.56^{a}
		Mean		7.80	0.3	0.11	44.7
	E2	1		$4.96^{b\ \mathbf{c}}$	0.14^{b}	$0.03^{b\ \mathbf{c}}$	27.77^{b}
		2		$5.67^{b\ \mathbf{b}}$	0.12^{b}	$0.11^{a\ \mathbf{b}}$	39.95^{a}
		3		$6.51^{a\ \mathbf{a}}$	0.56^{a}	$0.14^{a\ \mathbf{a}}$	38.94^{a}
		Mean		5.71	0.27	0.09	35.55
	Treatment	1		6.31^{b}	0.15^{b}	0.04^{c}	33.02^{c}
		2		6.36^{b}	0.16^{b}	0.12^{b}	43.2^{a}
		3		7.02^{a}	0.6^{a}	0.15^{a}	39.89^{b}
By fertilization treatment							
C_E				4.67^{b}	$0.4^{a\ \mathbf{a}}$	0.1^{a}	35.02^{b}
C_G				6.62^{a}	$0.34^{a\ \mathbf{b}}$	0.11^{a}	38.63^{a}